ISSN 2450–1654 | e-ISSN 2450–6478

2025, Vol. 21, Number 1

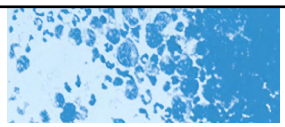

OFFICIAL JOURNAL OF THE POLISH SOCIETY OF CLINICAL ONCOLOGY

# Oncology IN CLINICAL PRACTICE



**Under the patronage of**

Akademia Czerniaka · Polska Grupa Raka Płuca · Polskie Towarzystwo Patologów · Polskie Towarzystwo Radioterapii Onkologicznej

VIA MEDICA

# ONCOLOGY
## IN CLINICAL PRACTICE

Official Journal of the Polish Society of Clinical Oncology, under the patronage of the Melanoma Academy, Polish Lung Cancer Group (PLCG), Polish Society of Pathologists, and Polish Society of Radiation Oncology (PSRO)

https://journals.viamedica.pl/oncology_in_clinical_practice





**Oncology in Clinical Practice** (ISSN 2450–1654, e-ISSN 2450–6478) is published six times a year by

VM Media Group sp. z o.o.
ul. Świętokrzyska 73, 80–180 Gdańsk, Poland
Phone: (+48 58) 320 94 94, fax: (+48 58) 320 94 60
e-mail: viamedica@viamedica.pl,
**http://www.viamedica.pl**

24-1973.001.001

**Editorial Address**

Klinika Nowotworów Płuca i Klatki Piersiowej
Narodowy Instytut Onkologii im. Marii Skłodowskiej-Curie — Państwowy Instytut Badawczy
ul. Roentgena 5, 02–781 Warszawa, Poland
Phone: (+48 22) 546 21 69
e-mail: sekretariat4@pib-nio.pl





**Current Impact Factor of "Oncology in Clinical Practice" (2023) is 0.3.**

**According to the statement of the Polish Ministry of Science and Higher Education publication in the journal has been awarded with 100 points.**

Editorial policies and author guidelines are published on journal website: http://journals.viamedica.pl/oncology_in_clinical_practice

the KF

THE KOSCIUSZKO FOUNDATION

# The 2025 Janczewski Award

For over two decades, the Kościuszko Foundation has been awarding the Bohdan and Zygmunt Janczewski Prize to Polish authors of the most outstanding scientific articles in the field of clinical medicine.

In this edition, the prize amounts to **$15,000**.

The award was established in 2004 by the renowned andrologist Zygmunt Janczewski, a professor at the former Medical Academy in Warsaw. It is granted every two years to a Polish physician permanently residing in Poland.

The competition will consider articles published in international medical journals in English within the last two years (2023–2024) preceding the award year. Applications will be accepted until May 15, 2025.

The award regulations and application form are available at: https://kfpoland.org

**Apply today!**

warsaw@thekf.org

https://kfpoland.org

ONCOLOGY
IN CLINICAL PRACTICE

Official Journal of the Polish Society of Clinical Oncology, under the patronage of the Melanoma Academy, Polish Lung Cancer Group (PLCG), Polish Society of Pathologists, and Polish Society of Radiation Oncology (PSRO)

https://journals.viamedica.pl/oncology_in_clinical_practice

2025, Vol. 21, Number 1

## ORIGINAL ARTICLES



## REVIEW ARTICLES



## CASE REPORTS

# Professor Krzysztof Krzemieniecki Award for the best case report or clinical vignette accepted for publication

## Case Report or Clinical Vignette Contest Policies

This policy defines the scope, requirements and regulations regarding **The Krzysztof Krzemieniecki Award** for the best case report or clinical vignette published in "Oncology in Clinical Practice" (OCP) 9th Edition.

1. The aim of the contest is to encourage submission of quality case reports and clinical vignettes related to oncological practice and to promote them in the scientific deliberations.
2. All respective manuscripts submitted to OCP between June 1, 2024 and May 31, 2025 and accepted for publication will qualify.
3. Manuscripts should be prepared in line with Authors' guidelines and should be submitted only through the manuscript system available at Journal's website: https://journals.viamedica.pl/oncology_in_clinical_practice
4. All submitted manuscripts will be evaluated during the peer review process and authors will be informed about their qualification for publication in OCP. Accepted papers will be evaluated by the Contest Committee based upon fulfillment of the Contest criteria as well as practical significance, originality, applicability and addressing of current/critical concerns.
5. The first author of the winning paper will be eligible for a prize of gross 1000,00 Euro gross (one thousand euro).
6. Results will be announced during the XXVIII National Congress of The Polish Society of Clinical Oncology and subsequently at the Journal website.
7. Winner will be notified via email.
8. Contest Committee may exclude a paper from participation in case of potential conflict of interest or ask submitting author for adequate clarifications.
9. The Sponsor at any stage and in any respect, will not participate in the evaluation of entries and selection of a winning paper.
10. The award amount shall be paid based on the copyright transfer agreement to the paper.
11. These Regulations are the sole and exclusive document defining the principles and conditions for the Contest. In all matters not regulated, decisions are made by The Organizer.

Contest Organizer:
VM Media Group sp. z o.o., seated at 73 Swietokrzyska Street, 80–180 Gdansk, Poland (Register of Entrepreneurs kept by the District Court for Gdansk, Commercial Division VII of the National Court Register under KRS No. 0000266430, VAT Reg. No. PL 583-28-39-187).

**Patronage** NOVARTIS

VIA MEDICA

ORIGINAL ARTICLE

Oncology in Clinical Practice
2025, Vol. 21, No. 1, 1–7
DOI: 10.5603/ocp.97982

ISSN 2450-1654
eISSN 2450-6478

# Impact of deep inspiration breath hold irradiation on dose reduction to the heart and left coronary artery in breast cancer

Piotr Winczura[1,*], Julianna Wejs-Maternik[1], Andrzej Blukis[1], Monika Antonowicz-Szydłowska[2], Patrycja Urbanowicz[3], Agnieszka Rakowiecka[1], Marcin Urbanowicz[4], Matteo Pepa[5], Samantha Dicuonzo[5], Barbara A. Jereczek-Fossa[5,6], Andrzej Badzio[2]

[1]Nu-Med Radiotherapy Center, Elbląg, Poland
[2]Department of Oncology and Radiotherapy, University Clinical Center, Gdańsk, Poland
[3]Department of Radiology, Regional Polyclinical Hospital in Elbląg, Poland
[4]Department of Radiology, Nu-Med, Elbląg, Poland
[5]Division of Radiotherapy, IEO European Institute of Oncology, IRCCS, Milan, Italy
[6]Department of Oncology and Hemato-oncology, University of Milan, Italy

**Abstract**

**Introduction.** Deep inspiration breath-hold (DIBH) is an effective and feasible approach to reducing the radiation dose to the heart in left-sided breast cancer radiotherapy (RT). This study aimed to assess the impact of DIBH on dose reduction to the heart and the left anterior descending coronary artery (LAD) in left-sided early breast cancer patients with intact breasts.

**Material and methods.** We compared RT plans of 42 patients from computed tomography datasets acquired for free breathing (FB) and DIBH techniques with 6 MeV photon tangential fields. The prescribed dose was 50 Gy in 25 fractions.

**Results.** DIBH enabled significant dose reduction to the heart and the LAD. A significantly lower mean heart dose (MHD) was observed in DIBH compared to FB planning (2.9 *vs.* 6.0 Gy, respectively; $p < 0.0001$). The considered LAD parameters, namely $D_{max}$ 0.2 $cm^3$, mean dose, and V45Gy, were all significantly reduced in DIBH compared to FB planning (33.3 *vs.* 47 Gy; $p < 0.0001$, 16.7 *vs.* 30.1 Gy; $p < 0.0001$ and 0.5 *vs.* 1.7 $cm^3$; $p < 0.0001$, respectively). Reduction in any of the LAD dose parameters was not correlated with MHD reduction. The LAD parameters were found to be significantly reduced in the group of patients with modest MHD reduction defined as < 2.8 Gy (31.2 *vs.* 46.9 Gy; $p = 0.0001$, 15 *vs.* 26.9 Gy; $p < 0.00001$, and 0.5 *vs.* 1.6 Gy; $p = 0.0005$, respectively).

**Conclusions.** DIBH has a pronounced impact on dose reduction to the LAD. This influence is not correlated with the MHD and is present even in patients with modest MHD reduction with DIBH.

**Keywords:** DIBH, breast cancer, radiotherapy

## Introduction

Adjuvant radiotherapy (RT) after breast-conserving surgery in breast cancer patients improves local control and overall survival. However, in patients with left-sided tumors, radiation increases cardiac toxicity. In a classic study, Darby et al. [1] demonstrated

*Correspondence: Piotr Winczura, MD PhD, Nu-Med Radiotherapy Center, ul. Królewiecka 146, 82–300 Elbląg, Poland (piotr.winczura@nu-med.pl)
Received: 2 December 2023; Accepted: 5 March 2024;
Early publication: 29 May 2024

that rates of major coronary events (myocardial infarction, necessity for coronary revascularization, and death from ischemic heart disease) increase linearly with the mean heart dose (MHD) by 7.4% per Gray (Gy) after left-sided breast cancer RT. These results have been independently validated by van den Boogard et al. [2]. Their study showed that for the first 9 years after radiation exposure, the risk of major coronary events increases by 16.5% per Gy [2]. Several techniques to optimize heart dose exist, namely deep inspiration breath-hold (DIBH), prone position, intensity-modulated RT, partial breast irradiation, and proton beam therapy [3–5]. Specifically, the DIBH procedure, which requires careful positioning and monitoring during treatment, is an effective and feasible technique that reduces the MHD by moving the heart away from the thoracic wall. Studies showed that DIBH irradiation decreases heart volume in the treatment field [5–9], MHD [5, 7, 10–17], and the radiation dose to the left anterior descending coronary artery (LAD) [5, 10, 12–18]. As radiation-induced heart injury leads to a higher risk of coronary events, we assumed that the dose to coronary vessels may be an important factor. In this study, we present an analysis of the MHD and different measures of radiation exposure of the LAD in patients treated with DIBH. We also present the development and prospective evaluation of DIBH in our Institution.

## Material and methods

Forty-two consecutive female left-sided early breast cancer patients planned for DIBH radiotherapy at the Radiotherapy Center NU-MED between 2016 and 2017 were analyzed retrospectively. All patients underwent breast-conserving surgery procedures and were referred for adjuvant RT. Patients after mastectomy or scheduled for adjuvant lymph node irradiation were excluded from the study. We also excluded all patients with invasive breast cancer who received external beam boost [either free breathing (FB) or DIBH] after whole breast irradiation due to heterogeneity of the boost. At the first visit, each patient had a consultation with the treating physician who explained the nature and rationale of the DIBH procedure. Good compliance is crucial in the DIBH procedure, so patients with poor lung function and unable to sustain breath were not considered optimal candidates. At the time of the study, no established criteria for DIBH irradiation in terms of MHD reduction were available at our Institution. Consequently, the treatment modality was chosen individually for each patient by the staff. Before the planned computed tomography (CT) simulation, patients were trained on the treatment machine and were considered eligible if they were able to hold their breath for at least 30 seconds. Surface monitoring system Align RT™ (VisionRT Ltd, London, UK) was used to check if the patient's chest wall was stable during the procedure.

The CT simulation was performed on the wing board in both FB and DIBH positions. Scans without intravenous contrast medium were acquired with a 3 mm slice width.

Target structures and organs at risk (OAR) were contoured both on FB and DIBH scans. Clinical target volume (CTV) included glandular tissue of the left breast down to the deep fascia, without the underlying muscle and rib cage. Planning target volume (PTV) was created by expanding the CTV by 5 mm isotropic margins. OAR were defined as the heart, LAD, and ipsilateral lung. The heart and the LAD were contoured manually by two independent radiation oncologists according to previously published guidelines [19]. The heart was contoured together with the pericardium starting superiorly and just inferiorly to the left pulmonary artery. When the LAD was not visible on CT scans, the interventricular groove was used as its surrogate. Lungs we contoured using an automatic segmentation tool.

### Treatment planning

Free breathing and DIBH CT data sets were transferred to the Eclipse™ planning system (Varian Medical Systems Palo Alto, CA, USA), and treatment plans with static 6 MV photon opposite conformal tangential fields with multileaf collimators (MLC) were created. The comparison of FB and DIBH plans is presented in Figure 1. An additional field-in-field approach was allowed to provide optimal dose distribution and PTV coverage. The total dose was 50 Gy in 25 fractions prescribed to the isocenter. In DIBH plans, virtual wedges were not allowed, as their exact position could not be exactly reproduced in case of automatic beam off. Some examples of beam's eye views for DIBH and FB plans are shown in Figure 2.

The following optimal dose constraints for OAR were used: V20Gy < 35% and a mean lung dose (MLD) < 20 Gy for the ipsilateral lung. The MHD was kept as low as possible, preferably lower than 4 Gy [20], but without penalizing PTV coverage [21].

In daily practice in our institution, the LAD is not considered an OAR, as no recommended dose constraints are available in the literature. For the study, we used three dosimetric parameters from the literature to describe dose distribution in the LAD. The first one was the mean LAD dose, which is the most commonly used parameter in studies assessing the influence of DIBH on coronary vessels [5, 8, 10, 12–14]. The second one was the maximum dose, which is very important as the LAD is a serial structure. Because of uncertainties about the exact position of the LAD due to its movements associated with heartbeat, we considered the maximum dose to the 0.2 $cm^3$ of the

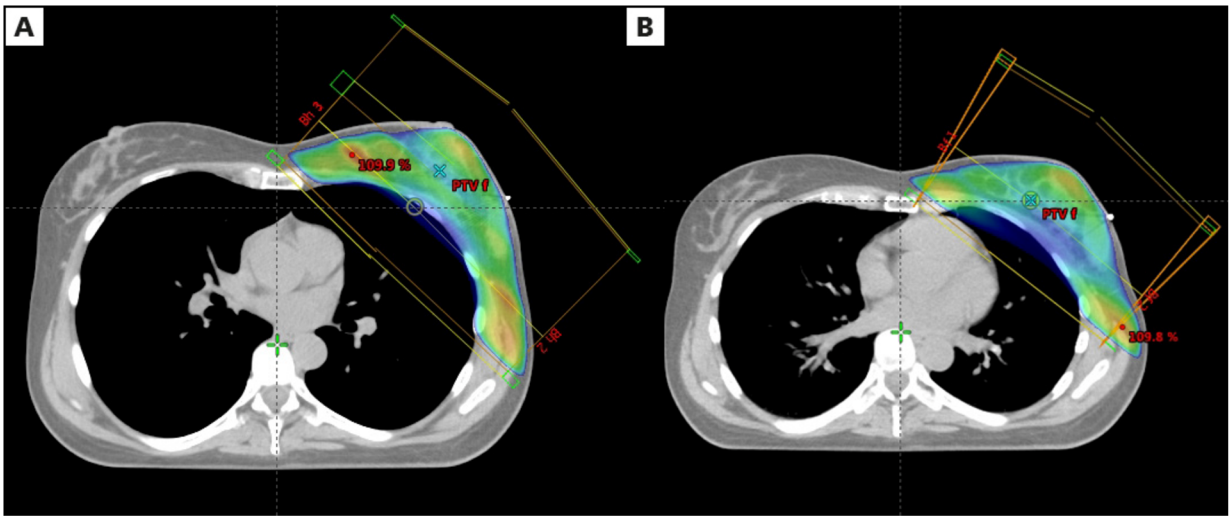


**Figure 1.** Axial views of computed tomography (CT) based radiation free breathing (FB) (**A**) and deep inspiration breath-hold (DIBH) (**B**) plans. The area in colour-wash represents volume covered by 95% isodose

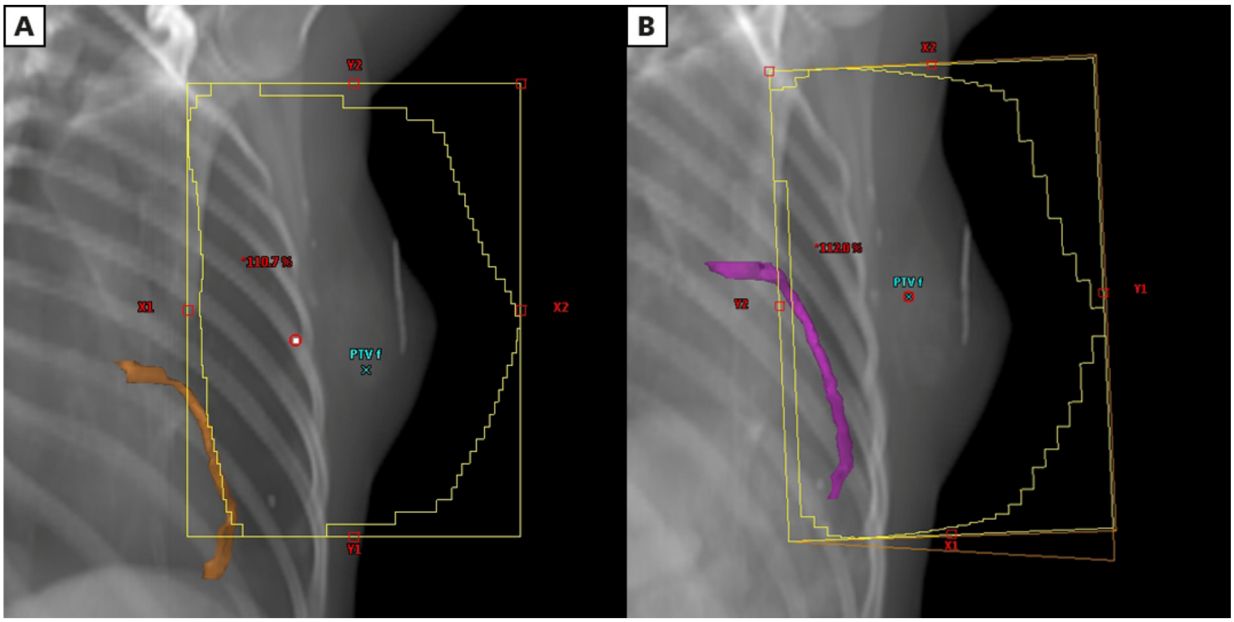


**Figure 2.** Beam's eye view (BEV) of the tangential radiation fields of the same patient planned for deep inspiration breath-hold (DIBH) (**A**) and free breathing (FB) (**B**). Note that in (**A**) the left anterior descending coronary artery (LAD) is situated at the edge of radiation field, while in (**B**) it is almost completely included inside

LAD instead of point maximum as a second constraint [9]. The third and last analyzed parameter was V45Gy as it is postulated that doses $\geq$ 45 Gy are associated with a higher risk of ischemic myocardial perfusion defects [22].

## Treatment verification and monitoring

Treatment was delivered with a Siemens Artiste linear accelerator. We used a voluntary technique for DIBH [23]. During the whole RT session, radiographers had direct audio-visual contact with the patient to give commands and instructions on breathing when needed. Before each fraction, the patient was asked to breathe in the same way as during the simulation. Two orthogonal 1 MV films were taken during the first 3 fractions to verify positioning and make changes if necessary. Surface monitoring system Align RT was used to achieve stable and reproducible patient position using a 3-mm tolerance limit. The beam was automatically turned off during treatment if the patient's surface was out of the limit.

Electronic portal images (EPI) were obtained daily from each treatment field and compared online with digitally reconstructed radiographs (DRR) before treatment delivery.

In the case of Align RT failure or poor compliance, patients were treated with FB plans prepared beforehand and could return to the DIBH procedure as soon as it was possible.

### Statistical methods

STATA 8.0 software was used for statistical analyses. Categorical variables were compared using a two-sided Pearson chi-square test. A dosimetric comparison was carried out by using a paired Student's t-test and Wilcoxon signed rank test. Statistical significance was considered at $p < 0.05$.

## Results

The characteristics of patients are presented in Table 1. In 32 patients (76%), MHD dose reduction with DIBH planning was considered clinically relevant, and they were treated with this technique. Only in one patient, the MHD was higher in DIBH than in FB, but this difference was 0.2 Gy and was considered clinically insignificant. The remaining 10 patients (24%) received the FB treatment.

**Table 1.** Patient characteristics

| | |
|---|---|
| **Age, mean (range)** | **53 (33–68)** |
| **Systemic treatment, no. (%)** | |
| Hormonal therapy | 36 (86%) |
| Chemotherapy | 16 (38%) |
| Trastuzumab | 8 (19%) |
| **Histology, no. (%)** | |
| Ductal invasive carcinoma | 33 (78%) |
| Lobular | 3 (8%) |
| Other | 6 (14%) |
| **T stage, no. (%)** | |
| $T_{is}$ | 1 (2%) |
| $T_1$ | 31 (74%) |
| $T_2$ | 9 (22%) |
| $T_3$ | 1 (2%) |
| **N stage, no. (%)** | |
| $N_0$ | 41 (98%) |
| $N_{1\ (mi)}$ | 1 (2%) |
| **CTV FB mean/median/range [cm$^3$]** | 904/778/344–2751 |
| **CTV DIBH mean/median/range [cm$^3$]** | 897/785/341–2630 |
| **CTV volume FB/DIBH** | p = 0.23* |
| **PTV FB mean/median/range [cm$^3$]** | 1279/1155/589–3511 |
| **PTV DIBH mean/median/range [cm$^3$]** | 1277/1151/591–3394 |
| **PTV volume FB/DIBH** | p = 0.82* |

*Student's t-test; CTV — clinical target volume; DIBH — deep inspiration breath hold; FB — free breathing; PTV — planning target volume

Significantly, a lower MHD was observed in DIBH compared to FB planning (2.9 *vs.* 6.0 Gy, respectively; $p < 0.0001$), and the average MHD reduction between DIBH and FB was 3.1 Gy. MHD < 4 Gy was achieved in 33 (78.6%) DIBH plans compared to 11 (26.2%) FB plans.

The analyzed LAD parameters, namely $D_{max}$ 0.2 cm$^3$, mean dose, and V45Gy, were all also significantly reduced in DIBH compared to FB planning (33.3 *vs.* 47 Gy; $p < 0.0001$, 16.7 *vs.* 30.1 Gy; $p < 0.0001$ and 0.5 *vs.* 1.7 cm$^3$; $p < 0.0001$, respectively). The mean reduction of the above-mentioned parameters achieved with DIBH planning was 13.7 Gy, 13.4 Gy, and 1.2 cm$^3$, respectively.

Such a reduction in any of the LAD dose parameters turned out not to be correlated with an MHD decrease. Therefore, we subsequently analyzed the impact of DIBH on the LAD parameters in patients with a modest MHD reduction, defined as < 2.8 Gy (n = 20). We found that these parameters were all significantly reduced in DIBH compared to FB plans (31.2 *vs.* 46.9 Gy; $p = 0.0001$, 15 *vs.* 26.6.9 Gy; $p < 0.00001$, and 0.5 *vs.* 1.6 Gy; $p = 0.0005$, respectively) (Tab. 2).

Deep inspiration breath-hold had a significant but not pronounced impact on ipsilateral lung irradiation. The MLD to the left lung was significantly lower in DIBH than in FB (9.8 *vs.* 11.1 Gy; $p < 0.00001$) as was V20Gy (18.6 *vs.* 20.9%; $p < 0.0001$). In 6 patients (14.3%), DIBH resulted in higher V20Gy and in 9 patients (21.4%) in a higher MLD.

## Discussion

Deep inspiration breath-hold in our Institution was proven to be a feasible and effective procedure for sparing heart in patients with left-sided early breast cancer treated with RT after breast-conserving surgery.

**Table 2.** Comparison of heart and left anterior descending coronary artery (LAD) doses between free breathing (FB) and deep inspiration breath-hold (DIBH) planning

| | FB [Gy] | DIBH [Gy] | Reduction [%] | p value |
|---|---|---|---|---|
| **Whole group (42 patients)** | | | | |
| MHD | 6.0 | 2.9 | 51.7 | < 0.00001 |
| $D_{max}$ 0.2 cm$^3$ | 47 | 33.3 | 21.5 | < 0.0001 |
| V45Gy | 1.7 | 0.5 | 70.6 | < 0.0001 |
| Mean LAD dose | 30.1 | 16.7 | 44.5 | < 0.0001 |
| **Modest MHD reduction group (20 patients)** | | | | |
| $D_{max}$ 0.2 cm$^3$ | 46.9 | 31.2 | 33.5 | 0.0001 |
| V45Gy | 1.6 | 0.5 | 68.7 | < 0.00001 |
| Mean LAD dose | 26.9 | 15 | 44,2 | 0.0005 |

MHD — mean heart dose

The benefits of DIBH in terms of MHD reduction in our cohort was 3.1 Gy and was consistent with other reported studies where it ranged from 1 to 3.4 Gy [5, 7, 12, 23]. It should also be mentioned that DIBH enabled achieving the optimal (< 4 Gy) MHD in more than 75% of patients while this constraint was fulfilled only in about one-quarter of FB subjects.

The study revealed a pronounced impact of DIBH on the LAD dose. To date, there are no established dose constraints to the coronary vessels as there are no prospective studies assessing the impact of absorbed doses on clinically relevant endpoints such as coronary events. Based on available clinical data, Piroth et al. [24] proposed constraints for left-sided breast-only RT. These include the MHD, mean LAD dose, and LAD V30 and V40 [24]. Dose to the left ventricle was also included as clinically relevant [22]. It is postulated that left ventricle V5 could be a predictor of acute coronary events after breast RT [2]. Nevertheless, the left coronary artery seems to be an important OAR in RT of left-sided breast cancers due to its anatomical location and importance, as it supplies blood to the left ventricle. This hypothesis is supported by large well-conducted studies showing that long-term cardiac mortality after breast cancer RT is associated mostly with coronary disease resulting in ischemic heart disease and myocardial infarction [23, 25]. According to these data, further studies on heart toxicity in breast cancer RT patients should take LAD, as an OAR, into consideration. In the era of conformal RT, this structure can be successfully identified and spared without compromising target coverage.

The most widely studied dosimetric parameter for the LAD is the mean dose [8, 11–13, 23]. In all published studies, mean doses to the LAD were significantly smaller in DIBH than in FB RT plans. However, there was considerable variability in the doses reported by the authors, which ranged from 5.5 to 21.9 Gy in DIBH and 11.4 to 31.7 Gy in FB. Dose reduction ranged from 5.9 to 10.3 Gy. These differences can be partially explained by different planning techniques and intra-observer variability in the contouring of coronary vessels, due to the scarcity of contouring guidelines at the time of the treatments and difficulties in delineation of small structures [19, 21, 23]. It should also be mentioned that, both in research and clinical settings, planning CT in breast cancer patients is performed without contrast media, which makes contouring less accurate. Some authors proposed adding an isotropic margin to the coronary artery to account for uncertainties of internal organ motion and intra-observer variability [13]. In our cohort, mean doses to the LAD in DIBH and FB were 16.7 and 30.1 Gy, respectively, with a resulting dose reduction of 13.4 Gy, in line with other mentioned studies.

No correlation between the reduction in the MHD and significant gain in the LAD dosimetric parameters was found. This can be explained by the anatomic location of the coronary vessel, which in DIBH is often situated at the edge of the radiation field (Fig. 1). As a result, even minor changes in thoracic geometry between DIBH and FB can cause substantial differences in dose distribution within this structure, while heart volume included in the radiation field would not change much. We also showed that, even in the group of patients with a modest reduction in the MHD in DIBH plans, there was still a significant improvement in all analyzed dose distribution parameters within the LAD. This finding suggests that the MHD may not be the most relevant parameter when assessing the risk of cardiac toxicity in breast cancer RT. It seems reasonable to assess the MHD in conjunction with the dose to the coronary artery, especially in patients with a low MHD. This hypothesis, however, requires further studies and correlation with clinical data.

The study demonstrated that DIBH yields lung dosimetric advantages both in terms of MLD and V20Gy. However, this effect was not as unequivocal as with the heart and the LAD, and it should be kept in mind that in a significant group of patients, DIBH plans were inferior to the FB technique in terms of the MLD and V20Gy. Some recent studies with significant groups of patients show similar results [5, 26–28]. In some patients with special concerns about lung toxicity, when DIBH is not sufficient to reduce the dose to the heart and the ipsilateral lung, radiotherapy in the prone position is a promising option [5]. Data on the influence of DIBH on the lung dose are limited, and this issue needs further research.

## Conclusions

Our study showed that the DIBH technique results in significant sparing of the coronary vessels in early left-sided breast cancer patients treated with postoperative RT. DIBH has a pronounced impact on dose reduction to the LAD. This influence is not correlated with the mean heart dose and is present even in patients with a modest mean heart dose reduction with DIBH.

## Article Information and Declarations

### Data availability statement

The data that support the findings of this study are available on request from the corresponding author.

### Ethics statement

The study is analysis based od the retrospective data (CT) that were completely anonymyzed. All medical procedures i.e. CT scans were performed as a part of routine radiotherapy planning. Taking these to account patients were not

asked to provide consent as well as ethical approval was not required.

### Author contributions

P.W.: conception and design, collection and assembly of data, data analysis and interpretation, manuscript writing; J.W.-M.: conception and design, collection and assembly of data, data analysis and interpretation; A.Blukis: conception and design, collection and assembly of data; M.A.-S., P.U., A.R. M.U.: collection and assembly of data; M.P., S.D.: data analysis and interpretation, manuscript writing; B.A.J.-F., A.Badzio: conception and design, data analysis and interpretation, manuscript writing.
All authors approved the final manuscript.

### Funding

The study was not financed/supported by any institution/company

### Acknowledgements

None.

### Conflict of interest

All authors declare no conflict of interest.

### Supplementary material

None.

## References

1. Darby SC, Ewertz M, McGale P, et al. Risk of ischemic heart disease in women after radiotherapy for breast cancer. N Engl J Med. 2013; 368(11): 987–998, doi: 10.1056/NEJMoa1209825, indexed in Pubmed: 23484825.
2. van den Bogaard VAB, Ta BDP, van der Schaaf A, et al. Validation and Modification of a Prediction Model for Acute Cardiac Events in Patients With Breast Cancer Treated With Radiotherapy Based on Three-Dimensional Dose Distributions to Cardiac Substructures. J Clin Oncol. 2017; 35(11): 1171–1178, doi: 10.1200/JCO.2016.69.8480, indexed in Pubmed: 28095159.
3. Smyth LM, Knight KA, Aarons YK, et al. The cardiac dose-sparing benefits of deep inspiration breath-hold in left breast irradiation: a systematic review. J Med Radiat Sci. 2015; 62(1): 66–73, doi: 10.1002/jmrs.89, indexed in Pubmed: 26229669.
4. Shah C, Badiyan S, Berry S, et al. Cardiac dose sparing and avoidance techniques in breast cancer radiotherapy. Radiother Oncol. 2014; 112(1): 9–16, doi: 10.1016/j.radonc.2014.04.009, indexed in Pubmed: 24813095.
5. Gaál S, Kahán Z, Paczona V, et al. Deep-inspirational breath-hold (DIBH) technique in left-sided breast cancer: various aspects of clinical utility. Radiat Oncol. 2021; 16(1): 89, doi: 10.1186/s13014-021-01816-3, indexed in Pubmed: 33985547.
6. Sixel KE, Aznar MC, Ung YC. Deep inspiration breath hold to reduce irradiated heart volume in breast cancer patients. Int J Radiat Oncol Biol Phys. 2001; 49(1): 199–204, doi: 10.1016/s0360-3016(00)01455-3, indexed in Pubmed: 11163515.
7. Stranzl H, Zurl B. Postoperative irradiation of left-sided breast cancer patients and cardiac toxicity. Does deep inspiration breath-hold (DIBH) technique protect the heart? Strahlenther Onkol. 2008; 184(7): 354–358, doi: 10.1007/s00066-008-1852-0, indexed in Pubmed: 19016033.
8. Swanson T, Grills IS, Ye H, et al. Six-year experience routinely using moderate deep inspiration breath-hold for the reduction of cardiac dose in left-sided breast irradiation for patients with early-stage or locally advanced breast cancer. Am J Clin Oncol. 2013; 36(1): 24–30, doi: 10.1097/COC.0b013e31823fe481, indexed in Pubmed: 22270108.
9. Wang W, Purdie TG, Rahman M, et al. Rapid automated treatment planning process to select breast cancer patients for active breathing control to achieve cardiac dose reduction. Int J Radiat Oncol Biol Phys. 2012; 82(1): 386–393, doi: 10.1016/j.ijrobp.2010.09.026, indexed in Pubmed: 21093165.
10. Vikström J, Hjelstuen MHB, Mjaaland I, et al. Cardiac and pulmonary dose reduction for tangentially irradiated breast cancer, utilizing deep inspiration breath-hold with audio-visual guidance, without compromising target coverage. Acta Oncol. 2011; 50(1): 42–50, doi: 10.3109/0284186X.2010.512923, indexed in Pubmed: 20843181.
11. Nissen HD, Appelt AL. Improved heart, lung and target dose with deep inspiration breath hold in a large clinical series of breast cancer patients. Radiother Oncol. 2013; 106(1): 28–32, doi: 10.1016/j.radonc.2012.10.016, indexed in Pubmed: 23199652.
12. Borst GR, Sonke JJ, den Hollander S, et al. Clinical results of image-guided deep inspiration breath hold breast irradiation. Int J Radiat Oncol Biol Phys. 2010; 78(5): 1345–1351, doi: 10.1016/j.ijrobp.2009.10.006, indexed in Pubmed: 20207496.
13. Hayden AJ, Rains M, Tiver K. Deep inspiration breath hold technique reduces heart dose from radiotherapy for left-sided breast cancer. J Med Imaging Radiat Oncol. 2012; 56(4): 464–472, doi: 10.1111/j.1754-9485.2012.02405.x, indexed in Pubmed: 22883657.
14. Lee HaY, Chang JS, Lee IkJ, et al. The deep inspiration breath hold technique using Abches reduces cardiac dose in patients undergoing left-sided breast irradiation. Radiat Oncol J. 2013; 31(4): 239–246, doi: 10.3857/roj.2013.31.4.239, indexed in Pubmed: 24501713.
15. Dincoglan F, Beyzadeoglu M, Sager O, et al. Dosimetric evaluation of critical organs at risk in mastectomized left-sided breast cancer radiotherapy using breath-hold technique. Tumori. 2013; 99(1): 76–82, doi: 10.1177/030089161309900113, indexed in Pubmed: 23549004.
16. Mast ME, van Kempen-Harteveld L, Heijenbrok MW, et al. Left-sided breast cancer radiotherapy with and without breath-hold: does IMRT reduce the cardiac dose even further? Radiother Oncol. 2013; 108(2): 248–253, doi: 10.1016/j.radonc.2013.07.017, indexed in Pubmed: 24044804.
17. Reardon KA, Read PW, Morris MM, et al. A comparative analysis of 3D conformal deep inspiratory-breath hold and free-breathing intensity-modulated radiation therapy for left-sided breast cancer. Med Dosim. 2013; 38(2): 190–195, doi: 10.1016/j.meddos.2013.01.002, indexed in Pubmed: 23453454.
18. Korreman SS, Pedersen AN, Josipović M, et al. Cardiac and pulmonary complication probabilities for breast cancer patients after routine end-inspiration gated radiotherapy. Radiother Oncol. 2006; 80(2): 257–262, doi: 10.1016/j.radonc.2006.07.020, indexed in Pubmed: 16905210.
19. Duane F, Aznar MC, Bartlett F, et al. A cardiac contouring atlas for radiotherapy. Radiother Oncol. 2017; 122(3): 416–422, doi: 10.1016/j.radonc.2017.01.008, indexed in Pubmed: 28233564.
20. Taylor C, Correa C, Duane FK, et al. Early Breast Cancer Trialists' Collaborative Group. Estimating the Risks of Breast Cancer Radiotherapy: Evidence From Modern Radiation Doses to the Lungs and Heart and From Previous Randomized Trials. J Clin Oncol. 2017; 35(15): 1641–1649, doi: 10.1200/JCO.2016.72.0722, indexed in Pubmed: 28319436.
21. White JTA, Arthur D, et al. Breast cancer atlas for radiation therapy planning: consenus definitions. http://www.nrgoncology.org/Portals/0/Resources/Atlases/BreastCancerAtlas.pdf.
22. Gayed IW, Liu HH, Yusuf SW, et al. The prevalence of myocardial ischemia after concurrent chemoradiation therapy as detected by gated myocardial perfusion imaging in patients with esophageal cancer. J Nucl Med. 2006; 47(11): 1756–1762, indexed in Pubmed: 17079807.
23. Clarke M, Collins R, Darby S, et al. Early Breast Cancer Trialists' Collaborative Group (EBCTCG). Effects of radiotherapy and of differences in the extent of surgery for early breast cancer on local

recurrence and 15-year survival: an overview of the randomised trials. Lancet. 2005; 366(9503): 2087–2106, doi: 10.1016/S0140-6736(05)67887-7, indexed in Pubmed: 16360786.
24. Piroth MD, Baumann R, Budach W, et al. Heart toxicity from breast cancer radiotherapy: Current findings, assessment, and prevention. Strahlenther Onkol. 2019; 195(1): 1–12, doi: 10.1007/s00066-018-1378-z, indexed in Pubmed: 30310926.
25. Cuzick J, Stewart H, Rutqvist L, et al. Cause-specific mortality in long-term survivors of breast cancer who participated in trials of radiotherapy. J Clin Oncol. 1994; 12(3): 447–453, doi: 10.1200/JCO.1994.12.3.447, indexed in Pubmed: 8120544.
26. Wolf J, Stoller S, Lübke J, et al. Deep inspiration breath-hold radiation therapy in left-sided breast cancer patients: a single-institution retrospective dosimetric analysis of organs at risk doses. Strahlenther Onkol. 2023; 199(4): 379–388, doi: 10.1007/s00066-022-01998-z, indexed in Pubmed: 36074138.
27. Vijeh L, Ahmed Y, Lee L, et al. Impact on Lung Dose in Left Breast Radiation Therapy Patients With Deep Inspiration Breath Hold Versus Free Breathing Technique. Int J Radiat Oncol Biol Phys. 2016; 96(2): E52, doi: 10.1016/j.ijrobp.2016.06.723.
28. Sripathi LK, Ahlawat P, Simson DK, et al. Cardiac Dose Reduction with Deep-Inspiratory Breath Hold Technique of Radiotherapy for Left-Sided Breast Cancer. J Med Phys. 2017; 42(3): 123–127, doi: 10.4103/jmp.JMP_139_16, indexed in Pubmed: 28974856.

VIA MEDICA

ORIGINAL ARTICLE

Oncology in Clinical Practice
2025, Vol. 21, No. 1, 8–14
DOI: 10.5603/ocp.98396

ISSN 2450-1654
eISSN 2450-6478

# Survival in adult osteosarcoma patients after resection of isolated pulmonary metastases — a single-center experience

Maciej Głogowski[1,*], Sebastian Szmit[2], Oliwia Głogowska[1], Iwona Ługowska[3], Łukasz Talarek[1], Mariusz Żmijewski[1], Piotr Rutkowski[3]

[1]Department of Lung Cancer and Thoracic Tumors, Maria Sklodowska-Curie National Research Institute of Oncology, Warsaw, Poland
[2]Department of Cardio-Oncology, Centre of Postgraduate Medical Education, Warsaw, Poland
[3]Department of Soft Tissue/Bone Sarcoma and Melanoma, Maria Sklodowska-Curie National Research Institute of Oncology, Warsaw, Poland

## Abstract

**Introduction.** Data on factors affecting disease recurrence and survival after pulmonary metastasectomy in adult osteosarcoma patients are still limited and inconclusive.

**Material and methods.** The study included 30 consecutive patients from a single institution who underwent resection of isolated osteosarcoma, with follow-up of pulmonary metastases over the period of 15 years between 1997 and 2012. Various perioperative variables were analyzed retrospectively to confirm the prognostic role of pulmonary surgery for overall and progression-free survival after metastasectomy. The multidisciplinary approach was implemented in qualification for repeated thoracic intervention.

**Results.** The overall 5-year survival rate (OS) after metastasectomy was 28% (median 27.5 months) and the 5-year progression-free survival rate (PFS) was 9% (median 6.33 months). Only radical pulmonary resection significantly influenced both OS (HR = 5.41; 95% CI 1.87–15.60, p = 0.002) and PFS (HR = 5.17; 95% CI 1.70–15.68, p = 0.004) after metastasectomy. The efficacy of thoracic surgery was independent of the patient's age, sex, number of operable lung metastases, bilateral presence of lung metastases, or time to the appearance of lung metastases after surgery for osteosarcoma. Five-year OS and PFS after radical and nonradical pulmonary metastasectomy were 35% *vs.* 0% (p = 0.002) and 11% *vs.* 0% (p = 0.004), respectively. In the observed group, 60 thoracotomies were performed; 3 or more procedures were needed in 8 (27%) patients.

**Conclusions.** Similar to the population of children and adolescents, radical pulmonary metastasectomy may be a curative treatment strategy in selected adult patients with metastatic osteosarcoma. Repeated procedures are necessary in many cases.

**Keywords:** osteosarcoma, pulmonary metastasectomy, adult patients, outcome

## Introduction

The lung is the most frequent site of metastases in osteosarcoma. Osteosarcoma lung metastases are detected during initial diagnosis or as a recurrence after radical multimodal treatment. Approximately 20% of osteosarcoma patients have metastatic disease at the

*Correspondence: Maciej Głogowski, MD PhD, Department of Lung Cancer and Thoracic Tumors, Maria Sklodowska-Curie National Research Institute of Oncology, ul. Roentgena 5, 02–781 Warsaw, Poland (maciej.glogowski@pib-nio.pl)
Received: 3 December 2023; Accepted: 12 January 2024;
Early publication: 19 February 2024

time of initial diagnosis, and the majority of these are pulmonary metastases without other symptoms of cancer disease [1]. Additionally, 30–50% of patients after radical multimodal treatment may have disease recurrence with a high probability of isolated lung metastases [2]. Pulmonary metastases are the only location of osteosarcoma disease in about 50–80% of patients [1–4]. Long-term survival in these patients has improved with aggressive resection of pulmonary metastases with the use of combination chemotherapy [5]. Most previous studies concerned the pediatric and adolescent population due to the higher incidence of osteosarcoma in young patients, and their prognosis appears better [6]. Similarly, most articles on survival and prognostic factors after pulmonary metastasectomy refer to both osteosarcoma and soft tissue sarcoma together in adult patients although the biology, treatment, and prognosis of these two cancer types are different [6–8]. Important prognostic factors for survival after pulmonary metastasectomy include the disease-free interval, age, sex, number of lesions, time of occurrence of metastases (synchronous/metachronous), laterality of metastases, and completeness of resection [2, 4, 7–11].

The main objective of our study was to evaluate prognostic factors for survival in adult patients with osteosarcoma after pulmonary metastasectomy based on a single-center experience.

## Material and methods

From January 1997 to December 2012, 176 adult patients (over 18 years old) with high-grade osteosarcoma were diagnosed and treated at the Maria Sklodowska-Curie Institute, Oncology Centre (now Maria Sklodowska-Curie National Research Institute of Oncology) in Warsaw. Twenty-two (12.5%) patients had metastases at presentation, 154 (87.5%) had localized disease. Among patients with tumors localized after radical multidisciplinary treatment, 53 (34.4%) had metastatic disease, and 42 (79.2%) of them had metastases located only in the lung. Twenty-four (57%) of them underwent pulmonary metastasectomy, and 18 (43%) were considered unresectable due to the high probability of incomplete resection or fast progression during chemotherapy before planned metastasectomy. Among 22 patients with synchronous metastases, 6 had isolated resectable pulmonary metastases. Thus, we identified 30 consecutive adult patients with synchronous (6 patients) or metachronous (24 patients) pulmonary osteosarcoma metastases who underwent at least one pulmonary metastasectomy between 1997 and 2012. All patients had isolated pulmonary metastases without evidence of extrapulmonary disease at the time of pulmonary resection. Patients with synchronous pulmonary metastases underwent radical multimodal treatment of the primary tumor including surgery and standard perioperative chemotherapy before metastasectomy. Patients with metachronous metastases underwent multiagent chemotherapy (including mainly etoposide and ifosfamide as second-line systemic therapy in our institution) before metastasectomy. All patients qualified for metastasectomy had no progression of the disease after preoperative chemotherapy. Computed tomography (CT) scans were performed at least 4 weeks before surgery. The indications for pulmonary metastasectomy included primary tumor control, lack of other metastatic sites outside the lungs, and sufficient pulmonary reserve to avoid pulmonary failure after complete surgical resection of metastases. All lung resections were performed by thoracotomy, also in bilateral lesions. Mediastinal lymphadenectomy or sampling during lung metastasectomy was performed in all patients. Palpation of the lung tissue was carried out to detect metastases that were not identified earlier on CT scans. Follow-up after radical pulmonary resection included alternating chest radiographs and CT scans performed every 6 weeks in the first year, every 3 months in the second and third year, and every 6 months thereafter. Complete staging based on chest CT and bone scans was repeated if lung disease relapse was suspected. The next pulmonary metastasectomy was attempted in most patients with isolated pulmonary metastases after disease recurrence. The collection of follow-up data was completed in June 2020. The study was carried out according to the principles recommended by the bioethics commission at the Maria Skłodowska-Curie National Research Institute of Oncology in Warsaw. All patients signed informed consent.

The prognostic variables were extracted from medical records and included age at the time of the first metastasectomy, sex, number of lung metastases (as confirmed by pathologists), laterality of metastases, disease-free interval (DFI; calculated as the time from primary radical resection of osteosarcoma to initial diagnosis of pulmonary metastases) and how radical metastasectomy was. Complete resection was defined as the lack of tumor cells in the surgical margins of the resected lung examined macroscopically and histologically and surgical removal of all visible and palpable nodules. All bilateral procedures (including staged bilateral thoracotomies) that occurred within 6 weeks of each other were considered a single intervention in the analysis.

Overall survival (OS) was calculated as the time from the date of initial pulmonary metastasectomy to the date of death (complete) or the last follow-up (censored data). Progression-free survival (PFS) was calculated as the time from the date of initial pulmonary metastasectomy to the date of disease recurrence (complete) or the last follow-up (censored).

The Kaplan-Meier methods, log-rank test, and Cox's proportional hazards model were used to determine prognostic factors for both OS and PFS.

## Results

In the group of 30 adult patients after pulmonary metastasectomy for osteosarcoma, there were 20 (66.7%) men and 10 (33.3%) women. At the onset of lung involvement, the median age was 26 years (range 19-56). The disease-free interval (DFI) rate ranged from 0 months to 11 years, including 6 (20%) patients with a simultaneous diagnosis of the primary tumor and pulmonary metastasis. The lung was the first site of osteosarcoma recurrence after radical multimodal treatment of the primary site in 17 (57%) patients. In 7 (23%) patients locoregional recurrence was observed first and radically treated before detection of lung metastases. In 16 (53%) patients, lung metastases were found to be bilateral. Population characteristics are listed in Table 1.

After 30 initial thoracotomies, 6 (20%) patients underwent non-radical resection. In those patients, small lesions caused by disease dissemination that had not been visualized on the preoperative CT scans were detected during thoracotomy. A non-radical wedge resection was performed to confirm metastatic disease. All of the patients with non-radical operations died within 2 years due to progression despite intensive chemotherapy.

Twenty-four (80%) patients were qualified for radical resection based on macroscopic and microscopic examinations. However, in 19 patients one or more wedge resections were performed, and in 4 cases, lobectomy and pneumonectomy were performed in one subject. No metastases involving the hilar or mediastinal lymph nodes were found. The mean number of metastatic nodules resected was 4.9 (range: from 1 to 18 nodules).

The median follow-up time was 29 months (range: 5–209 months). Among 24 patients after radical resection, 3 (12.5%) patients were alive without recurrence after initial thoracotomy, 21 (87.5%) had disease progression: 17 (81%) patients had isolated pulmonary metastases, 11 (64.7%) underwent next pulmonary metastasectomy, and 8 (33%) were operated at least 3 times (range: 3–9) due to isolated pulmonary recurrence. The patient after 9 procedures was still alive without progression with overall survival of 90 months.

In the analyzed group of 30 patients, we performed 60 thoracotomies without postoperative death (Tab. 2).

The median OS rate after pulmonary metastasectomy in the entire group was 27.5 months, and the 5-year OS rate was 28%. Patients after radical resection had median OS of 33.5 months and a 5-year OS rate of 35%. Patients after nonradical resection had a significantly worse prognosis: median OS was 13.3 months, and the 5-year OS rate was 0%. (Tab. 3, Fig. 1).

In the univariate analysis, only radical pulmonary resection was a significantly important factor that influenced OS (Tab. 4). Multivariate analysis confirmed the independent importance of radical pulmonary resection for OS.

**Table 1.** Characteristics of 30 patients with osteosarcoma requiring thoracic surgery for lung metastases

| | |
|---|---|
| **Age [years]** | |
| Median | 26 |
| Quartiles | 24–36 |
| Min.–max. | 19–56 |
| **Sex** | |
| Female | 10 (33.3%) |
| Male | 20 (66.7%) |
| **Lung metastases** | |
| Synchronous | 6 (20.0%) |
| Metachronous | 24 (80.0%) |
| **Lung metastases** | |
| Unilateral | 14 (46.7%) |
| Bilateral | 16 (53.3%) |
| **Time to lung metastases occurrence after surgery due to osteosarcoma [months]** | |
| Median | 14.5 |
| Quartiles | 5.8–23.3 |
| Min.–max. | 0–133.5 |
| **Number of operable lung metastases** | |
| One | 10 (33.3%) |
| Two or three or four | 9 (30.0%) |
| Five and more | 11 (36.7%) |
| **Radical pulmonary metastasectomy** | |
| Yes | 24 (80.0%) |
| No | 6 (20.0%) |
| **Disease progression** | |
| Yes | 27 (90.0%) |
| No | 3 (10.0%) |
| **Death** | |
| Yes | 21 (70.0%) |
| No | 9 (30.0%) |

**Table 2.** Outcomes of 60 thoracotomies in 30 patients

| Status | Number of patients | Number of thoracotomies | | | | | |
|---|---|---|---|---|---|---|---|
| | | 1 | 2 | 3 | 4 | 5 | 9 |
| No evidence of disease | 7 | 3 | | 1 | | 2 | 1 |
| Alive with disease | 2 | 1 | | 1 | | | |
| Died due to disease | 21 | 15 | 3 | 2 | 1 | | |

**Table 3.** Survival estimates in relation to thoracic surgery

| | 2-year | | 5-year | | p-value |
|---|---|---|---|---|---|
| | Rate | SE | Rate | SE | |
| **Progression-free survival (PFS)** | | | | | |
| **All patients** | 0.13 | 0.06 | 0.09 | 0.06 | |
| **Radical pulmonary metastasectomy** | | | | | |
| No | 0 | 0 | 0 | 0 | p = 0.004 |
| *vs.* | | | | | |
| Yes | 0.17 | 0.08 | 0.11 | 0.07 | |
| **Overall survival (OS)** | | | | | |
| **All patients** | 0.53 | 0.09 | 0.28 | 0.09 | |
| **Radical pulmonary metastasectomy** | | | | | |
| No | 0.17 | 0.15 | 0 | 0 | p = 0.002 |
| *vs.* | | | | | |
| Yes | 0.63 | 0.1 | 0.35 | 0.1 | |

SE — survival estimate

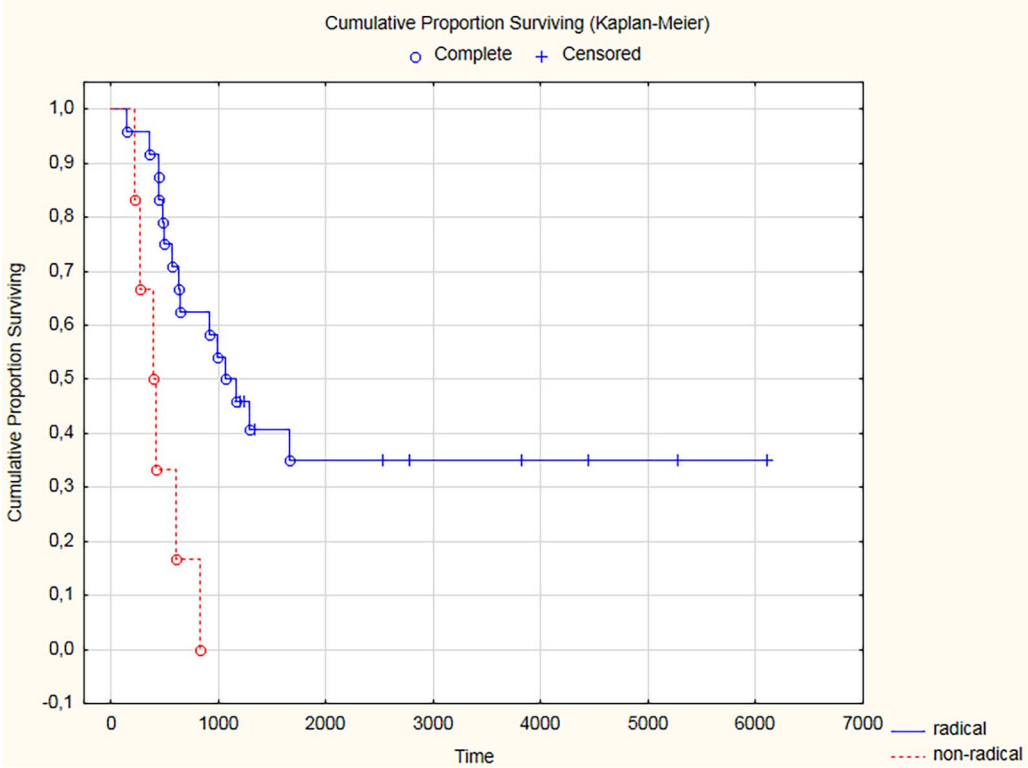


**Figure 1.** Survival estimates in relation to thoracic surgery

Median PFS in the entire group was 6.33 months, and the 5-year PFS rate was 9%. Patients after microscopically radical resection had a median PFS rate of 8.1 months and a 5-year PFS rate of 11%, which was a significantly better outcome compared to patients after non-radical resection: 3.3 months and 0%, respectively (Tab. 3).

Similarly, in the univariate and multivariate analysis, only radical pulmonary resection was significantly associated with longer PFS (Tab. 5).

## Discussion

Pulmonary metastasectomy has become the standard therapy for various metastatic malignancies in the lungs, including osteosarcomas. Therefore, we decided to report our institutional experience in pulmonary metastasectomy in the population of adult patients with osteosarcoma and to evaluate its role in extending OS and PFS. This was a retrospective study of adult patients who underwent pulmonary metastasectomy for synchronous and metachronous isolated

**Table 4.** Analysis of the clinically important factors that influenced overall survival (OS) in osteosarcoma patients after thoracic surgery for lung metastases

| Factor | Univariate analysis | | | Multivariate analysis | | |
|---|---|---|---|---|---|---|
| | HR | 95% CI | p-value | HR | 95% CI | p-value |
| **Age**<br>Older than median (≥ 27 y) *vs.* younger (≤ 26 y) | 0.57 | 0.23–1.38 | p = 0.21 | 0.43 | 0.16–1.13 | p = 0.08 |
| **Sex**<br>Female *vs.* male | 0.65 | 0.25–1.70 | p = 0.38 | 0.64 | 0.19–2.15 | p = 0.47 |
| **Time to lung metastasis occurrence after surgery for osteosarcoma [months]**<br>≤ 12 m *vs.* > 12 m | 1.72 | 0.72–4.12 | p = 0.22 | 1.44 | 0.48–4.31 | p = 0.52 |
| **Lung metastases**<br>Bilateral *vs*. unilateral | 1.39 | 0.59–3.29 | p = 0.45 | 0.59 | 0.16–2.24 | p = 0.44 |
| **Number of operable lung metastases**<br>More than one *vs.* one | 1.21 | 0.49–3.01 | p = 0.68 | 1.19 | 0.33–4.29 | p = 0.79 |
| **Radical pulmonary metastasectomy**<br>No *vs.* yes | 5.41 | 1.87–15.60 | p = 0.002 | 10.09 | 2.32–43.91 | p = 0.002 |

CI — confidence interval; HR — hazard ratio

**Table 5.** Analysis of the clinically important factors that influenced progression-free survival (PFS) in osteosarcoma patients after thoracic surgery for lung metastases

| Factor | Univariate analysis | | | Multivariate analysis | | |
|---|---|---|---|---|---|---|
| | HR | 95% CI | p-value | HR | 95% CI | p-value |
| **Age**<br>Older than median (≥ 27 y) *vs.* younger (≤ 26 y) | 0.47 | 0.21–1.06 | p = 0.07 | 0.60 | 0.23–1.52 | p = 0.28 |
| **Sex**<br>Female *vs.* male | 1.03 | 0.44–2.40 | p = 0.94 | 1.46 | 0.52–4.15 | p = 0.48 |
| **Time to lung metastasis occurrence after surgery for osteosarcoma [months]**<br>≤ 12 m *vs.* > 12 m | 1.50 | 0.69–3.26 | p = 0.31 | 1.59 | 0.64–3.95 | p = 0.32 |
| **Lung metastases**<br>Bilateral *vs*. unilateral | 1.31 | 0.61–2.82 | p = 0.49 | 0.51 | 0.18–1.46 | p = 0.21 |
| **Number of operable lung metastases**<br>More than one *vs.* one | 1.67 | 0.72–3.89 | p = 0.23 | 1.86 | 0.61–5.65 | p = 0.27 |
| **Radical pulmonary metastasectomy**<br>No *vs.* yes | 5.17 | 1.70–15.68 | p = 0.004 | 6.28 | 1.71–23.04 | p = 0.006 |

CI — confidence interval; HR — hazard ratio

pulmonary osteosarcoma metastases. To our knowledge, this is one of the largest series in the adult population after pulmonary metastasectomy for osteosarcoma reported by individual institutions.

The median age of our patients at the onset of lung involvement was 26 years (range 19–56). Aljubranet et al. [12] reported a series of 85 adult and adolescent patients after pulmonary metastases. The median age of their patients was 29 years (range 14–77), and 71 (83.5%) of them were < 18 years old. Only 47 (55.35%) of all patients underwent pulmonary metastasectomy. Furthermore, there were 35 (74.5%) complete pulmonary resections. Our rate for complete resections was similar (80%). The most frequent reasons for aborting complete surgery were small metastatic deposits in the lungs found during thoracotomy. This underlines the need for careful palpation of the lung during thoracotomy. Due to the high risk of micro-nodular dissemination in patients with metastatic pulmonary osteosarcoma, it seems that video-thoracoscopic surgery should be carefully considered only in patients with a single metastasis. The complete resection rate is variable in the literature, ranging between 65% and 91.5% [3, 13–16]. In our study, only radical resection was a significantly important predictor of long-term OS and PFS after pulmonary metastasectomy. The completeness of resection has been reported to be a better prognostic factor for overall survival in many studies including pediatric populations [1, 3, 7, 14, 16–18], but only two reports [3, 7] confirm this result for progression-free survival in metastatic osteosarcoma patients. Salah et al. [3] noted this association in 14 of 32 patients with metastatic lung osteosarcoma. Kempf-Bielack

et al. [7] reported on a larger group, but their study was not restricted only to lung metastases and the adult population.

The number of resected nodules and DFI have been often identified by many previous studies as important independent risk factors for long survival after lung metastasectomy in osteosarcoma patients [3, 7, 12, 13, 19]. Some studies have reported only the number of nodules as a statistically significant risk factor for OS, while DFI had no importance [14, 16, 18]. In contrast, Harting has reported the importance of DFI, and the number of pulmonary metastases was also insignificant [15]. Laterality of metastases has been identified as an independent risk factor only in a few studies [3, 18]. All of these reports included pediatric patients. Our study found that the above-described factors are nonsignificant for OS and PFS.

In our study, the 5-year survival rate was 28% in all groups, 35% in radically resected patients, and 0% in patients with unexpected nodule dissemination during thoracotomy. This result is similar to previous studies, including pediatric cases [1, 3, 7, 13–17, 19], and confirms the important and independent role of radical surgery in treating pulmonary metastases. A few reports described a survival rate of 5% in nonradical metastasectomy patients or between 10–16% in patients without metastatic surgery [12, 18, 20]. Furthermore, national or international registries have recorded 5-year survival for all patients with metastatic osteosarcoma at 19–24% [3, 19, 21], but it is worth emphasizing that aggressive radical surgery offers a higher probability of longer survival in carefully selected patients with pulmonary metastases. However, no randomized controlled trials have compared pulmonary metastasectomy with other treatment modalities [16, 21].

In our group of 30 patients after initial resection, 11 (37%) needed a repeated metastasectomy due to isolated recurrence of pulmonary osteosarcoma. In addition, 8 (27%) patients had 3 or more thoracotomies, and 4 patients were alive and disease-free at the last follow-up. It emphasizes the important role of repeated pulmonary metastasectomy in selected patients as a curative treatment. This phenomenon has been observed in many other studies, but complete surgery is still crucial as the treatment strategy for recurrent disease [3, 4, 14–16, 18–20, 22]. The next problem is maintaining a satisfactory quality of life with good cardiopulmonary exercise capacity after repeated thoracic surgery. A specialized multidisciplinary team is needed for patient care.

We are aware of several limitations to our study. The results should be interpreted with caution due to the retrospective design of the study and the relatively small number of patients. However, the limitations mentioned above result from the small incidence of osteosarcoma, especially in the adult population. Our well-defined patient cohort represented a relatively satisfactory study group. Additionally, chemotherapeutic regimens and surgical strategies have evolved substantially and rapidly over the last 20 years and treatment decisions are individualized according to tumor biology and unique patient characteristics in many tumor types, but not in osteosarcoma.

## Conclusions

Pulmonary metastasectomy may be a curative treatment strategy in selected adult patients with isolated pulmonary metastases of osteosarcoma, similar to the populations of children and adolescents. The possibility of radical resection seems to be the most important indication for pulmonary metastasectomy and repeat surgery. These procedures require careful collaboration of the multidisciplinary team and offer a satisfactory probability of longer survival with a good cardiopulmonary exercise capacity.

## Article Information and Declarations

### Data availability statement

All analyzed data is included in this article. Further inquiries may be directed to the corresponding author.

### Ethics statement

The study was conducted according to the criteria set by the declaration of Helsinki. Due to the retrospective nature of the study, local Bioethics Committee approval was not necessary.

### Author contributions

M.G.: study concepts and design, data acquisition, analysis and interpretation, quality control of data, literature review, manuscript preparation, manuscript editing, manuscript review; S.S.: statistical analysis, manuscript editing, manuscript review; O.G.: data acquisition, literature review, manuscript editing; Ł.Ł.: data acquisition, quality control data; Ł.T.: data acquisition; M.Ż.: data acquisition; P.R.: data acquisition, manuscript review.

All authors approved the final version of the manuscript.

### Funding

No external funding for the work was provided.

### Acknowledgements

The authors thank patients and their families for their participation in this study.

### Conflict of interest

The authors declare they have no conflict of interest.

### Supplementary material

None.

## References

1. Kager L, Zoubek A, Pötschger U, et al. Cooperative German-Austrian-Swiss Osteosarcoma Study Group.Primary metastatic osteosarcoma: presentation and outcome of patients treated on

neoadjuvant Cooperative Osteosarcoma Study Group protocols. J Clin Oncol. 2003; 21(10): 2011–2018, doi: 10.1200/JCO.2003.08.132, indexed in Pubmed: 12743156.
2. Gelderblom H, Jinks RC, Sydes M, et al. European Osteosarcoma Intergroup. Survival after recurrent osteosarcoma: data from 3 European Osteosarcoma Intergroup (EOI) randomized controlled trials. Eur J Cancer. 2011; 47(6): 895–902, doi: 10.1016/j.ejca.2010.11.036, indexed in Pubmed: 21216138.
3. Kempf-Bielack B, Bielack SS, Jürgens H, et al. Osteosarcoma relapse after combined modality therapy: an analysis of unselected patients in the Cooperative Osteosarcoma Study Group (COSS). J Clin Oncol. 2005; 23(3): 559–568, doi: 10.1200/JCO.2005.04.063, indexed in Pubmed: 15659502.
4. Blackmon SH, Shah N, Roth JA, et al. Resection of pulmonary and extrapulmonary sarcomatous metastases is associated with long-term survival. Ann Thorac Surg. 2009; 88(3): 877–84; discussion 884, doi: 10.1016/j.athoracsur.2009.04.144, indexed in Pubmed: 19699915.
5. ESMO/European Sarcoma Network Working Group. Bone sarcomas: ESMO Clinical Practice Guidelines for diagnosis, treatment and follow-up. Ann Oncol. 2014; 25 Suppl 3: iii113–iii123, doi: 10.1093/annonc/mdu256, indexed in Pubmed: 25210081.
6. Savage SA, Mirabello L. Using epidemiology and genomics to understand osteosarcoma etiology. Sarcoma. 2011; 2011: 548151, doi: 10.1155/2011/548151, indexed in Pubmed: 21437228.
7. Salah S, Fayoumi S, Alibraheem A, et al. The influence of pulmonary metastasectomy on survival in osteosarcoma and soft-tissue sarcomas: a retrospective analysis of survival outcomes, hospitalizations and requirements of home oxygen therapy. Interact Cardiovasc Thorac Surg. 2013; 17(2): 296–302, doi: 10.1093/icvts/ivt177, indexed in Pubmed: 23599187.
8. Lin AY, Kotova S, Yanagawa J, et al. Risk stratification of patients undergoing pulmonary metastasectomy for soft tissue and bone sarcomas. J Thorac Cardiovasc Surg. 2015; 149(1): 85–92, doi: 10.1016/j.jtcvs.2014.09.039, indexed in Pubmed: 25312228.
9. Kaifi JT, Gusani NJ, Deshaies I, et al. Indications and approach to surgical resection of lung metastases. J Surg Oncol. 2010; 102(2): 187–195, doi: 10.1002/jso.21596, indexed in Pubmed: 20648593.
10. Ceppa DP. Results of Pulmonary Resection: Sarcoma and Germ Cell Tumors. Thorac Surg Clin. 2016; 26(1): 49–54, doi: 10.1016/j.thorsurg.2015.09.007, indexed in Pubmed: 26611510.
11. Daw NC, Chou AJ, Jaffe N, et al. Recurrent osteosarcoma with a single pulmonary metastasis: a multi-institutional review. Br J Cancer. 2015; 112(2): 278–282, doi: 10.1038/bjc.2014.585, indexed in Pubmed: 25422914.
12. Aljubran AH, Griffin A, Pintilie M, et al. Osteosarcoma in adolescents and adults: survival analysis with and without lung metastases. Ann Oncol. 2009; 20(6): 1136–1141, doi: 10.1093/annonc/mdn731, indexed in Pubmed: 19153114.
13. Ferrari S, Briccoli A, Mercuri M, et al. Postrelapse survival in osteosarcoma of the extremities: prognostic factors for long-term survival. J Clin Oncol. 2003; 21(4): 710–715, doi: 10.1200/JCO.2003.03.141, indexed in Pubmed: 12586810.
14. Putnam JB, Roth JA, Wesley MN, et al. Survival following aggressive resection of pulmonary metastases from osteogenic sarcoma: analysis of prognostic factors. Ann Thorac Surg. 1983; 36(5): 516–523, doi: 10.1016/s0003-4975(10)60679-0, indexed in Pubmed: 6579887.
15. Harting MT, Blakely ML, Jaffe N, et al. Long-term survival after aggressive resection of pulmonary metastases among children and adolescents with osteosarcoma. J Pediatr Surg. 2006; 41(1): 194–199, doi: 10.1016/j.jpedsurg.2005.10.089, indexed in Pubmed: 16410132.
16. Chen F, Miyahara R, Bando T, et al. Prognostic factors of pulmonary metastasectomy for osteosarcomas of the extremities. Eur J Cardiothorac Surg. 2008; 34(6): 1235–1239, doi: 10.1016/j.ejcts.2008.07.032, indexed in Pubmed: 18757207.
17. Pfannschmidt J, Klode J, Muley T, et al. Pulmonary resection for metastatic osteosarcomas: a retrospective analysis of 21 patients. Thorac Cardiovasc Surg. 2006; 54(2): 120–123, doi: 10.1055/s-2005-872855, indexed in Pubmed: 16541354.
18. Meyer WH, Schell MJ, Kumar AP, et al. Thoracotomy for pulmonary metastatic osteosarcoma. An analysis of prognostic indicators of survival. Cancer. 1987; 59(2): 374–379, doi: 10.1002/1097-0142(19870115)59:2<374::aid-cncr2820590235>3.0.co;2-6, indexed in Pubmed: 3542182.
19. Briccoli A, Rocca M, Salone M, et al. High grade osteosarcoma of the extremities metastatic to the lung: long-term results in 323 patients treated combining surgery and chemotherapy, 1985-2005. Surg Oncol. 2010; 19(4): 193–199, doi: 10.1016/j.suronc.2009.05.002, indexed in Pubmed: 19515554.
20. Buddingh EP, Anninga JK, Versteegh MIM, et al. Prognostic factors in pulmonary metastasized high-grade osteosarcoma. Pediatr Blood Cancer. 2010; 54(2): 216–221, doi: 10.1002/pbc.22293, indexed in Pubmed: 19890902.
21. Treasure T, Fiorentino F, Scarci M, et al. Pulmonary metastasectomy for sarcoma: a systematic review of reported outcomes in the context of Thames Cancer Registry data. BMJ Open. 2012; 2(5), doi: 10.1136/bmjopen-2012-001736, indexed in Pubmed: 23048062.
22. Briccoli A, Rocca M, Salone M, et al. Resection of recurrent pulmonary metastases in patients with osteosarcoma. Cancer. 2005; 104(8): 1721–1725, doi: 10.1002/cncr.21369, indexed in Pubmed: 16155943.

VIA MEDICA

ORIGINAL ARTICLE

Oncology in Clinical Practice
2025, Vol. 21, No. 1, 15–27
DOI: 10.5603/ocp.98619

ISSN 2450-1654
eISSN 2450-6478

# The prevalence and impact of overweight and hypertension among patients with pancreatic cancer

Marta Fudalej[1,2,*], Izabella Cichowska[3], Anna Badowska-Kozakiewicz[1], Andrzej Deptała[1,2]

[1]Department of Oncology Propaedeutics, Medical University of Warsaw, Poland
[2]Department of Oncology, National Medical Institute of the Ministry of the Interior and Administration, Warsaw, Poland
[3]Department of Pathology, Military Institute of Medicine — National Research Institute, Warsaw, Poland

## Abstract

**Introduction.** Pancreatic cancer (PC) remains one of the most deadly malignancies with rising incidence. As therapeutical options seem unsatisfactory, great effort should be put into identifying and reducing risk factors as well as distinguishing possible factors influencing patient outcomes. The study aimed to describe the prevalence of overweight and hypertension among PC patients, analyse the possible association between overweight, hypertension and clinicopathological factors and distinguish variables influencing survival.

**Material and methods.** A retrospective analysis of medical records was performed. The study was designed in two branches: (1) the comparison of patients with hypertension (HTN group) and without; (2) the comparison of patients with BMI $\geq$ 25 and patients with BMI < 25. Statistical analysis with the usage of appropriate tests was conducted.

**Results.** No differences in survival between studied groups in the two branches were determined, even after subdividing into adjuvant and palliative types of treatment. Patients with HTN were more likely to be older, have diabetes and be diagnosed without distant metastases. BMI, ACEIs/ARBs use, diabetes, CRP/lymphocyte ratio (CLR) and AJCC IIb stage influenced survival. Patients with overweight/obesity were more likely to have an autoimmune disease, metastases in $\geq$ 4 lymph nodes (N2), tumour size between 2 and 4 cm (T2) and experience neutropenia as side effect of palliative chemotherapy. Higher BMI and CRP level influenced survival.

**Conclusions.** The exact effect of ACEIs/ARBs on cancerogenesis should be further studied. CLR appears to be a feasible marker for prognosis in PC.

**Keywords:** oncology, pancreatic cancer, hypertension, obesity

## Introduction

Pancreatic cancer (PC) remains one of the most deadly malignancies with a rising incidence. According to the 2020 Global Cancer Observatory (GLOBOCAN) report, PC accounts for almost as many deaths as cases and is currently the seventh leading cause of cancer death [1]. The incidence is projected to increase, reflecting the increasing prevalence of PC key risk factors [2]. Non-hereditary risk factors for PC could be divided into modifiable and non-modifiable. Modifiable encompass tobacco smoking, excessive alcohol consumption, pancreatitis, obesity, type 2 diabetes mellitus (DM), and metabolic syndrome, while non-modifiable factors include male sex, older age, and ethnicity [3]. PC survival rates remain unsatisfactory, after having slightly improved over the past 30 years from < 5% to 9% for overall survival (OS). Low survival rates are primarily associated with advanced, surgically unresectable stages of disease at the time

*Correspondence: Marta Fudalej, MD, Department of Oncology Propaedeutics, Medical University of Warsaw, ul. Erazma Ciołka 27, 01–445 Warsaw, Poland (marta.fudalej@wum.edu.pl)
Received: 20 December 2023; Accepted: 23 January 2024; Early publication: 5 March 2024

of diagnosis [4]. Other factors influencing survival include early distant metastases, resistance to conventional treatment schemes, and a highly desmoplastic tumor microenvironment. Pancreatic cancer treatment options remain limited, as no immunotherapeutic or anti-angiogenic regimens have been approved [5]. If possible, the current approach encompasses multidisciplinary treatment with surgery, chemotherapy, and chemoradiotherapy [6]. The two approved, most commonly used chemotherapy regimens are mFOLFIRINOX and gemcitabine with nab-paclitaxel. Despite aggressive chemotherapy, most patients eventually require palliative care and symptom management [7].

As therapeutical options seem unsatisfactory, great effort should be put into identifying and reducing risk factors and distinguishing possible factors influencing patient outcomes. The growing incidence points out metabolic syndrome and its components (insulin resistance, central obesity, hypertension, and features of atherogenic dyslipidemia) as some of the most significant risk factors [8, 9]. Due to population aging, it is estimated that the number of elderly PC patients will continue to rise [10]. The aging population is also associated with a higher prevalence of metabolic syndrome [11]. It seems crucial to focus on characterizing patients with PC concomitant with particular components of metabolic syndrome. More specific characterization might provide better patient care and impact further outcomes.

Our study aimed to describe the prevalence of overweight and hypertension among PC patients, analyze possible associations between overweight, hypertension, and clinicopathological factors, and distinguish variables influencing survival.

## Material and methods

### Patients, data collection, and study design

We retrospectively analyzed patients diagnosed with PC between 2012 and 2021 at the Central Clinical Hospital of the Ministry of Interior and Administration in Warsaw, Poland. Clinical data from patients were extracted from the hospital patient records. A total number of 175 patients was included in the study for analysis after excluding 52 patients with neuroendocrine tumors and 58 patients who received only one course of chemotherapy to reduce data variability and include information about adverse effects of chemotherapy. The study was designed in two branches:

1) comparison between patients with hypertension (HTN group) and patients without hypertension (non-HTN group);
2) comparison of patients with BMI $\geq$ 25 and patients with BMI < 25 (Fig. 1).

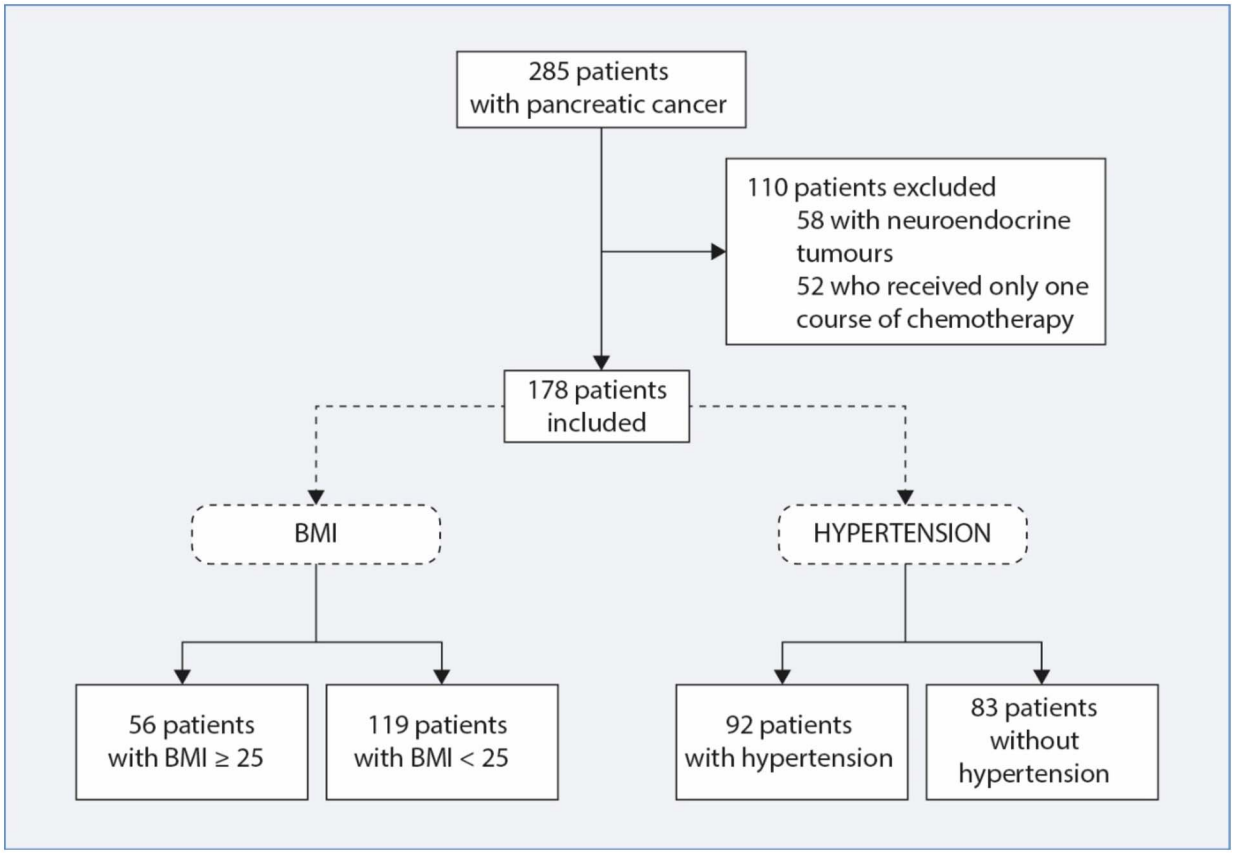


**Figure 1.** Summary of study design with exclusion criteria; BMI — body mass index

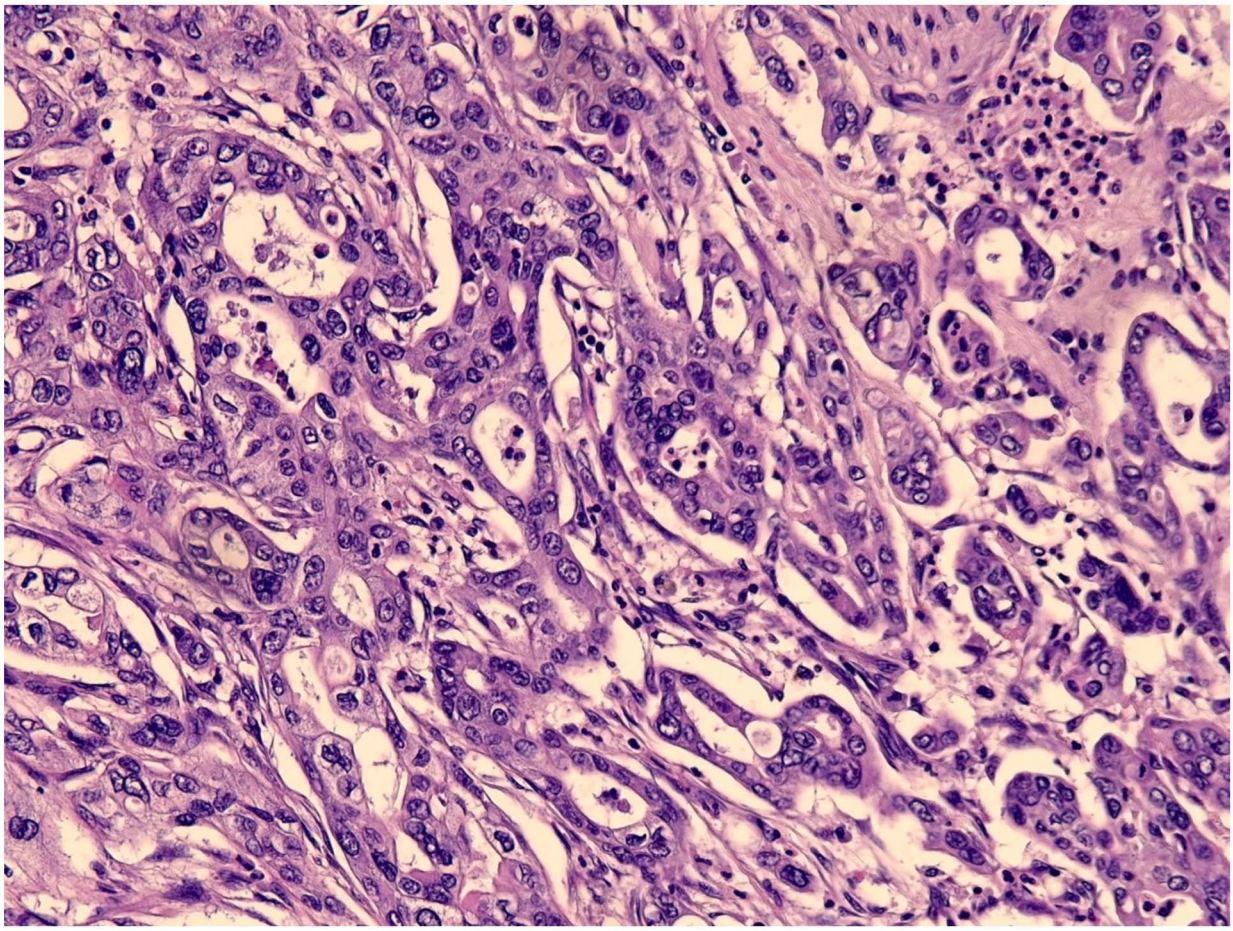

**Figure 2.** Histopathological image of pancreatic ductal adenocarcinoma (H&E, original magnification, 200×)

Analyzed data encompassed sex, age, weight, height, cigarette smoking, family history of cancers, history of other primary tumors, other diseases with described treatment methods, World Health Organization (WHO) performance status, pathological variables (tumor site, tumor size, histological grading, nodal involvement, tumor stage, resection margin) (Fig. 2), treatment data (type of the operation, vascular reconstruction, postoperative complications, adjuvant and palliative chemotherapy, ad side effects), laboratory findings before the first course of chemotherapy, survival, and progression time.

Body mass index (BMI) was calculated by dividing weight in kilograms (kg) by height in square meters (m). Data about weight and height were collected before the first course of chemotherapy.

Hypertension was defined based on one or more of the following criteria:

1) listed hypertension in patient history;
2) taking anti-hypertensive medication or
3) systolic blood pressure (SBP) in the clinic ≥ 140 mm Hg and/or diastolic blood pressure (DBP) ≥ 90 mm Hg following repeated examination.

In the analyses considering smoking, we took into account only active smoking. Laboratory findings were analyzed before chemotherapy. The C-reactive protein (CRP)/lymphocyte ratio (CLR) biomarker was additionally established. For statistical analysis, the cutoff value of 1.8 was confirmed based on the study by Fan et al. [12].

Diabetes mellitus was defined based on one or more of the following criteria:

1) diabetes listed in medical history;
2) two consecutive fasting glucose levels ≥ 140 mg/dL (7.8 mmol/L);
3) random plasma glucose ≥ 200 mg/dL (11.1 mmol/L) in patients with classic symptoms of hyperglycemia or hyperglycaemic crisis or
4) 2-hour plasma glucose ≥ 200 mg/dL (11.1 mmol/L) during an oral glucose tolerance test.

The study did not include abnormal cholesterol and triglyceride levels, as they were not routinely analyzed before the first course of chemotherapy.

Tumor staging was performed according to the American Joint Cancer Committee (AJCC) Staging Manual, 8th edition. Recurrence was detected with abdominal and chest computed tomography (CT) during the follow-up period. The study's primary endpoint was defined as OS. OS was calculated from the date of the histologically verified diagnosis (biopsies or material from surgeries) to the date of the last follow-up or death. Deaths were identified by reviewing the medical records.

### Statistical analysis

IBM SPSS 26 Statistics was used for statistical analysis. All analyzed variables were presented as means and standard deviations or frequencies with percentages. Estimation of mean differences between two independent groups was performed using the Mann-Whitney U test. Relationships between the two nominal variables were estimated using Pearson chi-squared or Fisher's exact test. Median OS was calculated using the Kaplan-Meier method, and differences were measured using the log-rank test, defined as the time from diagnosis until death (living patients were censored at the time of their last follow-up). Kaplan-Meier curves presented a summary of the data on survival probability. Univariate and multivariate analyses were conducted to examine the effect of single or multiple potential prognostic parameters on median OS. Cox regression models were presented as hazard ratios (HR) and were associated with a 95% confidence interval (CI). An alpha level of 0.05 was selected as statistically significant.

### Ethical approval

The study was approved by the Bioethics Committee of the Medical University of Warsaw (AKBE/144/2022). The work was carried out following the Code of Ethics of the World Medical Association (Declaration of Helsinki) on medical research involving human subjects and the ethical principle defined in the Farmington Consensus 1997.

## Results

### Group with hypertension

Of 175 PC patients, 92 (52.6%) were also diagnosed with HTN. From medical data, 53 schemes of hypertensive treatment were retrieved. Most of the patients were treated with two anti-hypertensive drugs (37.5%), predominantly with the combination of angiotensin-converting enzyme inhibitors/ /angiotensin II receptor blockers (ACEIs/ARBs) and $\beta$-blockers.

The majority of HTN patients were men (56.5%) with WHO performance status 1 (72.5%). The mean age was 66.3, with a range from 44 to 87. At the beginning of chemotherapy, the median BMI was 23.7 kg/m$^2$, while 39.8% of patients were overweight or obese. Regarding medical history, 50.0% had DM, 12.0% autoimmune disease, 9.8% other primary tumors, and 21.0% family history of cancers. History of active smoking concerned 33.8% of patients.

Most patients in the studied group were diagnosed with PC in the head of the pancreas (77.2%) with 52.2% having grade 2 while the most prevalent AJCC cancer stage was IIB (36.1%). Neuroinvasion was confirmed in 80.0% of the analyzed samples, while angioinvasion in 74.5%. Regarding treatment, 72.8% of patients underwent surgery (74.6% — the Whipple procedure), predominantly without further complications. Eleven of the operated patients (16.4%) required vascular reconstruction. Sixty-one patients (91.1%) received adjuvant chemotherapy, primarily based on gemcitabine (73.8%), with neutropenia as the most common side effect (65.6%). Eight-seven percent of patients eventually received palliative treatment with gemcitabine and nab-paclitaxel as the most common scheme (40.0%). Adverse effects were developed by 63.75% of palliatively treated patients, among which neutropenia was the most common.

Statistical analysis comparing the HTN group with the non-HTN group is presented in Table 1. Hypertension patients were more likely to be older ($p < 0.001$), have DM ($p = 0.033$), and have no distant metastases at the time of diagnosis ($p = 0.005$).

In Kaplan–Meier analysis, no significant differences concerning OS, disease-free survival (DFS), and progression-free survival (PFS) were confirmed (Tab. 1. Fig. 3–5).

The analyzed group was further subdivided into a group receiving adjuvant chemotherapy and a group receiving palliative chemotherapy (patients who presented with advanced disease at the time of diagnosis). In general, patients treated with adjuvant chemotherapy turned out to have significantly higher median OS than patients with advanced disease (20 months *vs.* 14, $p < 0.00012$). Nevertheless, no difference in survival between non-HTN and HTN groups was detected.

In the univariate analysis for survival in the HTN group, higher BMI ($p = 0.002$), using ACEIs/ /ARBs ($p = 0.003$), DM diagnosis ($p = 0.003$), and CLR $\leq 1.8$ ($p = 0.013$) were associated with longer survival. On the other hand, AJCC stage IIB ($p = 0.037$) was associated with shorter survival (Tab. 2).

Statistically significant prognostic factors were further analyzed in multivariate Cox regression using the backward method based on Wald statistics. ACEIs/ARBs use was the last excluded out of five studied prognostic factors, which means it was the strongest predictor of survival in the HTN group.

**Table 1.** Baseline characteristics of participants according to hypertension occurrence with statistical analysis

| Variable | Non-HTN group<br>Mean ± SD/n (%)/MD (95% CI) | HTN group<br>Mean ± SD/n (%)/MD (95% CI) | p-value |
|---|---|---|---|
| **Demography** | | | |
| Gender (male) | 35 (42.2%) | 52 (56.5%) | 0.070 |
| Age [years] | 60.95 ± 10.37 | 66.34 ± 8.33 | **< 0.001** |
| **Medical history** | | | |
| WHO status (0/1/2/0–1/1–2/2–3) | 3.7%/75.3%/16.0%/0.0%/3.7%/1.2% | 7.7%/72.5%/14.3%/2.2%/3.3%/0.0% | 0.517 |
| BMI (≥ 25) | 23 (32.4%) | 33 (39.8%) | 0.402 |
| History of smoking | 25 (39.1%) | 27 (33.8%) | 0.601 |
| Autoimmune disease | 9 (10.8%) | 11 (12.0%) | 1.000 |
| Diabetes mellitus | 28 (33.7%) | 46 (50.0%) | **0.033** |
| History of other CA | 7 (8.4%) | 9 (9.8%) | 0.799 |
| Family history of CA | 22 (34.3%) | 17 (21.0%) | 0.090 |
| Number of relatives with CA | 1.41 ± 0.67 | 1.35 ± 0.49 | 0.986 |
| **Histopathology** | | | |
| Localization of PC | | | 0.220 |
| Head | 75.9% | 77.2% | |
| Body | 7.2% | 7.6% | |
| Tail | 8.4% | 5.4% | |
| Head and body | 3.6% | 3.3% | |
| Body and tail | 1.2% | 6.5% | |
| Undetermined | 3.6% | 0.0% | |
| Grading (G1/G2/G3/Gx) | 12.0%/50.6%/13.3%/24.1% | 10.9%/52.2%/16.3%/20.7% | 0.901 |
| T (T1/T2/T3/T4/Tx) | 2.4%/14.5%/50.6%/4.8%/27.7% | 1.1%/19.6%/46.7%/3.3%/29.3% | 0.818 |
| N (N0/N1/N2/Nx) | 13.3%/39.8%/18.1%/28.9% | 20.7%/38.0%/13.0%/28.3% | 0.542 |
| M (M0/M1) | 50.6%/49.4% | 71.7%/28.3% | **0.005** |
| AJCC cancer stage (IA/IB/IIA/IIB/III/IV) | 1.3%/1.3%/5.0%/28.7%/13.8%/50.0% | 1.2%/9.6%/8.4%/36.1%/13.3%/31.3% | 0.072 |
| R (R0/R1/R2/None) | 32.5%/32.5%/2.4%/32.5% | 44.6%/28.3%/0.0%/27.2% | 0.210 |
| Neuroinvasion | 38 (86.4%) | 40 (80.0%) | 0.583 |
| Angioinvasion | 37 (82.2%) | 38 (74.5%) | 0.460 |
| **Treatment** | | | |
| Adverse effects — adjuvant chemotherapy | 28 (71.8%) | 51 (83.6%) | 0.209 |
| Neuropathy | 2 (5.1%) | 4 (6.6%) | 1.000 |
| Neutropenia | 22 (56.4%) | 40 (65.6%) | 0.402 |
| Hepatological | 3 (7.7%) | 3 (4.9%) | 0.676 |
| Adverse effects — palliative chemotherapy | 57 (80.3%) | 51 (77.3%) | 0.682 |
| Neutropenia | 33 (46.5%) | 33 (50.0%) | 0.734 |
| Hepatological | 7 (9.9%) | 4 (6.1%) | 0.535 |
| Neuropathy | 12 (16.9%) | 9 (13.6%) | 0.642 |
| Operative complications | 3 (5.3%) | 5 (7.4%) | 0.726 |
| **Laboratory findings** | | | |
| CEA ≥ 5 ng/mL | 20 (37.7%) | 21 (31.8%) | 0.562 |
| CA19-9 ≥ 37 IU/mL | 44 (62.0%) | 45 (53.6%) | 0.330 |
| CLR > 1.8 | 26 (57.8%) | 32 (57.1%) | 1.000 |
| LYM 1 × $10^3$/ µL | 2.13 ± 2.28 | 2.88 ± 6.00 | 0.289 |
| HGB [g/dL] | 12.34 ± 1.45 | 12.54 ± 1.58 | 0.407 |
| Plt 1 × $10^3$/ µL | 297.71 ± 158.85 | 290.12 ± 114.80 | 0.717 |
| CRP [mg/L] | 30.38 ± 61.82 | 14.57 ± 22.98 | 0.110 |
| **Survival** | | | |
| OS | 19.00 (15.89–22.11) | 20.00 (15.42–24.58) | 0.255 |
| DFS | 13.00 (6.22–19.78) | 12.00 (9.42–14.58) | 0.809 |
| PFS | 5.00 (4.13–5.87) | 7.00 (5.15–8.86) | 0.951 |

Bolded p-value — value statistically significant; AJCC — The American Joint Committee on Cancer; BMI — body mass index; CA — cancer; CA19-9 — carbohydrate antigen 19-9; CEA — carcinoembryonic antigen; CI — confidence interval; CLR — C-reactive protein/lymphocytes ratio; CRP — C-reactive protein; DFS — disease-free survival; HGB — hemoglobin; HTN — hypertension; LYM — lymphocytes; M — distant metastases; MD — median; N — nodal involvement; n — number; OS — overall survival; PC — pancreatic cancer; PFS — progression-free survival; PLT — platelets; R — resection margin; SD — standard deviation; T — tumor size; WHO status — World Health Organization performance status

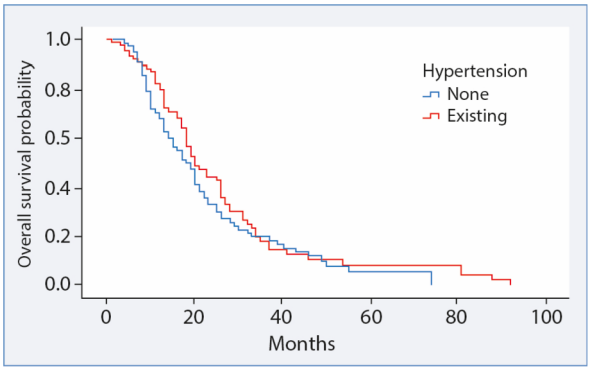


**Figure 3.** Overall survival of pancreatic cancer patients in the hypertension (HTN) and non-HTN groups

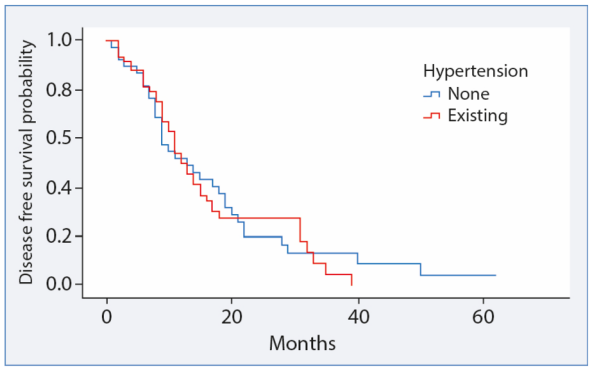


**Figure 4.** Disease-free survival of pancreatic cancer patients in the hypertension (HTN) and non-HTN groups

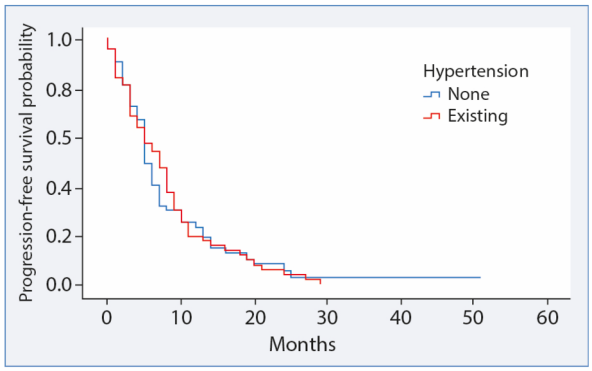


**Figure 5.** Progression-free survival of pancreatic cancer patients in the hypertension (HTN) and non-HTN groups

## Group with BMI ≥ 25

Of 175 PC patients, 56 (32.0%) were overweight or obese. Most were men (51.8%) with WHO performance status 1 (78.6%). The mean age was 62.7, with a range from 40 to 82. At the beginning of chemotherapy, the median BMI was 27.8 kg/m$^2$, with a mean of 28.5 kg/m$^2$ [standard deviation (SD) = 3.0, range 25.0–36.2].

**Table 2.** Univariate analysis of survival in the hypertension (HTN) group

| Variable | HR (95% CI) | p-value |
|---|---|---|
| **Age** | 1.014 (0.984–1.045) | 0.358 |
| **WHO performance status** | | |
| 0 | Ref | – |
| 1 | 0.192 (0.035–1.057) | 0.058 |
| 2 | 0.399 (0.093–1.707) | 0.215 |
| 0/1 | 0.264 (0.054–1.294) | 0.100 |
| 1/2 | 0.516 (0.046–5.841) | 0.593 |
| **BMI ≥ 25** | | |
| No | Ref | – |
| Yes | 0.384 (0.211–0.670) | **0.002** |
| **History of smoking** | | |
| No | Ref | – |
| Yes | 1.294 (0.742–2.258) | 0.364 |
| **Diabetes mellitus** | | |
| No | Ref | – |
| Yes | 0.399 (0.219–0.727) | **0.003** |
| **Family history of CA** | | |
| No | Ref | – |
| Yes | 0.674 (0.355–1.278) | 0.227 |
| **History of other CA** | | |
| No | Ref | – |
| Yes | 0.565 (0.265–1.205) | 0.139 |
| **Number of anti-hypertensive drugs** | | |
| 1 | Ref | – |
| 2 | 0.582 (0.075–4.541) | 0.606 |
| 3 | 0.521 (0.066–4.118) | 0.536 |
| 4 | 0.579 (0.072–4.628) | 0.606 |
| 5 | 0.150 (0.013–1.767) | 0.132 |
| **ACEIs/ARBs usage** | | |
| No | Ref | – |
| Yes | 0.170 (0.054–0.538) | **0.003** |
| **B-blockers usage** | | |
| No | Ref | – |
| Yes | 0.848 (0.414–1.738) | 0.653 |
| **CCBs usage** | | |
| No | Ref | – |
| Yes | 1.137 (0.573–2.257) | 0.713 |
| **Diuretics usage** | | |
| No | Ref | – |
| Yes | 0.744 (0.379–1.46) | 0.390 |
| **α-blockers usage** | | |
| No | Ref | – |
| Yes | 1.806 (0.636–5.131) | 0.267 |
| **AJCC cancer stage** | | |
| IB | Ref | – |
| IIA | 0.656 (0.247–1.741) | 0.398 |
| IIB | 2.035 (1.045–3.961) | **0.037** |
| III | 0.562 (0.312–1.0132) | 0.055 |
| IV | 0.792 (0.337–1.865) | 0.594 |

→

**Table 2 cont.** Univariate analysis of survival in the hypertension (HTN) group

| Variable | HR (95% CI) | p-value |
|---|---|---|
| **Adverse effects — adjuvant chth** | | |
| No | Ref | – |
| Yes | 1.003 (0.552–1.823) | 0.993 |
| **Neutropenia** | | |
| No | Ref | – |
| Yes | 0.763 (0.438–1.328) | 0.339 |
| **Adverse effects — palliative chth** | | |
| No | Ref | – |
| Yes | 0.968 (0.541–1.732) | 0.913 |
| **Neutropenia** | | |
| No | Ref | – |
| Yes | 1.625 (0.966–2.734) | 0.067 |
| **CLR > 1.8** | | |
| No | Ref | – |
| Yes | 1.886 (1.143–3.111) | **0.013** |
| **LYM 1 × $10^3$/ µL** | | |
| ≤ 1 | Ref | – |
| > 1 | 0.839 (0.356–1.977) | 0.688 |
| **CRP [mg/L]** | | |
| ≤ 5 | Ref | – |
| > 5 | 1.361 (0.807–2.297) | 0.247 |

Bolded p-value — value statistically significant; ACEIs — angiotensin-converting enzyme inhibitors; AJCC — The American Joint Committee on Cancer; ARBs — angiotensin II receptor blockers; BMI — body mass index; CA — cancer; CCBs — calcium channel blockers; chth — chemotherapy; CI — confidence interval; CLR — C-reactive protein/lymphocytes ratio; CRP — C-reactive protein; HR — hazard ratio; LYM — lymphocytes; Ref — reference

Regarding medical history, 58.9% of patients had HTN, 50.0% DM, 21.4% autoimmune disease, 7.14% other primary tumors, and 18.5% family history of cancers. History of active smoking concerned 30.2%.

Most patients in the studied group were diagnosed with PC in the head of the pancreas (78.6%) with 51.8% having grade 2 while the most prevalent AJCC cancer stage was IIB (21.6%). Neuroinvasion was confirmed in 93.5% of the analyzed samples while angioinvasion in 87.9%. Regarding treatment, 66.1% of patients underwent surgery (83.8% — the Whipple procedure), predominantly without further complications. Four of the operated patients (10.8%) required vascular reconstruction. Thirty-two (86.5%) received adjuvant chemotherapy, primarily based on gemcitabine (68.8%). Twenty-five suffered from adverse effects, predominantly neutropenia (76.0%). In total, 78.6% of patients eventually received palliative treatment, primarily based on gemcitabine with nab-paclitaxel (65.9%). Adverse effects were developed by 86.4% of palliatively treated patients, among which neutropenia was the most common.

Statistical analysis comparing groups with BMI < 25 and BMI ≥ 25 is presented in Table 3. Patients with overweight or obesity were more likely to have an autoimmune disease (p = 0.020), metastases in 4 or more lymph nodes (N2) (p = 0.041), tumor size between 2 and 4 cm (T2) (p = 0.022); they were more likely to experience neutropenia as a side effect of palliative chemotherapy (p = 0.014).

In Kaplan-Meier analysis, no significant differences concerning OS, DFS, and PFS were confirmed, even after subdividing into adjuvant and palliative types of treatment (Tab. 3, Fig. 6–8).

In the univariate analysis for survival in the studied group, higher BMI (p = 0.021) was associated with longer survival, whilst a CRP level higher than 5 mg/L (p = 0.025) with shorter survival (Tab. 4). In the further multivariate analysis, BMI was confirmed as the strongest predictor of survival.

## Discussion

Worldwide, HTN is the leading modifiable risk factor for premature deaths. The prevalence and absolute burden of HTN have increased over the past few years [13]. Approximately 60% of the population is diagnosed with HTN by the age of 60 years, and about 65% of men and 75% of women develop high blood pressure by 70. As the incidence of PC is also rising with age — 80% of the cases are diagnosed in people between 60 and 80 years of age, HTN is prevalent in this group [14]. In our study, over half of the analyzed group was diagnosed with HTN (52.6%), and the group with HTN was significantly older than the group without HTN (p < 0.001). In our previous analysis, DM was confirmed to be prevalent in PC patients [15]. Our results were in agreement with earlier studies, in which the prevalence of DM in PC patients was estimated to reach 40–65% [16]. In the current analysis, HTN patients were more likely to be diagnosed with DM (p = 0.033). Moreover, DM diagnosis was confirmed to be a prognostic factor for longer survival (p = 0.003). Reports regarding the impact of co-incidence of DM and PC on survival are ambiguous. Studies suggesting improved survival in DM patients discuss the positive effect of metformin on survival through various anti-cancer mechanisms [17, 18].

Drug therapy for HTN is recommended to come from one of four drug classes — calcium channel blockers (CCBs), thiazide diuretics, and ACEIs/ARBs. Two-drug treatment should be initiated in patients with blood pressure over 20/10 mmHg above the target [19]. In the studied group, most patients were treated with a two-drug combination, most with a combination of ACEIs/ARBS and $\beta$-blockers. In the univariate analysis, using ACEIs/ARBs was associated with longer survival (p = 0.003). In the

**Table 3.** Baseline characteristics of participants according to body mass index (BMI) with statistical analysis

| Variable | BMI < 25<br>Mean ± SD/n (%)/MD (95% CI) | BMI ≥ 25<br>Mean ± SD/n (%)/ MD (95% CI) | p-value |
|---|---|---|---|
| **Demography** | | | |
| Sex (male) | 47 (48.0%) | 29 (51.8%) | 0.738 |
| Age [years] | 64.88 ± 9.82 | 62.68 ± 8.48 | 0.069 |
| **Medical history** | | | |
| WHO status (0/1/2/01/1–2) | 4.2%/75.8%/15.8%/0.0%/4.2% | 5.4%/78.6%/14.3%/1.8%/0.0% | 0.374 |
| History of smoking | 35 (40.2%) | 16 (30.2%) | 0.279 |
| Hypertension | 50 (51.0%) | 33 (58.9%) | 0.402 |
| Autoimmune disease | 7 (7.1%) | 12 (21.4%) | **0.020** |
| Diabetes mellitus | 35 (35.7%) | 28 (50.0%) | 0.091 |
| History of other CA | 11 (11.2%) | 4 (7.1%) | 0.574 |
| Family history of CA | 28 (32.2%) | 10 (18.5%) | 0.083 |
| Number of relatives with CA | 1.46 ± 0.64 | 1.10 ± 0.31 | 0.087 |
| **Histopathology** | | | |
| Localisation of PC | | | 0.896 |
| Head | 79.6% | 78.6% | |
| Body | 7.1% | 8.9% | |
| Tail | 5.1% | 5.4% | |
| Head and body | 5.1% | 1.8% | |
| Body and tail | 2.0% | 3.6% | |
| Undetermined | 1.0% | 1.8% | |
| Grading (G1/G2/G3/Gx) | 13.3%/49.0%/14.3%/23.5% | 12.5%/51.8%/14.3%/21.4% | 0.987 |
| T (T1/T2/T3/T4/Tx) | 2.0%/13.3%/57.1%/5.1%/22.4% | 0.0%/28.6%/33.9%/3.6%/33.9% | **0.022** |
| N (N0/N1/N2/Nx) | 18.4%/45.9%/13.3%/22.4% | 14.3%/26.8%/25.0%/33.9% | **0.041** |
| M (M0/M1) | 64.3%/35.7% | 58.9%/41.1% | 0.604 |
| AJCC cancer stage (IA/IB/IIA/IIB/III/IV) | 1.1%/4.3%/7.7%/37.6%/12.9%/36.6% | 0.0%/7.8%/5.9%/21.6%/19.6%/45.1% | 0.341 |
| R (R0/R1/R2/None) | 45.9%/29.6%/0.0%/24.5% | 30.4%/35.7%/0.0%/33.9% | 0.157 |
| Neuroinvasion | 44 (78.6%) | 29 (93.5%) | 0.125 |
| Angioinvasion | 44 (75.9%) | 29 (87.9%) | 0.273 |
| **Treatment** | | | |
| Adverse effects — adjuvant chemotherapy | 49 (84.5%) | 25 (78.1%) | 0.566 |
| Neuropathy | 3 (5.2%) | 2 (6.3%) | 1.000 |
| Neutropenia | 40 (69.0%) | 19 (59.4%) | 0.366 |
| Hepatological | 5 (8.6%) | 1 (3.1%) | 0.416 |
| Adverse effects — palliative chemotherapy | 56 (73.7%) | 38 (86.4%) | 0.115 |
| Neutropenia | 30 (39.5%) | 28 (63.6%) | **0.014** |
| Hepatological | 7 (9.2%) | 4 (9.1%) | 1.000 |
| Neuropathy | 14 (18.4%) | 6 (13.6%) | 0.615 |
| Operative complications | 5 (6.6%) | 3 (8.1%) | 0.715 |
| **Laboratory findings** | | | |
| CEA ≥ 5 ng/mL | 22 (34.9%) | 13 (32.5%) | 0.834 |
| CA19-9 ≥ 37 IU/mL | 50 (55.6%) | 30 (60.0%) | 0.722 |
| CLR > 1.8 | 34 (54.0%) | 18 (60.0%) | 0.658 |
| LYM 1 × $10^3$/ µL | 3.09 ± 6.14 | 1.83 ± 0.69 | 0.707 |
| HGB g/dL | 12.29 ± 1.71 | 12.69 ± 1.22 | 0.161 |
| PLT 1 × $10^3$/ µL | 312.27 ± 150.45 | 267.64 ± 106.16 | 0.142 |
| CRP [mg/L] | 18.16 ± 41.80 | 23.26 ± 51.16 | 0.308 |
| **Survival** | | | |
| OS | 18.00 (15.27–20.73) | 22.00 (17.28–26.72) | 0.352 |
| DFS | 13.00 (9.17–16.83) | 14.00 (5.83–22.17) | 0.757 |
| PFS | 6.00 (4.62–7.38) | 7.00 (4.94–9.08) | 0.523 |

Bolded p-value — value statistically significant; AJCC — The American Joint Committee on Cancer; CA — cancer; CA19-9 — carbohydrate antigen 19-9; CEA — carcinoembryonic antigen; CI — confidence interval; CLR — C-reactive protein/lymphocytes ratio; CRP — C-reactive protein; DFS — disease-free survival; HGB — haemoglobin; LYM — lymphocytes; M — distant metastases; MD — median; N — nodal involvement; n — number; OS — overall survival; PC — pancreatic cancer; PFS — progression-free survival; PLT — platelets; R — resection margin; SD — standard deviation; T — tumour size; WHO status — World Health Organization performance status

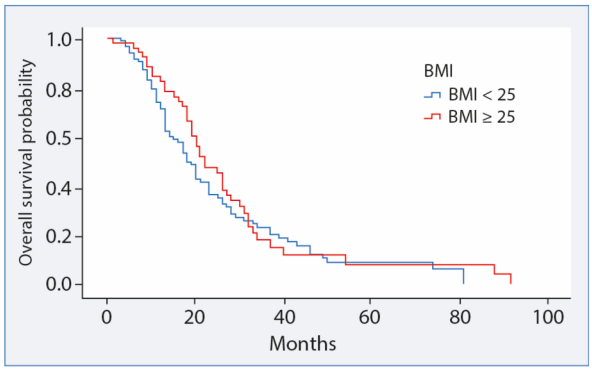


**Figure 6.** Overall survival of pancreatic cancer patients with body mass index (BMI) < 25 and BMI ≥ 25

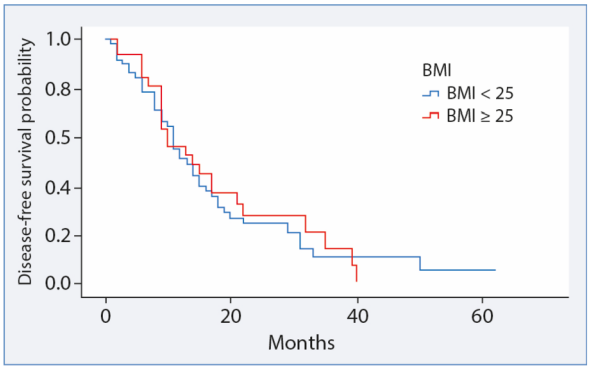


**Figure 7.** Disease-free survival of pancreatic cancer patients with body mass index (BMI) < 25 and BMI ≥ 25

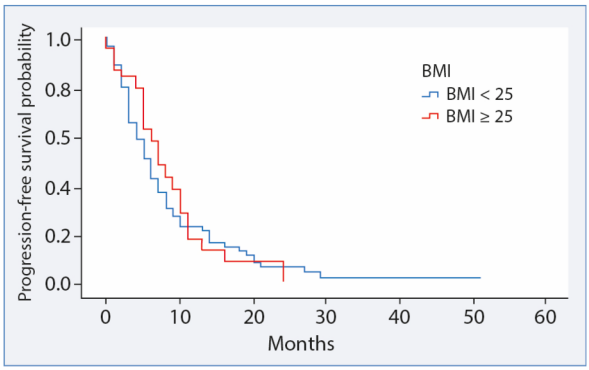


**Figure 8.** Progression-free survival of pancreatic cancer patients with body mass index (BMI) < 25 and BMI ≥ 25

subsequent multivariate Cox regression analysis using the backward method, it was the strongest predictor of survival in the HTN group. Similar to our analysis, in the study by Nakai et al. (2010) [20], the use of ACEIs/ARBs was associated with longer PFS and OS in patients with advanced PC receiving gemcitabine in monotherapy. Results from large population studies also imply that exposure to either ARBs or ACEI after PC diagnosis is significantly associated with improved survival [21]. Up-to-date

**Table 4.** Univariate analysis of survival in group with body mass index (BMI) ≥ 25

| Variable | HR (95% CI) | p-value |
|---|---|---|
| **Age** | 0.981 (0.943–1.020) | 0.330 |
| **WHO performance status** | | |
| 0 | Ref | – |
| 1 | 0.086 (0.005–1.531) | 0.095 |
| 2 | 0.674 (0.091–5.017) | 0.700 |
| 0/1 | 0.556 (0.064–4.815) | 0.594 |
| **BMI** | 0.853 (0.745–0.976) | **0.021** |
| **History of smoking** | | |
| No | Ref | – |
| Yes | 0.696 (0.348–1.390) | 0.304 |
| **Hypertension** | | |
| No | Ref | – |
| Yes | 1.383 (0.740–2.584) | 0.310 |
| **Diabetes Mellitus** | | |
| No | Ref | – |
| Yes | 1.202 (0.643–2.248) | 0.564 |
| **Autoimmune disease** | | |
| No | Ref | – |
| Yes | 0.964 (0.228–4.093) | 0.961 |
| **Family history of CA** | | |
| No | Ref | – |
| Yes | 0.751 (0.331–1.704) | 0.494 |
| **AJCC cancer stage** | | |
| IB | Ref | – |
| IIA | 0.528 (0.121–2.306) | 0.396 |
| IIB | 0.479 (0.130–1.757) | 0.267 |
| III | 0.591 (0.238–1.464) | 0.255 |
| IV | 1.005 (0.430–2.349) | 0.991 |
| **Tumour localisation** | | |
| Head | Ref | – |
| Body | 0.919 (0.214–3.945) | 0.909 |
| Tail | 0.753 (0.144–3.931) | 0.737 |
| Head and body | 7.137 (0.563–90.463) | 0.129 |
| Body and tail | 7.137 (0.563–90.463) | 0.129 |
| **Adverse effects — adjuvant chth** | | |
| No | Ref | – |
| Yes | 0.890 (0.440–1.837) | 0.771 |
| **Neutropenia** | | |
| No | Ref | – |
| Yes | 1.060 (0.557–2.018) | 0.860 |
| **Adverse effects — palliative chth** | | |
| No | Ref | – |
| Yes | 1.250 (0.646–2.419) | 0.507 |
| **Neutropenia** | | |
| No | Ref | – |
| Yes | 1.426 (0.770–2.644) | 0.259 |
| **CLR > 1.8** | | |
| No | Ref | – |
| Yes | 0.546 (0.275–1.087) | 0.085 |
| **LYM 1 × $10^3$/ µL** | | |
| ≤ 1 | Ref | – |
| > 1 | 0.58 (0.174–1.934) | 0.375 |
| **CRP [mg/L]** | | |
| ≤ 5 | Ref | – |
| > 5 | 1.447 (1.221–1.903) | **0.025** |

Bolded p-value – value statistically significant; AJCC — The American Joint Committee on Cancer; CA — cancer; chth — chemotherapy; CI — confidence interval; CLR — C-reactive protein/lymphocytes ratio; CRP — C-reactive protein; HR — hazard ratio; LYM — lymphocytes; Ref — reference

preclinical and clinical studies support the role of the renin-angiotensin system (RAS) in regulating tumor growth and metastasis in different neoplasms, encompassing PC [22]. In the pancreas, RAS components are considered to mediate growth and further lead to carcinogenesis [23]. Angiotensin II has two receptors prevalent in human tissue — the angiotensin II type 1 (AT1) and the angiotensin II type 2 (AT2). Stimulation of the AT1 receptor is associated with increased cell proliferation, growth, and reduced apoptosis. ACEIs inhibit angiotensin II systemic formation and its downstream effects through receptors. ARBs were designed to displace angiotensin II from the AT1 receptor [24]. Initial studies identified angiotensin II as a potent mediator of vascular endothelial growth factor (VEGF) expression in PC cells through an AT1-dependent pathway. The inhibition of its receptor by ARBs may inhibit tumor growth via suppression of VEGF-mediated angiogenesis [21]. One of ARBs, telmisartan, turned out to inhibit PC cell proliferation by inducing cell cycle arrest [25]. On the other hand, another ARB, losartan, reduced stromal collagen and hyaluronan production in PC models and, as a result, increased vascular perfusion and drug delivery [5]. Currently, losartan is under investigation in several PC clinical trials, including the combination of losartan with mFOLFIRINOX and beam proton radiation or the combination of losartan with gemcitabine (NCT01821729, NCT01276613). Moreover, a phase II clinical study on the efficacy of irbesartan with gemcitabine/nab-paclitaxel treatment for patients with advanced PC is designed, as in preclinical studies, irbesartan was proved to inhibit chemotherapy resistance and consequently improve the therapeutic efficacy in PC patients [26].

Our analysis did not present associations between CCBs, diuretics, or $\beta$-blocker use, and patient survival. Various studies analyzing the effect of anti-hypertensive treatment on PC patient survival demonstrate contradictory results. A meta-analysis by Jiang et al. (2022) [27] confirmed that the use of anti-hypertensive medication (ACEIs/ARBs, CCBs, diuretics, $\beta$-blockers) does not have a negative effect on overall survival of PC patients; thus, they should continue to use these drugs to prevent cardiovascular events. Yang et al. (2021) [28] suggested that $\beta$-blockers usage before PC diagnosis is not correlated with survival advantage; nevertheless, continuous use before and after diagnosis presented survival benefits. The mechanism remains unclear, and the authors noted the need for further prospective studies [28]. Previous analysis conducted by Udumyan et al. (2017) [29] revealed that patients using $\beta$-blockers had lower cancer-specific mortality rates, especially users with higher daily doses and localized disease at diagnosis. In a retrospective cohort study, the authors concluded that CCBs may prolong survival in PC patients [30]. Principe et al. (2022) [31] used CCBs, such as amlodipine, which inhibited pro-survival extracellular signal-regulated kinase (ERK) signaling *in vitro* and remarkably enhanced therapeutic responses to gemcitabine in both orthotopic xenografts and transgenic PC models. Further prospective studies are required to establish the exact impact of anti-hypertensive treatment on PC patient survival.

Although in our analysis, patients in the HTN group were significantly more likely to be diagnosed without distant metastases ($p = 0.005$), no impact of HTN on progression or survival was observed, even after further subdividing patients into receiving adjuvant or palliative therapy. Patients with comorbidities, such as hypertension, might be suspected to experience shorter survival or time to progression; nevertheless, in our study, this observation failed to achieve statistical significance. This phenomenon might be associated with receiving holistic care from doctors with both internal medicine and oncology specialties. Moreover, being hospitalized in a multi-specialist center provides patients with integrated care by multidisciplinary teams. Multidisciplinary teams might become an effective tool to facilitate collaboration between different professionals and further improve outcomes of patients with comorbidities. Similar to our study, in a single-center analysis of 2323 PC patients, HTN did not correlate with OS and showed no statistical significance in univariate analyses [32]. The study by Iede et al. (2022) [33] showed that median OS in the HTN group was significantly longer than in the non-HTN group; nevertheless, the multivariate analysis failed to identify the usage of anti-hypertensive drugs as an independent prognostic factor for OS in PC patients.

The CLR level reflects the equilibrium state between the systemic inflammatory and immunological response. An elevated CLR indicates a decrease in immune response and an increase in systemic inflammation [34]. It seems unclear if the CLR could serve as a prognostic marker in PC. In our previous analysis, higher CLR and CRP levels were significantly associated with poorer OS in PC and DM patients. In the current study, a higher CLR was also associated with shorter survival in the HTN group ($p = 0.013$). Similar results were obtained in the study by Fan et al. (2020) [12] in which a CLR > 1.8 was correlated with poorer survival of PC patients, both in univariate and multivariate analysis. On the other hand, in the group with BMI $\geq$ 25 analyzed in our study, the CLR failed to reach statistical significance as a prognostic marker; nevertheless, a higher CRP level was associated with shorter survival in this group. In the study by Yuan et al. (2021) [35], pre-diagnostic lev-

els of CRP were associated with reduced survival in PC patients, demonstrating that chronic inflammation is a significant risk factor for PC and influences further survival. A Mendelian randomization analysis confirmed the causal mechanism in which obesity induces chronic inflammation and contributes to PC development [36]. Moreover, an increase in CRP levels during chemotherapy with the mFOLFIRINOX regimen positively correlated with disease progression [37].

On the one hand, obesity is a well-known modifiable risk factor for PC; on the other hand, several studies confirmed that a higher BMI was correlated with longer survival in PC patients [32, 38–40]. These findings concur with our results, in which a higher BMI was also associated with longer survival in the group with HTN and the group with overweight/obesity. In the further multivariate analysis of the group with BMI $\geq$ 25, a higher BMI was the strongest predictor of survival. Interestingly, many previous studies have reported that a BMI higher than 25 kg/m$^2$ is associated with improved survival in other malignancies. This phenomenon was described as the "obesity paradox" [41]. Scientists trying to explain the obesity paradox underlie that measurement of obesity with BMI presents some limitations and cannot reflect metabolic and endocrine disruption [42]. Also, in some cancers, unintentional weight loss may occur before diagnosis; thus, weight at the time of diagnosis may be misleading [43]. On the other hand, it has been suggested that lack of cachexia in obese patients with advanced cancers may underlie this paradox [44]. Cachexia is a multifactorial syndrome defined by non-volitional weight loss, sarcopenia, anorexia, fatigue, weakness, loss of appetite, taste alterations, and early satiety [45]. It has been shown to affect approximately 50% of oncological patients and be driven by reduced food intake and specific alterations in metabolism caused by host-tumor interactions [46]. Insufficient food intake is a significant driver of weight loss, while metabolic changes and reduced activity contribute to the loss of muscle mass, called sarcopenia [47]. PC is associated with the highest frequency of developing cancer cachexia-sarcopenia syndrome, negatively influencing tolerance and response to treatment and survival [40]. In this context, obesity might correlate with better survival; however, rigorous and prospective studies are necessary to define the impact of obesity in the oncology setting.

This study had several limitations. It was a single-center study, and the juxtaposition of results collected in other clinical centers would have ensured a more reliable analysis. Moreover, we could not eliminate potential selection bias due to the retrospective character of the research. The outpatient medical records did not indicate the change in patients' weight both before diagnosis and during treatment. No data about exact blood pressure measurements was collected. Nonetheless, we firmly believe that our outcomes provide new insight into the relationship between being overweight, hypertension, and PC.

## Conclusions

Although hypertension and overweight are prevalent in PC patients, they seem to have no impact on outcomes. In the studied groups, we managed to distinguish some variables influencing survival. The exact effect of ACEIs/ARBs on cancerogenesis should be further investigated. The CLR seems to be a feasible marker of prognosis in PC.

## Article Information and Declarations

### Data availability statement

Correspondence and material requests should be addressed to M.F., A.B.K. or A.D.

### Ethics statement

The study was acknowledged by the Bioethics Committee of the Medical University of Warsaw (AKBE/144/2022). The work was carried out following the Code of Ethics of the World Medical Association (Declaration of Helsinki) on medical research involving human subjects, the ethical principle defined in the Farmington Consensus 1997.

### Author contributions

M.F.: conceptualization, data curation, investigation, writing — original draft, writing — review and editing; I.C.: writing — original draft; A.B.-K.: conceptualization, investigation, supervision, validation, writing — original draft, writing — review and editing; A.D.: conceptualization, data curation, investigation, supervision, validation, writing — original draft, writing — review and editing.

All authors have read and agreed to the published version of the manuscript.

### Funding

None.

### Acknowledgements

None.

### Conflict of interest

The authors declare no conflict of interest.

### Supplementary material

None.

## References

1. Sung H, Ferlay J, Siegel RL, et al. Global Cancer Statistics 2020: GLOBOCAN Estimates of Incidence and Mortality Worldwide for 36 Cancers in 185 Countries. CA Cancer J Clin. 2021; 71(3): 209–249, doi: 10.3322/caac.21660, indexed in Pubmed: 33538338.
2. Arnold M, Abnet CC, Neale RE, et al. Global Burden of 5 Major Types of Gastrointestinal Cancer. Gastroenterology. 2020; 159(1): 335–349.e15, doi: 10.1053/j.gastro.2020.02.068, indexed in Pubmed: 32247694.

3. Olakowski M, Bułdak Ł. Modifiable and Non-Modifiable Risk Factors for the Development of Non-Hereditary Pancreatic Cancer. Medicina (Kaunas). 2022; 58(8), doi: 10.3390/medicina58080978, indexed in Pubmed: 35893093.
4. Klein AP. Pancreatic cancer epidemiology: understanding the role of lifestyle and inherited risk factors. Nat Rev Gastroenterol Hepatol. 2021; 18(7): 493–502, doi: 10.1038/s41575-021-00457-x, indexed in Pubmed: 34002083.
5. Fudalej M, Kwaśniewska D, Nurzyński P, et al. New Treatment Options in Metastatic Pancreatic Cancer. Cancers (Basel). 2023; 15(8), doi: 10.3390/cancers15082327, indexed in Pubmed: 37190255.
6. McGuigan A, Kelly P, Turkington RC, et al. Pancreatic cancer: A review of clinical diagnosis, epidemiology, treatment and outcomes. World J Gastroenterol. 2018; 24(43): 4846–4861, doi: 10.3748/wjg.v24.i43.4846, indexed in Pubmed: 30487695.
7. Chung V, Sun V, Ruel N, et al. Improving Palliative Care and Quality of Life in Pancreatic Cancer Patients. J Palliat Med. 2022; 25(5): 720–727, doi: 10.1089/jpm.2021.0187, indexed in Pubmed: 34704841.
8. Park SK, Oh CM, Kim MH, et al. Metabolic syndrome, metabolic components, and their relation to the risk of pancreatic cancer. Cancer. 2020; 126(9): 1979–1986, doi: 10.1002/cncr.32737, indexed in Pubmed: 32012239.
9. Xia B, He Q, Pan Y, et al. Metabolic syndrome and risk of pancreatic cancer: A population-based prospective cohort study. Int J Cancer. 2020; 147(12): 3384–3393, doi: 10.1002/ijc.33172, indexed in Pubmed: 32580250.
10. Higuera O, Ghanem I, Nasimi R, et al. Management of pancreatic cancer in the elderly. World J Gastroenterol. 2016; 22(2): 764–775, doi: 10.3748/wjg.v22.i2.764, indexed in Pubmed: 26811623.
11. Saad MA, Cardoso GP, Martins Wd, et al. Prevalence of metabolic syndrome in elderly and agreement among four diagnostic criteria. Arq Bras Cardiol. 2014; 102(3): 263–269, doi: 10.5935/abc.20140013, indexed in Pubmed: 24676226.
12. Fan Z, Luo G, Gong Y, et al. Prognostic Value of the C-Reactive Protein/Lymphocyte Ratio in Pancreatic Cancer. Ann Surg Oncol. 2020; 27(10): 4017–4025, doi: 10.1245/s10434-020-08301-3, indexed in Pubmed: 32144621.
13. Mills KT, Stefanescu A, He J. The global epidemiology of hypertension. Nat Rev Nephrol. 2020; 16(4): 223–237, doi: 10.1038/s41581-019-0244-2, indexed in Pubmed: 32024986.
14. Zanini S, Renzi S, Limongi AR, et al. A review of lifestyle and environment risk factors for pancreatic cancer. Eur J Cancer. 2021; 145: 53–70, doi: 10.1016/j.ejca.2020.11.040, indexed in Pubmed: 33423007.
15. Badowska-Kozakiewicz A, Fudalej M, Kwaśniewska D, et al. Diabetes Mellitus and Pancreatic Ductal Adenocarcinoma-Prevalence, Clinicopathological Variables, and Clinical Outcomes. Cancers (Basel). 2022; 14(12), doi: 10.3390/cancers14122840, indexed in Pubmed: 35740504.
16. Lee W, Yoon YS, Han HS, et al. Prognostic relevance of preoperative diabetes mellitus and the degree of hyperglycemia on the outcomes of resected pancreatic ductal adenocarcinoma. J Surg Oncol. 2016; 113(2): 203–208, doi: 10.1002/jso.24133, indexed in Pubmed: 26799261.
17. Chen Ke, Qian W, Jiang Z, et al. Metformin suppresses cancer initiation and progression in genetic mouse models of pancreatic cancer. Mol Cancer. 2017; 16(1): 131, doi: 10.1186/s12943-017-0701-0, indexed in Pubmed: 28738823.
18. Gu Y, Zhang B, Gu G, et al. Metformin Increases the Chemosensitivity of Pancreatic Cancer Cells to Gemcitabine by Reversing EMT Through Regulation DNA Methylation of miR-663. Onco Targets Ther. 2020; 13: 10417–10429, doi: 10.2147/OTT.S261570, indexed in Pubmed: 33116621.
19. Flack JM, Adekola B. Blood pressure and the new ACC/AHA hypertension guidelines. Trends Cardiovasc Med. 2020; 30(3): 160–164, doi: 10.1016/j.tcm.2019.05.003, indexed in Pubmed: 31521481.
20. Nakai Y, Isayama H, Ijichi H, et al. Inhibition of renin-angiotensin system affects prognosis of advanced pancreatic cancer receiving gemcitabine. Br J Cancer. 2010; 103(11): 1644–1648, doi: 10.1038/sj.bjc.6605955, indexed in Pubmed: 20978506.
21. Keith SW, Maio V, Arafat HA, et al. Angiotensin blockade therapy and survival in pancreatic cancer: a population study. BMC Cancer. 2022; 22(1): 150, doi: 10.1186/s12885-022-09200-4, indexed in Pubmed: 35130875.
22. Khoshghamat N, Jafari N, Toloue-Pouya V, et al. The therapeutic potential of renin-angiotensin system inhibitors in the treatment of pancreatic cancer. Life Sci. 2021; 270: 119118, doi: 10.1016/j.lfs.2021.119118, indexed in Pubmed: 33548284.
23. Mandilaras V, Bouganim N, Yin H, et al. The use of drugs acting on the renin-angiotensin system and the incidence of pancreatic cancer. Br J Cancer. 2017; 116(1): 103–108, doi: 10.1038/bjc.2016.375, indexed in Pubmed: 27846200.
24. Messerli F, Bangalore S, Bavishi C, et al. Angiotensin-Converting Enzyme Inhibitors in Hypertension. Journal of the American College of Cardiology. 2018; 71(13): 1474–1482, doi: 10.1016/j.jacc.2018.01.058.
25. Yamana Y, Fujihara S, Kobara H, et al. MicroRNA profiles following telmisartan treatment in pancreatic ductal adenocarcinoma cells. J Cancer Res Ther. 2022; 18(Supplement): S305–S312, doi: 10.4103/jcrt.JCRT_104_20, indexed in Pubmed: 36510981.
26. Zhou T, Xie Y, Hou X, et al. Irbesartan overcomes gemcitabine resistance in pancreatic cancer by suppressing stemness and iron metabolism via inhibition of the Hippo/YAP1/c-Jun axis. J Exp Clin Cancer Res. 2023; 42(1): 111, doi: 10.1186/s13046-023-02671-8, indexed in Pubmed: 37143164.
27. Jiang W, He Ru, Lu Y, et al. The relationships between antihypertensive medications and the overall survival of patients with pancreatic cancer: a systematic review and meta-analysis. Expert Rev Gastroenterol Hepatol. 2022; 16(6): 547–553, doi: 10.1080/17474124.2022.2088506, indexed in Pubmed: 35686669.
28. Yang A, Zylberberg HM, Rustgi SD, et al. Beta-blockers have no impact on survival in pancreatic ductal adenocarcinoma prior to cancer diagnosis. Sci Rep. 2021; 11(1): 1038, doi: 10.1038/s41598-020-79999-0, indexed in Pubmed: 33441781.
29. Udumyan R, Montgomery S, Fang F, et al. Beta-Blocker Drug Use and Survival among Patients with Pancreatic Adenocarcinoma. Cancer Res. 2017; 77(13): 3700–3707, doi: 10.1158/0008-5472.CAN-17-0108, indexed in Pubmed: 28473530.
30. Tingle SJ, Severs GR, Moir JAG, et al. Calcium channel blockers in pancreatic cancer: increased overall survival in a retrospective cohort study. Anticancer Drugs. 2020; 31(7): 737–741, doi: 10.1097/CAD.0000000000000947, indexed in Pubmed: 32639282.
31. Principe DR, Aissa AF, Kumar S, et al. Calcium channel blockers potentiate gemcitabine chemotherapy in pancreatic cancer. Proc Natl Acad Sci U S A. 2022; 119(18): e2200143119, doi: 10.1073/pnas.2200143119, indexed in Pubmed: 35476525.
32. Neumann CCM, Schneider F, Hilfenhaus G, et al. Impact of Smoking, Body Weight, Diabetes, Hypertension and Kidney Dysfunction on Survival in Pancreatic Cancer Patients-A Single Center Analysis of 2323 Patients within the Last Decade. J Clin Med. 2023; 12(11), doi: 10.3390/jcm12113656, indexed in Pubmed: 37297851.
33. Iede K, Yamada T, Ueda M, et al. Do antihypertensive drugs really have antitumor effects? Baseline differences in hypertensive and non-hypertensive patients with advanced pancreatic cancer. Medicine (Baltimore). 2022; 101(29): e29532, doi: 10.1097/MD.0000000000029532, indexed in Pubmed: 35866833.
34. Cillóniz C, Torres A, Garcia-Vidal C, et al. COVID19-Researchers. The Value of C-Reactive Protein-to-Lymphocyte Ratio in Predicting the Severity of SARS-CoV-2 Pneumonia. Arch Bronconeumol. 2021; 57: 79–82, doi: 10.1016/j.arbres.2020.07.038, indexed in Pubmed: 34629674.
35. Yuan C, Morales-Oyarvide V, Khalaf N, et al. Prediagnostic Inflammation and Pancreatic Cancer Survival. J Natl Cancer Inst. 2021; 113(9): 1186–1193, doi: 10.1093/jnci/djab040.
36. Li Z, Jin L, Xia Lu, et al. Body mass index, C-reactive protein, and pancreatic cancer: A Mendelian randomization analysis to investigate causal pathways. Front Oncol. 2023; 13: 1042567, doi: 10.3389/fonc.2023.1042567, indexed in Pubmed: 36816931.

37. Shen F, Liu C, Zhang W, et al. Serum levels of IL-6 and CRP can predict the efficacy of mFOLFIRINOX in patients with advanced pancreatic cancer. Front Oncol. 2022; 12: 964115, doi: 10.3389/fonc.2022.964115, indexed in Pubmed: 35965580.
38. Eibl G, Cruz-Monserrate Z, Korc M, et al. Consortium for the Study of Chronic Pancreatitis, Diabetes, and Pancreatic Cancer. Diabetes Mellitus and Obesity as Risk Factors for Pancreatic Cancer. J Acad Nutr Diet. 2018; 118(4): 555–567, doi: 10.1016/j.jand.2017.07.005, indexed in Pubmed: 28919082.
39. Carreras-Torres R, Johansson M, Gaborieau V, et al. The Role of Obesity, Type 2 Diabetes, and Metabolic Factors in Pancreatic Cancer: A Mendelian Randomization Study. J Natl Cancer Inst. 2017; 109(9), doi: 10.1093/jnci/djx012, indexed in Pubmed: 28954281.
40. Hou YC, Chen CY, Huang CJ, et al. The Differential Clinical Impacts of Cachexia and Sarcopenia on the Prognosis of Advanced Pancreatic Cancer. Cancers (Basel). 2022; 14(13), doi: 10.3390/cancers14133137, indexed in Pubmed: 35804906.
41. Lee DH, Giovannucci EL. The Obesity Paradox in Cancer: Epidemiologic Insights and Perspectives. Curr Nutr Rep. 2019; 8(3): 175–181, doi: 10.1007/s13668-019-00280-6, indexed in Pubmed: 31129887.
42. Trestini I, Carbognin L, Bonaiuto C, et al. The obesity paradox in cancer: clinical insights and perspectives. Eat Weight Disord. 2018; 23(2): 185–193, doi: 10.1007/s40519-018-0489-y, indexed in Pubmed: 29492860.
43. Lennon H, Sperrin M, Badrick E, et al. The Obesity Paradox in Cancer: a Review. Curr Oncol Rep. 2016; 18(9): 56, doi: 10.1007/s11912-016-0539-4, indexed in Pubmed: 27475805.
44. Cespedes Feliciano EM, Kroenke CH, Caan BJ. The Obesity Paradox in Cancer: How Important Is Muscle? Annu Rev Nutr. 2018; 38: 357–379, doi: 10.1146/annurev-nutr-082117-051723, indexed in Pubmed: 29727593.
45. Arends J, Strasser F, Gonella S, et al. ESMO Guidelines Committee. Electronic address: clinicalguidelines@esmo.org. Cancer cachexia in adult patients: ESMO Clinical Practice Guidelines. ESMO Open. 2021; 6(3): 100092, doi: 10.1016/j.esmoop.2021.100092, indexed in Pubmed: 34144781.
46. Poulia KA, Sarantis P, Antoniadou D, et al. Pancreatic Cancer and Cachexia-Metabolic Mechanisms and Novel Insights. Nutrients. 2020; 12(6), doi: 10.3390/nu12061543, indexed in Pubmed: 32466362.
47. Fearon KCH, Glass DJ, Guttridge DC. Cancer cachexia: mediators, signaling, and metabolic pathways. Cell Metab. 2012; 16(2): 153–166, doi: 10.1016/j.cmet.2012.06.011, indexed in Pubmed: 22795476.

VIA MEDICA

ORIGINAL ARTICLE

Oncology in Clinical Practice
2025, Vol. 21, No. 1, 28–38
DOI: 10.5603/ocp.98228

ISSN 2450-1654
eISSN 2450-6478

# Higher neoantigen load correlates with better overall survival in Chinese lung adenocarcinoma patients

Xuemei Liu[1], Yongfeng Yu[1], Wenhui Song[2], Xiao Deng[2], Kaili Gu[2], Mengdi Yuan[2], Zeyu Jiang[2], Yu Wang[2,*], Yafei Zhang[2]

[1]Shanghai Chest Hospital, Shanghai Jiao Tong University School of Medicine, Shanghai, China
[2]MEDx (Suzhou) Translational Medicine Co., Ltd, Suzhou, China

**Abstract**

**Introduction.** Neoantigen load (NAL) has been extensively studied as a promising biomarker for immunotherapy. Recently it was also reported that NAL is associated with lung cancer patient survival, but the results were not consistent.

**Material and methods**. To further evaluate the prognostic value of NAL in lung cancer, we analyzed NAL in a cohort of 96 lung adenocarcinoma (AD) and 83 lung squamous cell carcinoma (SQ) patients from the Cancer Genome Atlas (TCGA). We found that high NAL correlates with better overall survival (OS) of AD patients but with worse OS of SQ patients. Next, we collected a total of 25 NSCLC patient samples and explored whole exome sequencing (WES) and a large targeted gene panel (Med1CDx panel containing 579 genes) for NAL and tumor mutation burden (TMB) analysis.

**Results.** We found that patients with both higher NAL and TMB, who underwent chemotherapy combined with immunotherapy, showed better OS and progression-free survival (PFS) in both AD and SQ subgroups. We also compared the concordance of NAL and TMB between WES and the Med1CDx panel. The $R^2$ for concordance of NAL and TMB prediction by WES and our Med1CDx panel was 0.81 and 0.86, respectively.

**Conclusions.** In this study, we showed that NAL is a useful biomarker for lung cancer OS prediction at least in the AD cohort. Furthermore, considering the high cost of WES, large targeted gene-panel-based NAL and TMB analysis could be a good alternative in clinical practical settings.

**Keywords:** neoantigen load, overall survival, lung adenocarcinoma, Chinese patients

## Introduction

Lung cancer has been the leading cause of death worldwide and the 2nd common cancer type in 2020, accounting for 1.8 million cases of 10 million deaths in 2020 [World Health Organization (WHO) website] [1]. Advanced molecular diagnostics and recognition of targetable oncogenic driver alterations have led to dramatic changes in non-small cell lung cancer (NSCLC) treatment in recent years. Many new effective targeted agents were developed and the treatment of some oncogene-addicted NSCLC, such as *EGFR*-mutated or *ALK*-rearranged NSCLC is well-established [2, 3]. Although these drugs have revolutionized clinical practice, only a fraction of susceptible patients will benefit, and acquired resistance to these agents remains a challenge. Individualized vaccines targeting neoantigens would be a good option for lung cancer therapy in the future. Neoantigens are protein fragments derived only from cancer cells. With this unique property, targeting neoantigen allows the patient's immune system to detect and attack cancer cells instead of attacking healthy cells [4, 5]. Neoantigens are classified into two types: shared and personalized neoantigens. While shared neoantigens are not specific to an individual or tumor type, personalized neoantigens are highly specific to individual

*Correspondence: Yu Wang, PhD, MEDx (Suzhou)Translational Medicine Co., Ltd, Suite 901, B5 Building, 218 Xinghu St., Suzhou Industrial Park, 215123 Suzhou, China (yu.wang@medxtmc.com)
Received: 16 November 2023; Accepted: 16 February 2024;
Early publication: 8 April 2024

tumors and are the basis of personalized neoantigen vaccines.

Identifying prognostic markers in cancer patients is essential because it allows the recognition of patient subpopulations that might anticipate different outcomes or might benefit from different types of therapies. Novel molecular prognostic biomarkers include such genes as *TP53*, *VEGF*, *TUBB3*, *Ki-67*, etc. However, despite an enormous amount of data available on molecular biomarkers, results are often not reproducible, partially due to the heterogeneity of study designs, techniques used, and data interpretation. Therefore, many molecular prognostic markers to date, have not managed to make their way into routine clinical use [6, 7]. Tumor mutation burden (TMB) and neoantigen load (NAL) have been extensively studied as promising biomarkers for predicting the anti-tumor effects of immune checkpoint inhibitors (ICIs) [8–12]. Several studies have reported the prognostic effect of TMB on the clinical benefits for patients with resected early-stage NSCLC, but the results are inconsistent. Two studies showed that a high TMB is associated with a favorable outcome in resected NSCLC patients [13, 14], but other reports demonstrated that TMB is not associated with overall survival of early-stage NSCLC patients, implying that TMB is not sufficient to predict NSCLC prognosis [15, 16]. However, utilizing computational tools to predict tumor NAL based on whole exome sequencing (WES) data has been confirmed to be a potentially useful method [17]. Recently, several studies have shown that NAL has good potential as a prognosis biomarker although the results were also contradictory. Gong et al. [18] showed that higher NAL exhibited better disease-free survival (DFS) for stage II/III Chinese lung squamous cell carcinoma (SQ) patients. However, another report demonstrated that high neoantigen burden was associated with significantly longer overall survival (OS) in the lung adenocarcinoma (AD) cohort of patients from Cancer Genome Atlas (TCGA) [19].

Tumor mutation burden and NAL analysis by WES is complicated and expensive due to large genomic space sequencing. Recent studies have shown that TMB can be accurately measured by smaller gene panels [9, 10, 20]. In this study, we assessed TMB and NAL by both WES and a large targeted gene panel and identified the correlation of TMB and NAL with clinical outcomes. The concordance of TMB and NAL measurements by WES and the large targeted gene panel was also determined. We expected to be able to provide more insights into biomarker discovery and identification for the prognosis of Chinese lung cancer patients. Personalized neoantigens predicted by WES were also compared with those from online public databases.

## Material and methods

### Cancer Genome Atlas data retrieval, neoantigen load calculation, and survival analysis

Thorsson et al. [21] presented an immunogenomic analysis of more than 10 000 tumors comprising 33 diverse cancer types by utilizing data compiled by TCGA. Clinical data for lung cancer patients was accessed and downloaded from https://gdc.cancer.gov/about-data/publications/panimmune. Predicted single nucleotide variant (SNV) and Indel neoantigen counts are available in this dataset. So we used predicted SNV, Indel neoantigen counts, and the sum of these two (NeoAll) to correlate with OS. Survfit objects were generated by surv_categorize() and survfit.formula() from R package survminer and survival. The ggsurvplot() function from R package ggplot2 was used to plot the Kaplan-Meier survival curve.

### Patient cohort

A total of 25 patients with pathologically confirmed NSCLC, including 17 AD and 8 SQ patients, were enrolled between 2017 Feb and 2018 Nov. Clinical data were retrieved from the electronic medical records. Data acquisition was in line with relevant legislation and institutional review board guidelines. All patients were followed up regularly in the Shanghai Chest Hospital until recurrent or last follow-up. All procedures involving human participants performed in this study were in accordance with the Declaration of Helsinki (as revised in 2013). The study was approved by the institutional committee board of the Shanghai Chest Hospital and informed consent was taken from all the participants.

### Whole exome and large targeted panel sequencing and tumor mutation burden calculation

Next-generation sequence (NGS) was performed using genomic DNA isolated from formalin-fixed paraffin-embedded (FFPE) samples with WES and a large targeted panel (Med1CDx panel including full coding sequences (CDS) regions of 579 genes, selected introns of 37 genes, which is designed for fusion calling). Deep sequencing was performed by the Hiseq X10 or NovaSeq platforms with a mean depth of 5000X. The bioinformatics workflow utilized a customized variant calling method based on GATK4 and Varscan, which contains SNP/InDel/CNV/SV calling.

Tumor mutation burden was determined as the average number of coding mutations per megabase (Mb) of genome examined following the method of FoundationOne panel [22]. All single nucleotide variations and Indels in the coding region including the synonymous alternation of targeted genes were counted for TMB calculation. Alterations listed as known somatic alterations in COSMIC hot spots were excluded, and truncations in tumor suppressor genes were not

counted. Sites presented in 1000G, ESP6500, and gnomAD with ≥ 1% frequency and synonymous SNV sites were filtered. The threshold for high TMB was determined by the 25th and 75th percentiles method used by the FoundationOne panel [22].

### Human leukocyte antigen typing, neoantigen prediction, and statistics analysis

Four-digit human leukocyte antigen (HLA) class I (HLA-A, HLA-B, and HLA-C) alleles of each patient were identified from WES data using Optitype (version 1.3.1, default parameters). The pvactools (version 1.5.8, default parameters) tool was used to predict binding of 8- to 11-mer mutant peptides to the patients' HLA alleles. Neoantigens predicted in this study were compared with those from the TSNAdb (version 4.0) database. Neoantigen load was calculated by dividing the total number of neoantigens in each sample by the CDS length (Mb) of the WES or Med1CDx panel. The Kaplan-Meier method and the log-rank test were performed to correlate survival of patients with genomic alterations and NAL. A $p \leq 0.05$ was considered statistically significant.

### Mutation spectra analysis and comparison between lung adenocarcinoma and lung squamous cell carcinoma patients

Raw sequence variants were called from WES data according to the GATK best practice analysis pipeline. Variant calling datasets were annotated by ANNOVAR. Screening of gene mutations from the bulk of raw variants sites followed the below analysis criteria: (1) > 25× coverage in the variant site; (2) variant allele frequency ≥ 5% and at least 5 individual mutant reads; (3) filter variants only observed on positive-strand or negative-strand; (4) filter sites presented in 1000 Genome Project with ≥ 1% frequency, NHLBI-ESP project with 6500 exomes with ≥ 1% frequency and the Genome Aggregation Database (gnomAD) with ≥ 1% frequency; (5) filter sequence variation frequency ≥ 5% and variants site < 20× coverage in normal control samples. Vcf files were converted to mutation annotation format (MAF) by vcf2maf and vep. The R packages maftools (https://bioconductor.org/packages/release/bioc/vignettes/maftools/inst/doc/maftools.html) were used to summarize, analyze, annotate, and visualize somatic MAF files. The tool deconstructSigs (https://rdrr.io/cran/deconstructSigs/) was used to identify signatures present in tumor samples.

## Results

### Cancer Genome Atlas neoantigen load analysis and correlation with overall survival

With the clinical data from TCGA, we were able to determine the cutoff value of predictive SNV, Indel, and total neoantigen counts. Patient samples and mutation numbers used to determine the cutoff values were: 96 AD and 83 SQ patients; 525 and 72 SNV neoantigen counts, 5 and 10 Indel neoantigen counts, 174 and 284 all neoantigens counts from AD and SQ, respectively. In this TCGA dataset, we showed that in AD, when the same survival probability was applied, high SNV/Indel/total neoantigen correlated with better overall survival. But in SQ, the results showed the opposite trend, high SNV/Indel/total neoantigen correlated with worse overall survival (Fig. 1A–F).

### Patient characteristics

The clinical characteristics of the patients are shown in Table 1. There were 17 AD patients and 8 SQ patients with a median age of 64 years (ranging between 34 and 83 years old). A total of 16 patients were former or current smokers: 53% (9/17) of AD patients versus 87.5% (7/8) of SQ patients (Tab. 1). The median cigarette consumption was 23 and 35 packs/year in AD and SQ patients, respectively. *EGFR* mutation occurred in 35% (6/17) of AD patients, but only in 12.5% (1/8) of SQ patients. For the treatment regime, 12 patients (12/25, 48%) received standard chemotherapy for at least one cycle.

### Tumor mutation burden concordance between the 579 gene panel and whole exome sequencing

Evidence has suggested that the TMB and tumor-specific neoantigens are potential determinants of the response to ICIs and can influence patient outcomes in immunotherapy [8–12]. Whole exome sequencing allows a direct measurement of TMB. However, routine implementation of WES in clinical practice is unsuitable because of high costs, labor and time intensiveness, and extensive data management. To test the potential utility of our in-house 579 gene Med1CDx panel in clinically predictive TMB estimates, DNA from 16 samples (including 11 AD and 5 SQ) was profiled. The Med1CDx panel showed a good correlation with WES for TMB estimation, with $R^2$ correlation values of 0.86 for all mutations.

### Analysis of personalized neoantigens derived from whole exome sequencing and Med1CDx panel

Whole exome sequencing and Med1CDx panel were applied to profile neoantigen spectra in 16 patients. Mutations occurring in the patients were assessed for predicted binding affinity to HLA alleles, and potential neoantigens were identified. In the WES data, 1733 neoantigens with binding affinities < 500 nM were identified. Of these, only 52 (3%) were observed through the Med1CDx panel, demonstrating that the large targeted gene panel failed to identify a broad spectrum of neoantigens as compared to WES. We found the most frequent shared missense mutation

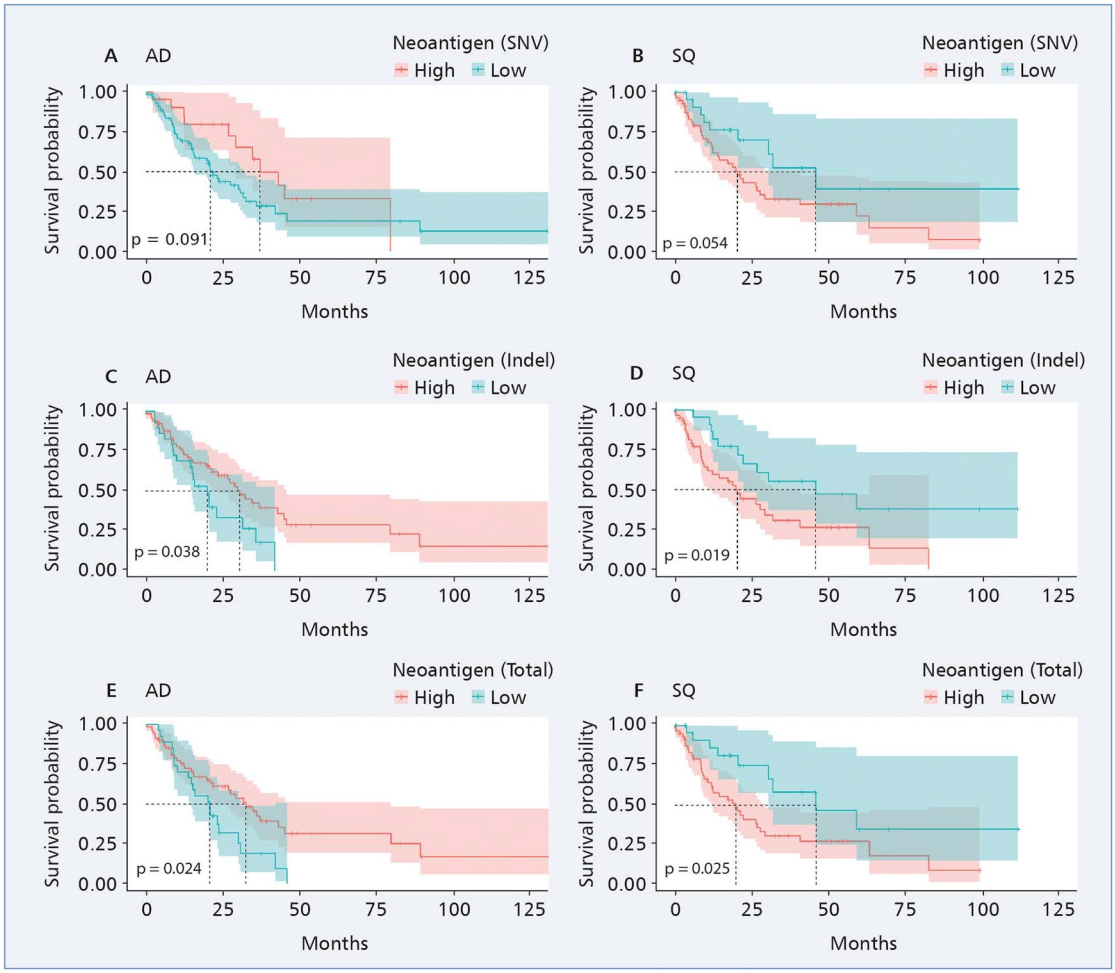


**Figure 1.** Correlation of neoantigen load with overall survival (OS) using Cancer Genome Atlas (TCGA) clinical data. Correlation of predicted single nucleotide variant (SNV) neoantigen (**A, B**), predicted Indel neoantigen (**C, D**), predicted total neoantigen (**E, F**) with OS

**Table 1.** Clinical characteristics of patients

| Characteristics | Number (%) |
|---|---|
| **Sex** | |
| Male | 18 (72) |
| Female | 7 (28) |
| **Age [years]** | |
| Range | 34–83 |
| Medium | 64 |
| < 65 | 13 (52) |
| ≥ 65 | 12 (48) |
| **Smoking status** | |
| Never | 9 (36) |
| Former/current | 16 (64) |
| **Stage** | |
| III | 5 (20) |
| IV | 20 (80) |
| **Histologic diagnosis** | |
| Adenocarcinoma | 17 (68) |
| Squamous cell carcinoma | 8 (32) |

detected by WES were *TTN*, *MUC16*, and *TP53*, occurring in 11,11, and 9 patients, respectively. The neoantigens derived from WES were compared with those in the online public database which contains 1.1 million neoantigens. Twelve neoantigens from 9 patients were identical to those from the public database, even though the HLA types are different (Tab. 2). Among these neoantigens, neoantigens derived from *TP53* gene mutation were the most frequent (3 samples), and 2 neoantigens were derived from the *PCDHA4* and *FFAR2* genes (Tab. 2).

## Neoantigen load analysis and correlation with progression-free survival and overall survival

The median number of NAL in all patients determined by WES was 3.0 neoantigens per Mb, while the median number called by the Med1CDx panel was 4.0. There was a linear relationship between neoantigens recovered from the Med1CDx panel and WES ($R^2 = 0.81$) (Fig. 2A, B). In the WES data, our data demonstrated that TMB and NAL were higher in the SQ subgroup than in the AD subgroup (Fig. 2C, D).

**Table 2.** Shared neoantigens between whole exome sequencing (WES) results and online public database of lung cancer

| Neoantigen (frequency) | Gene in database | HLA type in samples | HLA type in database |
|---|---|---|---|
| TYSPALIKM (3) | *TP53* | HLA-C*07:02 | HLA-A*23:01<br>HLA-A*24:02<br>HLA-C*04:01 |
| RAFGRGLHV (2) | *FFAR2* | HLA-C*12:03 | HLA-B*51:01<br>HLA-C*14:02 |
| VRDGGSPSL (2) | *PCDHA4* | HLA-C*06:02 | HLA-C*07:02<br>HLA-B*27:05 |
| IIHTGEKPY (1)<br>RTYTGEKPY (1) | *ZNF121*<br>*ZNF559* | HLA-C*03:03 | HLA-B*15:01 |
| LTRPVHNAAR (1)<br>ASHDERFKR (1) | *CDKN2A*<br>*KDM2A* | HLA-A*31:01 | HLA-A*33:03<br>HLA-A*11:01 |
| AMLKNTVTI (1) | *MAGEC1* | HLA-A*02:01 | HLA-A*02:01 |

HLA — human leukocyte antigen

Tumors with higher TMB carry higher NAL. Higher NAL was associated with improved overall survival using 10.3 neoantigens per Mb as a cutoff point (median OS not reached *versus* 11.0 months, log-rank p = 0.016) and progression-free survival (PFS) (median not reached *versus* 3.3 months, log-rank p = 0.03, 10.3 neoantigens per Mb as a cutoff point) (Fig. 2E, F).

### Mutation spectra and signatures in lung adenocarcinoma and lung squamous cell carcinoma samples

In the SNV class, transitions of C>T, and C>A were significantly mutated in both AD and SQ samples. In addition to these two variations, the prevalence of T>C transitions was observed in AD and C>G in SQ. The top 20 mutated genes were quite different between the AD and SQ subgroups, but *TP53* and *TTN* were in the top 3 genes (Fig. 3A, C). In AD, genes with the highest mutation rate were *TP53* (9/17,53%), *MUC16* (7/17, 41%), *TTN*, and *EGFR* (6/17, 35%). *TP53* and *TTN* were the most frequent mutations in SQ (7/8,88%). Other mutations that presented frequently in SQ included *KMT2D* and *RYR2* (5/8, 62%), *MUC16*/*GOLGA6L2*/*SYNE1*/*NCAM1*/*OBSCN*/*TPTE* (4/8, 50%) (Fig. 3B, D). *TP53* and *TTN* were also among the top 3 mutations in tobacco smokers, with *MUC16* and *KMT2D* as other frequent mutations in AD and SQ smokers, respectively. The genes mutated in non-smokers in both AD and SQ subtypes were very diverse, and the mutation rates were not high.

Analysis of the mutational somatic substitutions using the COSMIC Mutational Signatures database (v2 — March 2015) demonstrated that the AD mutations were distributed in Signatures 1, 3, 4, while the SQ mutations were mainly Signature 3 and 4 related (Fig. 3E, F). Signature 1 is common in all cancer types and most cancer samples. Signature 3 was reported in breast, ovarian, and pancreatic cancers, our results confirmed that this signature set was also presented in lung cancer samples. Signature 4 has been found in lung adenocarcinoma and lung squamous carcinoma and is considered to be associated with smoking and tobacco mutagens.

## Discussion

Neoantigen load, as a promising biomarker for predicting ICI efficacy, has been extensively studied, particularly in melanoma, lung cancer, and gynecological tumors [19, 23, 24]. In these types of cancer, NAL can predict anti-tumor effects of ICIs. However, research into neoantigens still faces challenges, such as the lack of an established standard protocol for neoantigen prediction or an optimized cutoff value for NAL. Previous research reported that large targeted panels are sufficient for most variant identification and NAL prediction [20, 21]. In this study, we compared a large targeted panel with WES to identify and profile NAL. Our data also showed that NAL measurement by the Med1CDx panel has a strong correlation with exome sequencing, which suggests that using a large gene panel for NAL prediction is feasible in NAL estimation. However, detailed neoantigen profiling demonstrated by the Med1CDx panel sequencing results failed to duplicate mutation estimated from WES data. Only 3% of the neoantigens identified by WES were observed through the Med1CDx panel, indicating that large targeted gene panels would not be appropriate for personalized neoantigen-based therapy development despite their convenience and advantages.

Currently, the association between NAL and genomic alterations is being studied to explore whether gene mutations can be utilized to estimate NAL for predicting the response to ICI therapies [11]. Common oncogene mutations can disrupt genome stability and alter immune status by creating novel antigens. Lyu et al. [25] found that that patients with mutant *TP53* exhibited enhanced tumor antigenicity and antigen presentation compared to those with wild-type *TP53*, and were more likely to benefit from ICI therapy. Besides common oncogenes, some rare gene mutations were also reported to cause an increase in NAL. Zhang et al. [26] reported that compared with patients with wild-type tumors, patients with *MUC16* mutant tumors have a significant increase in NAL, which is related to improved OS of patients with *MUC16* mutation containing NSCLC and melanoma. Research based on the TCGA indicated that *TP53*, *TTN*, and *MUC16* were the most frequently mutated genes in various cancers, including lung cancer [27]. Consistent with this, our study also found that these three genes have the highest mutation frequency in AD, while in SQ, *TP53* and *TTN* are the two genes

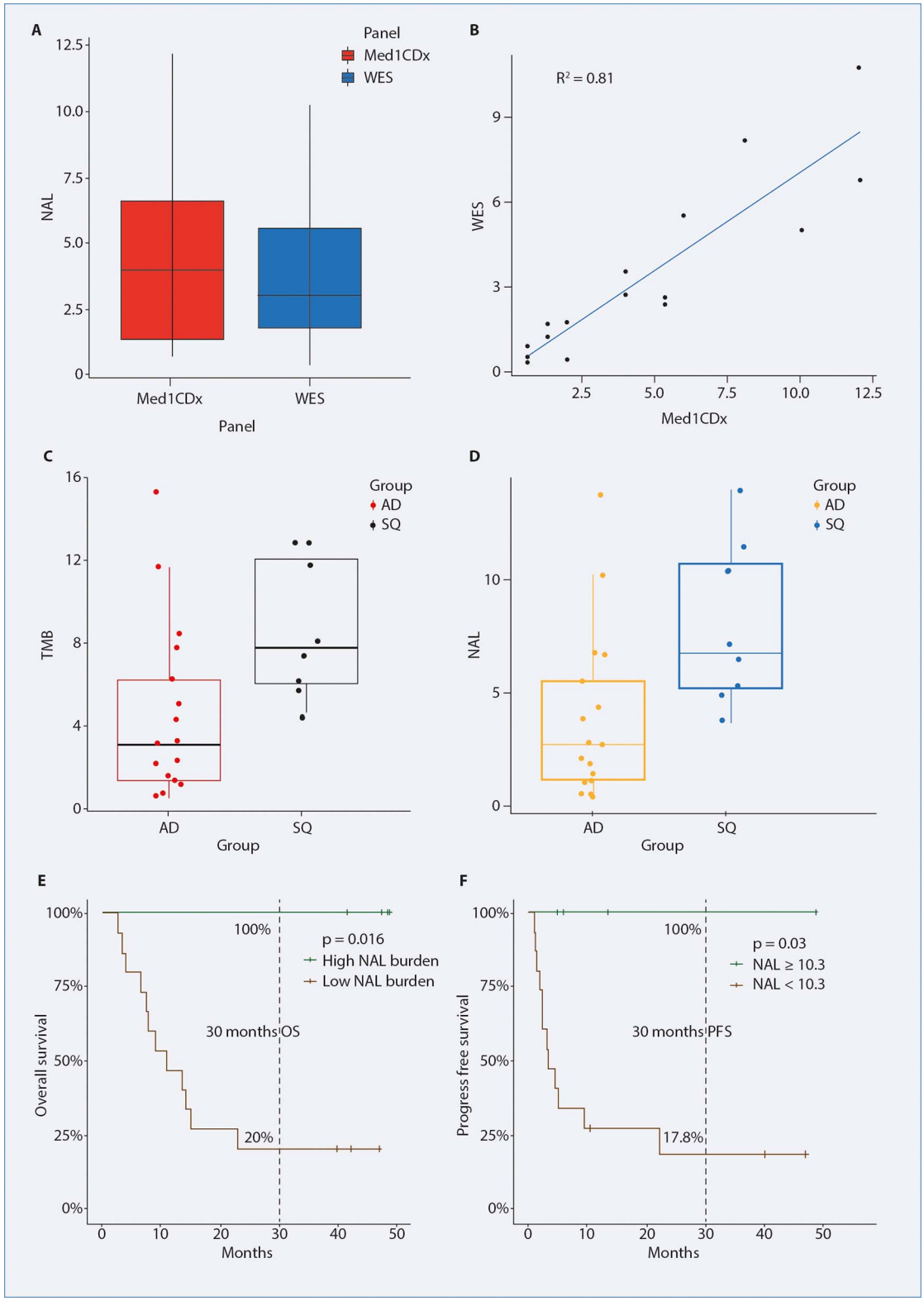


**Figure 2.** Tumor mutation burden (TMB) and tumor neoantigen load (NAL) analysis and association with clinical outcomes; **A.** NAL prediction by whole exome sequencing (WES) and Med1CDx panel; **B.** Correlation of NAL prediction by WES and Med1CDx panel; TMB value (**C**) and NAL (**D**) comparison in lung adenocarcinoma (AD) and lung squamous cell carcinoma (SQ) patients; Association of NAL with overall survival (OS) (**E**) and progression-free survival (PFS) (**F**)

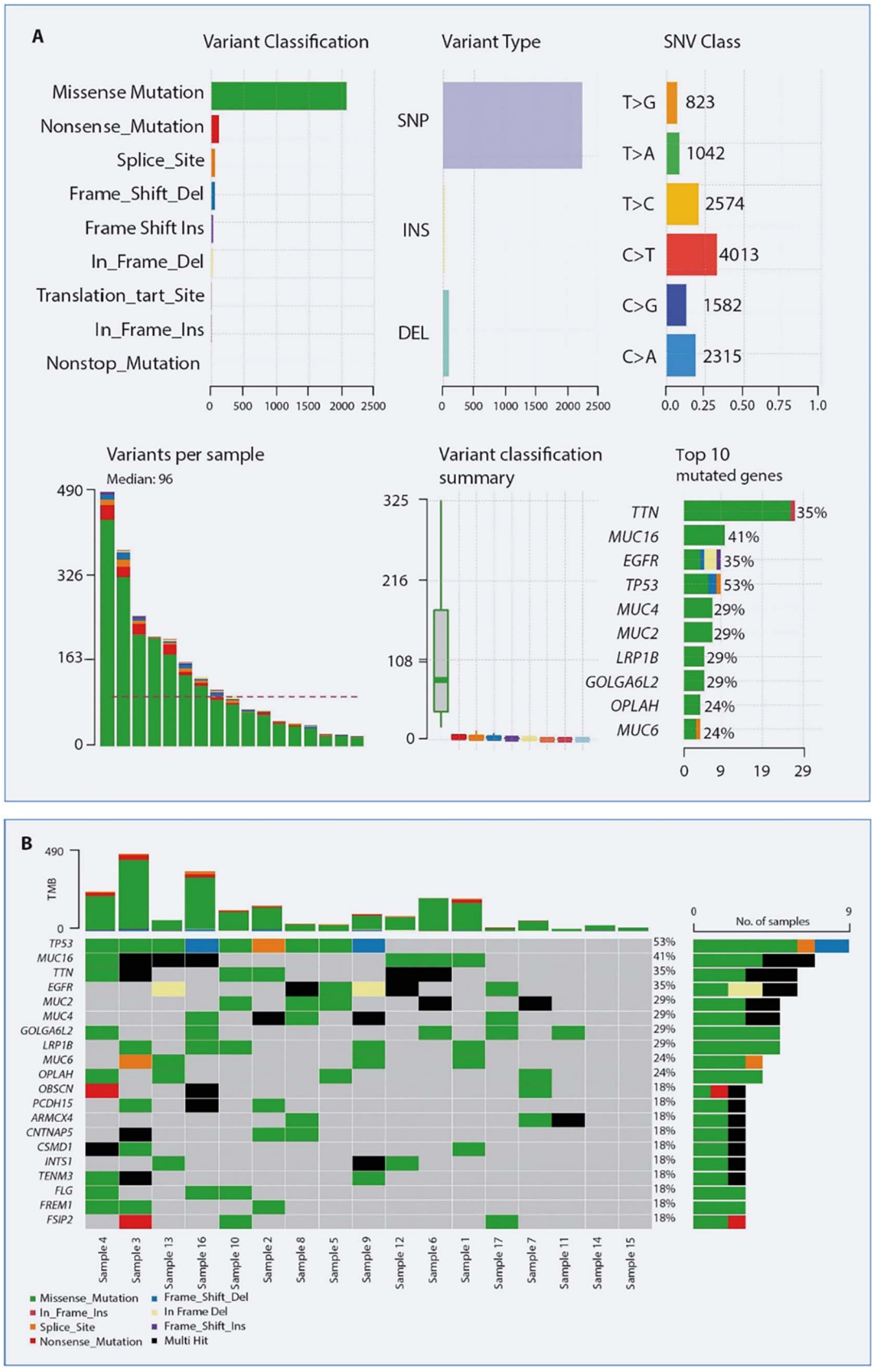


→

**Figure 3.** Mutation spectra and signatures of lung adenocarcinoma (AD) and lung squamous cell carcinoma (SQ) patients; **A, B.** Mutation spectra of AD patients; **C, D.** Mutation spectra of SQ patients; Mutation signatures of AD patients (**E**) and SQ patients (**F**)

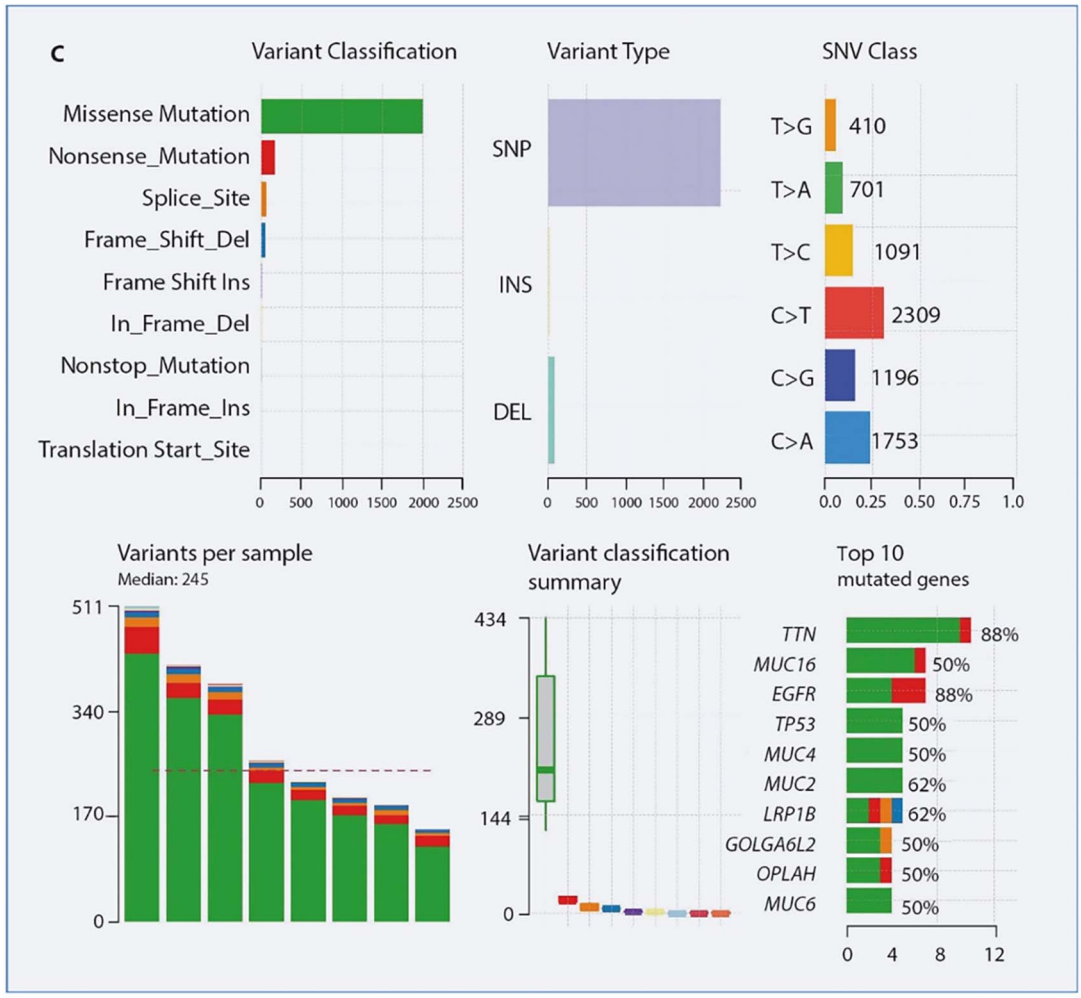


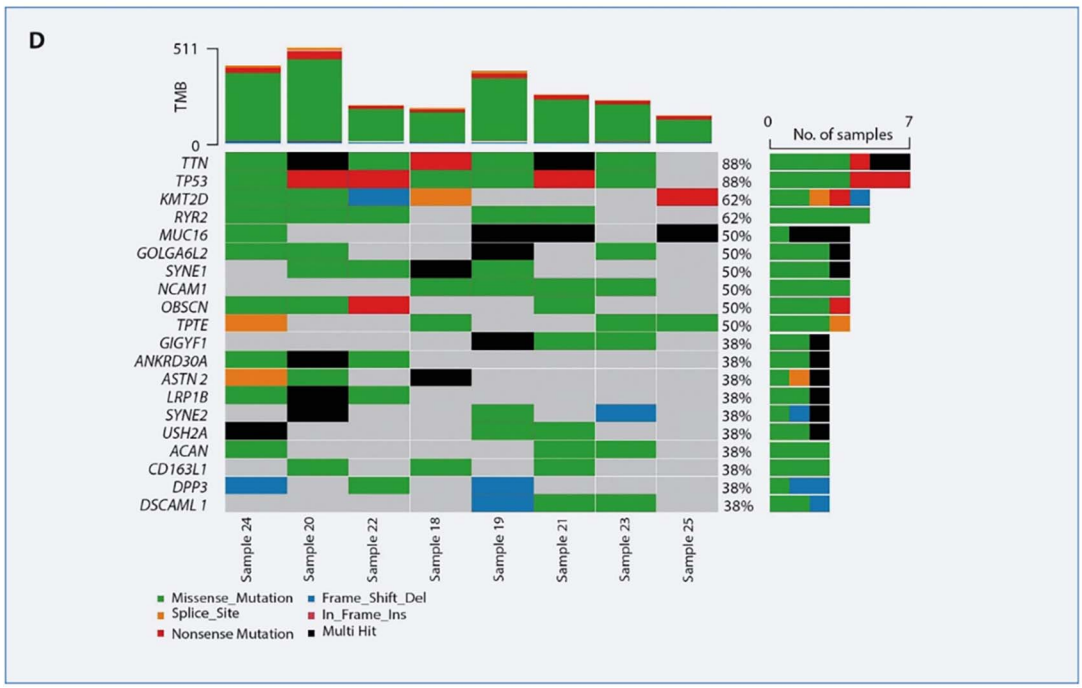


→

**Figure 3 cont.** Mutation spectra and signatures of lung adenocarcinoma (AD) and lung squamous cell carcinoma (SQ) patients; **A, B.** Mutation spectra of AD patients; **C, D.** Mutation spectra of SQ patients; Mutation signatures of AD patients (**E**) and SQ patients (**F**)

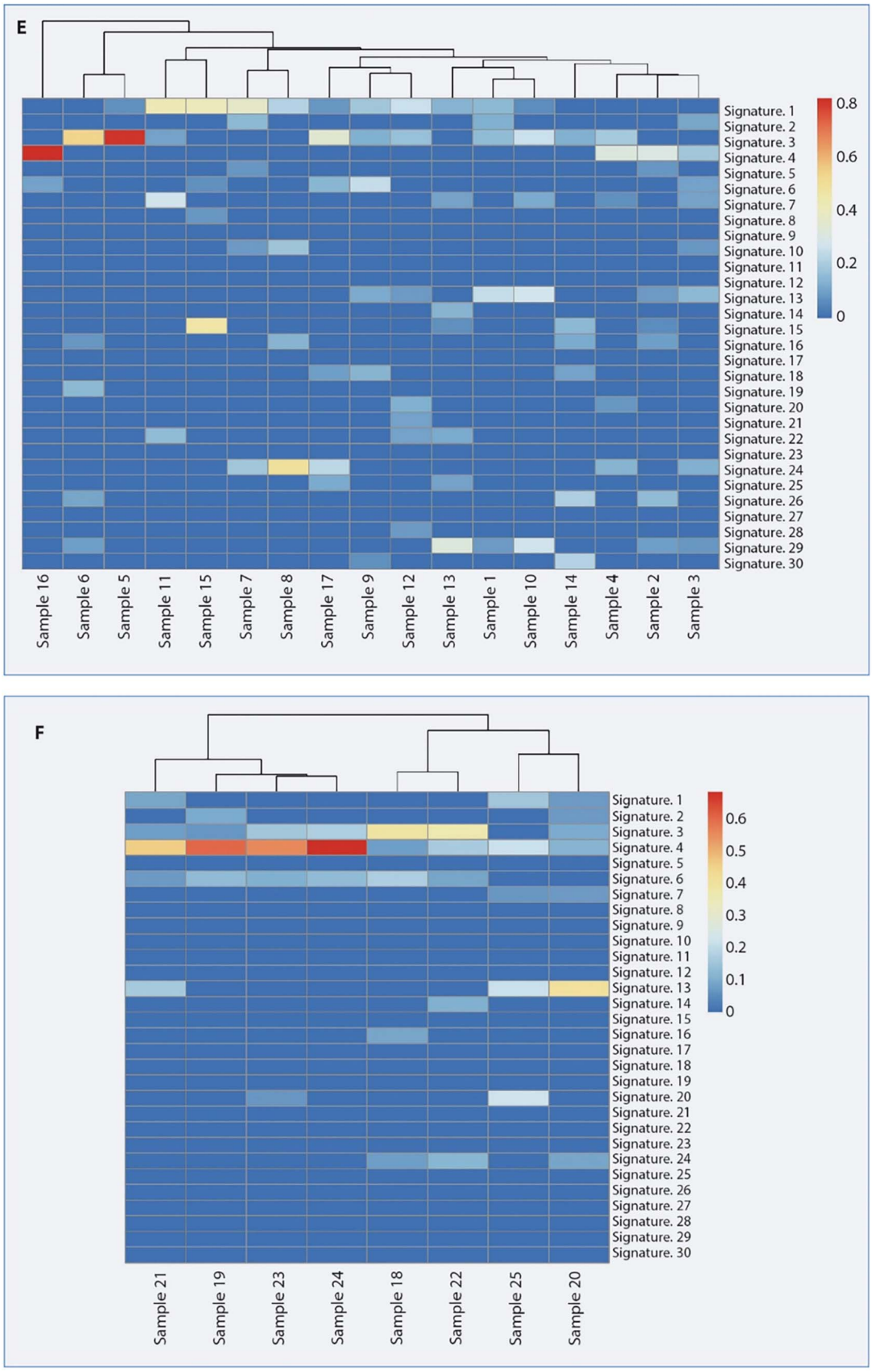


**Figure 3 cont.** Mutation spectra and signatures of lung adenocarcinoma (AD) and lung squamous cell carcinoma (SQ) patients; **A, B.** Mutation spectra of AD patients; **C, D.** Mutation spectra of SQ patients; Mutation signatures of AD patients (**E**) and SQ patients (**F**)

with the highest frequency. It is also possible that due to the high mutation frequency of *TP53* and *MUC16*, NAL is associated with the prognosis for AD and SQ in this study.

Recent studies have shown that neoantigens are not only associated with the response to anti-programmed cell death protein 1 (anti-PD-1) therapy in NSCLC patients but also are useful biomarkers for lung cancer prognosis and prediction of responses to chemotherapy in Chinese patients. A previous study analyzed NSCLC samples collected from patients treated with pembrolizumab and reported that higher NAL in tumors was associated with improved objective response and PFS [28]. Chae et al. [29] analyzed mutations in DNA repair genes using TCGA samples and found that NAL correlated with the expression of PD-1 and programmed death-ligand 1 (PD-L1) and tended to increase OS of patients with lung adenocarcinoma. High NAL is linked to DNA repair mutations and an increased number of tumor-infiltrating lymphocytes [24]. Although prognosis indication for neoantigen in lung cancer is promising, more detailed studies are still needed because contradictory results were obtained on the correlation of neoantigens with clinical outcomes of lung cancer subtypes. McGranahan et al. [19] reported that high NAL (defined as the upper quartile of NAL) was associated with significantly longer overall survival in lung AD but not SQ. Gong et al. [18] showed that higher NAL (> 2 neoantigens/Mb) exhibited better DFS for SQ but not AD patients. A benefit from adjuvant chemotherapy was correlated with lower NAL ($\leq$ 2 neoantigens/Mb). In our study, we demonstrated that high NAL is correlated with better overall survival in the AD subgroup in the clinical data retrieved from TCGA. In the 25-patient cohort, NAL could predict lung cancer prognosis in both AD and SQ patient subgroups both of which underwent a treatment strategy combining chemotherapy and immunotherapy.

Our study has a few limitations. Firstly, the study involved a relatively small sample size of participants. Given the potential implications of NAL for clinical decision-making, it is necessary to conduct further validation within a larger, independent patient cohort. Second, the method for calculating neoantigen load in this study differs from that of TCGA, although the impact on the observed trends may not be significant. In TCGA, the identification of potential neoantigen peptides was conducted using NetMHCpan v3.0 (Nielsen and Andreatta, 2016), and the neoantigen load refers to the number of pMHCs (peptides predicted to bind with MHC proteins). In our study, neoantigen prediction was carried out using the pvactools (version 1.5.8, default parameters). The NAL was calculated by dividing the total number of neoantigens by the CDS length in Mb of the WES or Med1CDx panel. Moreover, these two neoantigen algorithms were all based on the HLA-I binding prediction and did not account for other aspects of neoantigen production, including the processing and presentation of antigens, integration into the genome, and immune recognition. Last, all patients in this study were in stages III/IV, and the treatment regimens were primarily chemotherapy combined with immunotherapy. Therefore, the findings about the correlation between neoantigen and OS of AD patients are generally applicable to patients and treatments within this scope.

## Conclusions

In conclusion, our study demonstrated that NAL could be used as a useful prognosis marker to provide stratification for lung adenocarcinoma (LUAD) patient outcomes. Further studies with a larger cohort from multiple institutions are needed to validate the current data and confirm the prognostic role of NAL in different subtypes of lung cancer. The results of genomic alternation in this study also show that *TP53* and *MUC16* are among the genes with the highest mutation frequency in NSCLC and are involved in the correlation of NAL value and prognosis. In addition, we have shown that the Med1CDx panel (targeting 579 genes) can accurately assess TMB and NAL compared with WES, providing more evidence on the feasibility of using a large targeted gene panel in TMB and NAL analysis.

## Article Information and Declarations

### Data availability statement

All data are available.

### Ethics statement

The study was approved by the institutional committee board of Shanghai Chest Hospital and informed consent was taken from all the participants.

### Author contributions

X.L.: study design, results interpretation and writing of the manuscript; Y.Y.: study design, results interpretation and writing of the manuscript; W.S.: bioinformatics and statistical data analysis; X.D.: Bioinformatics and statistical data analysis; K.G.: patient clinical data analysis; M.Y.: neoantigens data analysis; Z.J.: revision of the manuscript; Y.W.: results interpretation and writing of the manuscript; Y.Z.: revision of the manuscript.

All authors have reviewed the manuscript and approved the final version.

### Funding

This work was funded by the National Key R&D Program of China (2016YFC1303300 to S.L.), the National Natural Science Foundation of China (82030045 to S.L.; 82172633 to YF.Y; 82002423 to WX.J), the Shanghai Municipal Science & Technology Commission Research Project (19411950500 to S.L.), the Shanghai Shenkang Action Plan (16CR3005A to

S.L.), the Shanghai Chest Hospital Project of Collaborative Innovation (YJXT20190105 to S.L.) the Yang Fan plan of Shanghai Science and Technology Commission Research Project (19YF1407300 to WX. J), and the Beijing Xisike Clinical Oncology Research Foundation (Y-HR2020MS-0982 to YF.Y.).

### Acknowledgements

We acknowledged MEDx (Suzhou) colleagues in technical advices.

### Conflict of interest

The authors declare no conflict interest.

### Supplementary material

There is no supplementary material.

## References

1. Sung H, Ferlay J, Siegel RL, et al. Global Cancer Statistics 2020: GLOBOCAN Estimates of Incidence and Mortality Worldwide for 36 Cancers in 185 Countries. CA Cancer J Clin. 2021; 71(3): 209–249, doi: 10.3322/caac.21660, indexed in Pubmed: 33538338.
2. Chan BA, Hughes BGM. Targeted therapy for non-small cell lung cancer: current standards and the promise of the future. Transl Lung Cancer Res. 2015; 4(1): 36–54, doi: 10.3978/j.issn.2218-6751.2014.05.01, indexed in Pubmed: 25806345.
3. Majeed U, Manochakian R, Zhao Y, et al. Targeted therapy in advanced non-small cell lung cancer: current advances and future trends. J Hematol Oncol. 2021; 14(1): 108, doi: 10.1186/s13045-021-01121-2, indexed in Pubmed: 34238332.
4. Blass E, Ott PA. Advances in the development of personalized neoantigen-based therapeutic cancer vaccines. Nat Rev Clin Oncol. 2021; 18(4): 215–229, doi: 10.1038/s41571-020-00460-2, indexed in Pubmed: 33473220.
5. Jiang T, Shi T, Zhang H, et al. Tumor neoantigens: from basic research to clinical applications. J Hematol Oncol. 2019; 12(1): 93, doi: 10.1186/s13045-019-0787-5, indexed in Pubmed: 31492199.
6. Šutić M, Vukić A, Baranašić J, et al. Diagnostic, Predictive, and Prognostic Biomarkers in Non-Small Cell Lung Cancer (NSCLC) Management. J Pers Med. 2021; 11(11), doi: 10.3390/jpm11111102, indexed in Pubmed: 34834454.
7. Thakur MK, Gadgeel SM. Predictive and Prognostic Biomarkers in Non-Small Cell Lung Cancer. Semin Respir Crit Care Med. 2016; 37(5): 760–770, doi: 10.1055/s-0036-1592337, indexed in Pubmed: 27732997.
8. Gubin MM, Artyomov MN, Mardis ER, et al. Tumor neoantigens: building a framework for personalized cancer immunotherapy. J Clin Invest. 2015; 125(9): 3413–3421, doi: 10.1172/JCI80008, indexed in Pubmed: 26258412.
9. Fancello L, Gandini S, Pelicci PG, et al. Tumor mutational burden quantification from targeted gene panels: major advancements and challenges. J Immunother Cancer. 2019; 7(1): 183, doi: 10.1186/s40425-019-0647-4, indexed in Pubmed: 31307554.
10. Büttner R, Longshore JW, López-Ríos F, et al. Implementing TMB measurement in clinical practice: considerations on assay requirements. ESMO Open. 2019; 4(1): e000442, doi: 10.1136/esmoopen-2018-000442, indexed in Pubmed: 30792906.
11. Zou XL, Li XB, Ke H, et al. Prognostic Value of Neoantigen Load in Immune Checkpoint Inhibitor Therapy for Cancer. Front Immunol. 2021; 12: 689076, doi: 10.3389/fimmu.2021.689076, indexed in Pubmed: 34992591.
12. Wang P, Chen Y, Wang C. Beyond Tumor Mutation Burden: Tumor Neoantigen Burden as a Biomarker for Immunotherapy and Other Types of Therapy. Front Oncol. 2021; 11: 672677, doi: 10.3389/fonc.2021.672677, indexed in Pubmed: 33996601.
13. Devarakonda S, Rotolo F, Tsao MS, et al. Tumor Mutation Burden as a Biomarker in Resected Non-Small-Cell Lung Cancer. J Clin Oncol. 2018; 36(30): 2995–3006, doi: 10.1200/JCO.2018.78.1963, indexed in Pubmed: 30106638.
14. Talvitie EM, Vilhonen H, Kurki S, et al. High tumor mutation burden predicts favorable outcome among patients with aggressive histological subtypes of lung adenocarcinoma: A population-based single-institution study. Neoplasia. 2020; 22(9): 333–342, doi: 10.1016/j.neo.2020.05.004, indexed in Pubmed: 32585428.
15. Jiang T, Shi J, Dong Z, et al. Genomic landscape and its correlations with tumor mutational burden, PD-L1 expression, and immune cells infiltration in Chinese lung squamous cell carcinoma. J Hematol Oncol. 2019; 12(1): 75, doi: 10.1186/s13045-019-0762-1, indexed in Pubmed: 31299995.
16. Yu H, Chen Z, Ballman KV, et al. Correlation of PD-L1 Expression with Tumor Mutation Burden and Gene Signatures for Prognosis in Early-Stage Squamous Cell Lung Carcinoma. J Thorac Oncol. 2019; 14(1): 25–36, doi: 10.1016/j.jtho.2018.09.006, indexed in Pubmed: 30253973.
17. Schumacher TN, Schreiber RD. Neoantigens in cancer immunotherapy. Science. 2015; 348(6230): 69–74, doi: 10.1126/science.aaa4971, indexed in Pubmed: 25838375.
18. Gong L, He R, Xu Y, et al. Neoantigen load as a prognostic and predictive marker for stage II/III non-small cell lung cancer in Chinese patients. Thorac Cancer. 2021; 12(15): 2170–2181, doi: 10.1111/1759-7714.14046, indexed in Pubmed: 34128337.
19. McGranahan N, Furness AJS, Rosenthal R, et al. Clonal neoantigens elicit T cell immunoreactivity and sensitivity to immune checkpoint blockade. Science. 2016; 351(6280): 1463–1469, doi: 10.1126/science.aaf1490, indexed in Pubmed: 26940869.
20. Garofalo A, Sholl L, Reardon B, et al. The impact of tumor profiling approaches and genomic data strategies for cancer precision medicine. Genome Med. 2016; 8(1): 79, doi: 10.1186/s13073-016-0333-9, indexed in Pubmed: 27460824.
21. Thorsson V, Gibbs DL, Brown SD, et al. Cancer Genome Atlas Research Network, Cancer Genome Atlas Research Network. The Immune Landscape of Cancer. Immunity. 2018; 48(4): 812–830.e14, doi: 10.1016/j.immuni.2018.03.023, indexed in Pubmed: 29628290.
22. Chalmers ZR, Connelly CF, Fabrizio D, et al. Analysis of 100,000 human cancer genomes reveals the landscape of tumor mutational burden. Genome Med. 2017; 9(1): 34, doi: 10.1186/s13073-017-0424-2, indexed in Pubmed: 28420421.
23. Van Allen EM, Miao D, Schilling B, et al. Genomic correlates of response to CTLA-4 blockade in metastatic melanoma. Science. 2015; 350(6257): 207–211, doi: 10.1126/science.aad0095, indexed in Pubmed: 26359337.
24. Zhu Y, Meng X, Ruan X, et al. Characterization of Neoantigen Load Subgroups in Gynecologic and Breast Cancers. Front Bioeng Biotechnol. 2020; 8: 702, doi: 10.3389/fbioe.2020.00702, indexed in Pubmed: 32754579.
25. Lyu Q, Lin A, Cao M, et al. Alterations in TP53 Are a Potential Biomarker of Bladder Cancer Patients Who Benefit From Immune Checkpoint Inhibition. Cancer Control. 2020; 27(1): 1073274820976665, doi: 10.1177/1073274820976665, indexed in Pubmed: 33356494.
26. Zhang L, Han X, Shi Y. Association of MUC16 Mutation With Response to Immune Checkpoint Inhibitors in Solid Tumors. JAMA Netw Open. 2020; 3(8): e2013201, doi: 10.1001/jamanetworkopen.2020.13201, indexed in Pubmed: 32845327.
27. Kim N, Hong Y, Kwon D, et al. Somatic mutaome profile in human cancer tissues. Genomics Inform. 2013; 11(4): 239–244, doi: 10.5808/GI.2013.11.4.239, indexed in Pubmed: 24465236.
28. Rizvi NA, Hellmann MD, Snyder A, et al. Cancer immunology. Mutational landscape determines sensitivity to PD-1 blockade in non-small cell lung cancer. Science. 2015; 348(6230): 124–128, doi: 10.1126/science.aaa1348, indexed in Pubmed: 25765070.
29. Chae YK, Anker JF, Bais P, et al. Mutations in DNA repair genes are associated with increased neo-antigen load and activated T cell infiltration in lung adenocarcinoma. Oncotarget. 2018; 9(8): 7949–7960, doi: 10.18632/oncotarget.23742, indexed in Pubmed: 29487705.

VIA MEDICA

REVIEW ARTICLE

Oncology in Clinical Practice
2025, Vol. 21, No. 1, 39–59
DOI: 10.5603/ocp.98716

ISSN 2450-1654
eISSN 2450-6478

# Malignant peripheral nerve sheath tumor — from genetics to multidisciplinary treatment

Anna M. Czarnecka[1,*], Paulina Chmiel[1], Paweł Sobczuk[1], Ewa Bartnik[2,3], Mateusz Spałek[1,4], Anna Szumera-Cieckiewicz[5], Marcin Zdzienicki[1], Sławomir Falkowski[1], Piotr Rutkowski[1]

[1]Department of Soft Tissue/Bone Sarcoma and Melanoma, Maria Sklodowska-Curie National Research Institute of Oncology, Warsaw, Poland.
[2]Institute of Genetics and Biotechnology, Faculty of Biology, University of Warsaw, Poland
[3]Institute of Biochemistry and Biophysics, Polish Academy of Sciences, Warsaw, Poland
[4]Department of Radiotherapy I, Maria Sklodowska-Curie National Research Institute of Oncology, Warsaw, Poland
[5]Department of Pathology, Maria Sklodowska Curie National Research Institute of Oncology, Warsaw, Poland

**Abstract**

Malignant peripheral nerve sheath tumor (MPNST) is an aggressive soft tissue sarcoma (STS); it originates from nervous tissue and typically develops in proximity to nerve trunks in the limbs and trunk. These tumors, constituting approximately 5% of soft tissue sarcomas, can either form spontaneously or arise from pre-existing neurofibromas. The majority (90%) of cases occur in individuals between the 2nd and 5th decades of life. The main risk factor for MPNST is von Recklinghausen disease (type 1 neurofibromatosis). The cornerstone of MPNST management involves radical surgical measures, specifically tumor excision within healthy tissue boundaries (wide local excision), which is complemented by adjuvant radiotherapy. In case of metastatic disease, palliative chemotherapy employing doxorubicin or a combination of doxorubicin and ifosfamide is utilized. Approximately 25–30% of patients experience clinical improvement after chemotherapy. Looking ahead, advancements in research on molecular biology may lead to the development of inhibitors demonstrating greater efficacy than traditional chemotherapy for MPNST patients. At present, ongoing clinical trials of the therapeutic management of MPNST encompass pembrolizumab, the combination of nivolumab with ipilimumab, pexydartinib (an inhibitor targeting KIT, CSF1R, and FLT3) in conjunction with sirolimus, sapanisertib (a TORC1/2 inhibitor), or LOXO-195 (an inhibitor of neurotrophic tyrosine kinase receptors NTRK type 1, 2, and 3).

**Keywords:** MPNST, malignant peripheral nerve sheath tumor, sarcoma, chemotherapy, NF1

## MPNST epidemiology

Malignant peripheral nerve sheath tumor (MPNST), previously known as malignant schwannoma or neurofibrosarcoma, is a rare neoplasm accounting for 4–5% of all sarcomas. According to the World Health Organization (WHO), MPNST should be categorized as a malignant form of tumor arising from nerve sheaths, as it originates from and displays differentiation towards any peripheral nerve sheath cell — not only Schwann cells [1]. The incidence of MPNST in the general population is approximately 0.001%, translating to a frequency of about 1 in 100 000 persons per year [2, 3]. Predominantly observed in adults, only 10–20% of cases manifest in individuals under 20 years old. Notably, half of these are associated with type I neurofibromatosis (NF1 or Recklinghausen syndrome), where MPNST arises from plexiform neurofibromas. The incidence increases to

*Correspondence: Prof. Anna M. Czarnecka, Department of Soft Tissue/Bone Sarcoma and Melanoma, Maria Sklodowska-Curie National Research Institute of Oncology, ul. Roentgena 5, 02–781 Warsaw, Poland, tel.: +48-22-546-24-55; fax: +48-22-643-93-75 (AnnaMalgorzata.Czarnecka@nio.gov.pl)
Received: 28 December 2023; Accepted: 3 January 2024;
Early publication: 27 February 2024

0.1% in this population, with an overall potential hazard of MPNST development ranging from 13% to 16%, significantly higher than the broader population. In practical terms, this implies that individuals with NF1 mutations have a risk of developing MPSNT that is 4600-fold greater than those in the general population. In male *NF1* mutation carriers, the incidence of MNST increases to approximately 70–80% [3–6]. Both sexes are affected with similar frequencies, however, men tend to develop the disease about 4 years earlier, across different populations (Caucasians, Afro-Americans, and Asians). The typical age range for individuals with sporadic MPNST falls between 30 and 60 years and for cases associated with NF1 mutations from 20 to 40 years.

Malignant peripheral nerve sheath tumors predominantly manifest in the limbs (in 30% of patients) and the trunk (approximately 50% of cases, including occurrences in the retroperitoneal space). However, they may also arise in other areas, such as the head and neck region (around 20%). Instances of intracranial MPNST not associated with cranial nerves are rare and occur sporadically [7]. Metastases typically involve the lungs, pleura, and bones during MPNST progression [3]. About 11% of these types of neoplasms form in previously irradiated areas, and the median time to development of MPNST from prior radiation is 15 years [8]. The primary factors contributing to the development of MPNST include the presence of pre-existing benign plexiform neurofibromas, prior radiotherapy, inherited genetic alterations (splicing mutations, point mutations, deletions, duplications, or insertions), and large deletions and microdeletions (< 1.5 Mb) encompassing a whole *NF1* alongside neighboring genes (escalating the risk up to 25%) [2, 5].

Generally, MPNST patients face a poor prognosis with surgical excision as the only highly effective clinical option. During treatment, metastatic disease is identified in 40 to 68% of patients, while local recurrence occurs in 40 to 65% of patients [3, 9, 10]. Furthermore, 5-year overall survival is approximately 52%, which demonstrates the aggressive course of the disease [11]. Moreover, these patients showed an increased risk of developing another cancer, including a second MPNST but also lung or breast cancers.

## MPNST biology and genetics

The genes most commonly subject to mutations in MPNST include *NF1, EED* (Embryonic Ectoderm Development), *SUZ12* (Polycomb Repressive Complex 2 Subunit), *TP53*, and *CDKN2A* (Cyclin Dependent Kinase Inhibitor 2A); their mutations are present in 87.5%, 56.1%, 32.5%, 40.3%, and 75% cases, respectively [12]. Somatic mutations in *NF1*, *CDKN2A/B*, and *PRC2* can be found in the majority of MPNST cases, irrespective of the origin. However, the genetics of those neoplasms are complex and involve not only mutations in single genes but also epigenetic changes and disorders within the tumor microenvironment contributing to malignant transformation [13]. The basis for the development of NF1 and the factor increasing the risk of MPNST are the germline mutations in the tumor suppressor gene *NF1* (neurofibromin 1) located on chromosome 17q11.2 [14]. The types of mutations that cause the NF1 phenotype include complete gene deletions, insertions, stop, and splicing mutations [15]. In about 50% of cases, the disease is due to a novel mutation and is not familial, the risk increases with the age of the father as these mutations are associated with replication errors during the mitosis of spermatocyte stem cells I (spermatogonia) [16]. The *NF1* gene is large, over 350 kbp long, and encompasses 60 exons that undergo alternative splicing, leading to a differentiated expression of isoforms in various tissues. Reduced activity of the gene's encoded protein neurofibromin, a Rat sarcoma (RAS) GTPase tumor suppressor, leads to the activation of the RAS kinase and subsequently of effector pathways correlated, among others, with malignant transformation. The level of neurofibromin expression is inversely correlated with the extent of RAS activation and its related signaling pathways, as well as the responsiveness of cells to their inhibitors [17]. Active RAS kinase leads to activation of two main effector pathways: the MAPK RAS/RAF/MEK/ERK pathway and the Akt/mTOR pathway, which control cellular functions, including responses to external stimuli like growth factors or chemokines [18, 19]. Both these pathways have been described as activated in many types of sarcomas, including MPNST [20]. Furthermore, inhibition of RAS kinase was shown to suppress MPNST cell growth both *in vitro* and *in vivo* [21]. Among others, it has been demonstrated that elevated expression, indicated by positive IHC staining of the Akt, mTOR, and pS6RP proteins is associated with shorter overall survival (OS) in patients diagnosed with MPNST [22].

Understanding genetic data is crucial in considering the use of the inhibitors of the previously mentioned pathways, e.g. mTOR inhibitors, in MPNST therapy. In cell-line-based *in vitro* experiments, these drugs markedly restrained the proliferation, invasiveness, and migration of MPNST cells [22, 23]. Nevertheless, it is essential to be aware that the activation of the mentioned pathways is not exclusively contingent on the absence of functional neurofibromin. It can also be upregulated due to activating somatic mutations in specific components of the pathways or their regulators [12, 24]. Given the heterogeneous nature of the interactions and the potential for concurrent activating mutations in multiple genes, the application of selective inhibitors

targeting RAS-dependent pathways might prove ineffective in clinical practice. This is exemplified by sorafenib, which functions as a RAS/Raf inhibitor. [25]. Single cases of successful treatment with sorafenib have been published, in the case of metastatic disease [26], a phase II trial of both sorafenib in monotherapy, also in combination with dacarbazine (S 400 mg BID and D 1000 mg/m$^2$ q3w), did not show a high percentage of responses in MPNST patients (NCT00217620) [27]. Furthermore, the indicator of the activation of the RAS/RAF/MEK/ERK pathway is persistent phosphorylation of ERK (Extracellular signal-regulated kinase) and MEK (Mitogen-activated protein kinase). The activation of MEK enhances invasiveness, migration, and angiogenesis while experimental deactivation of MEK inhibits the development of MPNST in an *in vitro* model [24, 28]. Administering a MEK inhibitor (PD0325901) led to the suppression of growth in both plexiform neurofibromas and MPNST in mice [29], and the activity of this inhibitor is increased by retinoids, including ATRA (all-trans retinoic acid) [30]. The effectiveness of the MEK inhibitor has been confirmed in *in vitro* studies in combination with a double mTOR1/2 inhibitor INK128 [17]. Also, there are a few cases of potential application of other inhibitors specific to MEK, such as trametinib [31, 32]. This categorizes MEK inhibitors among the potential medications for advanced stages of MPNST that necessitate systemic intervention. Presently, an ongoing phase II trial, SARC031 (NCT03433183), is assessing the efficacy of the MEK inhibitor selumetinib (AZD6244) in combination with the mTOR inhibitor sirolimus for patients with MPNST. It is noteworthy that even with the dual targeting approach, no substantial clinical outcomes were observed, suggesting the presence of additional mutations crucial to the carcinogenesis process. Results of the SARC016 clinical trial of the combination of bevacizumab and everolimus (mTOR inhibitor) showed a clinical benefit rate [(CBR); the number of patients experiencing a complete response (CR), a partial response (PR), or stable disease (SD) for $\geq$ 4 months] of 12%, which was evaluated as ineffective [33]. The SARC023 (NCT02008877) trial with the mTOR inhibitor everolimus and the Hsp90 inhibitor also showed no efficacy for this indication [34]. Molecular analyses, including microarray studies, may prove beneficial in the future for assessing resistance mechanisms and choosing the most effective therapy for MPNST patients [35]. Concerning poor clinical outcomes of the above-mentioned trials, initial data indicated that the combination of inhibitors of various kinases — canertinib (inhibitor of EGFR, Her2, and ErbB4) and sorafenib — inhibits the proliferation and decreases the viability of MPNST cells, which is not true for monotherapy with sunitinib, crizotinib, or sorafenib [36]. Though the development of the canertinib molecule did not lead to clinical success because of its toxicity, further attempts at targeted therapy are ongoing because of the changes in the expression of the genes characteristic for MPNST. Although *NF1* gene inactivation with loss of neurofibromin expression is a characteristic mutation of MPNST, bi-allelic *NF1* loss is insufficient for malignant transformation [37]. This was confirmed in mouse models, in which *NF1* gene inactivation in Schwann cell precursors resulted in plexiform neurofibroma development. Malignant peripheral nerve sheath tumor development requires additional genetic alterations [38]. As mentioned previously, mutations in such genes as *TP53, CDKN2A, EGFR*, and *SUZ12* have been reported as secondary alterations supporting malignant progression [39–42]. Arranging the disorders into a progression model based on current research, it seems most likely that *CDKN2A* mutations have been found in almost all cases of atypical plexiform neurofibromas, presenting the first step of progression [43]. Furthermore, *TP53, EGFR*, and *SUZ12* alterations are common in MPNST. However, mutations in these genes do not occur in benign lesions, suggesting that these alterations represent later steps in progression. The *SPP1* (osteopontin) gene was found to show significant differences in expression between benign neurofibromas and MPNST (85-fold higher in MPNST) and switching it off decreases the proliferation and migration of MPNST cell lines. Furthermore, the expression of SPP1 is controlled by the Wnt pathway, whose involvement in the progression to MPNST has also been demonstrated [44]. Additionally, numerous other genetic perturbations have been described in MPNST so far — on average 18 chromosome aberrations were observed, among them 8q, 7p, and 17q duplications, and the loss of 9p, 11q, 13q, or 17p are the most prevalent [45]. Moreover, numerous chromosome aberrations have been identified in MPNST resulting in the duplication of such genes as *LOXL2, MET*, *BIRC5, EGFR, DAB2, MSH2, CCNE2, DAB2, DDX15, CDK6, HGF, ITGB4, KCNK12, LAMA3*, and *PDGFRA*; and the deletions of *GLTSCR2, CDH1, CTSB, GATA3, SULT2A1, EGR1, GLTSCR2, MMP13, p16/INK4a, RASSF2, HMMR/RHAMM, LICAM2, NM-23H1* and *TP53* [46]. Among genes that undergo amplification in MPNST, attention should be also paid to topoisomerase 2a (TOP2A), which, as a main target of doxorubicin, takes part in DNA replication, broadly implicated in STS treatment. TOP2A amplification was confirmed in a large group of patients and correlates with shorter survival and metastasis occurrence [47]. The level of TOP2A expression in MPNST can be even 24-fold higher than in benign neurofibromas and correlates with sensitivity to doxorubicin [48]. Assaying TOP2A expression

could potentially be useful to determine sensitivity to chemotherapy and its choice.

In consequence, the activation of receptor tyrosine kinases can also lead to the activation of the above-mentioned pathways [49]. Among regulatory tyrosinase kinases, an important role is played by the epidermal growth factor receptor (EGFR), whose overexpression in an animal model was sufficient for transformation of neurofibromas into MPNST [50]. The observations were not confirmed in clinical trials, as EGFR inhibitors did not demonstrate effectiveness in MPNST [51]. Interestingly, the sonic hedgehog (SHH) and WNT/ß-catenin/CCND1 pathways were also found to be involved in MPNST pathogenesis, dividing these tumors into two potential groups susceptible to different targeted treatments. SHH pathway inhibition was shown to prevent growth and malignant progression [52]. Surprisingly, in MPNST in contrast to other STS types, a decrease in the expression of many genes encoding proteins (mRNA) and microRNA is observed. New research also confirmed these observations, showing that the majority (82 out of 90 evaluated) of miRNAs were found to be downregulated in the MPNST group in comparison to the plexiform neurofibromas [53]. This deregulation appears to depend on the inactivation of the p53 protein [54]. This is also most probably caused by the hypermethylation of gene promoters and the activation of inhibiting microRNAs, such as among others miR-29c [55, 56]. The gene hypermethylation pattern has also been proposed as a diagnostic MPNST marker, and a specific methylation pattern (H3K27me3) distinguishes MPNST from tumors of the neurofibroma, schwannoma, nerve sheath myxoma, or ganglioneuroma type. Moreover, sporadic MPNST cases without epigenetic inactivation (hypermethylation) of *NF1* after a repeat of the pathomorphological analysis turned out to be another type of STS or cellular Schwannoma [57]. Taking into consideration the confirmed role of the above-mentioned *SUZ12* and *EED* in gene silencing, there are promising investigations of drugs targeting epigenetic regulators. The Histone Deacetylase 1 (HDAC) inhibitor I/II romidepsin (trade name *Istodax*) shows a strong synergism in combination with the double mTORC1/2 inhibitor (INK128) on MPNST cell lines [17]. Patients with MPNST were included in a phase II trial with panobinostat (trade name Farydak) — a non-selective HDAC inhibitor — however, this drug did not show high activity in STS patients, as only 12.5% were progression-free after six months of treatment [58]. It was also indicated that typical chemotherapy based on doxorubicin and ifosfamide [regimen ifosfamide (AI) with a 5 g/m$^2$ total dose of ifosfamide and 60 mg/m$^2$ doxorubicin per cycle] could be efficient in MPNST patients with the aforementioned loss of H3K27me3 [59]. Contradictory data stated that even in the absence of SUZ12, the main catalytic subunits retain their epigenetic functions. Genetic and pharmacological analyses established that EZH2 (one of the main catalytic subunits) is functionally stable, excluding a PRC2-independent function. Moreover, in the absence of EZH2, EZH1 is overexpressed and functionally compensates for the loss of function [60].

The tumor microenvironment, characterized by NF1 heterozygosity, plays a role in the development of both plexiform neurofibromas and their transformation into malignancy through the secretion of growth factors, chemokines, and proinflammatory factors. This occurs via an intricate network of interactions between the tumor and the surrounding stromal cells. The tumor cells secrete c-KIT ligand and transforming growth factor *beta* (TGF-B), which draw in mast cells and fibroblasts, respectively. The mast cells release the platelet-derived growth factor (PDGF) and the vascular epidermal growth factor (VEGF), which through fibroblast and epithelial cell recruitment increase tumor growth and angiogenesis. Studies showed that inhibition of VEGF can result in a 50% reduction of xenograft tumor growth in comparison to controls, mainly due to a decrease in angiogenesis and an increase in apoptosis. However, these results were not confirmed in clinical trials [61]. Moreover, autocrine secretion of chemokines CXCR4 and CXCL12 enhances the progression of these changes [2]. Hypoxia-inducible factor (HIF-1a) expression is detected in around 75% of MPNST cases and is linked to an adverse prognosis [62]. Moreover, MPNSTs are characterized by scant PD-L1 expression, or lack of expression, and significant infiltration by CD8+ lymphocytes, which limits the possibility of using immunotherapy [63]. The activation of the tumor microenvironment and genetic alterations happen concurrently, and when these processes coincide, benign tumors undergo transformation into MPNST.

## Histopathology

Malignant peripheral nerve sheath tumors originate from neuroectodermal cells, especially from nerve roots, plexuses, and both cranial and peripheral nerves. Intracranial MPNSTs develop from multipotential precursor cells located within the brain parenchyma [3, 4]. The presence of nerve elements or the occurrence of the tumor in individuals with *NF1* mutations raises suspicion of MPNST. However, establishing a definitive diagnosis can often be challenging. The nerve sheath from which the tumor originated can be found in at most 39%-56% of patients. Notably, MPNST exhibits the highest rate of incorrect initial histological diagnoses among all STS, reaching up to 78%, particularly when diagnosed outside of reference centers for sarcoma treatment. To qualify an STS as MPNST, the tumor must meet one of three

specific criteria: 1) development in a peripheral nerve, 2) development from nerve sheaths of a prior benign neoplasm (neurofibroma or others), or 3) histological characteristics of differentiated Schwann cells can be identified in the tumor [3, 64, 65].

Malignant peripheral nerve sheath tumors may occur in the classical form — spindle cell shaped, but also in the pleomorphic and epithelioid (epithelial) form [3]. Malignant peripheral nerve sheath tumors are characterized by a diverse morphology. In histological sections, MPNSTs present as white to flesh-colored lesions. The classical form of MPNST is similar to fibrosarcoma, as it is composed of bundles of spindle-shaped cells. Prominent histological characteristics of MPNST involve the existence of interwoven strands displaying varying cell counts, vascular patterns reminiscent of hemangiopericytoma, cell arrangements forming palisades or rosettes, subendothelial accumulation of neoplastic cells, regions displaying geographic necrosis, and perineural or intraneural dissemination when linked with nerves. It is crucial to emphasize that these characteristics are not specific. Normal properties of Schwann cells (nerve sheath) are also observed in preparations. Malignant peripheral nerve sheath tumor cells typically exhibit comma-shaped or wavy nuclei, nearly invisible cytoplasm, and often have a plexiform arrangement in tumors. When conducting a differential diagnosis consideration should be given to other types of sarcomas (such as sarcoma synoviale, leiomyosarcoma, rhabdomyosarcoma, and dedifferentiated liposarcoma), mesenchymal benign tumors (neurofibroma), and nonmesenchymal tumors, particularly melanoma [3, 66].

For MPNSTs arising from neurofibromas, it becomes crucial to differentiate typical and atypical neurofibromas and MPNSTs, as well as low and high grades of malignancy. The grading is based on the *Fédération Nationale des Centres de Lutte Contre le Cancer* (FNCLCC) system, considering the differentiation and intensity, mitotic index degree, and intensity of necrosis. Tumors identified as atypical neurofibroma or low-grade MPNSTs (FNCLCC 1, grade II as per WHO classification) are occasionally collectively categorized as atypical neurofibromatous neoplasm of uncertain biologic potential (ANNOUBP) and managed as precursor alterations to MPNST. These tumors exhibit cellular atypia, heightened cellularity with low mitotic activity (fewer than 5 mitoses per 10 fields of view) [67]. On the contrary, MPNSTs with a high malignancy grade (FNCLCC 2–3, III–IV per WHO classification) exhibit cellular atypia, elevated cellularity, the existence of necrotic foci, and a high level of mitotic activity (exceeding 10 per 10 high-power fields). Tumors demonstrating mitotic activity ranging from 5 to 10 per 10 high-power fields may fall into an intermediate category [67].

In contrast to other types of sarcomas, MPNSTs lack pathognomic mutations or molecular markers (rearrangements, mutations) allowing a definitive histopathological diagnosis, as in the Ewing sarcoma or malignant synovial tumor. A comprehensive panel of analyses and staining is required to differentiate MPNST from other STS. It includes IHC for S-100, Leu-7, EMA, vimentin, HMB-45, cytokeratins. Additionally, assessing the presence of the NF1 mutation in tumor material may be helpful. In patients with a confirmed NF1 mutation, any spindle cell sarcoma should be treated as potential MPNST, and additional staining is used for an eventual confirmation of this diagnosis [66].

A typical panel of staining for differential diagnosis for MPNST encompasses immunohistochemical (IHC) evaluation of the expression of endothelial cell marker (CD34), Schwann cell marker (S100), tumor suppressor (TP53), a protein inhibiting the cell cycle that is inactive in MPNST (p14INK4a), and cell proliferation marker (Ki-67) proteins [68]. Proper validation of marker expression can establish a diagnosis, but the staining pattern does not allow for patient stratification in selection of an appropriate treatment regimen. However, some of the IHC markers can be correlated with MPNST pathogenesis. For instance, cyclin D1 and osteopontin were associated with a positive NF1 status [69]. In some cases, an analysis of tumor ultrastructure may be necessary to establish the nerve sheath origin of the tumor [2]. Notably, the expression of the typical markers varies depending on the differentiation degree. For instance, S100 is a characteristic marker for Schwann cells; expression can be present or absent in undifferentiated MPNSTs [2]. Some MPNSTs, especially high-grade ones, can be positive for p53 protein staining; this is more commonly positive in tumors associated with NF1 than in sporadic MPNSTs [2, 70]. Employing additional staining with muscle markers to confirm or exclude the rhabdomyoblastic component [malignant triton tumors (MTT)], which serves as a negative prognostic factor (linked with shorter time to metastasis and shorter overall survival), is also beneficial for a differential diagnosis [71] (Fig. 1).

Novel markers that could help in better identification and stratification of patients with an MPNST diagnosis are still being sought. Though numerous potential markers occurring in most MNPST cases have been described, their implementation in routine histopathological diagnosis requires prior verification on larger patient cohorts in multicenter studies. Promising results concern markers associated with perturbations in the pathway linked to remodeling the spatial structure of chromatin of the Polycomb (PcG) type, i.e. the polycomb repressive complex 2 (PRC2)/polycomb repressive complex 2 subunit (SUZ12); their mutations have been found in 70%

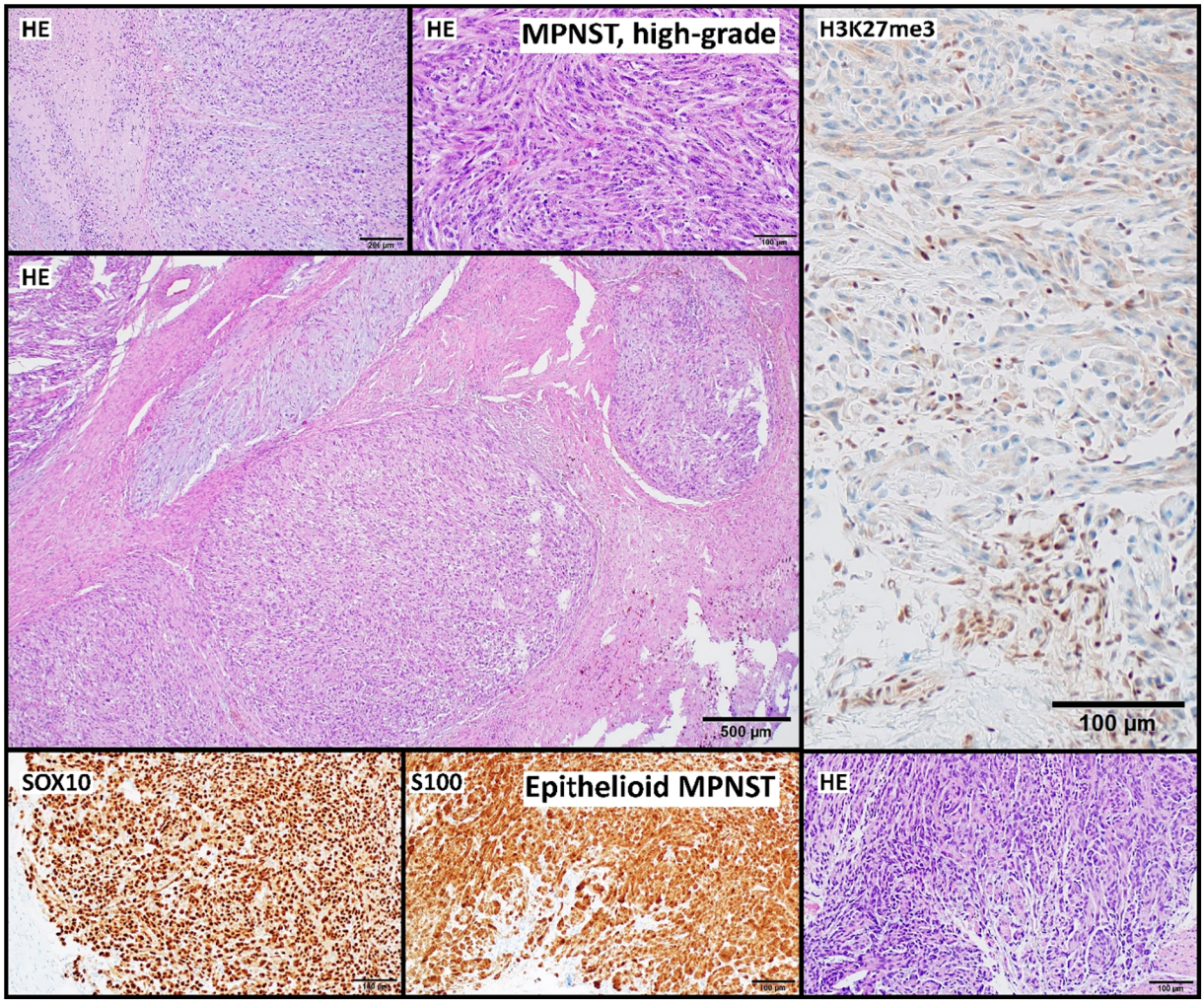


**Figure 1.** Malignant peripheral nerve sheath tumor (MPNST). The high-grade MPNST is composed mainly of spindle cells, with a mixture of hypo- and hypercellular areas and pleomorphism. Mitotic activity is focally seen, and the immunohistochemical methylation of lysine 27 of histone H3 (H3K27me3) loss is characteristic (see internal positive control in vessels and lymphocytes); epithelioid MPNST is a huge diagnostic challenge since it highly expresses Schwann cell marker (S100) and SOX10 and melanoma must be excluded; loss of INI1 expression supports the epithelioid MPNST diagnosis

of MPNSTs, but not in benign plexiform and atypical neurofibromas. The loss of methylation of lysine 27 of histone H3 (H3K27me3) can be a histological surrogate for PRC2. Complete loss of H3K27me3 is observed in about 50% of MPNSTs and seldom occurs in other tumors with similar morphology, which allows for confirmation of MPNST diagnosis with high sensitivity (98.7%) [72]. Furthermore, loss of H3Kme3 was found to be correlated with immunopositivity of myogenic immunohistochemical markers, such as desmin, while in cases with preserved expression, the staging revealed a correlation to neurogenic markers. After adjusting these findings to patients' outcomes, there has been a strong trend indicating involvement of H3Kme3 loss in aggressive skeletal muscle differentiation of MPNST [73] However, the specificity of this method is low (54.2%) which does not allow exclusion of MPNST when loss or partial loss of H3K27me3 is observed; also this marker can help define the histological subtype of MPNST [72].

In conclusion, the heterogeneous histopathological characteristics of MPNST demand a comprehensive approach, considering factors such as atypical neurofibromas, varying grades of malignancy, and the absence of pathognomonic molecular markers. Accurate diagnosis necessitates a thorough panel of analyses, including IHC for specific markers, and in some cases, ultrastructure analysis. The expression of markers and potential variations in staining patterns underscore the complexity of MPNST diagnosis, reinforcing the need for a multidisciplinary diagnostic strategy in clinical practice.

While certain histopathological markers can assist in predicting the response to specific treatments, they

are not employed in the diagnosis of MPNST due to their occurrence in various tumor types. Consequently, these markers are discussed in the section about specific types of treatment.

## Diagnosis

The clinical manifestation of MPNST is characterized mostly by the tumor's domination. The ailments experienced by patients depend on tumor localization. Given its development in strict association with nerve trunks, it frequently compresses them, which results in neurological symptoms and pain peripheral to the tumor. Significantly, sensory disturbances, weakness, and pain symptoms may manifest several months before the tumor becomes palpable, particularly in locations that are challenging to assess clinically, such as the retroperitoneal space. Individuals with MPNST commonly exhibit a swiftly enlarging, detectable mass, often associated with pain or neurological symptoms like paresthesia or muscle weakness. However, when the lesions are situated in the retroperitoneal or chest areas, diagnosis is frequently delayed due to nonspecific symptoms or the difficulty of detecting the tumor through physical examination.

Magnetic resonance imaging (MRI) is a widely employed imaging modality for STS, with the ongoing refinement of MRI technology contributing to enhancements in its sensitivity and specificity for tumor diagnosis. Magnetic resonance imaging is the best imaging method, allowing evaluation of the size and infiltration by the lesion and planning an appropriate surgical intervention, regardless of the localization of the tumor. In a recent meta-analysis incorporating fifteen studies involving 798 lesions, MRI demonstrated pooled sensitivity of 68%, and specificity of 93%, with various feature combinations. Notably, incorporating diffusion restriction significantly improved these metrics to 88% and 94%, respectively [74]. Furthermore, some studies showed a beneficial role of MRI in differentiating between benign and malignant peripheral nerve sheath tumors (PNSTs), facilitating appropriate treatment planning. The study evaluated differential diagnosis of malignant or benign PNSTs in the trunk or extremities, utilizing conventional contrast-enhanced MRI and diffusion-weighted imaging (DWI). The investigation showed significant distinctions in tumor size, margin, perilesional edema, and specific differences between benign and malignant PNSTs on both MRI and DWI. Notably, the absence of a split fat sign and mean apparent diffusion coefficient (ADC) values emerged as robust imaging indicators associated with MPNSTs [75]. Positron emission tomography (PET) also seems beneficial in diagnostics. Differentiating benign lesions from MPNSTs is possible using fludeoxyglucose (FDG) uptake — in most of the studies, benign lesions depict no or low FDG uptake, whereas malignant PNTs demonstrate moderate to high FDG accumulation. In general, standard uptake values (SUV) characteristic for MPNSTs oscillate around 4.1–10.4, with a cut-off value of 6.1 separating benign from malignant tumors with sensitivity of 94% and specificity of 91% [76, 77]. Furthermore, PET/CT can also be used for grading, biopsy guidance, and prognostic purposes in MPNST [78].

Conducting a biopsy for diagnostic purposes is a customary oncological procedure. Nevertheless, in instances of MPNST suspicion, its validity remains a subject of debate. Several studies highlight potential risks associated with nerve damage and enduring complications, with reports of persistent pain in approximately 30% of patients after biopsy [79]. Despite these concerns, biopsy has demonstrated notable efficacy in diagnosis, exhibiting almost 100% correlation with histological images of samples following surgical resection [80]. Furthermore, it has shown commendable 94% effectiveness in distinguishing between benign and malignant lesions [81]. There is no evidence supporting the superiority of an open biopsy over a core needle biopsy. The selection of the method primarily relies on the tumor's location and the preferences of the surgeon and patient. While a fine needle aspiration biopsy has limited utility in diagnosing the primary lesion, it proves valuable in identifying local recurrence or metastases [82]. In most cases, at the moment of MPNST diagnosis, the tumors are > 5 cm in size, and up to half of the patients experience metastasis, either to lymph nodes or distant sites, most frequently to the lungs or liver [9]. For this reason, in addition to visualizing the primary lesion, the presence of metastases should be excluded by conventional imaging techniques such as ultrasonography (USG), X-rays, computed tomography (CT), or positron emission tomography-computed tomography (PET-CT).

Most of the challenges in diagnosis involve patients with NF1 disease, in whom it is fundamental to evaluate the localization of neurofibromas, especially those that are inaccessible to physical examination, and to monitor their potential transformation to MPNST. Type I neurofibromatosis disease symptoms include numerous neurofibromas skin discoloration with a milk coffee color (*café au lait* spots), bone dysplasia, and Lisch nodules on the iris [83, 84]. Tumors situated in more central regions (the torso and proximal parts of the limbs) and those linked with large nerve trunks pose an increased risk of malignant transformation. It is crucial to initially assess the location and size of all benign lesions due to a substantial correlation between their quantity, the total volume of neurofibromas, and the likelihood of transformation into MPNST [85]. The optimal approach

involves whole-body magnetic resonance imaging, though it may not provide a definitive differentiation between MPNST and benign lesions [86], thus it is not an effective method for monitoring changes. However, recently an addition of DWI in diagnosis showed promising results, MPNST demonstrated significantly lower diffusivity ($p < 0.0001$) compared with benign lesions, and evaluation of this functional parameter resulted in 92% sensitivity and 98% specificity in characterizing NF1 patients' lesions [87]. Currently, there is an ongoing clinical trial aiming to characterize pre-malignant lesions in pediatric patients with NF1 syndrome (NCT04763109) [88]. Notably, Ferner et al. have shown that PET with FDG has good effectiveness in distinguishing benign neurofibromas and MPNST in NF1 patients. The sensitivity and specificity of PET-CT with FDG were 89% and 95%, respectively [89]. However, $SUV_{max}$ does not correlate with the grade of the neoplasm. These authors recommend the removal of tumors with $SUV_{max} > 3.5$, and in the case of an SUVmax between 2.5 and 3.5, treatment decisions should be taken after critical analysis including clinical data [89]. A meta-analysis involving 13 trials of PET-CT indicated that sensitivity ranges from 91% to 100%, while specificity between 72% and 95%. The optimal cut-off point for $SUV_{max}$, ensuring the highest sensitivity and specificity, varies from 3.1 to 6.1. However, existing data do not provide an unequivocal cut-off point for distinguishing between benign and malignant lesions. Some analyses suggest the potential to reduce false-positive results by incorporating delayed imaging (after 4 hours) [89, 90] or normalization of the $SUV_{max}$ coefficient to glucose capture by the liver or the body's dry weight [90, 91]. Also, monitoring of plexiform neurofibromas (PN) in NF1 patients showed efficacy, even in the case of asymptomatic patients, malignant lesions were detected with 100% sensitivity [92]. Polish guidelines on oncological diagnosis also recommend using PET tomography for this objective [93]. Nevertheless, there is still a debate regarding the superiority of these two imaging methods, as in some studies DWI performed better and yielded a specificity of 94% while FDG-PET/CT offered a specificity of 83% [94]. Ongoing research is exploring additional parameters that can be assessed in PET, such as metabolic tumor volume (MTV) and total lesion glycolysis (TLG), both of which demonstrate promising results. However, at the moment, there is no evidence justifying their routine use in practice [95]. Recently, a new non-invasive method to distinguish benign lesions from MPNST was proposed. Analysis of plasma cell-free DNA (cfDNA) originating from tumors showed that this fraction is lower in healthy patients and patients with benign lesions compared to patients with MPNST. Furthermore, these groups also differed in the length of cfDNA in the tumor fraction in plasma. This method showed 86% pretreatment accuracy (91% specificity, 75% sensitivity) [96].

Among symptoms that should lead to more in-depth identification of individuals with NF1 condition are new neurological disturbances, problems with sphincter control, a change in the neurofibroma's texture from 'soft' to 'hard,' rapid growth, or persistent pain lasting for more than one month and affecting sleep [97]. Patients with radiotherapy in their medical history, prior diagnosis of MPNST, and plexiform neurofibromas localized within the brachial plexus, lumbosacral plexus, sacral nerve roots, and the abdomen, and the lesser pelvis should undergo more careful surveillance, as these factors are associated with a more frequent transformation [89, 97].

## Treatment of localized disease

### Neoadjuvant treatment

Malignant peripheral nerve sheath tumors pose a therapeutic challenge due to limited options. The primary approach involves radical surgical excision with clear margins, i.e. R0 resection. Survival can be obtained solely following surgical excision with negative margins of the primary tumor, and if metastases are present also surgical removal of metastatic foci [4]. However, the propensity for local recurrence and metastasis post-surgery requires additional interventions. In this context, both radio- and chemotherapy have become integral components of therapy for risk reduction. [98]. If there is a risk of the tumor being non-resectable based on medical information and diagnostic imaging, neoadjuvant treatment should be considered. For this reason, presurgical treatment with neoadjuvant chemo- or radiotherapy may be a justified procedure in patients with tumors > 5 cm. Neoadjuvant treatment is also recommended for patients in whom rapidly decreasing the tumor mass is important, e.g. with tumors compressing surrounding nerves and causing considerable pain. Information about neoadjuvant chemotherapy in MPNST is constrained to retrospective examinations of individual cases and case series. Certain analyses indicate that R0 resections can be achieved after chemotherapy in patients with initially nonresectable tumors. A similar outcome was observed in the analysis of pediatric patients from centers in Germany and Italy, where complete resection was possible in 11 of 20 MPNST patients after neoadjuvant chemotherapy [99]. At present, there are no randomized trial data specifically assessing neoadjuvant chemotherapy for MPNST. However, in mixed populations of STS patients, meta-analyses indicate slight improvements in overall survival (OS) following neoadjuvant chemotherapy [9].

The multicenter phase II clinical trial SARC006 (NCT00304083) compared the effectiveness of neo-

adjuvant chemotherapy with etoposide, doxorubicin, and ifosfamide in individuals with nonresectable MPNSTs (grade III–IV), in which patients received 2 cycles of chemotherapy according to the AI regimen (ifosfamide and doxorubicin) and then 2 cycles of etoposide and ifosfamide (EI). After completing four cycles, eligible patients could proceed to receive definitive treatment, such as radiotherapy or surgery, and then they received 2 cycles of AI and 2 cycles of EI. After 4 cycles of treatment, objective responses (ORR) were obtained in 9 of 37 patients. However, this percentage was markedly reduced in patients carrying the NF1 mutation compared to those with sporadic MPNSTs (17.9% *vs*. 44.4%). Twenty--four patients achieved stable disease (SD); 22 patients underwent resection, radiotherapy, or a combination of both treatment methods, with a radical intent after 4 cycles of chemotherapy. Although the trial lacked adequate statistical power to demonstrate differences in responses between sporadic MPNST and NF1-associated MPNST due to the small patient cohort, a trend towards a diminished response to chemotherapy was observed in individuals with NF1. Furthermore, this study confirmed the significance of neoadjuvant chemotherapy for patients with initially non-resectable MPNSTs [100].

In the EUDRACT 2010 — 023484 — 17 (NCT01710176) trial, 3 courses of chemotherapy based on anthracycline and a full dose of ifosfamide (epirubicin 120 mg/m$^2$ + ifosfamide 9 g/m$^2$), given in neoadjuvant treatment were found to bring a 20% benefit for relapse-free survival (RFS) and OS [101]. Implementing this treatment approach enables the attainment of both radiological [response evaluation criteria in solid tumors (RECIST)] and metabolic (PET) responses. The substitution of doxorubicin with epirubicin may be linked to a reduced risk of cardiotoxicity [102]. In the recently published SG-STS 1001 trial, the regimen incorporating anthracycline (epirubicin 60 mg/m$^2$ on day 1 and 2 plus ifosfamide 3 g/m$^2$ on day 1, 2, 3; every 3 weeks) demonstrated greater efficacy when compared to EI chemotherapy (etoposide 150 mg/m$^2$ on day 1, 2, 3 plus ifosfamide 3 g/m$^2$ on day 1, 2, 3; every 3 weeks) [103]. Furthermore, a randomized, phase III trial evaluated the superiority of histology-specific neoadjuvant chemotherapy in comparison to standard AI neoadjuvant chemotherapy; the obtained results were not satisfactory. Estimated disease-free survival (DFS) and OS did not differ between those two groups, and a standard AI scheme was suggested as the primary choice in the neoadjuvant setting in MPNST [104].

Among the pediatric population with nonresectable MPNSTs undergoing treatment in Polish oncological centers, a favorable response (defined as a reduction in tumor size by more than 33%) to neoadjuvant chemotherapy (consisting of vincristine, ifosfamide, dactinomycin, doxorubicin or epirubicin, etoposide, and carboplatin) was observed in 47.6%. Negative predictive factors for chemotherapy response included the presence of NF1, along with high expressions of osteopontin, survivin, p53, and cyclin D. The response of patients with 3 or more negative predictive factors to therapy was significantly poorer. Differences in chemotherapy regimens used in children and adults and also the slightly different MPNST biology in these age groups should be taken into consideration. For this reason, data concerning treatment effectiveness in the pediatric population cannot be directly transferred to the adult population [105]. A prospective trial (NCT02180867) combining pazopanib with AI chemotherapy and radiotherapy in neoadjuvant treatment evaluated pathological response in MPNST (defined as response higher than 90%). The findings suggested that the addition of pazopanib improved pathological responses in the study group. Of the 37 patients (23 in the pazopanib group and 14 in the control group), the median pathological response was 95% in the pazopanib group and 50% in the control group [106]. Notably, a pathological response > 90% was associated with prolonged disease--specific survival in patients with MPNST [107].

## Surgery

As mentioned before, comprehensive treatment of MPNST involves radical surgery, precisely tumor excision within healthy tissue boundaries (R0 resection) through broad local excision, complemented by adjuvant radiotherapy. A tumor's resectability depends on its location. In the case of localization in the limbs, resection is possible in the majority of the patients. At times, it may be necessary to excise the primary nerve trunk, such as the sciatic nerve. Neoplasms localized centrally (often near the spine, with progression along nerve roots in the direction of the dural sac) are resectable in about 20% of cases [63]. Ensuring negative surgical margins (R0) is crucial in the treatment of MPNST patients, as numerous studies have indicated a significantly shorter survival time in individuals with positive surgical margins (R1/2) [66, 108–110]. In a French trial, patients who underwent R0 resection exhibited median disease-free survival nearly twice as long as those with R1 or R2 resections (47.8 *vs*. 24.4 *vs*. 24.4 months, respectively). Additionally, they demonstrated a significantly higher percentage of overall survival after 8 years (5.1% *vs*. 48.4% *vs*. 25.5%) [108]. Furthermore, resection with positive margins is also associated with almost 6-fold higher risk of local recurrence [111] and distant metastases [112]. In the case of R1 and R2 resections, a repeat of the surgery and/or post-surgical radio- and/or chemotherapy should be considered.

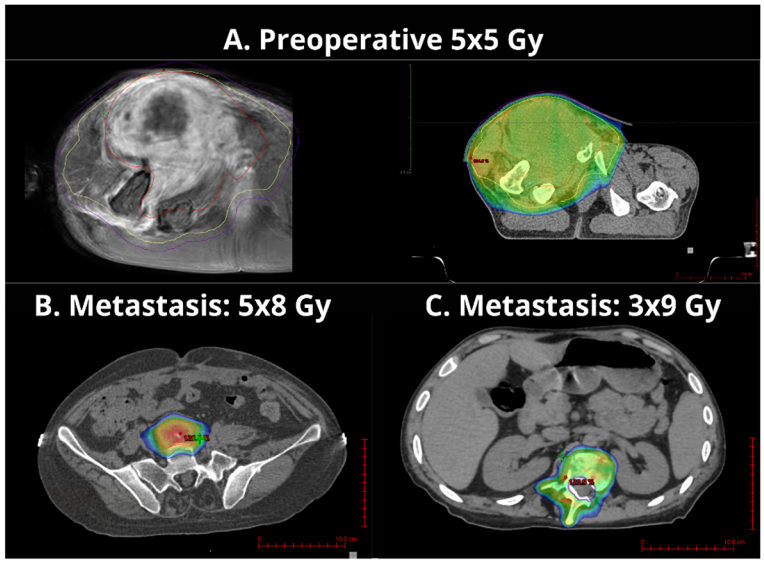


**Figure 2.** Malignant peripheral nerve sheath tumor — radiotherapy. The figure shows the planning of preoperative 5 × 5 Gy intensity-modulated radiotherapy in a patient with a locally advanced malignant peripheral nerve sheath tumor of the left groin (**A**) administered between the first and second doxorubicin-ifosfamide chemotherapy. However, due to disease progression (bone and lung oligometastases), he did not undergo surgery. He received stereotactic body radiotherapy for presacral (**B**) and spinal metastases (**C**) and palliative gemcitabine-docetaxel chemotherapy

### Adjuvant treatment — chemotherapy

The use of adjuvant chemotherapy in STS patients has been a subject of debate for numerous years. A meta-analysis comprising 18 randomized clinical trials involving individuals with locally advanced STS, without histopathological differentiation, revealed a positive impact of adjuvant chemotherapy on the control of local recurrence [odds ratio (OR) = 0.73; 95% confidence interval (CI) 0.56–0.94; p = 0.02) and distant metastases [hazard ratio (HR) = 0.67; 95% CI 0.56–0.82; p = 0.0001]. While adjuvant chemotherapy with doxorubicin alone showed no effect on OS (OR = 0.84; 95% CI 0.68–1.03; p = 0.009), its combination with ifosfamide exhibited a statistically significant improvement in OS (OR = 0.56; 95% CI 0.36–0.85; p = 0.01). Higher toxicity associated with the combination of doxorubicin and ifosfamide should be considered. Additionally, the meta-analysis encompassed various histological types of STS, and data specific to MPNST were not presented [113].

For completely excised tumors (R0) with a wide margin, post-operative treatment is generally believed to be unnecessary. Nevertheless, certain authors argue for the consideration of adjuvant chemotherapy in all cases of MPNSTs with a diameter exceeding 5 cm [99].

### Radical radiotherapy

It is important to emphasize that in this patient group, radiotherapy does not improve OS but decreases the risk of local recurrence [114]. In the case of no adjuvant radiotherapy, there is almost a 5-fold increased risk of local recurrence (HR = 4.51) [66]. An analysis conducted retrospectively at a single center, involving 134 patients treated for MPNST, highlighted the significant impact of factors related to radiotherapy on the local efficacy of combined treatment. Favorable outcomes were observed in patients receiving a dose exceeding 60 Gy, especially within the subgroup of individuals undergoing brachytherapy or intraoperative radiotherapy as part of perioperative treatment [115]. In MPNST localized in the paraspinal area or at the base of the skull after non-radical resection or without the possibility of performing surgery, an increasing role is played by radiotherapy using protons or heavy ions. This allows for obtaining high local efficacy with relatively small side effects [116, 117]. Available data from the literature are too sparse to draw unequivocal conclusions. The planning of treatment, which encompasses defining the clinical target volume and determining fractionation, aligns with recommendations for the perioperative treatment of STSs (Fig. 2).

## Treatment of recurrent or metastatic disease

Malignant peripheral nerve sheath tumors, characterized by a high degree of malignancy, present a significant risk of metastasis. Palliative chemotherapy, employing doxorubicin or doxorubicin with ifosfamide is administered in cases of widespread disease, with clinical improvement observed in about 25–30% of patients. However, recent study showed that 94.4% of MPNST patients do not receive palliative treatment in the course of the disease, indicating a gap

in palliative management [118]. Taking into consideration the effectiveness of molecularly targeted treatment for patients with gastrointestinal stromal tumors (GIST) and the relatively well-known molecular biology of MPNST, especially in patients with neurofibromatosis, there is hope that soon inhibitors will show higher effectiveness in these patients than typical chemotherapy. The overall 5-year survival rate for MPNST patients is 50–55%, with a poorer prognosis for patients in whom sarcoma developed in the course of neurofibromatosis. In this group, 5-year survival is approximately 20–30%. The time of DFS is also shorter for MPNST formed on the basis of NF1. These patients are also characterized by a higher risk of formation of new foci of unresectable neoplasms. [119] Despite these challenges, ongoing developments suggest an improving prognosis for NF1-related MPNST, approaching outcomes seen in sporadic sarcoma forms [120].

## Surgery

Surgical intervention is pivotal in managing both recurrent disease and isolated distant metastases. The resectability of recurrent tumors is typically lower compared to primary tumors. In some cases, achieving radical resection of the tumor may necessitate limb amputation. Given that MPNST often originates in connection with large nerve trunks, even limb-sparing surgery can result in substantial functional losses. While this approach is largely supported by individual case reports and retrospective studies from sarcoma treatment centers, guidelines provide less clarity on the matter [121–123]. Surgical decisions in such scenarios should be tailored to each patient, considering their prognosis. This individualized approach appears particularly advantageous for patients with favorable long-term DFS [124].

## Palliative radiotherapy

In the context of disease dissemination, palliative radiotherapy may be considered, similar to other STS. Guidelines acknowledge the potential use of radiotherapy for metastases, depending on individual patient indications and treatment center protocols [124]. However, the efficacy of such interventions remains inconclusive, with limited studies specifically addressing MPNST. Retrospective trials suggest the feasibility of using a mean dose of 40.8 Gy in 2.6 Gy fractions for palliative radiotherapy in this context [125]. Nevertheless, there was no observed impact on patients' OS ($p = 0.53$). An evaluation of the utility of radiotherapy in palliative treatment demonstrated satisfactory 73% 1-year local control (LC) of targeted lesions and 95% effectiveness in symptom control. It is important to note, however, that this study included only 2 MPNST patients, and results based on the histological type of sarcoma were not disclosed [126].

**Table 1.** Ifosfamide (AI) chemo regimen used for malignant peripheral nerve sheath tumor (MPNST) treatment — repeat every 21 days

| Drug | Dose | Administration | Comments |
|---|---|---|---|
| Dexamethasone | 8 mg | *i.v.* | |
| Ondansetron | 16 mg | *i.v.* | |
| **Doxorubicin** | **25 mg/m$^2$** | In 250 mL 0,9% NaCl *i.v.* 1 h infusion | Days 1–3 |
| 0.9% NaCl | 500 mL | *i.v.* | |
| Mannitol | 250 mL | *i.v.* | |
| Mesna | 800 mg | In 20 mL 5% glucose *i.v.* | |
| **Ifosfamide** | **2.5 g/m$^2$** | In 500 mL 5% glucose *i.v.* 3 h infusion | Days 1–4 |
| **Mesna** | **2.5 g/m$^2$** | | |
| Mesna | 800 mg | In 500 mL 5% glucose *i.v.* 1 h infusion | After 3 hours |
| Dexamethasone | 4 mg | *i.v.* | |

*i.v.* — intravenous; NaCl — sodium chloride

## Palliative chemotherapy

Like in other soft tissue sarcomas, anthracycline-based therapy continues to be the primary choice for initial treatment in patients with unresectable, locally advanced, or metastatic MPNSTs. Most current studies focus on the evaluation of anthracyclines in combination with other drugs in this indication. In NIO-PIB doxorubicin — ifosfamide regimen is used as described below (Tab. 1).

Required premedications:

- ondansetron 8–16 mg *per os* (*p.o.*)/*intravenous* (*i.v.*) 30 to 60 minutes pre-chemotherapy, then 8 mg *p.o.*/*i.v.* every 8 hours in two doses post-chemotherapy;
- dexamethasone 8 mg *p.o.*/*i.v.* 30 to 60 minutes pre-chemotherapy, then 4 mg *p.o.*/*i.v.* every 12 hours in two doses post-chemotherapy;
- aprepitant 125 mg *p.o.*/*i.v.* 30 to 60 minutes pre-chemotherapy on day 1, then 80 mg *p.o.* daily on days 2 and 3.

Additionally may be used:

- lorazepam 1 mg sublingually (SL) every 4–6 hours for nausea, sleep, or restlessness;
- prochlorperazine 10 mg *p.o.* every 4–6 hours for nausea or vomiting.

Due to potential drug toxicity, dose adjustments may be necessary. If the absolute neutrophil count (ANC) or platelet count decrease to 1.5–1 and $\leq$ 100–70 $\times$ $10^9$/L, respectively, dose modifications should be implemented, reducing each drug's dosage

to 80% of the initial dose. If these counts further decline below the indicated values, it is necessary to postpone the cycle by one week. For ifosfamide, the creatinine clearance (CrCl) should be estimated according to protocol guidelines. If CrCl falls below 50, ifosfamide administration should be discontinued. If renal function does not improve, monotherapy with doxorubicin is recommended. Adjustments are also warranted for adverse events graded as 3/4 according to the Common Terminology Criteria for Adverse Events (CTCAE), such as mucositis and nausea/vomiting. In such cases, the dose should be reduced to 80% of the initial dose. In instances of hepatic dysfunction, indicated by a 1.5–2 × upper limit normal (ULN) increase in bilirubin, doxorubicin should be administered at a reduced dose of 50%. If febrile neutropenia occurs, after recovery, all drugs in the cycles should be administered at a reduced dose of 80%. In the case of a CTCAE grade 1 neurological toxicity to ifosfamide, ifosfamide must be reduced in the next cycle. If a CTCAE grade 2 neurological toxicity appears or neurological toxicity worsens despite dose reduction ifosfamide must be stopped. Risk factors for CNS toxicity are a low serum albumin level, renal impairment, prior administration of cisplatin, poor performance status, CNS tumor, bulky pelvic disease, concomitant psychotropic drug use, and younger age. Methylene blue 50 mg four times a day intravenous infusion in 100 mL sodium chloride 0.9% over 30 minutes should be used to treat ifosfamide-induced encephalopathy.

Analysis of 12 clinical trials conducted by European Organisation for Research and Treatment of Cancer (EORTC) involving patients with advanced STS showed no disparities in the response rate (RR) (21% *vs*. 22%, p = 0.84), median of progression-free survival (PFS) (17 months *vs*. 16.1 months, p = 0.83), and OS (48 months *vs*. 51 months, p = 0.483) between the cohort with nonresectable or metastasized MPNST (n = 175) and other sarcoma subtypes (n = 2500) undergoing chemotherapy. The used regimen emerged as an independent factor for prognosing response to therapy and PFS but had no impact on OS, which was predominantly influenced by overall physical well-being [127]. Chemotherapy regimens were grouped into 4 categories: anthracycline in monotherapy (doxorubicin 75 mg/m$^2$, pegylated liposomal doxorubicin, epirubicin 75 mg/m$^2$, 3 × 50 mg/m$^2$, or 150 mg/m$^2$), ifosfamide in monotherapy (5 mg/m$^2$, 3 × 3 mg/m$^2$, 9 mg/m$^2$, 12 mg/m$^2$), doxorubicin with ifosfamide (50 mg/m$^2$ + 5 mg/m$^2$; 75 mg/m$^2$ + + 5 mg/m$^2$) and cyclofosfamide, vincristine, adriamycin and dacarbazine (CYVADIC). The results of this trial are presented in Table 2.

**Table 2.** Analysis of 12 EORTC clinical trials focusing on median progression-free survival (PFS) and one-year overall survival (OS) in patients with advanced MPNST, contingent on the initial chemotherapy regimen employed [127]

| Chemotherapy scheme | mPFS | 1-year OS |
|---|---|---|
| Anthracycline monotherapy 75 mg/m$^2$ q3w* | 17 (13.7–20.43) | 14.8% |
| Ifosfamide monotherapy q3w** | 9.4 (7.1–17.0) | 3.85% |
| Doxorubicin + ifosfamide (AI) q3w | 26.9 (22.4–35.1) | 25.2% |
| CYVADIC q4w*** | 10.4 (8.4–41.9) | 23.3% |

*For patients older than 65 years old reduce the dose to 60 mg/m$^2$; **Ifosfamide 3000 mg/m$^2$ + mesna 3000 mg/m$^2$ over 4 hours with 0.9% NaCl hydration before and after ifosfamide, days 1–3; ***The CYVADIC regimen administered to each patient consisted of cyclophosphamide [day (d) 2, 500 mg/m$^2$), vincristine (d1,1.5 mg/m$^2$, max 2.0 mg/body), doxorubicin (d1, 50 mg/m$^2$), and dacarbazine (d1–5, 250 mg/m$^2$). One cycle lasted 28 days

Patients administered the doxorubicin and ifosfamide regimen experienced prolonged PFS compared to those treated with anthracycline monotherapy (HR = 0.807; 95% CI 0.48–1.358), while individuals receiving ifosfamide monotherapy exhibited the shortest PFS time (HR = 2.018; 95% CI 1.155–3.327). Additionally, the AI regimen was correlated with the highest percentage of objective responses (HR = 6.283; 95% CI 2.342–16.852), whereas ifosfamide was linked to the lowest ORR (HR = 0.333; 95% CI 0.038–2.912) [127]. Moreover, based on a retrospective analysis, regimens combining doxorubicin and ifosfamide are associated with the lowest recurrence risk and the best percentage of responses in MPNST patients, even though in the EORTC62851 trials, no differences were observed in RR, OS, or PFS between treatments with doxorubicin at a dose of 75 mg/m$^2$ and the AI combination at doses of 50 mg/m$^2$ + 5 mg/m$^2$ in STS patients [128]. Furthermore, in the randomized phase III trial (EORT62012) that compared doxorubicin 75 mg/m$^2$ as a single-agent therapy to the combination of doxorubicin with a heightened dose of ifosfamide (10 mg/m$^2$), there was no observed impact on OS (12.8 *vs*. 14.3 months; HR = 0.83; 95% CI 0.67–1.03; p = 0.076). Nevertheless, individuals treated with the addition of ifosfamide demonstrated a notably extended PFS rate (7.4 *vs*. 4.7 months; HR = 0.74; 95% CI 0.6–0.9; p = 0.003) and a raised percentage of CR (26% *vs*. 14%; p = 0.0006). This trial involved 455 STS patients, but subgroup analyses for various sarcoma types, including MPNST, remain undisclosed [129].

Anthracycline monotherapy is characterized by worse PFS compared to regimens in combination with AI although in some cases, especially in patients in whom the main aim of treatment is control of metastatic disease, there is an option for monotherapy with anthracycline. If the aim of the treatment is

alleviation of pronounced symptoms associated, for instance, with invasion or pressure on nerves or obtaining a potential resectability of the tumor and/or metastases, adding ifosfamide to doxorubicin seems justified. In clinical practice, there is a need to choose a chemotherapy regimen based on the toxicity profile. The AI combination is more myelotoxic in comparison with doxorubicin in monotherapy [128, 129]. Leukopenia, neutropenia, neutropenic fever, anemia, or thrombocytopenia at grades 3 and 4 according to CTCAE occurred significantly more frequently in patients treated with the doxorubicin and ifosfamide regimen in the populations of STS patients [129]. In a pediatric population treated in Italian and German centers, the percentage of responses in patients treated with regimens containing ifosfamide was 65%, cyclofosfamide 17%, and other drugs (among them etoposide or cisplatin) 20%. The regimens either did or did not contain a minimal dose of anthracyclines, and analysis of the subgroups treated with this drug was not performed [99].

In the majority of retrospective analyses, doxorubicin was the most frequently utilized medication, either as single-agent therapy or in conjunction with ifosfamide. In a trial conducted by a French sarcoma group, 102 patients with metastatic or nonresectable disease (72%, 102/142) were administered a regimen incorporating doxorubicin. Among them, 38 (37%) received doxorubicin as a single-agent therapy, while 64 (63%) received it in combination with isoniazid [108]. In another single-center French trial (retrospective), 6 cycles of doxorubicin at 60 mg/m$^2$ were given, and, in patients with fitness levels 0–1, ifosfamide 2500 mg/m$^2$ was added on days 1–3 of the cycle. Because of the small group of patients (n = 21) with different degrees of disease progression and different statuses of surgery (and resectability degree), the chemotherapy effectiveness was not compared between regimens [130]. Anthracycline-based first-line chemotherapy remains the baseline treatment for advanced MPNST. Current studies assess anthracyclines in combination with other drugs. Analysis indicates comparable outcomes between MPNST and other STS. Regimens combining doxorubicin and ifosfamide show longer PFS and higher response rates. While anthracycline monotherapy is an option, adding ifosfamide is justified for symptom relief or potential resectability, considering regimen toxicity. Second-line chemotherapy may be contemplated following established STS treatment protocols; nevertheless, there are scarce data on its effectiveness in MPNST. Among the options is the combination of gemcitabine with docetaxel. Anthracycline-based therapy remains essential, emphasizing the need for ongoing research to refine MPNST treatment strategies.

## Targeted treatment and clinical trials

As mentioned above, standard chemotherapy showed limited effectiveness in MPNST. Thus searching for targeted therapies seems justified, as preclinical trials showed the expression of proteins such as MET, IGFR, PDGFRA, PDGFRB, and AXL that are the targets of known drugs [131]. Currently, no standard targeted therapy for patients with MPNST is recommended, and clinical data showed limited treatment responses in MPNST patients. Preclinical trials also indicated an important role for EGFR in MPNST development, but further investigations have shown that only in 3.1% of MPNSTs is EGFR phosphorylated and activated [132]. Molecular findings are further corroborated by the outcomes of a phase II trial, indicating the inefficacy of the EGFR inhibitor erlotinib in individuals with nonresectable or metastatic MPNSTs (18 of 20 cases demonstrated disease progression) [133]. The ineffectiveness in MPNST treatment was also observed in phase II trials with sorafenib (PFS = 1.7 m), imatinib (without PR or SD), dasatinib (SRC kinase inhibitor — Sprycel; without PR or SD after 4 cycles), and alisertib (Aurora A kinase inhibitor — MLN8237; 60% PSF after 12 weeks), a combination of bevacizumab with everolimus (without PR, SD in 3 patients — SARC016 trial), or a combination of ganetespib with sirolimus (HSP 90 and mTOR inhibitor; without PR, 1 SD after 4 cycles — SARC023 trial) [68, 134–137]. Also, a retrospective analysis of the above-mentioned phase II clinical trials, in terms of PFS achieved poor results with mean PFS of 1.77 months (95% CI 1.61–3.45). Progression-free survival at 4 months was 16%, which was significantly influenced by the increasing number of previous lines of treatment [138]. In contrast, a phase I/II study evaluating pexidartinib (KIT, CSF1R, and FLT3 inhibitor) combined with sirolimus (NCT02584647) showed promising results with all the enrolled patients achieving clinical benefit [139]. In all, 12 of 18 patients who could be evaluated (66.7%; 95% CI 41.15–85.64) experienced clinical benefit [3 PR and 9 SD, also median PFS and median OS in the MPNST group were 18.6 weeks (95% CI, noncalculable) and 145.1 weeks (95% CI, noncalculable), respectively] [140]. Trials combining standard cytotoxic therapy with targeted therapy have also been performed. Rriociclib, sorafenib, and olaratumab in combination with chemotherapy drugs did not show the expected improvement in treatment results [27, 141–143]. However, targeting neurotrophic tyrosine receptor kinases (NTRK) seems to be beneficial in patients with TRK-mutated solid tumors with an ORR of 34%; yet no specific results for MPNST have been posted [144]. Pazopanib (800 mg per day) — a multikinase tyrosine kinase inhibitor — based on the results of the clinical PALETTE

trial has been recommended as the standard treatment for patients with metastatic, non-adipocytic STS after failure of standard chemotherapy. In a small series of patients treated in one of the Korean centers, in 5 patients with MPNST, a partial response was observed in 1 and in 4 disease stabilization. mPFS was 6.5 months (0.7–12.3) and OS 8.9 months (3.5–14.3). PFS was significantly longer in patients with a diagnosis of liposarcoma or rhabdomyosarcoma, and comparable with PFS for patients with leiomyosarcoma, malignant fibrous histiocytoma/undifferentiated pleomorphic sarcoma, and sarcoma synoviale [145]. In a retrospective analysis of 156 STS patients treated in Japan, in 7 patients with MPNST none attained a PR, 3 had SD, 0 SD > 6 months. The MPNSTs exhibited significantly poorer response rates and PFS percentages compared to the general population and other histological types (PFS MPNST *vs.* non-MPNST: HR = 2.24; 95% CI 1.035–4.849; p = 0.03) [146]. Median PFS was 7.4 weeks and median OS 2.5 months [146]. A phase II trial with pazopanib found a 50% clinical benefit rate defined by RECIST in MPNST patients; mOS and mPFS were 5.4 and 10.6 months, respectively [147]. Also, the addition of pazopanib to standard chemotherapy with gemcitabine showed prolonged PFS in STS patients. A phase II study evaluated this combination with PFS of 4.4 months for combined therapy compared to 2.2 months for gemcitabine alone [148]. Pazopanib also showed therapeutic superiority over a selective mTOR inhibitor in MPNST, demonstrating greater clinical benefit and longer PFS. However, evaluating activity in this clinical trial, pazopanib demonstrated shorter PFS as compared to earlier randomized studies [149]. In a trial with Sapanisertib (TORC1/2 INK128 inhibitor), compared with pazopanib (NCT02601209), there was no superiority of any agent observed in patients with mPFS 2 and 2.1 months, respectively [150].

Due to the profile of the tumor microenvironment, MPNST is also a candidate for immunotherapy treatment. A study is currently being conducted on the use of dual anti-PD-1 and anti-CTLA4 blockade in patients with rare cancers, including MPNSTs (NCT02834013), [151]. Unfortunately, a previously conducted study of pembrolizumab as monotherapy was closed due to low recruitment (NCT02691026). Also, the use of immunotherapy in combination with targeted therapy showed a clinical effect in MPNST patients. The multi-tyrosine kinase inhibitor lenvatinib in combination with pembrolizumab allowed for achieving a partial response (PR) in the cohort of patients with MPNST and mPFS of 32 months (4.3–51.1) [152]. Also, the addition of the immunomodulator — alrizomadlin (which restores TP53 function, activating p53-mediated apoptosis in tumor cells) — to pembrolizumab showed clinical benefit in MPNST with an overall response rate and stable disease in 53% of patients according to the RECIST criteria [153]. Currently, a phase I trial of vaccine therapy for patients with unresectable or recurrent MPNST is ongoing. Vaccines utilizing a genetically modified virus may target and eliminate tumor cells expressing the neurofibromin 1 (*NF1*) gene while sparing surrounding normal cells. Additionally, they have the potential to stimulate the body's immune response, contributing to eradication of tumor cells.

## Survival and prognostic factors

In general, MPNST patients face poor prognosis. Data concerning prognostic and predictive factors in MPNST differs depending on the authors' experience, mainly due to the relatively rare occurrence of this type of tumor, and the heterogenous course of the disease. Lately, nomograms that have been created to predict OS for MPNST patients indicate the prognostic value of histological type, disease advancement, and systemic treatment [154]. Patients who underwent complete lesion removal and had tumors under 5 cm when diagnosed, who exhibited low-grade progression, were more likely to survive 5 years. Classical clinical and pathological prognostic factors for MPNST now include:

- localization (better prognosis if localized in the limbs);
- tumor size ($\leq$ 5 cm);
- NF1 (worsens the prognosis);
- mitotic index;
- grading;
- degree of necrosis;
- previous exposure to radiation during the course of another disease (possibility of MPNST induction).

The size of the tumor is one of the most commonly correlated factors associated with a poor prognosis [112, 120, 155, 156]. Discrepancies concern the cut-off point, but in general, it is assumed that tumors with a diameter over 5 cm are associated with shorter survival, but in some analyses, an even poorer prognosis is observed for tumors > 15 cm [110]. The large tumor size is also associated with a shorter time to chemotherapy failure [130]. The next significant factor is the tumor histological malignancy grade (G). Malignant peripheral nerve sheath tumor with a high malignancy grade are characterized by significantly shorter progression-free survival and overall survival [66, 108, 109, 120], which is related to, among others, a significantly higher risk of distant metastasis development [66, 112]. Grade III malignant tumors are associated with a 1.5 shorter progression-free survival and even 3.5-fold worse overall survival than grade I and II tumors [108]. Furthermore, based on

histologic grading using the FNCLCC system, an unfavorable outcome was associated with a higher grade, thus no deaths were observed in patients with grade 1 MPNST [157].

Besides size, a significant factor is tumor localization. A deep localization of the tumor e.g. in the retroperitoneal space is a negative prognostic factor for DFS and OS [108]. Patients with axial tumor localization have shorter DFS and OS than patients with tumors located on the limbs [110]. Intracranial tumors can be associated with better outcomes, while core localization has the worst prognosis both for OS and disease-specific survival [158]. However, no significant difference was observed in OS between cutaneous or subcutaneous MPNSTs, regardless of location [159]. The presence of distant metastases is a negative prognostic factor [120]. Factors influencing the development of distant metastases in MPNST are both the size of the tumor and the involvement of local lymph nodes. Patients with distant metastases, especially metastases in multiple locations, have the worst mOS prognosis [160]. Local progression of the disease (e.g. infiltration of adjoining structures) is also associated with poorer DFS and OS [108]. Our own experience confirmed that the main factors influencing patient prognosis are tumor size at diagnosis, high grade, and R0 resection, which confirms the outcomes of previous research [161].

Considerable debates revolve around the impact of the *NF1* mutation on survival outcomes for MPNST patients. Some studies indicate markedly inferior treatment responses and reduced survival duration in individuals with NF1-associated MPNST, as opposed to sporadic MPNST, with a 5-year overall survival rate that is shortened by up to 50% [66, 99, 162]. Taking into consideration only analyses published after 2000, Kolberg et al. [120] have demonstrated that the *NF1* mutation does not significantly affect differences in survival. These variations could stem from advancements in monitoring strategies for patients with *NF1* mutations, and the prompt initiation of treatment upon detection of alarming symptoms or irregularities in imaging studies. Additionally, it is noteworthy that the familial presence of MPNST is a risk factor for early disease onset in individuals with *NF1* mutations [163]. Notably, a meta-analysis on prognostic factors for MPNST involving 28 studies, showed that, in addition to classical factors, *NF1* status remains one of the most important factors influencing prognosis [164]. Also, when it comes to the pediatric population, the main factor influencing prognosis seems to be the *NF1* status, with MPNST patients associated with the NF1 syndrome facing poorer prognosis; also, no treatment modalities were shown to influence prognosis in this group [165, 166]. A less frequently observed negative prognostic factor is female sex [66].

As mentioned before, prior radiation is a risk factor for developing MPNST, it is one of the cancers most frequently correlated with radiotherapy, and its development on this basis is associated with an aggressive course of the disease and higher risk of disease-specific death [8, 167].

## Summing up and conclusions

Malignant peripheral nerve sheath tumor is a highly aggressive tumor that develops from peripheral nerves, often linked to nerve trunks in the limbs and torso. It can arise either *de novo* or from pre-existing neurofibromas, displaying a notable association with type 1 neurofibromatosis (von Recklinghausen disease). Diagnosis is confirmed through histopathological examination, usually obtained through an open biopsy. Standard excision for tumors under 5 cm in diameter is a common practice, with similar principles applied to patients with type 1 neurofibromatosis, which necessitates vigilant monitoring and potential excision or biopsy in suspicious cases. Distinguishing between benign neurofibromas and potential sarcomatous foci remains a clinical challenge, where PET-CT is useful. Radical surgery, involving broad local excision, is a cornerstone in neurosarcoma management, often complemented by adjuvant radiotherapy for R1/2 resections. Neoadjuvant chemotherapy precedes surgery in selected cases. For locally advanced or generalized cases, palliative chemotherapy — typically doxorubicin or doxorubicin with ifosfamide — gives a clinical improvement in 25–30% of patients [9, 98, 168]. Future endeavors should focus on elucidating genetic changes driving MPNST transformation, progression, and metastasis, which necessitates longitudinal studies with comprehensive patient observation, biobanking, and analysis of clinical and radiological data [68]. Although treatment outcomes for MPNST have seen few changes, recent progress in understanding its biology and pathogenesis has paved the way for promising preclinical and clinical trials, offering hope for identifying active therapies and biomarkers. Ongoing research evaluating novel treatments, including immunotherapy and combination chemotherapy or targeted approaches is well-justified [169].

## Article Information and Declarations

### Author contributions

A.M.C., S.F., P.R.: conception and supervision; All authors — writing.

### Funding

2019/35/O/NZ2/03761 National Science Centre Grant (AMC).

### Acknowledgements

This work was supported by the National Science Centre's grant (2019/35/O/NZ2/03761).

### Conflict of interest

The authors declare that there are no conflicts of interest.

### Supplementary material

None.

## References


1. WHO Classification of Tumours Editorial Board. Soft Tissue and Bone Tumours. WHO Classification of Tumours, 5th Edition. World Health Organization 2013.
2. Hirbe A, Gutmann D. The management of neurofibromatosis type 1-associated malignant peripheral nerve sheath tumors: challenges, progress, and future prospects. Expert Opinion on Orphan Drugs. 2017; 5(8): 623–631, doi: 10.1080/21678707.2017.1348294.
3. Pala-Sadza A, Zajączkiewicz H, Banaś-Samson R, et al. Rzadki przypadek złośliwego nerwiaka osłonkowego jamy nosa. Polski Przegląd Otorynolaryngologiczny. 2014; 3(4): 210–213, doi: 10.1016/j.ppotor.2014.08.004.
4. Boczej R, Walas R, Motyka M. Olbrzymi guz złośliwy nerwów obwodowych. Chirurgia Polska. 2013; 15(2): 141–145.
5. De Raedt T, Brems H, Wolkenstein P, et al. Elevated risk for MPNST in NF1 microdeletion patients. Am J Hum Genet. 2003; 72(5): 1288–1292, doi: 10.1086/374821, indexed in Pubmed: 12660952.
6. Evans DGR, Baser ME, McGaughran J, et al. Malignant peripheral nerve sheath tumours in neurofibromatosis 1. J Med Genet. 2002; 39(5): 311–314, doi: 10.1136/jmg.39.5.311, indexed in Pubmed: 12011145.
7. Mackel CE, Medeiros I, Moore BE, et al. Intracranial Malignant Peripheral Nerve Sheath Tumors Not Associated with a Cranial Nerve: Systematic Review and Illustrative Case. World Neurosurg. 2021; 156: 76–91, doi: 10.1016/j.wneu.2021.09.072, indexed in Pubmed: 34563719.
8. Miao R, Wang H, Jacobson A, et al. Radiation-induced and neurofibromatosis-associated malignant peripheral nerve sheath tumors (MPNST) have worse outcomes than sporadic MPNST. Radiother Oncol. 2019; 137: 61–70, doi: 10.1016/j.radonc.2019.03.015, indexed in Pubmed: 31078939.
9. Farid M, Demicco EG, Garcia R, et al. Malignant peripheral nerve sheath tumors. Oncologist. 2014; 19(2): 193–201, doi: 10.1634/theoncologist.2013-0328, indexed in Pubmed: 24470531.
10. Shurell E, Tran LM, Nakashima J, et al. Gender dimorphism and age of onset in malignant peripheral nerve sheath tumor preclinical models and human patients. BMC Cancer. 2014; 14: 827, doi: 10.1186/1471-2407-14-827, indexed in Pubmed: 25398666.
11. Mowery A, Clayburgh D. Malignant peripheral nerve sheath tumors: Analysis of the national cancer database. Oral Oncol. 2019; 98: 13–19, doi: 10.1016/j.oraloncology.2019.09.010, indexed in Pubmed: 31525622.
12. Brohl AS, Kahen E, Yoder SJ, et al. The genomic landscape of malignant peripheral nerve sheath tumors: diverse drivers of Ras pathway activation. Sci Rep. 2017; 7(1): 14992, doi: 10.1038/s41598-017-15183-1, indexed in Pubmed: 29118384.
13. Brosseau JP, Le LuQ. Heterozygous Tumor Suppressor Microenvironment in Cancer Development. Trends Cancer. 2019; 5(9): 541–546, doi: 10.1016/j.trecan.2019.07.004, indexed in Pubmed: 31474359.
14. Pemov A, Li H, Patidar R, et al. NISC Comparative Sequencing Program, NCI DCEG Cancer Genomics Research Laboratory. The primacy of NF1 loss as the driver of tumorigenesis in neurofibromatosis type 1-associated plexiform neurofibromas. Oncogene. 2017; 36(22): 3168–3177, doi: 10.1038/onc.2016.464, indexed in Pubmed: 28068329.
15. Messiaen LM, Callens T, Mortier G, et al. Exhaustive mutation analysis of the NF1 gene allows identification of 95% of mutations and reveals a high frequency of unusual splicing defects. Hum Mutat. 2000; 15(6): 541–555, doi: 10.1002/1098-1004(200006)15:6<541::AID-HUMU6>3.0.CO;2-N, indexed in Pubmed: 10862084.
16. Jadayel D, Fain P, Upadhyaya M, et al. Paternal origin of new mutations in Von Recklinghausen neurofibromatosis. Nature. 1990; 343(6258): 558–559, doi: 10.1038/343558a0.
17. Kahen EJ, Brohl A, Yu D, et al. Neurofibromin level directs RAS pathway signaling and mediates sensitivity to targeted agents in malignant peripheral nerve sheath tumors. Oncotarget. 2018; 9(32): 22571–22585, doi: 10.18632/oncotarget.25181, indexed in Pubmed: 29854299.
18. Lee S, Rauch J, Kolch W. Targeting MAPK Signaling in Cancer: Mechanisms of Drug Resistance and Sensitivity. Int J Mol Sci. 2020; 21(3), doi: 10.3390/ijms21031102, indexed in Pubmed: 32046099.
19. Zou Z, Tao T, Li H, et al. mTOR signaling pathway and mTOR inhibitors in cancer: progress and challenges. Cell & Bioscience. 2020; 10(1), doi: 10.1186/s13578-020-00396-1.
20. Watson AL, Keller BJ, Williams KA, et al. Correction: Co-targeting the MAPK and PI3K/AKT/mTOR pathways in two genetically engineered mouse models of schwann cell tumors reduces tumor grade and multiplicity. Oncotarget. 2020; 11(39): 3618–3620, doi: 10.18632/oncotarget.27349, indexed in Pubmed: 33062197.
21. Arshad T. A novel pan-RAS inhibitor for malignant peripheral nerve sheath tumors. J Clin Oncol. 2022; 40(16_suppl): e23531–e23531, doi: 10.1200/jco.2022.40.16_suppl.e23531.
22. Endo M, Yamamoto H, Setsu N, et al. Prognostic significance of AKT/mTOR and MAPK pathways and antitumor effect of mTOR inhibitor in NF1-related and sporadic malignant peripheral nerve sheath tumors. Clin Cancer Res. 2013; 19(2): 450–461, doi: 10.1158/1078-0432.CCR-12-1067, indexed in Pubmed: 23209032.
23. Varin J, Poulain L, Hivelin M, et al. Dual mTORC1/2 inhibition induces anti-proliferative effect in NF1-associated plexiform neurofibroma and malignant peripheral nerve sheath tumor cells. Oncotarget. 2016; 7(24): 35753–35767, doi: 10.18632/oncotarget.7099, indexed in Pubmed: 26840085.
24. Zou CY, Smith KD, Zhu QS, et al. Dual targeting of AKT and mammalian target of rapamycin: a potential therapeutic approach for malignant peripheral nerve sheath tumor. Mol Cancer Ther. 2009; 8(5): 1157–1168, doi: 10.1158/1535-7163.MCT-08-1008, indexed in Pubmed: 19417153.
25. Adnane L, Trail PA, Taylor I, et al. Sorafenib (BAY 43-9006, Nexavar), a dual-action inhibitor that targets RAF/MEK/ERK pathway in tumor cells and tyrosine kinases VEGFR/PDGFR in tumor vasculature. Methods Enzymol. 2006; 407: 597–612, doi: 10.1016/S0076-6879(05)07047-3, indexed in Pubmed: 16757355.
26. Gudena V, Verma N, Post G, et al. Metastatic chest wall malignant schwannoma responding to sorafenib: case report and literature review. Cancer Biol Ther. 2008; 7(6): 810–813, doi: 10.4161/cbt.7.6.5932, indexed in Pubmed: 18376142.
27. D'Adamo DR, Keohan ML, Carvajal RD, et al. A phase II trial of sorafenib (S) and dacarbazine (D) in leiomyosarcoma (LMS), synovial sarcoma (SS), and malignant peripheral nerve sheath tumor (MPNST). J Clin Oncol. 2011; 29(15_suppl): 10025–10025, doi: 10.1200/jco.2011.29.15_suppl.10025.
28. Torres KE, Zhu QS, Bill K, et al. Activated MET is a molecular prognosticator and potential therapeutic target for malignant peripheral nerve sheath tumors. Clin Cancer Res. 2011; 17(12): 3943–3955, doi: 10.1158/1078-0432.CCR-11-0193, indexed in Pubmed: 21540237.
29. Jessen WJ, Miller SJ, Jousma E, et al. MEK inhibition exhibits efficacy in human and mouse neurofibromatosis tumors. J Clin Invest. 2013; 123(1): 340–347, doi: 10.1172/JCI60578, indexed in Pubmed: 23221341.
30. Fischer-Huchzermeyer S, Dombrowski A, Wilke G, et al. MEK inhibitors enhance therapeutic response towards ATRA in NF1 associated malignant peripheral nerve sheath tumors (MPNST) in-vitro. PLoS One. 2017; 12(11): e0187700, doi: 10.1371/journal.pone.0187700, indexed in Pubmed: 29131833.
31. Hitchen N, Cross M, Laking G, et al. Sporadic Metastatic Malignant Peripheral Nerve Sheath Tumour with an NF1 Mutation Responding to Trametinib: A Case Report. Case Rep Oncol. 2023; 16(1): 1–6, doi: 10.1159/000528743, indexed in Pubmed: 36743881.

32. Nagabushan S, Lau L, Barahona P, et al. Efficacy of MEK inhibition in a recurrent malignant peripheral nerve sheath tumor. npj Precision Oncology. 2021; 5(1), doi: 10.1038/s41698-021-00145-8, indexed in Pubmed: 33580196.
33. Widemann BC, Lu Y, Reinke D, et al. Targeting Sporadic and Neurofibromatosis Type 1 (NF1) Related Refractory Malignant Peripheral Nerve Sheath Tumors (MPNST) in a Phase II Study of Everolimus in Combination with Bevacizumab (SARC016). Sarcoma. 2019; 2019: 7656747, doi: 10.1155/2019/7656747, indexed in Pubmed: 31427883.
34. Kim A, Lu Y, Okuno SH, et al. Targeting Refractory Sarcomas and Malignant Peripheral Nerve Sheath Tumors in a Phase I/II Study of Sirolimus in Combination with Ganetespib (SARC023). Sarcoma. 2020; 2020: 5784876, doi: 10.1155/2020/5784876, indexed in Pubmed: 32089640.
35. Peacock JD, Cherba D, Kampfschulte K, et al. Molecular-guided therapy predictions reveal drug resistance phenotypes and treatment alternatives in malignant peripheral nerve sheath tumors. J Transl Med. 2013; 11: 213, doi: 10.1186/1479-5876-11-213, indexed in Pubmed: 24040940.
36. Brosius S, Roth K, Carroll S. Combinatorial treatment of malignant peripheral nerve sheath tumors with tyrosine kinase inhibitors hinders proliferation and survival. The FASEB Journal. 2013; 27(S1), doi: 10.1096/fasebj.27.1_supplement.1088.4.
37. Cichowski K, Shih TS, Schmitt E, et al. Mouse models of tumor development in neurofibromatosis type 1. Science. 1999; 286(5447): 2172–2176, doi: 10.1126/science.286.5447.2172, indexed in Pubmed: 10591652.
38. Yang FC, Ingram DA, Chen S, et al. Nf1-dependent tumors require a microenvironment containing Nf1+/– and c-kit-dependent bone marrow. Cell. 2008; 135(3): 437–448, doi: 10.1016/j.cell.2008.08.041, indexed in Pubmed: 18984156.
39. De Raedt T, Beert E, Pasmant E, et al. PRC2 loss amplifies Ras-driven transcription and confers sensitivity to BRD4-based therapies. Nature. 2014; 514(7521): 247–251, doi: 10.1038/nature13561, indexed in Pubmed: 25119042.
40. Legius E, Dierick H, Wu R, et al. TP53 mutations are frequent in malignant NF1 tumors. Genes Chromosomes Cancer. 1994; 10(4): 250–255, doi: 10.1002/gcc.2870100405, indexed in Pubmed: 7522538.
41. Perry A, Kunz SN, Fuller CE, et al. Differential NF1, p16, and EGFR patterns by interphase cytogenetics (FISH) in malignant peripheral nerve sheath tumor (MPNST) and morphologically similar spindle cell neoplasms. J Neuropathol Exp Neurol. 2002; 61(8): 702–709, doi: 10.1093/jnen/61.8.702, indexed in Pubmed: 12152785.
42. Zhang M, Wang Y, Jones S, et al. Somatic mutations of SUZ12 in malignant peripheral nerve sheath tumors. Nat Genet. 2014; 46(11): 1170–1172, doi: 10.1038/ng.3116, indexed in Pubmed: 25305755.
43. Beert E, Brems H, Daniëls B, et al. Atypical neurofibromas in neurofibromatosis type 1 are premalignant tumors. Genes Chromosomes Cancer. 2011; 50(12): 1021–1032, doi: 10.1002/gcc.20921, indexed in Pubmed: 21987445.
44. Thomas LE, Winston J, Rad E, et al. Evaluation of copy number variation and gene expression in neurofibromatosis type-1-associated malignant peripheral nerve sheath tumours. Hum Genomics. 2015; 9(1): 3, doi: 10.1186/s40246-015-0025-3, indexed in Pubmed: 25884485.
45. Brekke HR, Ribeiro FR, Kolberg M, et al. Genomic changes in chromosomes 10, 16, and X in malignant peripheral nerve sheath tumors identify a high-risk patient group. J Clin Oncol. 2010; 28(9): 1573–1582, doi: 10.1200/JCO.2009.24.8989, indexed in Pubmed: 20159821.
46. Yang J, Du X. Genomic and molecular aberrations in malignant peripheral nerve sheath tumor and their roles in personalized target therapy. Surg Oncol. 2013; 22(3): e53–e57, doi: 10.1016/j.suronc.2013.06.003, indexed in Pubmed: 23830351.
47. Skotheim RI, Kallioniemi A, Bjerkhagen B, et al. Topoisomerase-II alpha is upregulated in malignant peripheral nerve sheath tumors and associated with clinical outcome. J Clin Oncol. 2003; 21(24): 4586–4591, doi: 10.1200/JCO.2003.07.067, indexed in Pubmed: 14673046.
48. Amirnasr A, Verdijk RM, van Kuijk PF, et al. Expression and inhibition of BRD4, EZH2 and TOP2A in neurofibromas and malignant peripheral nerve sheath tumors. PLoS One. 2017; 12(8): e0183155, doi: 10.1371/journal.pone.0183155, indexed in Pubmed: 28813519.
49. Li H, Velasco-Miguel S, Vass WC, et al. Epidermal growth factor receptor signaling pathways are associated with tumorigenesis in the Nf1:p53 mouse tumor model. Cancer Res. 2002; 62(15): 4507–4513, indexed in Pubmed: 12154062.
50. Wu J, Patmore DM, Jousma E, et al. EGFR-STAT3 signaling promotes formation of malignant peripheral nerve sheath tumors. Oncogene. 2014; 33(2): 173–180, doi: 10.1038/onc.2012.579, indexed in Pubmed: 23318430.
51. Albritton KH, Rankin C, Coffin CM, et al. Phase II study of erlotinib in metastatic or unresectable malignant peripheral nerve sheath tumors (MPNST). J Clin Oncol. 2006; 24(18_suppl): 9518–9518, doi: 10.1200/jco.2006.24.18_suppl.9518.
52. Suppiah S, Mansouri S, Mamatjan Y, et al. Multiplatform molecular profiling uncovers two subgroups of malignant peripheral nerve sheath tumors with distinct therapeutic vulnerabilities. Nat Commun. 2023; 14(1): 2696, doi: 10.1038/s41467-023-38432-6, indexed in Pubmed: 37164978.
53. Amirnasr A, Verdijk RM, van Kuijk PF, et al. Deregulated microRNAs in neurofibromatosis type 1 derived malignant peripheral nerve sheath tumors. Sci Rep. 2020; 10(1): 2927, doi: 10.1038/s41598-020-59789-4, indexed in Pubmed: 32076030.
54. Subramanian S, Thayanithy V, West RB, et al. Genome-wide transcriptome analyses reveal p53 inactivation mediated loss of miR-34a expression in malignant peripheral nerve sheath tumours. J Pathol. 2010; 220(1): 58–70, doi: 10.1002/path.2633, indexed in Pubmed: 19890883.
55. Feber A, Wilson GA, Zhang Lu, et al. Comparative methylome analysis of benign and malignant peripheral nerve sheath tumors. Genome Res. 2011; 21(4): 515–524, doi: 10.1101/gr.109678.110, indexed in Pubmed: 21324880.
56. Presneau N, Eskandarpour M, Shemais T, et al. MicroRNA profiling of peripheral nerve sheath tumours identifies miR-29c as a tumour suppressor gene involved in tumour progression. Br J Cancer. 2013; 108(4): 964–972, doi: 10.1038/bjc.2012.518, indexed in Pubmed: 23175151.
57. Röhrich M, Koelsche C, Schrimpf D, et al. Methylation-based classification of benign and malignant peripheral nerve sheath tumors. Acta Neuropathol. 2016; 131(6): 877–887, doi: 10.1007/s00401-016-1540-6, indexed in Pubmed: 26857854.
58. Cassier PA, Lefranc A, Amela EY, et al. A phase II trial of panobinostat in patients with advanced pretreated soft tissue sarcoma. A study from the French Sarcoma Group. Br J Cancer. 2013; 109(4): 909–914, doi: 10.1038/bjc.2013.442, indexed in Pubmed: 23922114.
59. Seno N, Fukushima T, Gomi D, et al. Successful treatment with doxorubicin and ifosfamide for mediastinal malignant peripheral nerve sheath tumor with loss of H3K27me3 expression. Thorac Cancer. 2017; 8(6): 720–723, doi: 10.1111/1759-7714.12498, indexed in Pubmed: 28876532.
60. Wassef M, Luscan A, Aflaki S, et al. EZH1/2 function mostly within canonical PRC2 and exhibit proliferation-dependent redundancy that shapes mutational signatures in cancer. Proc Natl Acad Sci U S A. 2019; 116(13): 6075–6080, doi: 10.1073/pnas.1814634116, indexed in Pubmed: 30867289.
61. Katz D, Lazar A, Lev D. Malignant peripheral nerve sheath tumour (MPNST): the clinical implications of cellular signalling pathways. Expert Rev Mol Med. 2009; 11: e30, doi: 10.1017/S1462399409001227, indexed in Pubmed: 19835664.
62. Fukushima S, Endo M, Matsumoto Y, et al. Hypoxia-inducible factor 1 alpha is a poor prognostic factor and potential therapeutic target in malignant peripheral nerve sheath tumor. PLoS One. 2017; 12(5): e0178064, doi: 10.1371/journal.pone.0178064,

indexed in Pubmed: 28558056.
63. Shurell E, Singh AS, Crompton JG, et al. Characterizing the immune microenvironment of malignant peripheral nerve sheath tumor by PD-L1 expression and presence of CD8+ tumor infiltrating lymphocytes. Oncotarget. 2016; 7(39): 64300–64308, doi: 10.18632/oncotarget.11734, indexed in Pubmed: 27588404.
64. Lehnhardt M, Daigeler A, Homann HH, et al. [Importance of specialized centers in diagnosis and treatment of extremity-soft tissue sarcomas. Review of 603 cases]. Chirurg. 2009; 80(4): 341–347, doi: 10.1007/s00104-008-1562-2, indexed in Pubmed: 18523742.
65. Sandrucci S, Trama A, Quagliuolo V, et al. Accreditation for centers of sarcoma surgery. Updates Surg. 2017; 69(1): 1–7, doi: 10.1007/s13304-016-0382-z, indexed in Pubmed: 27502605.
66. Le Guellec S, Decouvelaere AV, Filleron T, et al. Malignant Peripheral Nerve Sheath Tumor Is a Challenging Diagnosis: A Systematic Pathology Review, Immunohistochemistry, and Molecular Analysis in 160 Patients From the French Sarcoma Group Database. Am J Surg Pathol. 2016; 40(7): 896–908, doi: 10.1097/PAS.0000000000000655, indexed in Pubmed: 27158754.
67. Rodriguez FJ, Folpe AL, Giannini C, et al. Pathology of peripheral nerve sheath tumors: diagnostic overview and update on selected diagnostic problems. Acta Neuropathol. 2012; 123(3): 295–319, doi: 10.1007/s00401-012-0954-z, indexed in Pubmed: 22327363.
68. Kim A, Stewart DR, Reilly KM, et al. Malignant Peripheral Nerve Sheath Tumors State of the Science: Leveraging Clinical and Biological Insights into Effective Therapies. Sarcoma. 2017; 2017: 7429697, doi: 10.1155/2017/7429697, indexed in Pubmed: 28592921.
69. Krawczyk MA, Karpinsky G, Izycka-Swieszewska E, et al. Immunohistochemical assessment of cyclin D1 and p53 is associated with survival in childhood malignant peripheral nerve sheath tumor. Cancer Biomark. 2019; 24(3): 351–361, doi: 10.3233/CBM-181572, indexed in Pubmed: 30883338.
70. Zhou H, Coffin CM, Perkins SL, et al. Malignant peripheral nerve sheath tumor: a comparison of grade, immunophenotype, and cell cycle/growth activation marker expression in sporadic and neurofibromatosis 1-related lesions. Am J Surg Pathol. 2003; 27(10): 1337–1345, doi: 10.1097/00000478-200310000-00006, indexed in Pubmed: 14508395.
71. Kamran SC, Howard SA, Shinagare AB, et al. Malignant peripheral nerve sheath tumors: prognostic impact of rhabdomyoblastic differentiation (malignant triton tumors), neurofibromatosis 1 status and location. Eur J Surg Oncol. 2013; 39(1): 46–52, doi: 10.1016/j.ejso.2012.09.001, indexed in Pubmed: 23084090.
72. Mito JK, Qian X, Doyle LA, et al. Role of Histone H3K27 Trimethylation Loss as a Marker for Malignant Peripheral Nerve Sheath Tumor in Fine-Needle Aspiration and Small Biopsy Specimens. Am J Clin Pathol. 2017; 148(2): 179–189, doi: 10.1093/ajcp/aqx060, indexed in Pubmed: 28898989.
73. Ito Y, Kohashi K, Endo M, et al. Clinicopathological and prognostic significance of H3K27 methylation status in malignant peripheral nerve sheath tumor: correlation with skeletal muscle differentiation. Virchows Arch. 2021; 479(6): 1233–1244, doi: 10.1007/s00428-021-03189-0, indexed in Pubmed: 34432163.
74. Wilson MP, Katlariwala P, Low G, et al. Diagnostic Accuracy of MRI for the Detection of Malignant Peripheral Nerve Sheath Tumors: A Systematic Review and Meta-Analysis. AJR Am J Roentgenol. 2021; 217(1): 31–39, doi: 10.2214/AJR.20.23403, indexed in Pubmed: 33909462.
75. Yun JS, Lee MH, Lee SM, et al. Peripheral nerve sheath tumor: differentiation of malignant from benign tumors with conventional and diffusion-weighted MRI. Eur Radiol. 2021; 31(3): 1548–1557, doi: 10.1007/s00330-020-07234-5, indexed in Pubmed: 32894357.
76. Benz MR, Czernin J, Dry SM, et al. Quantitative F18--fluorodeoxyglucose positron emission tomography accurately characterizes peripheral nerve sheath tumors as malignant or benign. Cancer. 2010; 116(2): 451–458, doi: 10.1002/cncr.24755, indexed in Pubmed: 19924789.
77. Nishida Y, Ikuta K, Ito S, et al. Limitations and benefits of FDG-PET/CT in NF1 patients with nerve sheath tumors: A cross-sectional/longitudinal study. Cancer Sci. 2021; 112(3): 1114–1122, doi: 10.1111/cas.14802, indexed in Pubmed: 33415792.
78. Assadi M, Velez E, Najafi MH, et al. PET Imaging of Peripheral Nerve Tumors. PET Clin. 2019; 14(1): 81–89, doi: 10.1016/j.cpet.2018.08.013, indexed in Pubmed: 30420224.
79. Pendleton C, Howe BM, Spinner RJ. Percutaneous image-guided biopsy in malignant peripheral nerve sheath tumors. Acta Neurochir (Wien). 2021; 163(2): 515–519, doi: 10.1007/s00701-020-04556-7, indexed in Pubmed: 32901394.
80. Pianta M, Chock E, Schlicht S, et al. Accuracy and complications of CT-guided core needle biopsy of peripheral nerve sheath tumours. Skeletal Radiol. 2015; 44(9): 1341–1349, doi: 10.1007/s00256-015-2185-6, indexed in Pubmed: 26078215.
81. Graham DS, Russell TA, Eckardt MA, et al. Oncologic Accuracy of Image-guided Percutaneous Core-Needle Biopsy of Peripheral Nerve Sheath Tumors at a High-volume Sarcoma Center. Am J Clin Oncol. 2019; 42(10): 739–743, doi: 10.1097/COC.0000000000000591, indexed in Pubmed: 31436746.
82. Wakely PE, Ali SZ, Bishop JA. The cytopathology of malignant peripheral nerve sheath tumor: a report of 55 fine-needle aspiration cases. Cancer Cytopathol. 2012; 120(5): 334–341, doi: 10.1002/cncy.21195, indexed in Pubmed: 22434579.
83. Tonsgard JH. Clinical manifestations and management of neurofibromatosis type 1. Semin Pediatr Neurol. 2006; 13(1): 2–7, doi: 10.1016/j.spen.2006.01.005, indexed in Pubmed: 16818170.
84. Evans DGR, Baser ME, McGaughran J, et al. Malignant peripheral nerve sheath tumours in neurofibromatosis 1. J Med Genet. 2002; 39(5): 311–314, doi: 10.1136/jmg.39.5.311, indexed in Pubmed: 12011145.
85. Mautner VF, Asuagbor FA, Dombi E, et al. Assessment of benign tumor burden by whole-body MRI in patients with neurofibromatosis 1. Neuro Oncol. 2008; 10(4): 593–598, doi: 10.1215/15228517-2008-011, indexed in Pubmed: 18559970.
86. Derlin T, Tornquist K, Münster S, et al. Comparative effectiveness of 18F-FDG PET/CT versus whole-body MRI for detection of malignant peripheral nerve sheath tumors in neurofibromatosis type 1. Clin Nucl Med. 2013; 38(1): e19–e25, doi: 10.1097/RLU.0b013e318266ce84, indexed in Pubmed: 23242059.
87. Well L, Salamon J, Kaul MG, et al. Differentiation of peripheral nerve sheath tumors in patients with neurofibromatosis type 1 using diffusion-weighted magnetic resonance imaging. Neuro Oncol. 2019; 21(4): 508–516, doi: 10.1093/neuonc/noy199, indexed in Pubmed: 30496452.
88. Baca N, Majlessipour F, Xie Y, et al. Characterization of pre--malignant lesions in patients with pediatric neurofibromatosis type 1 using a novel whole-body magnetic resonance imaging technique. J Clin Oncol. 2023; 41(16_suppl): TPS10637–TPS10637, doi: 10.1200/jco.2023.41.16_suppl.tps10637.
89. Ferner RE, Golding JF, Smith M, et al. [18F]2-fluoro-2-deoxy-D--glucose positron emission tomography (FDG PET) as a diagnostic tool for neurofibromatosis 1 (NF1) associated malignant peripheral nerve sheath tumours (MPNSTs): a long-term clinical study. Ann Oncol. 2008; 19(2): 390–394, doi: 10.1093/annonc/mdm450, indexed in Pubmed: 17932395.
90. Salamon J, Veldhoen S, Apostolova I, et al. 18F-FDG PET/CT for detection of malignant peripheral nerve sheath tumours in neurofibromatosis type 1: tumour-to-liver ratio is superior to an SUVmax cut-off. Eur Radiol. 2014; 24(2): 405–412, doi: 10.1007/s00330-013-3020-x, indexed in Pubmed: 24097302.
91. Chirindel A, Chaudhry M, Blakeley JO, et al. 18F-FDG PET/CT qualitative and quantitative evaluation in neurofibromatosis type 1 patients for detection of malignant transformation: comparison of early to delayed imaging with and without liver activity normalization. J Nucl Med. 2015; 56(3): 379–385, doi: 10.2967/jnumed.114.142372, indexed in Pubmed: 25655626.
92. Azizi AA, Slavc I, Theisen BE, et al. Monitoring of plexiform neurofibroma in children and adolescents with neurofibromatosis

type 1 by [ F]FDG-PET imaging. Is it of value in asymptomatic patients? Pediatr Blood Cancer. 2018; 65(1), doi: 10.1002/pbc.26733, indexed in Pubmed: 28771999.
93. Krzakowski M, Rutkowski P, Jassem J, et al. Zalecenia w zakresie zastosowania badań pozytonowej emisyjnej tomografii w onkologii. NOWOTWORY Journal of Oncology. 2011; 61(1): 57–69.
94. Ahlawat S, Blakeley JO, Rodriguez FJ, et al. Imaging biomarkers for malignant peripheral nerve sheath tumors in neurofibromatosis type 1. Neurology. 2019; 93(11): e1076–e1084, doi: 10.1212/WNL.0000000000008092, indexed in Pubmed: 31395668.
95. Tovmassian D, Razak MA, London K. The Role of [$^{18}$F]FDG-PET/CT in Predicting Malignant Transformation of Plexiform Neurofibromas in Neurofibromatosis-1. Int J Surg Oncol. 2016; 2016: 1–7, doi: 10.1155/2016/6162182, indexed in Pubmed: 28058117.
96. Szymanski JJ, Sundby RT, Jones PA, et al. Cell-free DNA ultra-low-pass whole genome sequencing to distinguish malignant peripheral nerve sheath tumor (MPNST) from its benign precursor lesion: A cross-sectional study. PLoS Med. 2021; 18(8): e1003734, doi: 10.1371/journal.pmed.1003734, indexed in Pubmed: 34464388.
97. Ferner RE, Huson SM, Thomas N, et al. Guidelines for the diagnosis and management of individuals with neurofibromatosis 1. J Med Genet. 2007; 44(2): 81–88, doi: 10.1136/jmg.2006.045906, indexed in Pubmed: 17105749.
98. Casali PG, Abecassis N, Bauer S, et al. Soft tissue and visceral sarcomas: ESMO–EURACAN Clinical Practice Guidelines for diagnosis, treatment and follow-up. Ann Oncol. 2018; 29(Suppl 4): iv51–iv67, doi: 10.1093/annonc/mdy096, indexed in Pubmed: 29846498.
99. Carli M, Ferrari A, Mattke A, et al. Pediatric malignant peripheral nerve sheath tumor: the Italian and German soft tissue sarcoma cooperative group. J Clin Oncol. 2005; 23(33): 8422–8430, doi: 10.1200/JCO.2005.01.4886, indexed in Pubmed: 16293873.
100. Higham CS, Steinberg SM, Dombi E, et al. SARC006: Phase II Trial of Chemotherapy in Sporadic and Neurofibromatosis Type 1 Associated Chemotherapy-Naive Malignant Peripheral Nerve Sheath Tumors. Sarcoma. 2017; 2017: 8685638, doi: 10.1155/2017/8685638, indexed in Pubmed: 29138631.
101. Gronchi A, Stacchiotti S, Verderio P, et al. Short, full-dose adjuvant chemotherapy (CT) in high-risk adult soft tissue sarcomas (STS): long-term follow-up of a randomized clinical trial from the Italian Sarcoma Group and the Spanish Sarcoma Group. Ann Oncol. 2016; 27(12): 2283–2288, doi: 10.1093/annonc/mdw430, indexed in Pubmed: 27733375.
102. Hirbe AC, Cosper PF, Dahiya S, et al. Neoadjuvant Ifosfamide and Epirubicin in the Treatment of Malignant Peripheral Nerve Sheath Tumors. Sarcoma. 2017; 2017: 3761292, doi: 10.1155/2017/3761292, indexed in Pubmed: 28546782.
103. Gronchi A, Ferrari S, Quagliuolo V, et al. Histotype-tailored neoadjuvant chemotherapy versus standard chemotherapy in patients with high-risk soft-tissue sarcomas (ISG-STS 1001): an international, open-label, randomised, controlled, phase 3, multicentre trial. Lancet Oncol. 2017; 18(6): 812–822, doi: 10.1016/S1470-2045(17)30334-0, indexed in Pubmed: 28499583.
104. Gronchi A, Palmerini E, Quagliuolo V, et al. Neoadjuvant Chemotherapy in High-Risk Soft Tissue Sarcomas: Final Results of a Randomized Trial From Italian (ISG), Spanish (GEIS), French (FSG), and Polish (PSG) Sarcoma Groups. J Clin Oncol. 2020; 38(19): 2178–2186, doi: 10.1200/jco.19.03289, indexed in Pubmed: 32421444.
105. Karpinsky G, Krawczyk MA, Izycka-Swieszewska E, et al. Tumor expression of survivin, p53, cyclin D1, osteopontin and fibronectin in predicting the response to neo-adjuvant chemotherapy in children with advanced malignant peripheral nerve sheath tumor. J Cancer Res Clin Oncol. 2018; 144(3): 519–529, doi: 10.1007/s00432-018-2580-1, indexed in Pubmed: 29332262.
106. Weiss A, Chen YL, Scharschmidt T, et al. Pathological response in children and adults with large unresected intermediate-grade or high-grade soft tissue sarcoma receiving preoperative chemoradiotherapy with or without pazopanib (ARST1321): a multicentre, randomised, open-label, phase 2 trial. Lancet Oncol. 2020; 21(8): 1110–1122, doi: 10.1016/s1470-2045(20)30325-9, indexed in Pubmed: 32702309.
107. Shurell-Linehan E, DiPardo BJ, Elliott IA, et al. Pathologic Response to Neoadjuvant Therapy is Associated With Improved Long-term Survival in High-risk Primary Localized Malignant Peripheral Nerve Sheath Tumors. Am J Clin Oncol. 2019; 42(5): 426–431, doi: 10.1097/COC.0000000000000536, indexed in Pubmed: 30913092.
108. Valentin T, Le Cesne A, Ray-Coquard I, et al. Management and prognosis of malignant peripheral nerve sheath tumors: The experience of the French Sarcoma Group (GSF-GETO). Eur J Cancer. 2016; 56: 77–84, doi: 10.1016/j.ejca.2015.12.015, indexed in Pubmed: 26824706.
109. Hwang InK, Hahn SM, Kim HS, et al. Outcomes of Treatment for Malignant Peripheral Nerve Sheath Tumors: Different Clinical Features Associated with Neurofibromatosis Type 1. Cancer Res Treat. 2017; 49(3): 717–726, doi: 10.4143/crt.2016.271, indexed in Pubmed: 28052660.
110. Longhi A, Errani C, Magagnoli G, et al. High grade malignant peripheral nerve sheath tumors: outcome of 62 patients with localized disease and review of the literature. J Chemother. 2010; 22(6): 413–418, doi: 10.1179/joc.2010.22.6.413, indexed in Pubmed: 21303750.
111. Bishop AJ, Zagars GK, Torres KE, et al. Malignant Peripheral Nerve Sheath Tumors: A Single Institution's Experience Using Combined Surgery and Radiation Therapy. Am J Clin Oncol. 2018; 41(5): 465–470, doi: 10.1097/COC.0000000000000303, indexed in Pubmed: 27281262.
112. Stucky CC, Johnson K, Gray R, et al. Malignant Peripheral Nerve Sheath Tumors (MPNST): The Mayo Clinic Experience. Ann Surg Oncol. 2011; 19(3): 878–885, doi: 10.1245/s10434-011-1978-7, indexed in Pubmed: 21861229.
113. Pervaiz N, Colterjohn N, Farrokhyar F, et al. A systematic meta-analysis of randomized controlled trials of adjuvant chemotherapy for localized resectable soft-tissue sarcoma. Cancer. 2008; 113(3): 573–581, doi: 10.1002/cncr.23592, indexed in Pubmed: 18521899.
114. Anghileri M, Miceli R, Fiore M, et al. Malignant peripheral nerve sheath tumors. Cancer. 2006; 107(5): 1065–1074, doi: 10.1002/cncr.22098, indexed in Pubmed: 16881077.
115. Wong WW, Hirose T, Scheithauer BW, et al. Malignant peripheral nerve sheath tumor: analysis of treatment outcome. Int J Radiat Oncol Biol Phys. 1998; 42(2): 351–360, doi: 10.1016/s0360-3016(98)00223-5, indexed in Pubmed: 9788415.
116. DeLaney TF, Liebsch NJ, Pedlow FX, et al. Long-term results of Phase II study of high dose photon/proton radiotherapy in the management of spine chordomas, chondrosarcomas, and other sarcomas. J Surg Oncol. 2014; 110(2): 115–122, doi: 10.1002/jso.23617, indexed in Pubmed: 24752878.
117. Jensen AD, Uhl M, Chaudhri N, et al. Carbon Ion irradiation in the treatment of grossly incomplete or unresectable malignant peripheral nerve sheaths tumors: acute toxicity and preliminary outcome. Radiat Oncol. 2015; 10: 109, doi: 10.1186/s13014-015-0414-8, indexed in Pubmed: 25943106.
118. Voth C, Wu X, Keirns D, et al. Analysis of demographic characteristics of malignant peripheral nerve sheath tumor in adults: A National Cancer Database study. J Clin Oncol. 2023; 41(16_suppl): e23555–e23555, doi: 10.1200/jco.2023.41.16_suppl.e23555.
119. Zou C, Smith KD, Liu J, et al. Clinical, pathological, and molecular variables predictive of malignant peripheral nerve sheath tumor outcome. Ann Surg. 2009; 249(6): 1014–1022, doi: 10.1097/SLA.0b013e3181a77e9a, indexed in Pubmed: 19474676.
120. Kolberg M, Høland M, Agesen TH, et al. Survival meta-analyses for >1800 malignant peripheral nerve sheath tumor patients with and without neurofibromatosis type 1. Neuro Oncol. 2013; 15(2): 135–147, doi: 10.1093/neuonc/nos287, indexed in Pubmed: 23161774.

121. Hirozane T, Nakayama R, Yamaguchi S, et al. Recurrent malignant peripheral nerve sheath tumor presenting as an asymptomatic intravenous thrombus extending to the heart: a case report. World J Surg Oncol. 2022; 20(1): 8, doi: 10.1186/s12957-021-02473-2, indexed in Pubmed: 34996471.
122. Lee CS, Huh JiS, Chang JW, et al. The early detection of recurrence of malignant peripheral nerve sheath tumor by frequent magnetic resonance imaging. J Korean Neurosurg Soc. 2010; 47(1): 51–54, doi: 10.3340/jkns.2010.47.1.51, indexed in Pubmed: 20157379.
123. Marickar YM, Abraham B. Malignant peripheral nerve sheath tumour - A long story: Case report. Int J Surg Case Rep. 2020; 77: 618–623, doi: 10.1016/j.ijscr.2020.11.061, indexed in Pubmed: 33395859.
124. Gronchi A, Miah AB, Tos APD, et al. Soft tissue and visceral sarcomas: ESMO–EURACAN–GENTURIS Clinical Practice Guidelines for diagnosis, treatment and follow-up. Ann Oncol. 2021; 32(11): 1348–1365, doi: 10.1016/j.annonc.2021.07.006, indexed in Pubmed: 34303806.
125. Kahn J, Gillespie A, Ondos J, et al. Radiation Therapy in Management of Sporadic and Neurofibromatosis Type 1 (NF1) Associated Malignant Peripheral Nerve Sheath Tumors (MPNST). International Journal of Radiation Oncology*Biology*Physics. 2012; 84(3): S638, doi: 10.1016/j.ijrobp.2012.07.1704.
126. Boyce-Fappiano D, Damron EP, Farooqi A, et al. Hypofractionated Radiation Therapy for Unresectable or Metastatic Sarcoma Lesions. Adv Radiat Oncol. 2022; 7(3): 100913, doi: 10.1016/j.adro.2022.100913, indexed in Pubmed: 35647398.
127. Kroep JR, Ouali M, Gelderblom H, et al. First-line chemotherapy for malignant peripheral nerve sheath tumor (MPNST) versus other histological soft tissue sarcoma subtypes and as a prognostic factor for MPNST: an EORTC Soft Tissue and Bone Sarcoma Group study. Ann Oncol. 2011; 22(1): 207–214, doi: 10.1093/annonc/mdq338, indexed in Pubmed: 20656792.
128. Santoro A, Tursz T, Mouridsen H, et al. Doxorubicin versus CYVADIC versus doxorubicin plus ifosfamide in first-line treatment of advanced soft tissue sarcomas: a randomized study of the European Organization for Research and Treatment of Cancer Soft Tissue and Bone Sarcoma Group. J Clin Oncol. 1995; 13(7): 1537–1545, doi: 10.1200/JCO.1995.13.7.1537, indexed in Pubmed: 7602342.
129. Judson I, Verweij J, Gelderblom H, et al. European Organisation and Treatment of Cancer Soft Tissue and Bone Sarcoma Group. Doxorubicin alone versus intensified doxorubicin plus ifosfamide for first-line treatment of advanced or metastatic soft-tissue sarcoma: a randomised controlled phase 3 trial. Lancet Oncol. 2014; 15(4): 415–423, doi: 10.1016/S1470-2045(14)70063-4, indexed in Pubmed: 24618336.
130. Zehou O, Fabre E, Zelek L, et al. Chemotherapy for the treatment of malignant peripheral nerve sheath tumors in neurofibromatosis 1: a 10-year institutional review. Orphanet J Rare Dis. 2013; 8: 127, doi: 10.1186/1750-1172-8-127, indexed in Pubmed: 23972085.
131. Torres KE, Liu J, Young E, et al. Expression of'drugable' tyrosine kinase receptors in malignant peripheral nerve sheath tumour: potential molecular therapeutic targets for a chemoresistant cancer. Histopathology. 2011; 59(1): 156–159, doi: 10.1111/j.1365-2559.2011.03867.x, indexed in Pubmed: 21771036.
132. Tawbi H, Thomas D, Lucas DR, et al. Epidermal growth factor receptor expression and mutational analysis in synovial sarcomas and malignant peripheral nerve sheath tumors. Oncologist. 2008; 13(4): 459–466, doi: 10.1634/theoncologist.2007-0166, indexed in Pubmed: 18448562.
133. Albritton KH, Rankin C, Coffin CM, et al. Phase II study of erlotinib in metastatic or unresectable malignant peripheral nerve sheath tumors (MPNST). J Clin Oncol. 2006; 24(18_suppl): 9518–9518, doi: 10.1200/jco.2006.24.18_suppl.9518.
134. Widemann B, Meyer C, Cote G, et al. SARC016: Phase II study of everolimus in combination with bevacizumab in sporadic and neurofibromatosis type 1 (NF1) related refractory malignant peripheral nerve sheath tumors (MPNST). J Clin Oncol. 2016; 34(15_suppl): 11053–11053, doi: 10.1200/jco.2016.34.15_suppl.11053.
135. Kim A, Reinke D, Cichowski K, et al. SARC023: Phase I/II trial of ganetespib in combination with sirolimus for refractory sarcomas and malignant peripheral nerve sheath tumors (MPNST). J Clin Oncol. 2014; 32(15_suppl): TPS10603–TPS10603, doi: 10.1200/jco.2014.32.15_suppl.tps10603.
136. Chugh R, Wathen JK, Maki RG, et al. Phase II multicenter trial of imatinib in 10 histologic subtypes of sarcoma using a bayesian hierarchical statistical model. J Clin Oncol. 2009; 27(19): 3148–3153, doi: 10.1200/JCO.2008.20.5054, indexed in Pubmed: 19451433.
137. Maki RG, D'Adamo DR, Keohan ML, et al. Phase II study of sorafenib in patients with metastatic or recurrent sarcomas. J Clin Oncol. 2009; 27(19): 3133–3140, doi: 10.1200/JCO.2008.20.4495, indexed in Pubmed: 19451436.
138. Akshintala S, Mallory N, Lu Y, et al. Outcome of patients with refractory malignant peripheral nerve sheath tumors (MPNST) enrolled on phase 2 trials. J Clin Oncol. 2019; 37(15_suppl): e22534–e22534, doi: 10.1200/jco.2019.37.15_suppl.e22534.
139. Manji G, Patwardhan P, Lee S, et al. Phase 1/2 study of combination therapy with pexidartinib and sirolimus to target tumor-associated macrophages in malignant peripheral nerve sheath tumors. J Clin Oncol. 2016; 34(15_suppl): TPS11070–TPS11070, doi: 10.1200/jco.2016.34.15_suppl.tps11070.
140. Manji GA, Van Tine BA, Lee SM, et al. A Phase I Study of the Combination of Pexidartinib and Sirolimus to Target Tumor-Associated Macrophages in Unresectable Sarcoma and Malignant Peripheral Nerve Sheath Tumors. Clin Cancer Res. 2021; 27(20): 5519–5527, doi: 10.1158/1078-0432.CCR-21-1779, indexed in Pubmed: 34321280.
141. Davis L, Latour E, Burch R, et al. A phase Ib study of ribociclib in combination with doxorubicin in advanced soft tissue sarcomas (aSTS). J Clin Oncol. 2020; 38(15_suppl): 11548–11548, doi: 10.1200/jco.2020.38.15_suppl.11548.
142. Striefler JK, Brandes F, Baur A, et al. Combination therapy with Olaratumab/doxorubicin in advanced or metastatic soft tissue sarcoma -a single-Centre experience. BMC Cancer. 2020; 20(1): 68, doi: 10.1186/s12885-020-6551-y, indexed in Pubmed: 31996176.
143. Tap WD, Wagner AJ, Schöffski P, et al. ANNOUNCE Investigators. Effect of Doxorubicin Plus Olaratumab vs Doxorubicin Plus Placebo on Survival in Patients With Advanced Soft Tissue Sarcomas: The ANNOUNCE Randomized Clinical Trial. JAMA. 2020; 323(13): 1266–1276, doi: 10.1001/jama.2020.1707, indexed in Pubmed: 32259228.
144. Hyman D, Kummar S, Farago A, et al. Abstract CT127: Phase I and expanded access experience of LOXO-195 (BAY 2731954), a selective next-generation TRK inhibitor (TRKi). Cancer Res. 2019; 79(13_Supplement): CT127–CT127, doi: 10.1158/1538-7445.am2019-ct127.
145. Yoo KH, Kim HS, Lee SuJ, et al. Efficacy of pazopanib monotherapy in patients who had been heavily pretreated for metastatic soft tissue sarcoma: a retrospective case series. BMC Cancer. 2015; 15: 154, doi: 10.1186/s12885-015-1160-x, indexed in Pubmed: 25885855.
146. Nakamura T, Matsumine A, Kawai A, et al. The clinical outcome of pazopanib treatment in Japanese patients with relapsed soft tissue sarcoma: A Japanese Musculoskeletal Oncology Group (JMOG) study. Cancer. 2016; 122(9): 1408–1416, doi: 10.1002/cncr.29961, indexed in Pubmed: 26970174.
147. Nishida Y, Urakawa H, Nakayama R, et al. Phase II clinical trial of pazopanib for patients with unresectable or metastatic malignant peripheral nerve sheath tumors. Int J Cancer. 2020; 148(1): 140–149, doi: 10.1002/ijc.33201, indexed in Pubmed: 32638374.
148. Ryan C, Degnin C, Cranmer L, et al. A randomized phase II study of gemcitabine (G) alone or with pazopanib (P) in refractory soft tissue sarcoma (STS). J Clin Oncol. 2020; 38(15_suppl): 11515–11515, doi: 10.1200/jco.2020.38.15_suppl.11515.
149. Ingham M, Mahoney M, Remotti F, et al. A randomized phase II study of MLN0128 (M) versus pazopanib (P) in patients (pt)

with advanced sarcoma (Alliance A091304). J Clin Oncol. 2020; 38(15_suppl): 11562–11562, doi: 10.1200/jco.2020.38.15_suppl.11562.
150. CT02601209. Sapanisertib or Pazopanib Hydrochloride in Treating Patients With Locally Advanced or Metastatic Sarcoma. December 2023. https://clinicaltrials.gov/study/NCT02601209.
151. Patel SP, Othus M, Chae YK, et al. A Phase II Basket Trial of Dual Anti-CTLA-4 and Anti-PD-1 Blockade in Rare Tumors (DART SWOG 1609) in Patients with Nonpancreatic Neuroendocrine Tumors. Clin Cancer Res. 2020; 26(10): 2290–2296, doi: 10.1158/1078-0432.CCR-19-3356, indexed in Pubmed: 31969335.
152. Movva S, Avutu V, Chi P, et al. A pilot study of lenvatinib plus pembrolizumab in patients with advanced sarcoma. J Clin Oncol. 2023; 41(16_suppl): 11517–11517, doi: 10.1200/jco.2023.41.16_suppl.11517.
153. Somaiah N, Tine BV, Chmielowski B, et al. A phase 2 study of alrizomadlin, a novel MDM2/p53 inhibitor, in combination with pembrolizumab for treatment of patients with malignant peripheral nerve sheath tumor (MPNST). J Clin Oncol. 2023; 41(16_suppl): e14627–e14627, doi: 10.1200/jco.2023.41.16_suppl.e14627.
154. Yan P, Huang R, Hu P, et al. Nomograms for predicting the overall and cause-specific survival in patients with malignant peripheral nerve sheath tumor: a population-based study. J Neurooncol. 2019; 143(3): 495–503, doi: 10.1007/s11060-019-03181-4, indexed in Pubmed: 31089923.
155. Zou C, Smith KD, Liu J, et al. Clinical, pathological, and molecular variables predictive of malignant peripheral nerve sheath tumor outcome. Ann Surg. 2009; 249(6): 1014–1022, doi: 10.1097/SLA.0b013e3181a77e9a, indexed in Pubmed: 19474676.
156. LaFemina J, Qin LX, Moraco NH, et al. Oncologic outcomes of sporadic, neurofibromatosis-associated, and radiation-induced malignant peripheral nerve sheath tumors. Ann Surg Oncol. 2013; 20(1): 66–72, doi: 10.1245/s10434-012-2573-2, indexed in Pubmed: 22878618.
157. Wakeman KM, Zhang QS, Bandhlish A, et al. Fédération Nationale Des Centres de Lutte Contre Le Cancer (FNCLCC) Grading, Margin Status and Tumor Location Associate With Survival Outcomes in Malignant Peripheral Nerve Sheath Tumors. Am J Clin Oncol. 2022; 45(1): 28–35, doi: 10.1097/COC.0000000000000877, indexed in Pubmed: 34962906.
158. Martin E, Muskens IS, Coert JH, et al. Treatment and survival differences across tumor sites in malignant peripheral nerve sheath tumors: a SEER database analysis and review of the literature. Neurooncol Pract. 2019; 6(2): 134–143, doi: 10.1093/nop/npy025, indexed in Pubmed: 31386019.
159. Kromer CM, Yacoub N, Xiong D, et al. Analysis of Survival Differences Between Cutaneous and Subcutaneous Malignant Peripheral Nerve Sheath Tumors. Dermatol Surg. 2023; 49(4): 322–329, doi: 10.1097/DSS.0000000000003717, indexed in Pubmed: 36763849.
160. Xu Y, Xu G, Liu Z, et al. Incidence and prognosis of distant metastasis in malignant peripheral nerve sheath tumors. Acta Neurochir (Wien). 2021; 163(2): 521–529, doi: 10.1007/s00701-020-04647-5, indexed in Pubmed: 33219865.
161. Sobczuk P, Teterycz P, Zdzienicki M, et al. Clinicopathological prognostic and predictive factors of malignant peripheral nerve sheath tumors (MPNST) survival and treatment efficacy. J Clin Oncol. 2019; 37(15_suppl): e22537–e22537, doi: 10.1200/jco.2019.37.15_suppl.e22537.
162. Porter DE, Prasad V, Foster L, et al. Survival in Malignant Peripheral Nerve Sheath Tumours: A Comparison between Sporadic and Neurofibromatosis Type 1-Associated Tumours. Sarcoma. 2009; 2009: 756395, doi: 10.1155/2009/756395, indexed in Pubmed: 19360115.
163. Malbari F, Spira M, B Knight P, et al. Malignant Peripheral Nerve Sheath Tumors in Neurofibromatosis: Impact of Family History. J Pediatr Hematol Oncol. 2018; 40(6): e359–e363, doi: 10.1097/MPH.0000000000001156, indexed in Pubmed: 29683959.
164. Cai Z, Tang X, Liang H, et al. Prognosis and risk factors for malignant peripheral nerve sheath tumor: a systematic review and meta-analysis. World J Surg Oncol. 2020; 18(1): 257, doi: 10.1186/s12957-020-02036-x, indexed in Pubmed: 32998743.
165. Martin E, Coert JH, Flucke UE, et al. Neurofibromatosis-associated malignant peripheral nerve sheath tumors in children have a worse prognosis: A nationwide cohort study. Pediatr Blood Cancer. 2020; 67(4): e28138, doi: 10.1002/pbc.28138, indexed in Pubmed: 31889416.
166. van Noesel MM, Orbach D, Brennan B, et al. Outcome and prognostic factors in pediatric malignant peripheral nerve sheath tumors: An analysis of the European Pediatric Soft Tissue Sarcoma Group (EpSSG) NRSTS-2005 prospective study. Pediatr Blood Cancer. 2019; 66(10): e27833, doi: 10.1002/pbc.27833, indexed in Pubmed: 31241238.
167. Bartlett EK, Sharma A, Seier K, et al. Histology-Specific Prognostication for Radiation-Associated Soft Tissue Sarcoma. JCO Precis Oncol. 2022; 6: e2200087, doi: 10.1200/PO.22.00087, indexed in Pubmed: 36240470.
168. Widemann BC, Italiano A. Biology and Management of Undifferentiated Pleomorphic Sarcoma, Myxofibrosarcoma, and Malignant Peripheral Nerve Sheath Tumors: State of the Art and Perspectives. J Clin Oncol. 2018; 36(2): 160–167, doi: 10.1200/JCO.2017.75.3467, indexed in Pubmed: 29220302.
169. Widemann BC, Italiano A. Biology and Management of Undifferentiated Pleomorphic Sarcoma, Myxofibrosarcoma, and Malignant Peripheral Nerve Sheath Tumors: State of the Art and Perspectives. J Clin Oncol. 2018; 36(2): 160–167, doi: 10.1200/JCO.2017.75.3467, indexed in Pubmed: 29220302.

VIA MEDICA

REVIEW ARTICLE

Oncology in Clinical Practice
2025, Vol. 21, No. 1, 60–70
DOI: 10.5603/ocp.99119

ISSN 2450-1654
eISSN 2450-6478

# Distal and proximal epithelioid sarcoma — differences in diagnosis and similarities in treatment

Maria Krotewicz[1], Anna M. Czarnecka[1,*], Piotr Błoński[1,2], Jakub Śledź[1,3], Bartłomiej Szostakowski[1], Anna Szumera-Ciećkiewicz[4], Ewa Bartnik[5,6], Piotr Rutkowski[1]

[1]Department of Soft Tissue/Bone Sarcoma and Melanoma, Maria Sklodowska-Curie National Research Institute of Oncology, Warsaw, Poland
[2]Faculty of Medicine, Medical University of Warsaw, Poland
[3]Specialist Treatment Center, Nowowiejski Hospital, Medical University of Warsaw, Poland
[4]Department of Pathology, Maria Sklodowska-Curie National Research Institute of Oncology, Warsaw, Poland
[5]Institute of Genetics and Biotechnology, Faculty of Biology, University of Warsaw, Poland
[6]Institute of Biochemistry and Biophysics, Polish Academy of Sciences, Warsaw, Poland

**Abstract**

Epithelioid sarcoma (ES) comprises two subtypes, distal and proximal. Initially, the distinction between these variants was based on tumor location, but subsequent research highlighted numerous functional differences between them. Proximal ES is distinguished by the molecular deletion of INI1, while classic ES is characterized by retained dysfunctional INI1 expression. Classic ES features elevated expression of GLI3, FYN, and CXCL12, along with overactive Notch/Hedgehog pathways and class 1 human leukocyte antigens (HLA). In contrast, proximal ES demonstrates MYC overexpression and upregulation of genes associated with the cell cycle, chromatin metabolism, and protein synthesis. The differences in clinical presentation underscore the necessity for tailored treatment approaches for each ES subtype. New therapeutic strategies are crucial, especially for the aggressive proximal variant. Tazemetostat, an oral selective inhibitor of the histone methyltransferase enhancer of zeste homolog 2 (EZH2), has recently gained FDA approval as a first-line treatment for ES patients.

**Keywords:** sarcoma, epithelioid, INI, surgery, chemotherapy, tazemetostat

## Introduction

Epithelioid sarcoma (ES) is a malignant epithelioid soft tissue tumor of yet undefined etiology. It was first reported by Laskowski in 1961 [1] and then described and named by Enzinger in 1970 [2]. Epithelioid sarcoma is rare with 0.02–0.05 cases per 100 000 people. The reported incidences of epithelioid sarcoma are collected, among others, in the Surveillance, Epidemiology, and End Results (SEER) database supported by the National Cancer Institute of the United States and in the RARECAREnet database in Europe. The RARECAREnet collection gathers data on cancer diagnosed in patients in 27 countries of the European Union. Collected data on ES age-adjusted incidence rates differ in the United States (0.05/100 000) and in the European Union (0.03/100 000) [3].

Epithelioid sarcoma often resembles benign entities in histopathology and therefore initial misdiagnosis is common. Epithelioid sarcoma has high recurrence and metastasis rates (around 70% and 50%, respectively), and poor prognosis [4]. The average survival rate in the absence of distant metastases is estimated at 88 months and 8 months for patients with distant metastases [5, 6]. Metastases are diagnosed in 40% to 50% of cases and mostly localized in regional lymph nodes, lungs, bone, brain, and liver [7], and

*Correspondence: Prof. Anna M. Czarnecka, Department of Soft Tissue/Bone Sarcoma and Melanoma, Maria Sklodowska-Curie National Research Institute of Oncology, ul. Roentgena 5, 02–781 Warsaw, Poland, tel.: +48-22-546-24-55; fax: +48-22-643-93-75 (anna.czarnecka@gmail.com)
Received: 25 January 2024; Accepted: 10 February 2024; Early publication: 5 March 2024

early diagnosis may improve survival for ES patients. Epithelioid sarcoma affects mainly adolescents although it may also be diagnosed in adults (18–79 years old) [4, 8]. Several studies revealed male predominance in ES diagnoses [3, 5]. The most common localization of ES is the upper or lower limb [4, 5]. Typically, ES is diagnosed as a nodule within the subcutis or in deep soft tissues. The nodules grow slowly over the years particularly in the hand and forearm area [9, 10]. Tumors localized in distal extremities are defined as the distal type of ES. The proximal type of ES, less frequent but with a more aggressive clinical course, was described within the perineum and genital region first time in 1997 [11]. The proximal type of epithelioid sarcoma usually accounts for one-third of all ES cases [12]. These two variants of ES differ from each other in localization, epidemiology, and pathological features.

## Macro- and microscopic characteristics of distal and proximal types of epithelioid sarcoma

Distal epithelioid sarcoma, also called conventional or classic, most often occurs in the extremities. It affects different distally located anatomic sites of fingers, hands, and arms in particular in association with tendons or aponeuroses, rarely with bones [2, 9, 13]. Distal ES less often affects the lower leg [14]. The second variant of ES, i.e. the proximal type, also described as the axial or large-cell type, tends to affect soft tissues of the perineum, pelvis, genital tract, head, neck, proximal extremities, and other sites [11, 15–17].

Distal epithelioid sarcoma commonly occurs as a small, solid, superficial, and slowly growing potentially ulcerated nodule or a cluster of nodules. The nodules may be well-circumscribed as well as fused into lobulated masses [3]. Generally, it often grows slowly and is asymptomatic. Histological examination revealed that distal ES is composed of spindle, polygonal, and polyhedral (as in the epithelium) epithelioid cells, containing deeply eosinophilic cytoplasm and often with loss of cellular connections [7, 9]. Polynuclear giant cells occasionally are found in histological preparations [18]. Central palisaded hyalinizing necrosis of the nodule with possible calcification is frequently observed [2, 3]. Tumor tissue of the distal ES contains large numbers of inflammatory cells, hyalinized collagen, vascular invasion, and the deposition of hemosiderin, fibrin, or mucin [2, 3, 7]. Binucleated cells are observed in the smears obtained from lymph node metastases [19].

Proximal ES has a different clinical picture. It forms nonspecific soft tissue masses deep in trunk organs or the proximal part of a limb, commonly with hemorrhage and necrosis [11]. Epithelioid sarcoma presents in histopathology as disintegrated large and round epithelioid cells containing eccentrically located vesicular pleomorphic nuclei, prominent nucleoli, and abundant eosinophilic cytoplasm, with or without paranuclear globules of intermediate filaments characteristic of the rhabdoid phenotype [7, 11, 19, 20]. In the microscopic image, binucleated and multinucleated cells are observed [20]. Mixed multinucleated osteoclast-like cells and signet cells are in aggregations next to the epithelioid cells [20]. The aggregations are separated by fibrous septa [20]. Images of cells in the tumor tissue in proximal ES show greater atypia compared to the distal type [18, 20]. Mitoses are more frequent in proximal ES [20].

## Epidemiology and prognosis of distal and proximal types of epithelioid sarcoma

Distal ES is rare in children and older people but commonly occurs in adolescents and young adults (20–40 years of age, median age 26 years) with a predominance in men [10, 21]. The proximal subtype affects older adults more often than the distal subtype; they are between 20 and 65 years of age, with a median age of 40 years, at diagnosis and a slight predominance of men [7, 9, 19, 21]. Proximal ES comprises fewer than one-third of ES cases [22]. Trauma is cited in 20–25% of ES cases as the cause of tumor appearance [23].

The type of ES is one of the prognostic factors in a clinical rating [8, 24]. The proximal variant of ES is considered more aggressive, and it metastasizes earlier than the distal type [9, 19, 25]. The poorer prognosis in proximal ES may be caused by inadequate surgical resectability associated with the tumor's deeper and more proximal location [7].

Other prognostic factors concerning both ES variants include age, tumor size, vascular invasion, deep location, higher mitotic rate and lack of lymphocyte infiltrate in the primary tumor [5, 9, 25, 26]. A better prognosis is associated with a diagnosis age below 55 years and adequate surgery [4], tumor size below 2 cm (in tumors greater than 2 cm necrosis and vascular invasion are observed) [27], absence of metastasis and low grade (I and II) [4]. Positive prognostic factors are a single localized disease stage and no regional spread [28]. The presence of distant metastases is a poorer prognostic factor compared to the finding of metastasis in regional lymph nodes [29]. Conflicting evidence was reported in terms of an association between sex and prognosis [29, 30]; however, a large study of the SEER database showed no differences in survival between male and female ES patients [31]. Pediatric patients have a better prognosis due to more frequent diagnoses of distal ES and low metastasis rate [21]. Patients who underwent any surgery had a better prognosis, confirming that

surgery is a positive prognostic factor [14, 25, 31]. The postoperative prognosis depends on radicality of local resection [29]. The median local recurrence rate, measured as time from the date of diagnosis to the occurrence of relapse in the primary tumor after surgical treatment, was 13 months (range 6–82 months) in 35% of cases [5]. In patients diagnosed with ES, lymphatic spread is also observed (20–45% of ES cases) [10, 32, 33].

## Immunohistochemical profile of distal and proximal types of epithelioid sarcoma

Analysis of immunoreactivity weakly confirms the difference between distal and proximal variants of epithelioid sarcoma (Tab. 1 [2, 3, 12, 15, 17, 18, 20, 25, 34–41]). Both proximal and distal variants of ES show great immunophenotypic similarity. Consequently, the distinction between the two variants of epithelioid sarcoma is unclear. Therefore, proximal and distal types of epithelioid sarcoma are also considered a continuum of the same disease [21].

Tumor tissue of ES possesses a unique immunophenotype, expressing epithelial and mesenchymal markers [3, 18]. The most common epithelial antigens expressed in epithelioid sarcoma are cytokeratins (Fig. 1), i.e. proteins building the intermediate filament cytoskeleton in epithelial cells. Cytokeratins are expressed in both the distal and proximal variants of epithelioid sarcoma (88.2%), especially cytokeratin 8 and 18 [3, 7, 12]. These keratins typically are co-expressed in normal epithelial cells. Moreover, cytokeratin K8 and K18 are the first to be expressed during embryogenesis [42]. Cytokeratins K8 and K18 are also expressed in most carcinomas and therefore are useful markers in immunohistochemical analysis of tumors. Cytokeratins of high molecular weight, K5 and K6, are usually not detected in ES tumor tissue [17].

Epithelioid sarcoma tumor tissue also shows strong expression of the epithelial membrane antigen (EMA) [12, 18, 20], a member of a family of transmembrane mucin glycoproteins, which is localized on the apical cellular surface of normal epithelial cells. Expression of E-cadherin, a protein that creates epithelial cellular connections was not observed in tumor tissue of distal and proximal ES [12]. Samples of both types of ES tissue overexpress CA125 [12, 34]. Moreover, the serum glycoprotein CA125 level depends on the progression of both tumor variants, tumor growth, and clinical treatment [34, 43]. Epithelial tissue has been reported as one of the main sources of CA125 [44]. Expression of serum antigen CA125 and lack of E-cadherin expression may be useful ES diagnostic epithelial markers. Serum and tissue CA125 level analysis is recommended for monitoring the course of the proximal ES variant [43].

Mesenchymal antigens detected in ES tumors include, among others, vimentin and CD34. Vimentin is a building protein of intermediate filaments in cells of mesenchymal origin and is used to confirm the mesenchymal origin of these tumors. It is expressed in both variants of ES [15, 18, 20, 35–37]. Transmembrane phosphoglycoprotein CD34 is expressed in ES [3, 12, 18, 38]. High expression of angiogenesis factors VEGF-A and VEGF-C has been detected in both ES variants, while proximal ES often shows overexpression of MYC, a proto-oncogene involved in cell cycle regulation. Immunohistochemistry for MYC can be positive in proximal ES [12]. Smooth muscle actin and desmin were usually negative in ES tissue, as was expression of the S-100 protein [3, 18, 20].

In distal and proximal variants of epithelioid sarcoma nuclear positivity for ERG, an ETS-family transcription factor, was detected [39]. ERG represents endothelial markers. It controls endothelial cell differentiation and is used as a marker of endothelial cell neoplasms [39]. The role and origin of ERG in epithelioid sarcoma is unknown. Expression of other endothelial markers such as adhesion molecule CD31, claudin 5, or another transcription factor Prox1 was

**Table 1.** Biomarkers used in the diagnosis of distal and proximal epithelioid sarcoma (ES) types

| | Distal type | Proximal type | References |
|---|---|---|---|
| **Epithelial markers** | | | |
| Cytokeratin 5 | – | – | [17] |
| Cytokeratin 6 | – | – | [17] |
| Cytokeratin 8 | + | + | [7, 12] |
| Cytokeratin 18 | + | + | [7, 12] |
| EMA | + | + | [12, 20] |
| E-cadherin | – | – | [12] |
| CA125 | + | + | [12, 34] |
| **Mesenchymal markers** | | | |
| Vimentin | + | + | [15, 18, 20, 35–37] |
| CD34 | + | + | [3, 12, 18, 38] |
| VEGF-A | + | + | [12] |
| VEGF-C | + | + | [12] |
| Smooth muscle actin | – | – | [3, 18] |
| Desmin | – | – | [3, 18] |
| **Endothelial markers** | | | |
| ERG | + | + | [39] |
| CD31 | – | – | [39] |
| Claudin 5 | – | – | [39] |
| **Gene expression markers** | | | |
| SMARCB1 | – | – | [12, 17, 20, 25, 40] |
| EZH2 | + | + | [41] |

EMA — epithelial membrane antigen

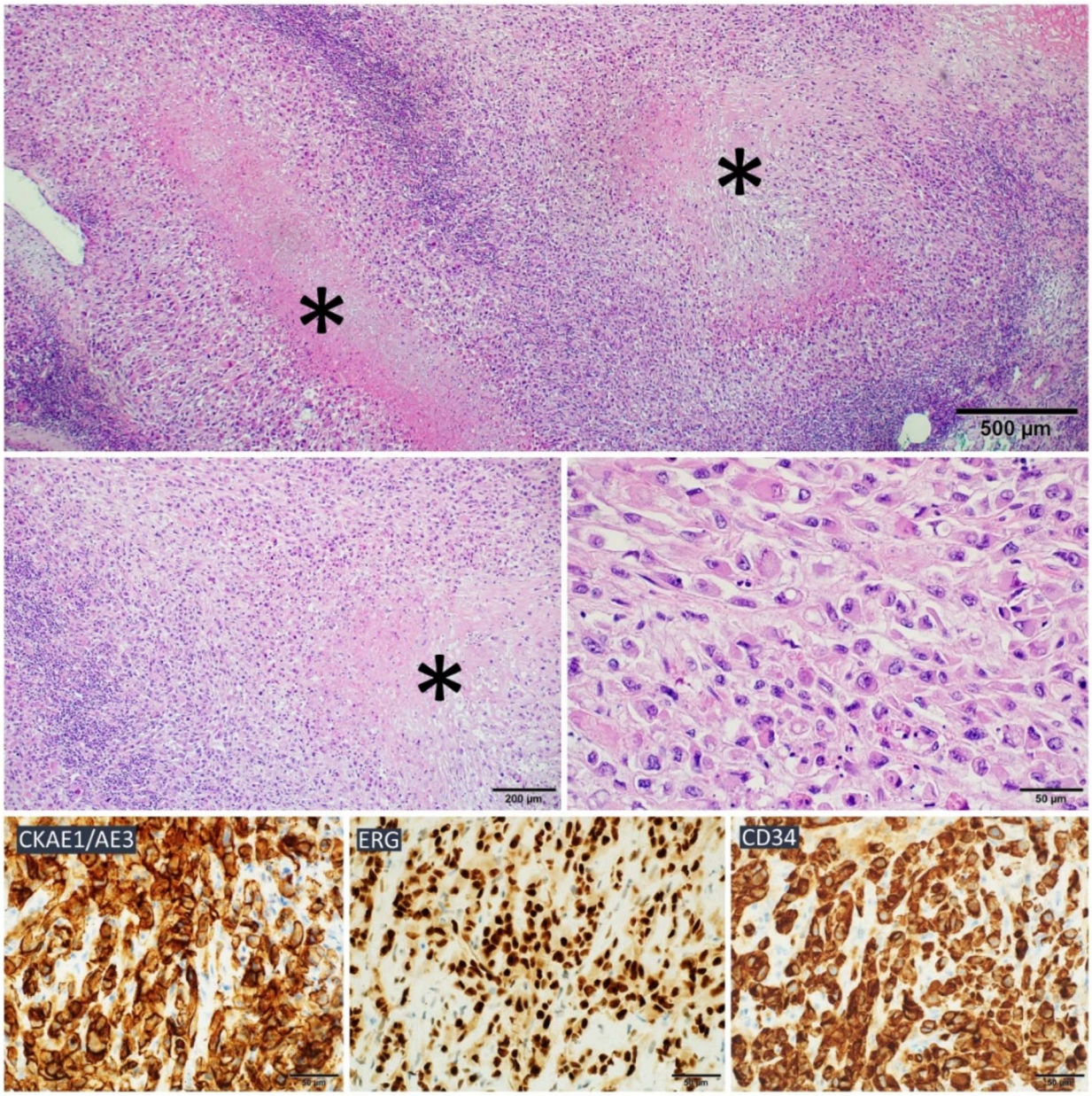


**Figure 1.** Histopathological images of epithelioid sarcoma (ES); tumor composed of malignant epithelioid cells, with geographical necrosis (*) and infiltration by inflammatory cells, mainly lymphocytes; cytokeratins [CKAE1/AE3, CK8/18 and epithelial membrane antigen (EMA)] and vascular markers (CD34 and ERG) are usually positive

not detected in either variant of endothelial sarcoma [39]. Melanosomal glycoprotein HMB45 was not detected in ES [18, 37]; this is useful in its distinction from malignant melanoma [18].

The most diagnostically useful finding is the lack of SMARCB1 (known as integrase interactor INI-1, hSNF5, or BAF 47) protein expression in ES tumor cells [12, 17, 20, 25, 40]. The INI1 protein is a subunit of the Switch/Sucrose Non-Fermentable (SWI/SNF) complex, which plays a crucial role in regulating gene expression by altering the structure of chromatin. SMARCB1/INI1 expression loss is commonly used as a marker of ES [45]. SMARCB1/INI1 is a protein of the BRG1/BRM-associated factor (BAF) complex engaged in remodeling chromatin by nucleosome repositioning, and it suppresses tumor development [46]. SMARCB1 loss has been identified as the sole mutation leading to the initiation of tumor development [46]. The loss of expression of INI1 is characteristic both of classic and proximal ES. In particular, deletion of INI1 is found in proximal ES, while classic ES is characterized by retained dysfunctional INI1 expression. Moreover, classic ES is also characterized by high expression of glioma-associated oncogene

family zinc finger 3 (GLI3), tyrosine-protein kinase fyn (FYN), as well as stromal cell-derived factor 1, also known as C-X-C motif chemokine 12 (CXCL12) [40]. Moreover, proximal ES exhibits MYC overexpression and genomic patterns influencing cell cycle, chromatin metabolism, and protein synthesis. Conversely, classic ES displays heightened activation of Notch/Hedgehog pathways and immune regulation, associated with elevated expression of class 1 human leukocyte antigens (HLA) and enhanced immune infiltration [47].

## Genetic characteristics of distal and proximal types of epithelioid sarcoma

The loss of SMARCB1 (abbreviation of the full gene name SWI/SNF Related, Matrix Associated, Actin Dependent Regulator of Chromatin, Subfamily B, Member 1) expression in ES tumors presented above has a genetic cause. SMARTCB1 is ubiquitously expressed in the nuclei of all normal cells. Moreover, SMARCB1 is a tumor suppressor gene located on chromosome 22 at band 22q11. It encodes BAF47, a subunit of the SWI/SNF (Sucrose Non-Fermentable, SNF) complex which regulates genes, the cell cycle, and signaling pathways [3, 17, 21, 48]. Therefore, inactivation of SMARCB1 leads to genomic instability, cell cycle progression, and abnormal signaling pathway activation [17]. The loss of SMARCB1 has been associated with induction of metaplasia [46]. Both variants of epithelioid sarcoma are characterized by peculiar chromosomal translocations caused by new gene fusions, and numerous rearrangements and deletions. Deletion of *SMARCB1* has been reported in classical and proximal types of ES [26, 49]. Both homozygous and heterozygous deletions of at least two exons in the *SMARCB1* gene were observed in proximal and distal ES variants [26, 49, 50]. The loss of SMARCB1 may also be due to silencing of *SMARCB1* gene expression caused by point mutations, interaction with microRNA, or epigenetic mechanisms [3, 51, 52]. Moreover, it was reported that the loss of SMARCB1/INI1 expression in the tumor cells is related to persistent activation of various pathways engaged in tumor progression, such as phosphatidylinositol 3-kinase (PI3K)/AKT/mTOR signaling pathway, the sonic hedgehog signaling pathway, or the Polycomb pathway [51, 53, 54]. Activation of these pathways leads to induction of cellular proliferation, motility, and survival [51, 53]. Within the tumor tissue, there is a subpopulation of cells exhibiting pluripotent embryonic stem cell characteristics, called cancer stem cells (CSCs), that are not involved in tumor initiation, proliferation, recurrence, metastasis, or drug resistance [55]. Successful tumor initiation and proliferation is based on transformation of normal progenitor cells into cancer stem cells. Analyses of sensitive CSC biomarkers are currently being conducted for use in personalized treatment [55]. The interaction between inactivation of *SMARCB1*/*INI1* and upregulation of enhancer of zeste homolog 2 (EZH2), a member of the polycomb group genes, which are epigenetic regulators of transcription in ES tumorigenesis, has been demonstrated [56]. The role of EZH2 in cancer initiation, progression, and metastasis has been described [56]. Therefore, EZH2 is an important therapeutic target for treating epithelioid sarcoma [17].

The BAF complex mutation has been found in 25% of cancers. BAP1 (BRCA1-associated protein 1) mutations gene have been reported in some cases of epithelioid sarcoma. Moreover, alterations in the *cyclin-dependent kinase inhibitor 2a* (*CDKN2A*), and *neurofibromin 2* (*NF2*) genes, encoding for tumor suppressor proteins, have been identified in epithelioid sarcoma cases [46, 57].

Epithelioid sarcoma biomarker gene expression analysis identified slight differences between distal and proximal ES samples [40] (Tab. 2 [2–4, 7–9, 11, 12, 15, 16, 18–21, 24–26, 40, 45, 49, 58, 59]). The source of distal and proximal ES dissimilarity may be differences in translocations: t(8;22)(q22;q11) in the distal ES variant and t(10;22) in the proximal ES variant [21]. The genetic differences are associated with expression patterns of certain genes related to SMARCB1/INI1 [40]. RNA sequencing profiling conducted on proximal and distal ES samples identified MYC pathway overexpression in the proximal ES variant and Sonic Hedgehog and Notch pathway overexpression in the distal ES variant [3].

## Diagnosis of distal and proximal types of epithelioid sarcoma

Diagnosis of epithelioid sarcoma is often incorrect and delayed due to its rarity, slow growth, and unalarming benign signs. Epithelioid sarcoma, especially the distal variant, mimics numerous diagnoses such as fibrosarcoma, synovial sarcoma, fibrous histiocytic sarcoma, malignant rhabdoid tumor, epithelioid hemangioendothelioma, anaplastic carcinoma, melanoma, or rheumatoid nodules [3, 7, 60, 61]. Nodules of ES slowly extend into deeper tissues reaching sometimes a size greater than 20 cm, causing pain, muscle weakness, movement restriction, paresthesia, and fever of unknown origin [20, 37, 61, 62]. Initial misdiagnoses of ES also relate to its proximal variant. Worse diagnosis of proximal ES may be caused by its rarity and deeper and more proximal location of the tumor. This often leads to a subsequent increase in ES size and risk of metastases. Appropriate and timely diagnosis management is crucial to restrict ES recurrence, metastasis, and mortality. Metastases to lymph

**Table 2.** Comparison of distal and proximal types of epithelioid sarcoma (ES)

| | **Distal epithelioid sarcoma** | **Proximal epithelioid sarcoma** | **Reference** |
|---|---|---|---|
| Place of occurrence | Extremities; distal sites of hands and feet, particularly associated with tendons or aponeuroses | Soft tissue of perineum, pelvis, genital tract, head, neck, proximal parts of extremities | [11, 15, 16, 18] |
| Incidence | More frequent | Less frequent (approximately one-third of all ES cases) | [11, 12] |
| Demography | Predominantly affects male adolescents and young adults | Tends to affect older individuals | [8] |
| Macroscopic image | Superficial, slowly growing, solid nodule or cluster of nodules. Potentially ulcerated | Nonspecific tissue masses deep in healthy tissues. Hemorrhage and necrosis are common | [3, 11] |
| Histological features | Pseudogranulomatous appearance. Spindle, polygonal, polyhedral epithelioid cells with deeply eosinophilic cytoplasm. Often the loss of cellular connections. Occasionally polynuclear giant cells. Often central palisaded hyalinizing necrosis with possible calcification. Numerous inflammatory cells. Hyalinized collagen, vascular invasion, deposits of hemosiderin, fibrin, or mucin. Binucleated cells in the smear of nodal metastasis | Disintegrated large and round epithelioid cells with abundant eosinophilic cytoplasm, eccentrical vesicular pleomorphic nuclei, and prominent nucleoli. Possible paranuclear globules of intermediate filaments and rhabdoid phenotype. Multinucleated osteoclast-like and signet cells are aggregated adjacent to the epithelioid cells and separated from each other with fibrous septa. Absence of granulomatous appearance. Atypia and mitotic rates are greater compared to the distal type | [2, 3, 7, 9, 11, 18–20] |
| Molecular characteristics | Common: Loss of SMARCB1/INI-1 expression | | [26, 45, 49] |
| | t(8;22)(q22;q11), Enrichment in Sonic Hedgehog and Notch pathways | t(10;22), Overexpression of MYC pathway activity signature | [3, 4, 21] |
| | Trend toward lower dysadherin expression | Trend toward higher dysadherin expression | [58] |
| | Higher expression of *FYN, CXCL12, NID2, KRT7, SMARCB1, MMP2, BASP1, VASN, ACTA2, THBS1, ICAM2, ABCA8, TGFBR2, PDE2A, EPHA4, CD44* and *CDH5* genes than in proximal ES | Higher expression of *SHC1, C19orf33, RIPK4, EPHA2, SLCO4A1, THBS3, AC091180.3, RRAS, ITGA2B, APLP1, KRT8, FBXL6, FJX1, CACNG6, KRT18, CENPV, MUC1* and *MAP2K2* genes than in distal ES | [40] |
| Course of the disease | Poor prognosis, 10-year OS for patients with localized disease is approximately 50%, and 10% for patients who developed distant metastases | Increased risk of developing distant metastases and worse overall survival, compared to the distal type | [8, 9, 19, 24, 25] |
| Response to the treatment | Moderate activity of anthracycline — and gemcitabine-based regimens | Trend toward a higher response rate to anthracycline-based regimens, with a lower response rate to gemcitabine-based regimens, compared to the distal type | [59] |

OS — overall survival

nodes, lungs, pleura, and skin have been documented in patients with epithelioid sarcoma [9, 38].

Correct diagnosis requires the use of many diagnostic tools including computed tomography scan, magnetic resonance imaging, X-ray, ultrasound-guided biopsy, and histological and immunohistochemical analysis [20, 37, 63, 64]. However, it should be noted that immunohistochemistry is not a substitute for microscopic histological images and should be analyzed in parallel with them [65]. The use of molecular genetics methods for diagnostic ES detection is increasingly indicated. A methodological approach following the World Health Organization (WHO) instructions should form the basis for further therapeutic management [66]. This approach requires changes in diagnostic management such as integration of morphology with immunochemistry and molecular genetics and involvement of sarcoma expert pathologists and clinicians [66]. Tumor appearance and location on preoperative imaging using computed tomography scans and magnetic resonance imaging allow determining the anatomical site of the tumor, its volume, percentage of tumor necrosis, areas of hemorrhage, bone and neurovascular bundle involvement [6, 67]. Collection of tumor tissue material by biopsy allows analysis of microscopic images of cells, immunohistochemical evaluation, and DNA sequencing [19]. Using these methods allows the identification of epithelioid sarcoma and the determination of its variants, proximal and distant.

## Therapy of distal and proximal types of epithelioid sarcoma

The therapy for both variants of epithelioid sarcoma is still controversial. Surgical management with or without adjuvant/neoadjuvant radiotherapy and chemotherapy is still the most acceptable and effective method [63, 68]. The location and size of the ES tumor, presence of metastases, and the patient's age determine further treatment management. When the mass is localized, complete surgical resection (amputation or resection with wide margins — R0) with high-dose radiotherapy and chemotherapy is usually recommended, aiming at low local recurrence rates [7]. Some clinicians suggest ultrasound examination and sentinel node biopsy to check for undiscovered lymph node metastasis [24, 67]. Flap reconstruction and isolated limb perfusion are sometimes used [3, 24].

Presurgical embolization can help reduce tumor vascularity, and neo-adjuvant or adjuvant radiotherapy is useful in reducing the local recurrence rate [69]. To obtain cytoreduction allowing the decrease of tumor size and immediate treatment of metastases, neoadjuvant chemotherapy may be applied [67]. In addition to primary tumor resection, lymph node surgery may be required, and an appropriate lymph node basin should always be evaluated with imaging before surgery [67]. R1 and R2 resections are associated with high risk of recurrence and shorter overall survival (OS) [3]. Radiation therapy aims to prevent recurrence, especially after microscopically and macroscopically incomplete surgical ES resection [24]. Conventional fractionation, as well as hypofractionated radiotherapy, may be used [24, 70]. However, even complete surgical excision with clear margins does not prevent tumor recurrence, as even the first report by Enzinger indicated a local recurrence rate of 85% [7, 71].

## Surgical management in the treatment of distal and proximal types of ES

Surgery is a potentially curative treatment for localized ES, in case of both primary and recurrent tumors [14]. Misdiagnosis of ES delays the treatment process and can lead to significant proliferation of tumor tissue and metastases. Therefore, patients should be referred to specialized sarcoma centers that are equipped with NGS and may provide gene fusion analysis. Figure 2 shows photographs of the foot of a misdiagnosed patient unsuccessfully treated for two years for ulceration of the toe at a chronic wound clinic and a local orthopedic clinic where a full-thickness skin graft was used. The graft was rejected due to proliferation of tumor tissue. Subsequently, resection of the distal phalanx and amputation of the first phalanx were performed, after which the pathological tissue was excised. Due to the rapid recurrence of the tumor and the diagnosis of distal ES, the patient underwent amputation of the lower limb in our Institute (Fig. 2).

R0 surgical resection with a wide tumor-free margin is crucial for the treatment of both proximal and distal ES types [29]. Surgery of the distal sarcoma type depends on the size and localization of the tumor and most often amputation of the finger or limb

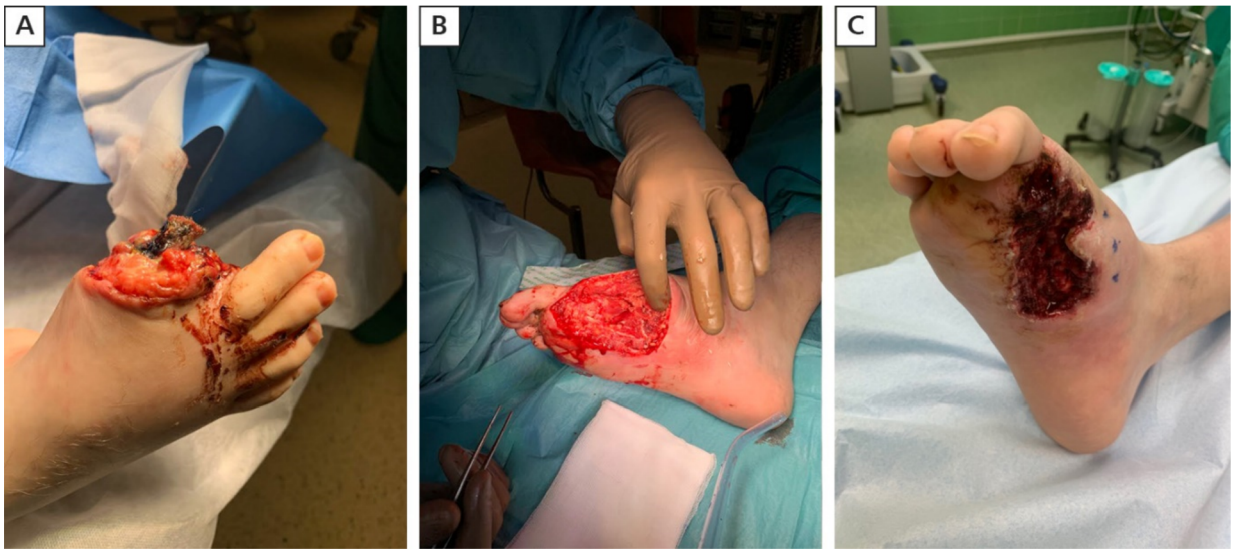


**Figure 2.** Patient with acral epithelioid sarcoma misdiagnosed as a toe ulcer and treated for two years with a full-thickness skin graft, which failed, in a chronic wound clinic and at the local orthopedic service. This was followed by resection of the distal phalange and first-ray amputation, after which the resected pathology specimen was diagnosed as non-radical resection of the epithelioid sarcoma. Due to fast relapse, the patient underwent lower leg amputation; **A.** Failed skin graft after resection of the distal phalange; **B.** Intraoperative image of the first ray amputation; **C.** Preamputation image of the foot with recurrence in the postoperative wound

in which the tumor is located is performed, although a neoadjuvant multidisciplinary treatment approach may enable limb sparing surgery [10, 61]. Achieving R0 margins (i.e. margins free of tumor cells on microscopic evaluation), when removing a tumor, is often difficult due to its spread via the synovial space routes, especially in the distal type of ES [29, 61]. The presence of tumor tissue in surgical margins on macroscopic or microscopic pathological evaluation (R2 or R1 margins) has been associated with high risk of recurrence and reduces the survival rate of ES patients. In several studies, researchers have observed that amputation of lesioned limbs does not increase the survival rates of ES patients compared to sparring surgery with R0 resection [29]. However, when multiple local recurrences of tumor occur, removal of the affected limb becomes a necessity [29]. It is worth adding that even complete surgical excision with clear margins does not always prevent ES recurrence; the course of both ES types is unpredictable, and late recurrences were also reported [7]. Epithelioid sarcoma staging may often be supported by sentinel lymph node biopsy (SLNB), as SLNB is indicated in patients suffering from sarcomas with high risk of regional lymphatic spread such as ES [72]. However, retrospective analysis including 217 patients undergoing ES therapy showed that prophylactic removal of most or all of the lymph nodes draining the area around the primary ES tumor significantly increased overall survival rates and tumor-specific survival rates [73].

## The role of systemic treatment in es management

Chemotherapy for ES uses a broad spectrum of cytostatics, such as doxorubicin, ifosfamide, vincristine, cyclophosphamide, actinomycin D, and gemcitabine [3, 24, 67]. However, cytostatics are not highly effective in reducing ES growth. Increasing knowledge about the role of lack of SMARCB1 in developing epithelioid sarcoma makes it possible to design new, more effective personalized ES therapy [46]. Lack of SMARCB1 is associated with the BAF complex loss and upregulation of EZH2, which is a catalytic subunit of PRC2 (Polycomb repressive complex 2) [46]. Inhibition of EZH2 leads to regaining control of gene expression regulation [74]. Tazemetostat is an oral selective inhibitor of the histone methyltransferase — enhancer of zeste homolog 2 (EZH2) approved as the first-line treatment for ES. EZH2 is a histone methyltransferase that catalyzes the trimethylation of histone H3 at lysine 27 (H3K27me3) and plays a role in the regulation of gene expression by modifying chromatin structure. Tazemetostat specifically targets and inhibits the activity of EZH2. By doing so, it interferes with the addition of methyl groups to histones, and this inhibition leads to changes in the expression of genes involved in cell growth and survival and enables inhibition of the growth of ES cells. For example, repression of the INK4A-ARF locus, which encodes the p16INK4a and p14ARF tumor suppressors, is a well-documented effect of EZH2, so inhibition of EZH upregulates these tumor suppressors. EZH2 has also been implicated in promoting epithelial-mesenchymal transition (EMT) — a process associated with increased cell motility and invasiveness, which is again stopped by EZH inhibition [25, 74].

New chemical compounds targeting mTOR and c-MET signaling pathways are also studied [67]. Novel therapeutic strategies are needed to treat highly aggressive epithelioid sarcoma, especially for the proximal ES variant [64, 75]. Differences in the clinical presentation of patients with different ES types indicate the need for different treatment procedures. Analyses of sensitive CSC biomarkers are currently being conducted for use in personalized treatment [55]. Use of pazopanib, a tyrosine kinase inhibitor, was also reported in ES tumor cases, but the results were also not satisfactory [3]. Dasatinib (multi-kinase inhibitor) efficacy in ES was investigated in the SARC0009 single-arm trial and multiple immunotherapy trials are ongoing including studies with immune checkpoint inhibitors targeting the PD-1/PD-L1 pathway as well as CTLA-4/CD80/86 signaling. Pembrolizumab, as well as a combination of nivolumab with ipilimumab, were investigated in ES [76].

## Conclusions

There are two subtypes of ES — distal and proximal [23, 66]. The differences in the functional structure of these two variants described in the scientific literature have resulted in an update of the WHO classification of soft tissue tumors [23]. Initially, distal and proximal terms were related to the location of the tumor. It is now known that there are many more differences between the two types of ES (Tab. 2). However, it should be noted that both proximal and distal ES variants also show great similarity, mainly in the immunophenotype and genotype, therefore, both ES types are also considered a disease continuum [21]. At the molecular level, deletion of INI1 is found in proximal ES, while in classic ES is characterized by retained dysfunctional INI1 expression. While classic ES has high expression of GLI3, FYN, and CXCL12, along with overexpression of the Notch/Hedgehog pathways and class 1 human leukocyte antigens (HLA), proximal ES exhibits overexpression of MYC and genes involved in the cell cycle, chromatin metabolism, and protein synthesis [40, 47]. Differences in the clinical presentation of patients with different ES types indicate the need for different treatment approaches. New therapeutic

strategies are needed to treat highly aggressive ES, especially for the proximal variant of ES. Tazemetostat is an oral selective inhibitor of the histone methyltransferase EZH2 recently approved by the FDA as the first-line treatment for ES patients.

## Article Information and Declarations

### Author contributions

A.M.C., P.R.: conception and design; B.S., A.S.-C.: figures; all authors: writing and editing.

### Funding

AMC work was supported by National Science Centre grant No.: 2019/35/O/NZ2/03761.

### Acknowledgements

AMC work was supported by National Science Centre grant No.: 2019/35/O/NZ2/03761.

### Conflict of interest

All authors declare no conflict of interest.

### Supplementary material

None.

## References

1. Laskowski J. Sarcoma aponeuroticum. Nowotwory. 1961; 11: 61–67.
2. Enzinger FM. Epithelioid sarcoma. A sarcoma simulating a granuloma or a carcinoma. Cancer. 1970; 26(5): 1029–1041, doi: 10.1002/1097-0142(197011)26:5<1029::aid-cncr2820260510>3.0.co;2-r.
3. Czarnecka AM, Sobczuk P, Kostrzanowski M, et al. Epithelioid Sarcoma-From Genetics to Clinical Practice. Cancers (Basel). 2020; 12(8), doi: 10.3390/cancers12082112, indexed in Pubmed: 32751241.
4. Elsamna ST, Amer K, Elkattawy O, et al. Epithelioid sarcoma: half a century later. Acta Oncol. 2020; 59(1): 48–54, doi: 10.1080/0284186X.2019.1659514, indexed in Pubmed: 31478778.
5. Spillane AJ, Thomas JM, Fisher C. Epithelioid sarcoma: the clinicopathological complexities of this rare soft tissue sarcoma. Ann Surg Oncol. 2000; 7(3): 218–225, doi: 10.1007/BF02523657, indexed in Pubmed: 10791853.
6. McCarville MB, Kao SC, Dao TV, et al. Magnetic resonance and computed tomography imaging features of epithelioid sarcoma in children and young adults with pathological and clinical correlation: a report from Children's Oncology Group study ARST0332. Pediatr Radiol. 2019; 49(7): 922–932, doi: 10.1007/s00247-019-04389-2, indexed in Pubmed: 30929036.
7. Armah H, Parwani A. Epithelioid Sarcoma. Arch Pathol Lab Med. 2009; 133(5): 814–819, doi: 10.5858/133.5.814, indexed in Pubmed: 19415960.
8. Frezza AM, Botta L, Pasquali S, et al. An epidemiological insight into epithelioid sarcoma (ES): The open issue of distal-type (DES) versus proximal-type (PES). Ann Oncol. 2017; 28: v525, doi: 10.1093/annonc/mdx387.013.
9. Chase D, Enzinger F. Epithelioid sarcoma. Diagnosis, prognostic indicators, and treatment. Am J Surg Pathol. 1985; 9(4): 241–263, indexed in Pubmed: 4014539.
10. Farzaliyev F, Steinau HU, Ring A, et al. Classic Type of Epithelioid Sarcoma of the Distal Upper Extremity: Clinical and Oncological Characteristics. Hand (N Y). 2023; 18(6): 1037–1043, doi: 10.1177/15589447221075745, indexed in Pubmed: 35187970.
11. Guillou L, Wadden C, Coindre JM, et al. "Proximal-type" epithelioid sarcoma, a distinctive aggressive neoplasm showing rhabdoid features. Clinicopathologic, immunohistochemical, and ultrastructural study of a series. Am J Surg Pathol. 1997; 21(2): 130–146, doi: 10.1097/00000478-199702000-00002, indexed in Pubmed: 9042279.
12. Sakharpe A, Lahat G, Gulamhusein T, et al. Epithelioid sarcoma and unclassified sarcoma with epithelioid features: clinicopathological variables, molecular markers, and a new experimental model. Oncologist. 2011; 16(4): 512–522, doi: 10.1634/theoncologist.2010-0174, indexed in Pubmed: 21357725.
13. Raoux D, Péoc'h M, Pedeutour F, et al. Primary epithelioid sarcoma of bone: report of a unique case, with immunohistochemical and fluorescent in situ hybridization confirmation of INI1 deletion. Am J Surg Pathol. 2009; 33(6): 954–958, doi: 10.1097/PAS.0b013e31819b92d5, indexed in Pubmed: 19342946.
14. Lu H, Xu Q, Chen X, et al. Clinical characteristics and survival analysis of patients with limb epithelioid sarcoma. Medicine (Baltimore). 2022; 101(30): e29969, doi: 10.1097/MD.0000000000029969, indexed in Pubmed: 35905199.
15. Kaya EA, Broadbent TJ, Thomas CJ, et al. Primary Epithelioid Sarcoma of Orbit: A Case Report and Review of the Literature. Case Rep Oncol Med. 2018; 2018: 3989716, doi: 10.1155/2018/3989716, indexed in Pubmed: 30652038.
16. Zhang Y, Mirpuri TM, Ho CL. Primary Epithelioid Sarcoma Manifesting as a Fungating Scalp Mass - Imaging Features and Treatment Options. A Case Report and Literature Review. J Radiol Case Rep. 2021; 15(11): 1–9, doi: 10.3941/jrcr.v15i11.4326, indexed in Pubmed: 35516973.
17. Del Savio E, Maestro R. Beyond SMARCB1 Loss: Recent Insights into the Pathobiology of Epithelioid Sarcoma. Cells. 2022; 11(17), doi: 10.3390/cells11172626, indexed in Pubmed: 36078034.
18. Li Y, Cao G, Tao X, et al. Clinicopathologic features of epithelioid sarcoma: report of seventeen cases and review of literature. Int J Clin Exp Pathol. 2019; 12(8): 3042–3048, indexed in Pubmed: 31934143.
19. Gajdzis P, Laé M, Klijanienko J. FNA of epithelioid sarcoma: Curie Institute experience and critical review of the literature. Cancer Cytopathol. 2018; 126(11): 934–941, doi: 10.1002/cncy.22052, indexed in Pubmed: 30291790.
20. Mannan AA, Rifaat AA, Kahvic M, et al. Proximal-type epithelioid sarcoma in the groin presenting as a diagnostic dilemma. Pathol Oncol Res. 2010; 16(2): 181–188, doi: 10.1007/s12253-009-9203-8, indexed in Pubmed: 19757197.
21. Noujaim J, Thway K, Bajwa Z, et al. Epithelioid Sarcoma: Opportunities for Biology-Driven Targeted Therapy. Front Oncol. 2015; 5: 186, doi: 10.3389/fonc.2015.00186, indexed in Pubmed: 26347853.
22. Pendse AA, Dodd LG. Fine-needle-aspiration cytology of a proximal type epithelioid sarcoma: A case report. Diagn Cytopathol. 2015; 43(10): 859–862, doi: 10.1002/dc.23294, indexed in Pubmed: 26138930.
23. Fletcher CDM, Unni K, Mertens F. World Health Organization Classification of Tumours. Pathology and Genetics of Tumours of Soft Tissue and Bone. IARC Press, Lyon 2002.
24. Casanova M, Ferrari A, Collini P, et al. Italian Soft Tissue Sarcoma Committee. Epithelioid sarcoma in children and adolescents: a report from the Italian Soft Tissue Sarcoma Committee. Cancer. 2006; 106(3): 708–717, doi: 10.1002/cncr.21630, indexed in Pubmed: 16353216.
25. Alves A, Constantinidou A, Thway K, et al. The evolving management of epithelioid sarcoma. Eur J Cancer Care (Engl). 2021; 30(6): e13489, doi: 10.1111/ecc.13489, indexed in Pubmed: 34278633.
26. Folpe AL. Selected topics in the pathology of epithelioid soft tissue tumors. Mod Pathol. 2014; 27 Suppl 1: S64–S79, doi: 10.1038/modpathol.2013.175, indexed in Pubmed: 24384854.
27. Needs T, Fillman EP. Epithelioid Sarcoma. In: StatPearls [Internet]. StatPearls Publishing, Treasure Island (FL) 2023.
28. Baratti D, Pennacchioli E, Casali PG, et al. Epithelioid sarcoma: prognostic factors and survival in a series of patients treated at a single institution. Ann Surg Oncol. 2007; 14(12): 3542–3551, doi: 10.1245/s10434-007-9628-9, indexed in Pubmed: 17909905.
29. de Visscher SA, van Ginkel RJ, Wobbes T, et al. Epithelioid sarcoma: Still an only surgically curable disease. Cancer. 2006; 107(3): 606–612, doi: 10.1002/cncr.22037, indexed in Pubmed: 16804932.

30. Zhang S, Jing C, Liu H, et al. Epithelioid sarcoma: A single--institutional retrospective cohort study of 36 cases. J Orthop Surg (Hong Kong). 2021; 29(3): 23094990211029349, doi: 10.1177/23094990211029349, indexed in Pubmed: 34405755.
31. Jawad MU, Extein J, Min ES, et al. Prognostic factors for survival in patients with epithelioid sarcoma: 441 cases from the SEER database. Clin Orthop Relat Res. 2009; 467(11): 2939–2948, doi: 10.1007/s11999-009-0749-2, indexed in Pubmed: 19224301.
32. Frezza AM, Sbaraglia M, Lo Vullo S, et al. The natural history of epithelioid sarcoma. A retrospective multicentre case-series within the Italian Sarcoma Group. Eur J Surg Oncol. 2020; 46(7): 1320–1326, doi: 10.1016/j.ejso.2020.03.215, indexed in Pubmed: 32307188.
33. Rekhi B, Thomas A. A case of retroperitoneal tumor displaying epithelial differentiation, prominent myxoid stroma and loss of INI1/SMARCB1. Pathologica. 2021; 113(6): 456–462, doi: 10.32074/1591-951X-250, indexed in Pubmed: 34974552.
34. Kato H, Hatori M, Watanabe M, et al. Epithelioid sarcomas with elevated serum CA125: report of two cases. Jpn J Clin Oncol. 2003; 33(3): 141–144, doi: 10.1093/jjco/hyg030, indexed in Pubmed: 12672792.
35. Mukai M, Torikata C, Iri H, et al. Cellular differentiation of epithelioid sarcoma. An electron-microscopic, enzyme-histochemical, and immunohistochemical study. Am J Pathol. 1985; 119(1): 44–56, indexed in Pubmed: 2580443.
36. Chbani L, Guillou L, Terrier P, et al. Epithelioid sarcoma: a clinicopathologic and immunohistochemical analysis of 106 cases from the French sarcoma group. Am J Clin Pathol. 2009; 131(2): 222–227, doi: 10.1309/AJCPU98ABIPVJAIV, indexed in Pubmed: 19141382.
37. Magetsari R, Dwianingsih EK, Putro YA, et al. Primary rhabdoid epithelioid sarcoma of the left thigh mimicking epithelioid rhabdomyosarcoma: A diagnostic pitfall. Int J Surg Case Rep. 2020; 70: 188–192, doi: 10.1016/j.ijscr.2020.04.002, indexed in Pubmed: 32417737.
38. Diaz-Perez JA, Spasic S, Velez-Torres JM, et al. Epithelioid Sarcoma of the Peripheral Nerve: Clinicopathologic Series of Three Cases and Literature Review. Am J Clin Pathol. 2021; 155(5): 729–737, doi: 10.1093/ajcp/aqaa180, indexed in Pubmed: 33247294.
39. Miettinen M, Wang Z, Sarlomo-Rikala M, et al. ERG Expression in Epithelioid Sarcoma. Am J Surg Pathol. 2013; 37(10): 1580–1585, doi: 10.1097/pas.0b013e31828de23a, indexed in Pubmed: 23774169.
40. Rasmussen SV, Jin JX, Bickford LR, et al. Functional genomic analysis of epithelioid sarcoma reveals distinct proximal and distal subtype biology. Clin Transl Med. 2022; 12(7): e961, doi: 10.1002/ctm2.961, indexed in Pubmed: 35839307.
41. Ramaglia M, D'Angelo V, Iannotta A, et al. High EZH2 expression is correlated to metastatic disease in pediatric soft tissue sarcomas. Cancer Cell Int. 2016; 16: 59, doi: 10.1186/s12935-016-0338-x, indexed in Pubmed: 27471434.
42. Moll R, Divo M, Langbein L. The human keratins: biology and pathology. Histochem Cell Biol. 2008; 129(6): 705–733, doi: 10.1007/s00418-008-0435-6, indexed in Pubmed: 18461349.
43. Lee HI, Kang KH, Cho YM, et al. Proximal-type epithelioid sarcoma with elevated serum CA 125: report of a case with CA 125 immunoreactivity. Arch Pathol Lab Med. 2006; 130(6): 871–874, doi: 10.5858/2006-130-871-PESWES, indexed in Pubmed: 16740043.
44. Lokshin A, Bast RC, Rodland K. Circulating Cancer Biomarkers. Cancers (Basel). 2021; 13(4), doi: 10.3390/cancers13040802, indexed in Pubmed: 33671847.
45. Mularz K, Harazin-Lechowska A, Ambicka A, et al. Specificity and sensitivity of INI-1 labeling in epithelioid sarcoma. Loss of INI1 expression as a frequent immunohistochemical event in synovial sarcoma. Pol J Pathol. 2012; 63(3): 179–183, doi: 10.5114/pjp.2012.31502, indexed in Pubmed: 23161234.
46. Cooper GW, Hong AL. SMARCB1-Deficient Cancers: Novel Molecular Insights and Therapeutic Vulnerabilities. Cancers (Basel). 2022; 14(15), doi: 10.3390/cancers14153645, indexed in Pubmed: 35892904.
47. Frezza A, Sigalotti L, Savio ED, et al. Epitheliod sarcoma: Molecular insights into proximal versus classic variant. J Clin Oncol. 2020; 38(15_suppl): e23552–e23552, doi: 10.1200/jco.2020.38.15_suppl.e23552.
48. Wang X, Haswell JR, Roberts CWM. Molecular pathways: SWI/SNF (BAF) complexes are frequently mutated in cancer–mechanisms and potential therapeutic insights. Clin Cancer Res. 2014; 20(1): 21–27, doi: 10.1158/1078-0432.CCR-13-0280, indexed in Pubmed: 24122795.
49. Sullivan LM, Folpe AL, Pawel BR, et al. Epithelioid sarcoma is associated with a high percentage of SMARCB1 deletions. Mod Pathol. 2013; 26(3): 385–392, doi: 10.1038/modpathol.2012.175, indexed in Pubmed: 23060122.
50. Modena P, Lualdi E, Facchinetti F, et al. SMARCB1/INI1 tumor suppressor gene is frequently inactivated in epithelioid sarcomas. Cancer Res. 2005; 65(10): 4012–4019, doi: 10.1158/0008-5472.CAN-04-3050, indexed in Pubmed: 15899790.
51. Kohashi K, Oda Y. Oncogenic roles of SMARCB1/INI1 and its deficient tumors. Cancer Sci. 2017; 108(4): 547–552, doi: 10.1111/cas.13173, indexed in Pubmed: 28109176.
52. Nacev BA, Jones KB, Intlekofer AM, et al. The epigenomics of sarcoma. Nat Rev Cancer. 2020; 20(10): 608–623, doi: 10.1038/s41568-020-0288-4, indexed in Pubmed: 32782366.
53. Imura Y, Yasui H, Outani H, et al. Combined targeting of mTOR and c-MET signaling pathways for effective management of epithelioid sarcoma. Mol Cancer. 2014; 13: 185, doi: 10.1186/1476-4598-13-185, indexed in Pubmed: 25098767.
54. Darr J, Klochendler A, Isaac S, et al. Loss of IGFBP7 expression and persistent AKT activation contribute to SMARCB1/Snf5-mediated tumorigenesis. Oncogene. 2014; 33(23): 3024–3032, doi: 10.1038/onc.2013.261, indexed in Pubmed: 23851500.
55. Chico MA, Mesas C, Doello K, et al. Cancer Stem Cells in Sarcomas: In Vitro Isolation and Role as Prognostic Markers: A Systematic Review. Cancers (Basel). 2023; 15(9), doi: 10.3390/cancers15092449, indexed in Pubmed: 37173919.
56. Duan R, Du W, Guo W. EZH2: a novel target for cancer treatment. J Hematol Oncol. 2020; 13(1): 104, doi: 10.1186/s13045-020-00937-8, indexed in Pubmed: 32723346.
57. Schaefer IM, Al-Ibraheemi A, Qian X. Cytomorphologic Spectrum of SMARCB1-Deficient Soft Tissue Neoplasms. Am J Clin Pathol. 2021; 156(2): 229–245, doi: 10.1093/ajcp/aqaa223, indexed in Pubmed: 33608696.
58. Izumi T, Oda Y, Hasegawa T, et al. Prognostic significance of dysadherin expression in epithelioid sarcoma and its diagnostic utility in distinguishing epithelioid sarcoma from malignant rhabdoid tumor. Mod Pathol. 2006; 19(6): 820–831, doi: 10.1038/modpathol.3800599, indexed in Pubmed: 16557275.
59. Frezza AM, Jones RL, Lo Vullo S, et al. Anthracycline, Gemcitabine, and Pazopanib in Epithelioid Sarcoma: A Multi-institutional Case Series. JAMA Oncol. 2018; 4(9): e180219, doi: 10.1001/jamaoncol.2018.0219, indexed in Pubmed: 29800950.
60. Thway K, Jones RL, Noujaim J, et al. Epithelioid Sarcoma: Diagnostic Features and Genetics. Adv Anat Pathol. 2016; 23(1): 41–49, doi: 10.1097/PAP.0000000000000102, indexed in Pubmed: 26645461.
61. Alexander L. Epithelioid Sarcoma of Upper Extremity: Diagnostic Dilemma With Therapeutic Challenges. Cureus. 2021; 13(3): e14156, doi: 10.7759/cureus.14156, indexed in Pubmed: 33936870.
62. Sajko N, Murphy S, Tran A. Undifferentiated epithelioid sarcoma presenting as a fever of unknown origin: a case report. J Med Case Rep. 2019; 13(1): 24, doi: 10.1186/s13256-018-1951-1, indexed in Pubmed: 30684969.
63. Asano N, Yoshida A, Ogura K, et al. Prognostic Value of Relevant Clinicopathologic Variables in Epithelioid Sarcoma: A Multi--Institutional Retrospective Study of 44 Patients. Ann Surg Oncol. 2015; 22(8): 2624–2632, doi: 10.1245/s10434-014-4294-1, indexed in Pubmed: 25663591.
64. Zegarra Buitron E, Vidal Panduro DA, Morales Luna D. Clinicopathological Characteristics, Treatment, and Survival in Patients Diagnosed With Proximal-Type Epithelioid Sarcoma: A Case Report and Systematic Review. Cureus. 2022; 14(12): e32962, doi: 10.7759/cureus.32962, indexed in Pubmed: 36712724.

65. Carbone A, Gloghini A, Volpe R. The value of immunohistochemistry in the diagnosis of soft tissue sarcomas. Ann Oncol. 1992; 3 Suppl 2: S51–S54, doi: 10.1093/annonc/3.suppl_2.s51, indexed in Pubmed: 1622866.
66. Sbaraglia M, Bellan E, Dei Tos AP. The 2020 WHO Classification of Soft Tissue Tumours: news and perspectives. Pathologica. 2021; 113(2): 70–84, doi: 10.32074/1591-951X-213, indexed in Pubmed: 33179614.
67. Mahajan A, Sen I, Hazra D, et al. Management of Epithelioid Sarcoma of the Inguinal Region with Vascular Invasion. Indian J Surg. 2016; 78(4): 315–317, doi: 10.1007/s12262-015-1401-x, indexed in Pubmed: 27574351.
68. Yuan J, Li X, Yu S. Molecular targeted therapy for advanced or metastatic soft tissue sarcoma. Cancer Control. 2021; 28: 10732748211038424, doi: 10.1177/10732748211038424, indexed in Pubmed: 34844463.
69. Dangoor A, Seddon B, Gerrand C, et al. UK guidelines for the management of soft tissue sarcomas. Clin Sarcoma Res. 2016; 6: 20, doi: 10.1186/s13569-016-0060-4, indexed in Pubmed: 27891213.
70. Spałek MJ, Koseła-Paterczyk H, Borkowska A, et al. Combined Preoperative Hypofractionated Radiotherapy With Doxorubicin--Ifosfamide Chemotherapy in Marginally Resectable Soft Tissue Sarcomas: Results of a Phase 2 Clinical Trial. Int J Radiat Oncol Biol Phys. 2021; 110(4): 1053–1063, doi: 10.1016/j.ijrobp.2021.02.019, indexed in Pubmed: 33600887.
71. Sobanko JF, Meijer L, Nigra TP. Epithelioid sarcoma: a review and update. J Clin Aesthet Dermatol. 2009; 2(5): 49–54, indexed in Pubmed: 20729965.
72. Chmiel P, Krotewicz M, Szumera-Ciećkiewicz A, et al. Review on Lymph Node Metastases, Sentinel Lymph Node Biopsy, and Lymphadenectomy in Sarcoma. Curr Oncol. 2024; 31(1): 307–323, doi: 10.3390/curroncol31010020, indexed in Pubmed: 38248105.
73. Liu QK, Yu XJ, Wang YG, et al. Risk factors for lymph node metastasis of soft tissue sarcomas of the head, neck, and extremities, and the clinical significance of negative lymph node dissection. J Orthop Surg Res. 2022; 17(1): 167, doi: 10.1186/s13018-022-03050-3, indexed in Pubmed: 35303897.
74. Straining R, Eighmy W. Tazemetostat: EZH2 Inhibitor. J Adv Pract Oncol. 2022; 13(2): 158–163, doi: 10.6004/jadpro.2022.13.2.7, indexed in Pubmed: 35369397.
75. Russi S, Sgambato A, Bochicchio AM, et al. CHIR99021, trough GSK-3$\beta$ Targeting, Reduces Epithelioid Sarcoma Cell Proliferation by Activating Mitotic Catastrophe and Autophagy. Int J Mol Sci. 2021; 22(20), doi: 10.3390/ijms222011147, indexed in Pubmed: 34681807.
76. Meissner M, Napolitano A, Thway K, et al. Pharmacotherapeutic strategies for epithelioid sarcoma: are we any closer to a non-surgical cure? Expert Opin Pharmacother. 2023; 24(12): 1395–1401, doi: 10.1080/14656566.2023.2224500, indexed in Pubmed: 37326105.

VIA MEDICA

CASE REPORT

Oncology in Clinical Practice
2025, Vol. 21, No. 1, 71–77
DOI: 10.5603/ocp.98628

ISSN 2450-1654
eISSN 2450-6478

# Cloaked up osteosarcoma: chondroblastoma-like osteosarcoma — a case report and literature review

Sivaranjani Selvaraj[1,*], Prashanth Jayapal[2], Suma Mysore Narayana[1], Champaka Gopal[1]

[1]Department of Pathology, Kidwai Memorial Institute of Oncology, Bengaluru, India
[2]Department of Radiodiagnosis, Kidwai Memorial Institute of Oncology, Bengaluru, India

**Abstract**

Osteosarcoma (OS) is the most common nonhematopoietic bone malignancy. Chondroblastoma-like osteosarcoma is an extremely uncommon variant with only 26 cases reported in medical literature in English. Given its rarity, diagnosis and management can be challenging. Osteosarcoma patients frequently receive inadequate care and incorrect diagnoses, which can lead to recurrences. Hereby, we report a rare case of osteosarcoma in an untypical location with a review of the literature. The case of an 18-year-old male with chondroblastoma-like osteosarcoma in the body of the sternum highlights diagnostic pitfalls and emphasizes the importance of morphology.

**Keywords:** chondroblastoma-like osteosarcoma, aggressive chondroblastoma, osteosarcoma of sternum

## Introduction

Osteosarcoma (OS) is the most common primary nonhematopoietic malignant bone tumor [1–3]. The term osteosarcoma has been defined as a high-grade bone tumor in which tumor cells produce osteoid or woven bone. Osteosarcomas have multiple described, histological and anatomical variants, including conventional OS (osteoblastic, chondroblastic, and fibroblastic OS), small cell, telangiectatic, giant cell-rich variants, and others [1–3]. However, this rare entity identified as chondroblastoma-like osteosarcoma (CBLOS), which accounts for fewer than 1% of all osteosarcomas, has unique histological and clinical characteristics. This disparate entity needs to be distinguished from chondroblastic OS and chondroblastoma, which are two closely related yet distinct entities. In the English medical literature, there are not many case reports or brief case series. Usually affecting bones of the foot, osteosarcomas seem to affect predominantly young individuals. As far as we understand, there are no case reports of these tumors emerging from flat bones. We have reviewed the literature, and hereby report a case of an 18-year-old male, with this exceptionally rare malignancy of bone in an uncommon site. The significance of using relevant diagnostic imaging and identifying histological features in establishing the diagnosis of CBLOS is highlighted based on our experience.

## Case report

An 18-year-old male patient presented with swelling and pain in the anterior part of the chest which increased during coughing or heavy breathing. He had no history of chronic disease. Physical examination revealed a bulge over the sternum measuring 5 × 3 cm, which was fixed, nontender, and hard in consistency.

The findings from the computed tomography (CT) scan of the chest and abdomen showed an expansile lesion involving the body of the sternum measuring 4.3 × 4.6 × 7.1 cm, with an enhancing soft tissue component within the lesion showing significant rings and arc type of calcification and multiple areas of the cortical breach, with an extension of soft tissue into subcutaneous and muscular planes. Posteriorly, the lesion was abutting the pericardium with no obvious invasion. No intrathoracic extension was identified (Fig. 1). With these findings, a radiological suspicion

*Correspondence: Doctor Sivaranjani Selvaraj, Department of Pathology, Kidwai Memorial Institute of Oncology, Marigowda Road, 560027 Bengaluru, India (sivaranjani0892@gmail.com)
Received: 22 December 2023; Accepted: 16 January 2024; Early publication: 15 February 2024

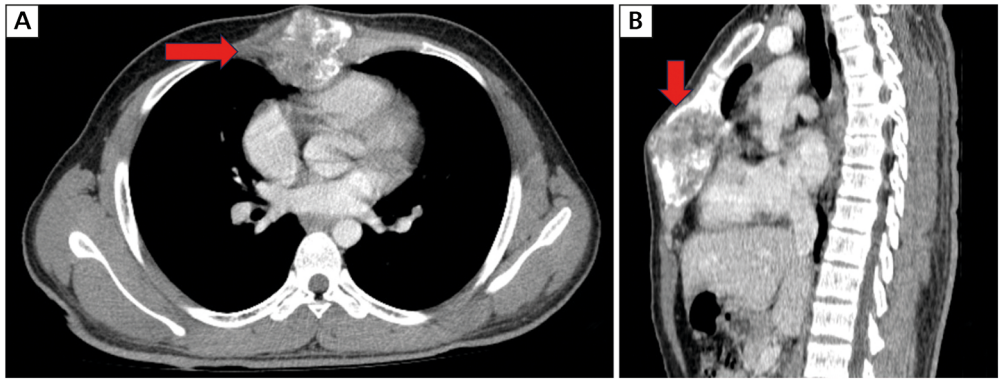


**Figure 1.** Computed tomography chest — expansile lesion involving the body of sternum (marked by red arrow) with an enhancing soft tissue component within the lesion showing significant rings and arc type of calcification and extension into adjacent soft tissue; **A.** Coronal; **B.** Sagittal

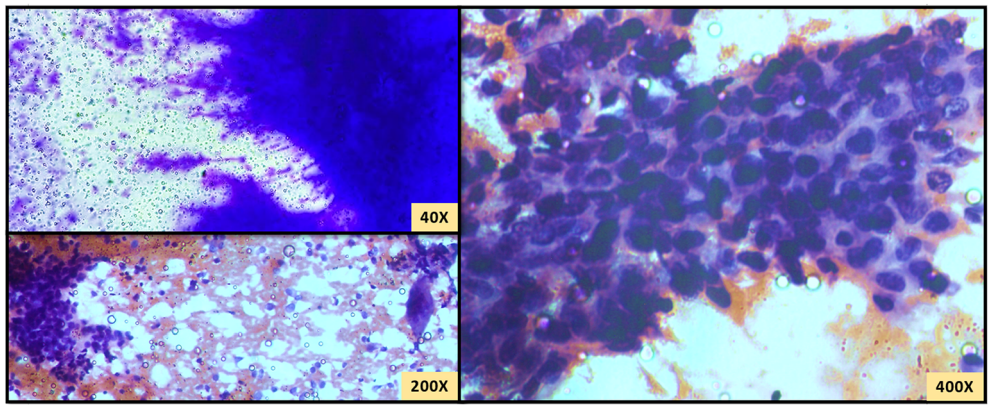


**Figure 2.** Fine needle aspiration smears of sternal lesion — shows clusters as well as dispersed tumor cells exhibiting grooving with interspersed osteoclast-type giant cells embedded in chondroid matrix like background material

of expansile bone neoplasm with chondroid matrix arose. However, a conclusive opinion could not be provided.

Fine needle aspiration was performed from the lesion, which showed a giant cell-rich cartilaginous neoplasm with tumor cells in clusters, exhibiting ovoid and polygonal cells with fine chromatin and occasional grooves. Many osteoclast-type giant cells were observed. A focally chondroid-like matrix was noted (Fig. 2). A needle core biopsy (Jamshidi needle) was performed. Histologically, the tumor tissue displayed a cellular neoplasm composed of round-to-polygonal cells exhibiting nuclear grooves with moderate cytologic atypia, arranged in lobules and sheets intervened by scattered osteoclastic type of giant cells. Chicken wire-like calcification was noted with cartilaginous areas. No malignant osteoid was identified. The lesion was suggestive of a chondroblastoma. Further, we performed Immunohistochemistry for confirmation, which showed positivity for DOG1 and a low KI67 proliferation index (7%). Though this needle core biopsy was not representative of the lesion, the possibility of aggressive chondroblastoma was considered, keeping in mind the location and radiological findings.

Given the aggressive radiological picture exhibiting soft tissue and muscular plane involvement, sternal resection with chest wall reconstruction using a titanium mesh was done. On gross examination, a grey-white tumor measuring $7.5 \times 4.5 \times 4$ cm was identified in the body of the sternum, which was gritty to cut along, with areas of necrosis and hemorrhage.

Histopathological examination of the sternal resection showed similar features to the J-needle biopsy performed earlier, with an infiltrative growth pattern toward the soft tissues, moderate anaplasia of the tumoral cells, and lace-like malignant osteoid (Fig. 3). A final diagnosis of chondroblastoma-like osteosarcoma was confirmed. The histopathological report confirmed soft tissue involvement; however, it had tumor-free margins all over the specimen. The specimen was assigned a TNM stage of pT1 [8$^{th}$ edition TNM staging system for bone tumors of the American Joint Committee on Cancer (AJCC) and the International Union Against Cancer (UICC)].

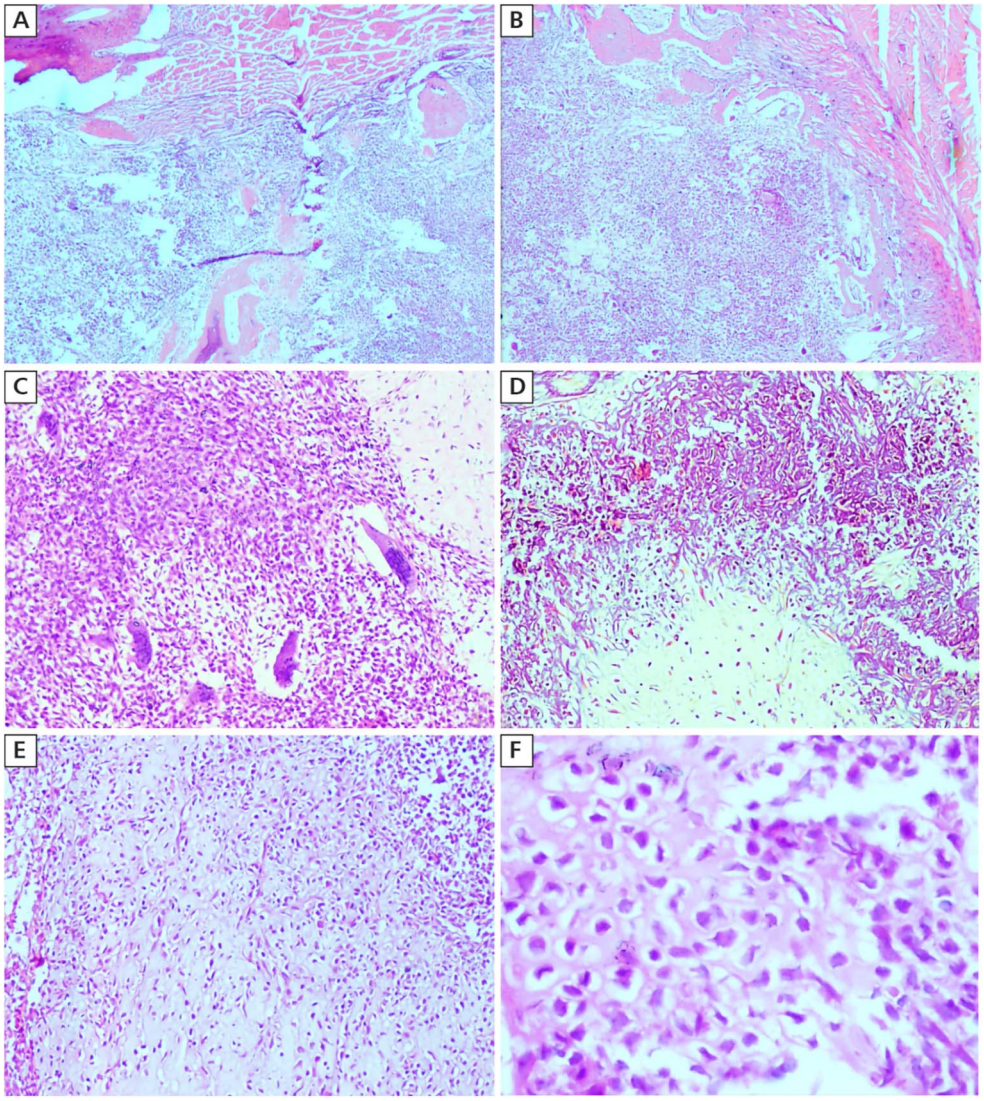


**Figure 3.** Chondroblastoma-like osteosarcomas, histology — infiltrative tumor involving soft tissue, muscular plane, and bone tissue (**A, B**), composed of round to oval cells with a grooved nucleus. Numerous scattered multi-nucleated osteoclast-like giant cells are noted (**C**) with a chicken-wire type of calcification (**D**). Tumor cells produce variable amounts of lace-like osteoid matrix (**E**) exhibiting moderate to severe nuclear atypia (**F**)

The postoperative period was uneventful with no complications or neurovascular deficits. At the end of 2 months, chest radiographs revealed an intact mesh with good osteointegration. (Fig. 4). The patient was started on adjuvant chemotherapy after 2 months of surgery i.e., adriamycin and cisplatin. We followed up with the patient for 16 months, and he was doing well and was disease-free.

## Discussion

In children and young adults, OS are the most prevalent primary non-hematopoietic bone cancer [1–3]. They could be osteogenic, chondrogenic, or fibroblastic. In 1990, the term 'chondroblastoma-like osteosarcoma' was coined by Schajowicz et al. [4]. It is an extremely rare and little-known histological subtype of osteosarcoma, with just a handful of cases reported in English literature [4, 5]. The vast majority of the reported cases present in the 3$^{rd}$ decade of life. The most frequent sites of involvement are metatarsal bones (4 cases), femur (3), ribs (3), humerus (2), tibia (2), and single cases at the fibula, ischium, phalanx, talus, and ilium [4–6]. Unlike these previous case reports and series, this is the first case reported in the sternum. The majority of the reported CBLOS patients had a minor trauma after which they developed painless mass or pain [1–7]. The pain in our case was attributed to the site, as the sternum is the most sensitive site. The locations and radiological patterns of involvement by CBLOS are varied. The first case reported in 1990 was a 12-year-old male child who was diagnosed with CBLOS in the tibia [4].

Chondroblastoma-like osteosarcoma has been radiologically described predominantly in the diaphysis of long bones exhibiting a mixed pattern composed of a lytic and sclerotic pattern, with either thin or absent cortices, and expansile radiolucent area, focal punctate calcifications leading to a laminar periosteal reaction and endosteal scalloping [4, 5]. Chondroblastoma-like osteosarcomas also involve soft tissues and have a destructive penetration of the host bone, as demonstrated by radiology [6–8]. Radiologically, chondroblastoma-like osteosarcoma was previously described as an expansile lytic lesion with endosteal erosions and focal punctate calcifications. It was observed that the entire bone was affected in those with metatarsal involvement. Differential diagnosis with use of radiology includes considering giant cell tumors [7–9], aneurysmal bone cysts [7, 9, 10], chondromyxoid fibroma [11] and chondroblastoma, Ewing sarcoma, fibrous dysplasia, chondrosarcoma, Langerhans cell histiocytosis. We had similar differentials in our case, but we did not take into account the aggressive nature of the tumor The cases that have been reported in the English literature are summarized in Table 1 [4, 6, 7, 9–12].

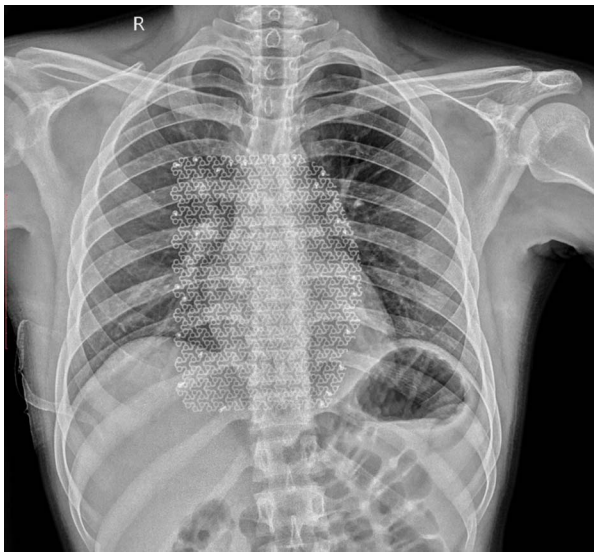


**Figure 4.** Chest X-ray (post sternal resection and reconstruction with mesh)

**Table 1.** Literature review

| No. | Source, year | Age [years]/ /sex | Site | Size | Radiological features | Treatment | Follow-up |
|---|---|---|---|---|---|---|---|
| 1. | Schajowicz et al. [4], 1990 | 12/M | Tibia | NA | NA | NA | NA |
| 2. | Bahrami et al. [6], 2010 — 17 cases | 13–72/M, 8/F | Metatarsus (3)<br>Femur (3)<br>Rib (3)<br>Humerus (2)<br>Talus (1)<br>Phalanx (1)<br>Tibia (1)<br>Fibula (1)<br>Ischium (1)<br>Ilium (1) | NA | 13/14 malignant or with suspicion of malignancy<br>1/14 equivocal | NA | 7 ANED<br>6 LR<br>2 Metastasis<br>2 DOD |
| 3. | Byatnal et al. [7], 2013 | 17/M | Jaw | 6 cm | NA | NA | NA |
| 4. | Martin et al. [9], 2014 | 32/M | Distal tibia | NA | GCT | Curettage followed by resection | 12 years, multiple LR |
| 5. | Aycan et al. [10], 2015 | 10/M | First metatarsal | | GCT versus ABC | Resection | ANED<br>6 months |
| 6. | Ramos Pascua et al. [11], 2018 | 30/M | Tibia | 6 cm | Benign versus malignant | Aggressive curettage | ANED<br>7 years |
| 7. | Gaeta et al. [12], 2022 — 6 cases | 20/M<br>9/M<br>63/F<br>54/M<br>14/M<br>14/M | 1st metatarsal<br>1st metatarsal<br>Scaphoid<br>VI rib<br>Vertebra<br>3rd metacarpel | NA | 2/6 malignant or with suspicion of malignancy<br>4/6 Equivocal | 4/6 Wide resection<br>1/6 Marginal Resection<br>1/6 Curretage | 4 ANED<br>1 LR<br>1 DOD |
| 8. | Current case | 18/M | | 7.5 cm | Equivocal | Resection | ANED<br>30 months |

ABC — aneurysmal bone cyst; ANED — alive with no evidence of disease; DOD — died of disease; F — demale; GCT — giant cell tumor; LR — local recurrence; M — male; NA — not available

Chondroblastoma-like osteosarcoma has a presentation similar to that of osteosarcoma, however, it has a younger age of presentation than malignant chondroblastoma [6]. Bahrami et al. [6] reviewed 17 CBLOS cases; two patients had recurrence, and one of them developed recurrence over 14 years after initial resection. Two patients died of disease, one due to local recurrence in the cervical C7 vertebra, and one had widespread metastases over 26 years. This behavior of this type of osteosarcoma contrasts with that of conventional osteosarcoma, which is known to have a worse prognosis and faster disease progression when associated with metastases. Our patient also underwent morbid surgery amounting to complete resection of sternum along with the tumor. However, the patient responded well, with no recurrence or metastasis in the sixteen-month follow-up period.

Although chondroblastoma-like osteosarcoma is a completely distinct entity from chondroblastoma, we shall discuss them together as chondroblastoma--like osteosarcoma has a significant historical and morphologic relationship to chondroblastoma. It was first described in 1990 by Schajowicz et al. [4] who coined the term chondroblastoma-like osteosarcoma. Despite being called chondroblastoma, it is a rare variant of osteosarcoma.

Clinically, the tumor presents mostly in males, of a wide age range, and has an indolent course, with only a minority of the reported cases developing pulmonary metastases and local recurrences [9]. This neoplasm has a predilection for the lower extremities, most commonly involving the metatarsus, tibia, and femur. Our case, however, had sternal pain and swelling on a flat bone — the sternum.

Radiologically, most of the cases reveal findings that are suggestive of or consistent with malignant tumors. This tumor is known to show lesions that are 'expansile and lytic, with an infiltrative growth pattern; destroying cortical bone'. Aneurysmal bone cysts, chondroblastomas, giant cell tumors, and chondrosarcoma are among the radiological differential diagnoses [4, 5, 7, 8]. Our case had an expansile sternal tumor with the destruction of soft tissue and muscular planes, implying an aggressive growth pattern. However, the findings did not classically correspond to an osteosarcoma and were leaning more toward a chondroblastoma with aggressive growth.

Histologically, this distinct neoplasm is characterized by hypocellular and hypercellular areas. The cellular areas resemble the features of chondroblastoma with abnormal malignant osteoid deposition and destruction of the adjacent nonneoplastic bone [6]. The tumor has an 'infiltrative growth pattern composed of small cells exhibiting ovoid, folded, or grooved nuclei with eosinophilic pale cytoplasm, resembling the neoplastic cells enmeshed in chondroid matrix observed in chondroblastoma along with varying amounts of chicken wire calcification.' In addition, it also has areas with larger cells displaying more nuclear atypia, with few atypical mitotic figures and evidence of malignant osteoid deposition [4, 5, 7–9]. Our case displayed the described features of chondroblastoma with the unique features pertaining to CBLOS exhibiting interspersed islands of plasmacytoid, polygonal osteoblasts, and areas of malignant lace-like osteoid deposition.

The largest reported study by Bahrami et al. and a review of CBLOS by Hmada et al. [8] included, respectively, 17 patients and 22 patients. In the study by Bahrami et al. [6], 10 of the 17 patients had available follow-up information: '2 had died from the disease, 2 had developed lung metastases, and 6 of them had local recurrence'. In the study by Hmada et al. [8], the authors reviewed 5 cases in addition to the 17 cases reported by Bahrami et al. [6]. Three patients had follow-up data, and only one of them developed local recurrence.

The primary differential diagnosis for CBLOS is chondroblastoma, which is a benign neoplasm with cartilage production that is mostly seen in the second decade of life. It is located in an epiphyseal region or metaphyseal/epiphyseal region of the long bones. The characteristics that point towards CBLOS are older age and usually non-epiphyseal location (although it can be epiphyseal) [4, 6, 7], with histopathological characteristics in addition to the chondroblastoma. These are malignant osteoid production/formation, nuclear atypia, and increased and atypical mitoses, with destructive permeation resulting in bone/soft tissue infiltration and, tumor necrosis [4, 6, 7]. On the other hand, conventional chondroblastic OS is less likely to be misdiagnosed as CBLOS, as it presents with deposition of high-grade hyaline cartilage that exhibits severe atypia and lacunae [1]. Chondrosarcoma, which again displays hyaline cartilage matrix deposition with malignant chondrocytes exhibiting significant nuclear atypia that reside in lacunae [1], would not be considered a differential in histopathological diagnosis. As we know, the histological picture has to be correlated with radiological and clinical findings to include or rule out the possibility of CBLOS. The comparison of clinical, radiological, and histopathologic characteristics of chondroblastoma, malignant chondroblastoma [13, 14], and CBLOS is presented in Table 2.

Gaeta et al. [12] studied clinicopathologic and molecular data of 6 cases of CBLOS and compared these with 6 cases of chondroblastoma with atypical features. Immunohistochemistry (IHC) for H3.3 K36M and H3.3 G34W can be used to differentiate chondroblastoma and giant cell tumor respectively. Molecular profiling by whole exome sequencing (WES) was performed on two of the CBLOS and

**Table 2.** Comparison of chondroblastoma (CB), malignant chondroblastoma, and chondroblastoma-like osteosarcoma (CBLOS)

| Characteristics | Chondroblastoma | Malignant chondroblastoma | Chondroblastoma-like osteosarcoma |
|---|---|---|---|
| **Clinical** | Typically affects individuals in the second decade of life<br>Predominantly presents with localized pain, often centered around the affected joint<br>Benign behavior with a low rate of metastasis | Occurs in older age groups compared to conventional CB<br>Presents with persistent or worsening pain and may exhibit signs of local invasion<br>Characterized by a more aggressive clinical course, including a higher risk of recurrence and metastasis. | Occurs at the intermediate age range between CB and malignant CB<br>Clinical presentation may resemble CB but with a higher tendency for aggressive behavior.<br>However, better prognosis compared to malignant CB and conventional osteosarcoma |
| **Radiological** | Well-defined, eccentrically located lytic lesions with sclerotic margins on plain radiographs<br>May demonstrate lobulated or soap-bubble appearances | Radiographic features include permeative bone destruction, cortical breach, and soft tissue extension<br>Aggressive appearance with a higher likelihood of associated soft tissue masses | Radiologically heterogeneous, combining features of chondroblastoma and osteosarcoma<br>Presence of both lytic and sclerotic components, as well as areas of mineralization and osteoid formation |
| **Histopathological** | Sheets of round to polygonal cells with eosinophilic cytoplasm<br>Central nuclei and characteristic "chicken-wire" calcifications in hyaline cartilage | Increased cellularity, nuclear atypia, and mitotic figures<br>Necrosis may be present, indicating aggressive behavior | Combination of chondroblastoma-like areas and osteosarcomatous components<br>Presence of malignant osteoid and cartilaginous matrices |
| **H3.3 K36M point mutation** | Present (~95%) | Absent | Absent |

11 conventional high-grade osteosarcomas to compare them. The authors found that H3.3 K36M was positive in 2 of the 6 cases. In the limited two cases of WES by next-generation sequencing, they identified that CBLOS share a similar appearance to conventional high-grade osteosarcomas, with RTK-RAS, NOTCH, and Hippo being the significant oncogenic pathways involved. A point mutation in histone H3.3 K36M is identified in 95% of chondroblastomas [15, 16]. As far as we are aware, no credible reports of H3K36M have been found in tumors other than chondroblastoma, even though the Catalogue of Somatic Mutations in Cancer (COSMIC) database contains more than a million tumors [17]. Therefore, it seems that a positive H3K36M IHC test will almost always rule out a malignant chondroblastoma and CBLOS in differential diagnosis.

## Conclusions

Despite osteosarcomas being extremely unusual, one should take into account chondroblastoma-like osteosarcoma when considering differentials for chondroblastoma and chondroblastic OS, especially when radiological features are atypical and the lesion is aggressive. Awareness of this entity can facilitate timely and effective intervention that will improve patient prognosis as CBLOS are known to have an indolent course.

## Article Information and Declarations

### Ethics statement

Consent was obtained from patient.

### Author contributions

S.S.: collection of case details and writing manuscript; P.J: collection of case details; S.M.N., C.G.: supervision and review of manuscript.

### Funding

None funding.

### Acknowledgements

We thank the department of medical oncology and surgical oncology for their contribution.

### Conflict of interest

All authors declare no conflict of interest.

### Supplementary material

None.

## References


1. Fletcher CDM, Bridge JA, Hogendoorn PCW, Mertens F. (ed.). World Health Organization classification of tumors of soft tissue and bone. 4th ed. IARC Press, Lyon 2013.
2. Klein M, Siegal G. Osteosarcoma. Am J Clin Pathol. 2006; 125(4): 555–581, doi: 10.1309/uc6kqhld9lv2kenn.
3. Picci P. Osteosarcoma (Osteogenic sarcoma). Orphanet J Rare Dis. 2007; 2(1), doi: 10.1186/1750-1172-2-6.
4. Schajowicz F, Próspero Jde, Cosentino E. Case report 641. Skelet Radiol. 1990; 19(8): 603–606, doi: 10.1007/bf00241285.
5. Bacchini P, Inwards C, Biscaglia R, et al. Chondroblastoma-Like Osteosarcoma. Orthopedics. 1999; 22(3): 337–339, doi: 10.3928/0147-7447-19990301-11.
6. Bahrami A, Unni K, Bertoni F, et al. Chondroblastoma Like Osteosarcoma: A Clinicopathologic Review of 17 Cases. In Laboratory investigation (Vol. 90). Nature Publishing Group, New York 2010: 15A.
7. Byatnal AA, Rao ACK, Solomon MC, et al. A guise of osteosarcoma: chondroblastoma-like. Indian J Dent Res. 2013; 24(5): 631–634, doi: 10.4103/0970-9290.123418, indexed in Pubmed: 24355968.
8. Hmada YAl, Bernieh A, Morris RW, et al. Chondroblastoma-like Osteosarcoma. Arch Pathol Lab Med. 2020; 144(1): 15–17, doi: 10.5858/arpa.2019-0191-RA, indexed in Pubmed: 31389716.
9. Martin KL, Firestone DE, McGarry SV, et al. Chondroblastoma-like osteosarcoma. Pathol Int. 2014; 64(8): 409–411, doi: 10.1111/pin.12182, indexed in Pubmed: 25143130.
10. Aycan OE, Vanel D, Righi A, et al. Chondroblastoma-like osteosarcoma: a case report and review. Skeletal Radiol. 2015; 44(6): 869–873, doi: 10.1007/s00256-014-2068-2, indexed in Pubmed: 25492634.
11. Ramos Pascua LR, Casas Ramos P, Arias Martín F, et al. Aggressive curettage of a chondroblastoma-like osteosarcoma of the proximal end of the tibia. A case report with seven-year follow-up. Skeletal Radiol. 2018; 47(6): 853–857, doi: 10.1007/s00256-017-2860-x, indexed in Pubmed: 29307095.
12. Gaeta R, Righi A, Gambarotti M, et al. Chondroblastoma-like osteosarcoma: a clinicopathological and molecular study of a rare osteosarcoma variant. Histopathology. 2022; 81(3): 389–401, doi: 10.1111/his.14721, indexed in Pubmed: 35791778.
13. Kyriakos M, Land VJ, Penning HL, et al. Metastatic chondroblastoma. Report of a fatal case with a review of the literature on atypical, aggressive, and malignant chondroblastoma. Cancer. 1985; 55(8): 1770–1789, doi: 10.1002/1097-0142(19850415)55:8<1770::aid-cncr2820550825>3.0.co;2-q, indexed in Pubmed: 3978565.
14. Papke DJ, Hung YP, Schaefer IM, et al. Clinicopathologic characterization of malignant chondroblastoma: a neoplasm with locally aggressive behavior and metastatic potential that closely mimics chondroblastoma-like osteosarcoma. Mod Pathol. 2020; 33(11): 2295–2306, doi: 10.1038/s41379-020-0604-2, indexed in Pubmed: 32601382.
15. Amary MF, Berisha F, Mozela R, et al. The H3F3 K36M mutant antibody is a sensitive and specific marker for the diagnosis of chondroblastoma. Histopathology. 2016; 69(1): 121–127, doi: 10.1111/his.12945, indexed in Pubmed: 26844533.
16. Behjati S, Tarpey PS, Presneau N, et al. Distinct H3F3A and H3F3B driver mutations define chondroblastoma and giant cell tumor of bone. Nat Genet. 2013; 45(12): 1479–1482, doi: 10.1038/ng.2814, indexed in Pubmed: 24162739.
17. Tate JG, Bamford S, Jubb HC, et al. COSMIC: the Catalogue Of Somatic Mutations In Cancer. Nucleic Acids Res. 2019; 47(D1): D941–D947, doi: 10.1093/nar/gky1015, indexed in Pubmed: 30371878.

VIA MEDICA

CASE REPORT

Oncology in Clinical Practice
2025, Vol. 21, No. 1, 78–85
DOI: 10.5603/ocp.98755

ISSN 2450-1654
eISSN 2450-6478

# Can erythrodermic psoriasis be considered a paraneoplastic syndrome in patients with metastatic occult gastric cancer?

Ali Fuat Gürbüz[1,*], Murat Araz[1], Fatih Kılıç[2], Oğuzhan Yıldız[1], Muzaffer Uğraklı[1], Mehmet Zahid Koçak[1], Melek Karakurt Eryılmaz[1], Fahriye Kılınç[3], Mehmet Artaç[1]

[1]Department of Medical Oncology, Faculty of Medicine, Necmettin Erbakan University, Konya, Türkiye
[2]Department of Dermatology, Faculty of Medicine, Necmettin Erbakan University, Konya, Türkiye
[3]Department of Pathology, Faculty of Medicine, Necmettin Erbakan University, Konya, Türkiye

**Abstract**

**Introduction.** Erythrodermic psoriasis is a relatively rare form of psoriasis. It has many etiologies including infection, inflammatory skin diseases, malignancy, and systemic drug reactions. It may be seen more frequently in hematological malignancies. To our knowledge, this is the first reported case of paraneoplastic erythrodermic psoriasis in gastric cancer.

**Case report.** A 59-year-old male patient, who was diagnosed with psoriasis 5 years earlier, presented with severe erythroderma resistant to both local and immunosuppressive treatments. During treatment, he was diagnosed with pathological and radiological metastatic occult gastric cancer and treated with a modified FOLFOX-6 chemotherapy protocol that was planned every 14 days. After six cycles of chemotherapy, a clinically significant benefit was observed in control examination. Extensive skin lesions almost completely resolved after chemotherapy. Erythroderma and pruritus symptoms completely regressed. The patient continues his treatment.

**Conclusions.** Erythrodermic psoriasis may be considered a paraneoplastic syndrome associated with malignant disorders, and therefore paraneoplastic syndrome should be considered in the treatment of these patients.

**Keywords:** erythrodermic psoriasis, occult gastric cancer, paraneoplastic syndrome, chemotherapy

## Introduction

Erythrodermic psoriasis (EP) is a clinical form that patients with psoriasis may experience at any time in their lives. It is characterized by diffuse erythema and varying degrees of desquamation, which may be accompanied by general malaise, fever, lymphadenopathy, and protein loss. It can be caused by various factors including infection, inflammatory skin conditions, malignancy, and systemic drug reactions [1]. Paraneoplastic syndromes are defined as signs and symptoms that may appear when substances released by tumor cells alter normal functions of nearby cells or tissues. Their incidence is not well defined although they are more frequent in hematologic cancers. Moreover, they can appear either at the beginning or during the course of the disease [2]. We present a case of a 59-year-old man with a new onset of erythrodermic psoriasis and concurrent metastatic occult gastric cancer (GC). To our knowledge, this is the first reported case of paraneoplastic EP with metastatic occult GC.

*Correspondence: Ali Fuat Gürbüz, MD, Department of Medical Oncology, Faculty of Medicine, Necmettin Erbakan University, 14280, Konya, Türkiye; tel. +90332 223 7266 (dr.alifuatg@gmail.com)
Received: 2 January 2024; Accepted: 2 February 2024;
Early publication: 5 March 2024

## Case

A 59-year-old male who had been followed up with a diagnosis of psoriasis vulgaris for about five years presented to the dermatology outpatient clinic with signs of peeling skin, diffuse redness, chills, and

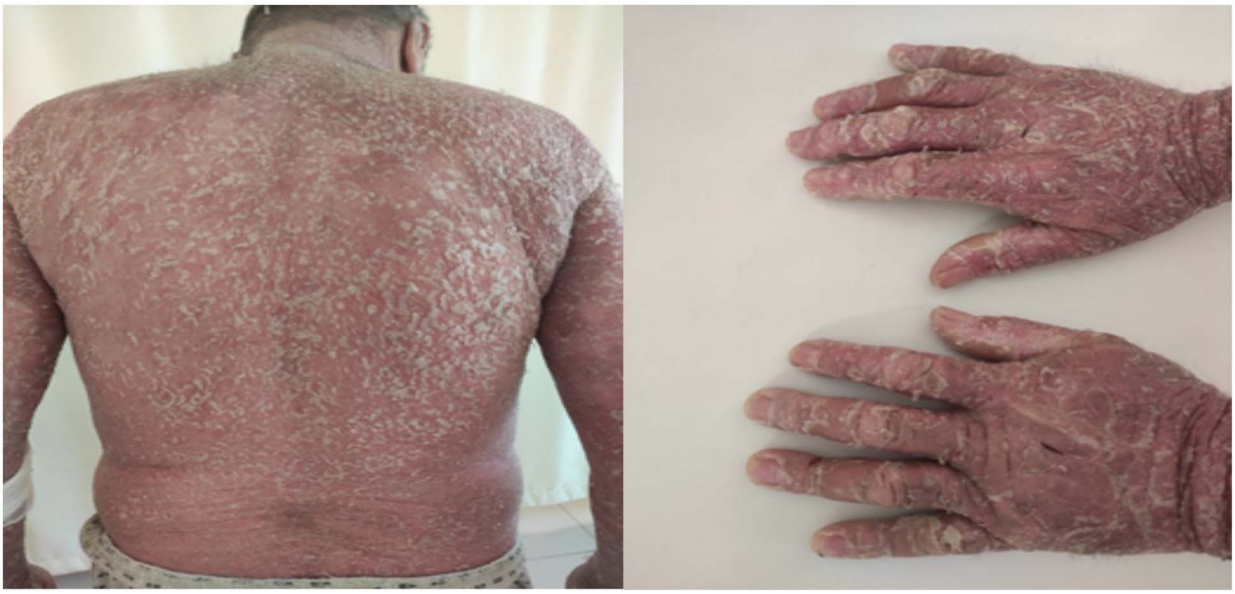

**Figure 1.** Dermatological lesions at the time of diagnosis

shivering. The patient stated that the skin changes that had started on his hands and feet spread rapidly all over his body and were accompanied by joint pain. Dermatological examination revealed diffuse erythema and desquamation including the scalp (Fig. 1). No significant dystrophy was found in the fingernails of the hands and feet, but pitting was observed in the fingernails of the hands.

Firstly, topical treatment was initiated. The initial Psoriasis Area Severity Index (PASI) score was 15. The patient was evaluated for moderate-severe plaque psoriasis. He was treated with betamethasone plus calcipotriol, but there was no improvement in the PASI score. The conventional treatment with acitretin was started at 25 mg once daily before a biological agent. Acitretin has been added as an emollient and topical corticosteroid treatment as a topical treatment.

The patient was evaluated in terms of treatment effectiveness in the 12$^{th}$ week of his conventional treatment. The PASI score was calculated as 33. The patient did not have a PASI50 response in the induction phase, and the dose of acitretin was changed to 35 mg once daily.

After further 12 weeks, the results of using acitretin 35 mg once daily were evaluated. The PASI score was calculated at 31.2. Systemic acitretin treatment was considered unsuccessful due to failure to obtain a PASI50 response after 24 weeks of acitretin use.

Systemic treatment was started with acitretin and adalimumab, and an anti-tumor necrosis factor-alpha (anti-TNF) agent was initiated. The patient's baseline PASI score was calculated at 23.7. The patient received 80 mg of what? at the first application and 40 mg after 1 week, and then the treatment was continued with 40 mg of adalimumab administered subcutaneously every 2 weeks at regular intervals. Although we recommended the continuation of adalimumab, it was discontinued due to the patient's decision.

The patient presented at the dermatology clinic 4 months later, and diffuse psoriatic plaques and erythroderma were observed throughout the body. The patient, whose general condition was moderate, was hospitalized and followed up.

Additional systemic diseases, trauma, drugs, infections, or other similar trigger factors were questioned in the patient's history, but these were not ascertained. With a history of psoriasis vulgaris, diffuse erythroderma, desquamation, arthritis and secondary malnutrition, fever, chills and shivering on dermatological examination, the patient was diagnosed with severe EP. A punch biopsy was taken from the lesion on the right knee to support the current clinical diagnosis with histopathological examination (Fig. 2 and 3). The pathology result was reported as psoriasis form dermatitis. The patient had a history of using acitretin, a conventional systemic treatment, and adalimumab, an anti-TNF antibody. For this reason, standard treatment with secukinumab (300 mg loading dose), an anti-interleukin-17 antibody was started. Following induction treatment at 0, 1, 2, 3, and 4 weeks, monthly maintenance treatment was planned. Although there was some regression in diffuse skin erythema and desquamation in the 4$^{th}$ week of secukinumab treatment (Fig. 4), skin lesions continued to be prominent. The patient received a total of five loadings and two maintenance doses of secukinumab.

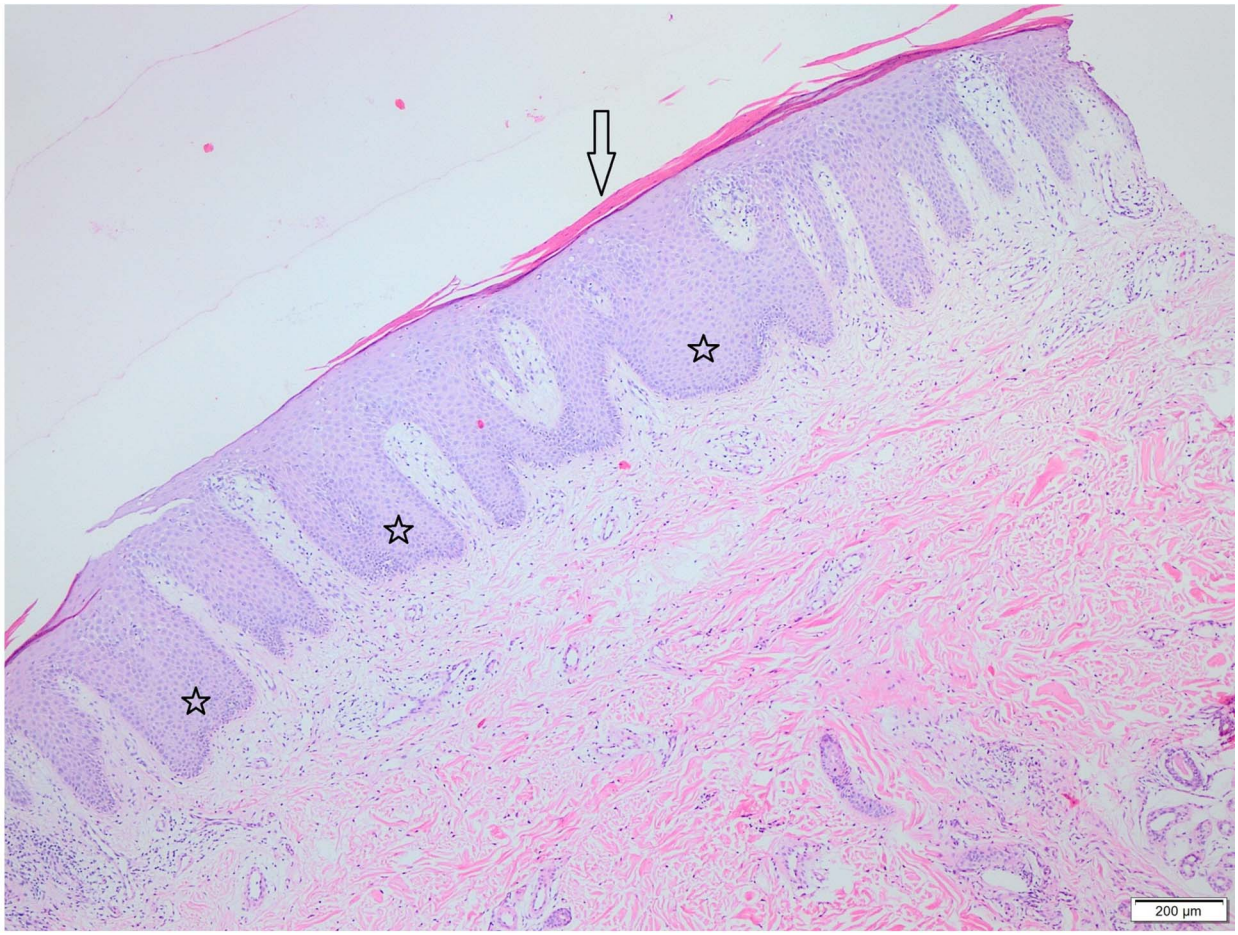


**Figure 2.** Hyperkeratosis on the surface, parakeratosis (arrow), acanthosis, retinal elongation and some have confluence (stars) at the lower ends, hypogranulosis (Hematoxylin/Eosin, 40×)

The patient was referred to the gastroenterology department due to dyspepsia, loss of appetite, and weight loss during treatment. An upper gastrointestinal system endoscopy was performed, and a biopsy was taken from a nodular edematous lesion in the corpus mucosa extending to the cardia along the level of the small curvature (Fig. 5). The pathology report indicated chronic gastritis.

The patient underwent whole-body imaging, and abdominal computer tomography (CT) revealed malignant wall thickening and minimal contrast enhancement starting from the cardia of the stomach and extending along the small curvature (Fig. 6). Lymphadenopathies were present in the root of the mesentery, starting around the celiac trunk and extending to the periportal, paraaortic and aortic bifurcations, with the largest lymphadenopathy having a short diameter of up to 2.5 cm, and there are also lymphadenopathies with a short diameter of less than 1 cm in the peripancreatic area. No malignant mass was detected in the pancreas and the biliary tract. Hypodense nodular lesions suggestive of metastasis were found in both adrenal glands, measuring 2.7 × 3.5 cm on the right and 3 × 2.7 cm on the left, with a Hounsfield unit of more than 20 HU. No evidence of metastasis was found on the thorax CT. Liver dynamic magnetic resonance imaging revealed a 7.5 cm lesion in the posterior superior part of the right lobe of the liver (Fig. 7), which did not have a typical appearance in terms of metastasis since no signal intensity loss was observed in the arterial portal and late phase sections after intravenous contrasting. No malign cells or tissue were observed in the rebiopsy taken from the stomach. It was reported as benign. A liver wedge biopsy was performed by an interventional radiologist for diagnostic purposes. In the pathology report, it was interpreted as carcinoma metastasis subtype unclassified, CDX-2, TTF-1; and HEPAR were negative, while cytokeratin 7 and 20 were positive. No loss of expression was observed for MLH1, MSH2, MSH6, and PMS2 proficient mismatch repair (pMMR). CERBB2 was positive (score 3) and PDL-1 TPS negative (Dako Clone 22C3). Due to these findings, we investigated the stomach and the pancreatobiliary system as the primary focus.

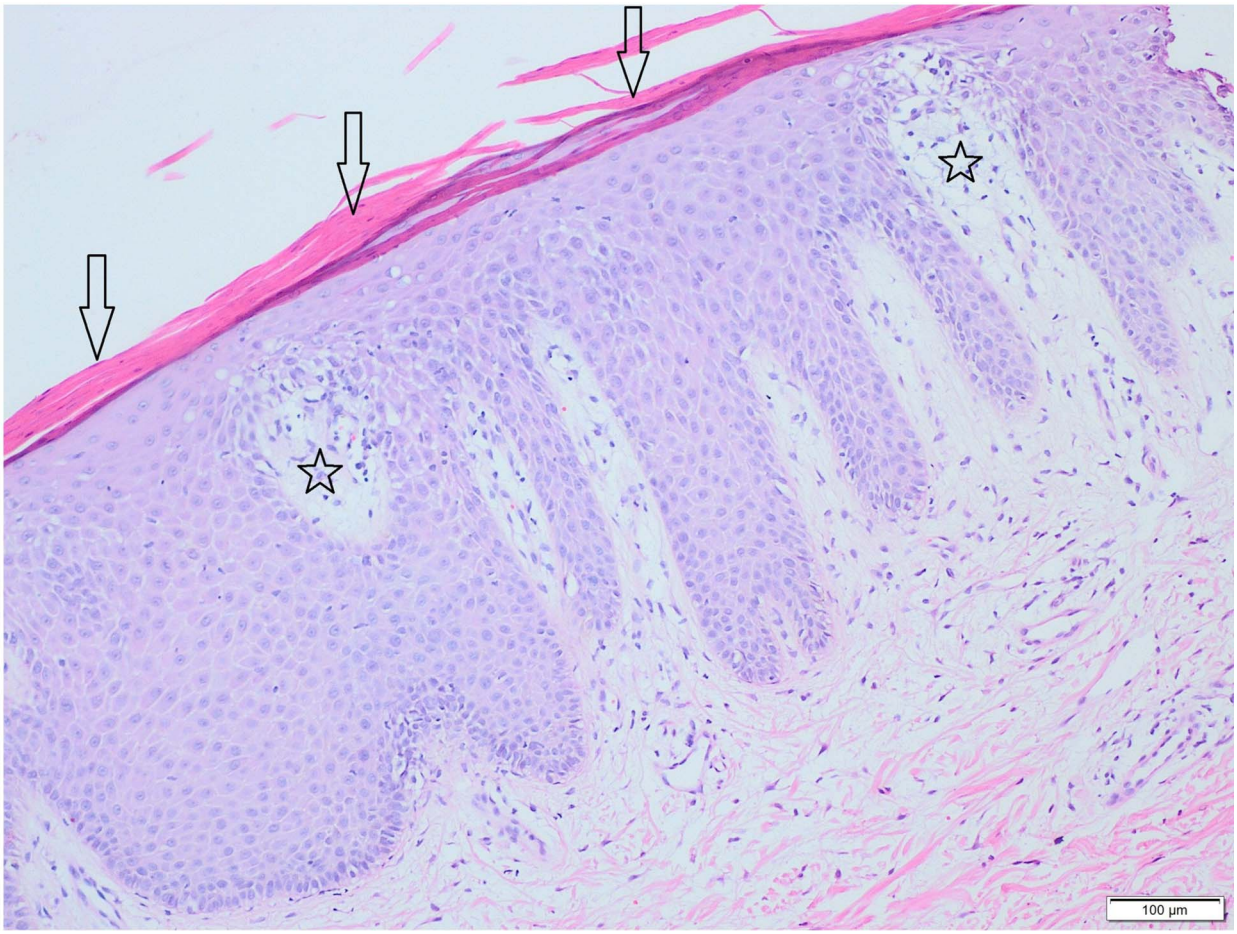


**Figure 3.** Closer view of skin texture. Persistent parakeratosis (arrows), edema of the papillary dermis, dilated capillaries (stars), and few perivasciluar lymphocytes are seen (Hematoxylin/Eosin, 100×)

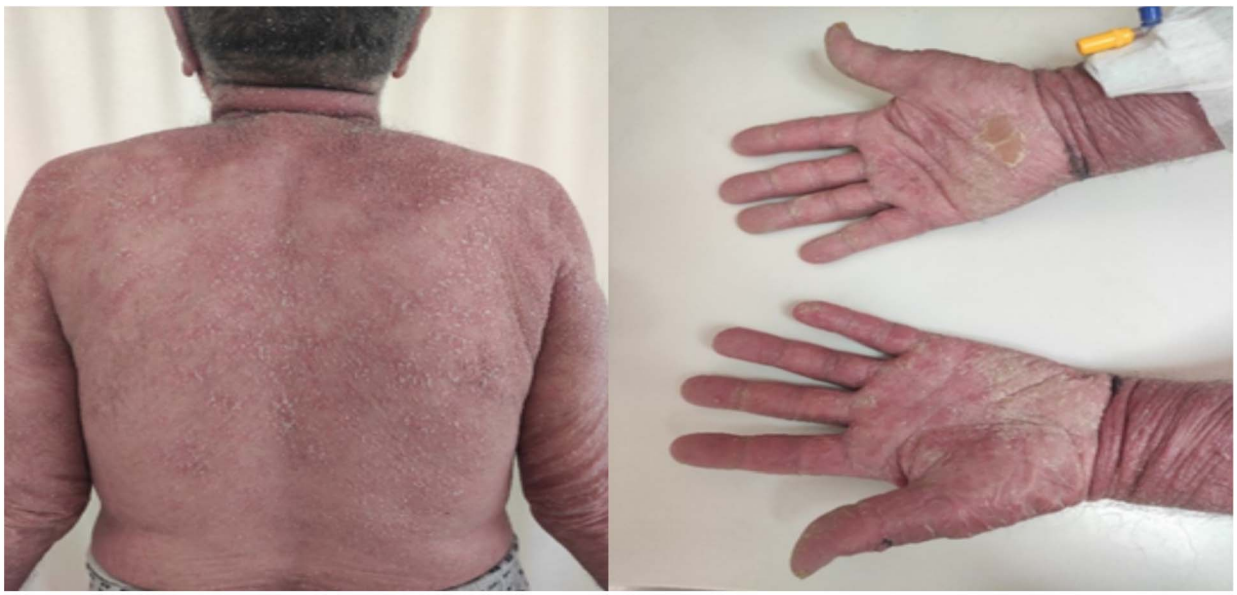

**Figure 4.** After secukinumab 4$^{th}$ week loading dose treatment

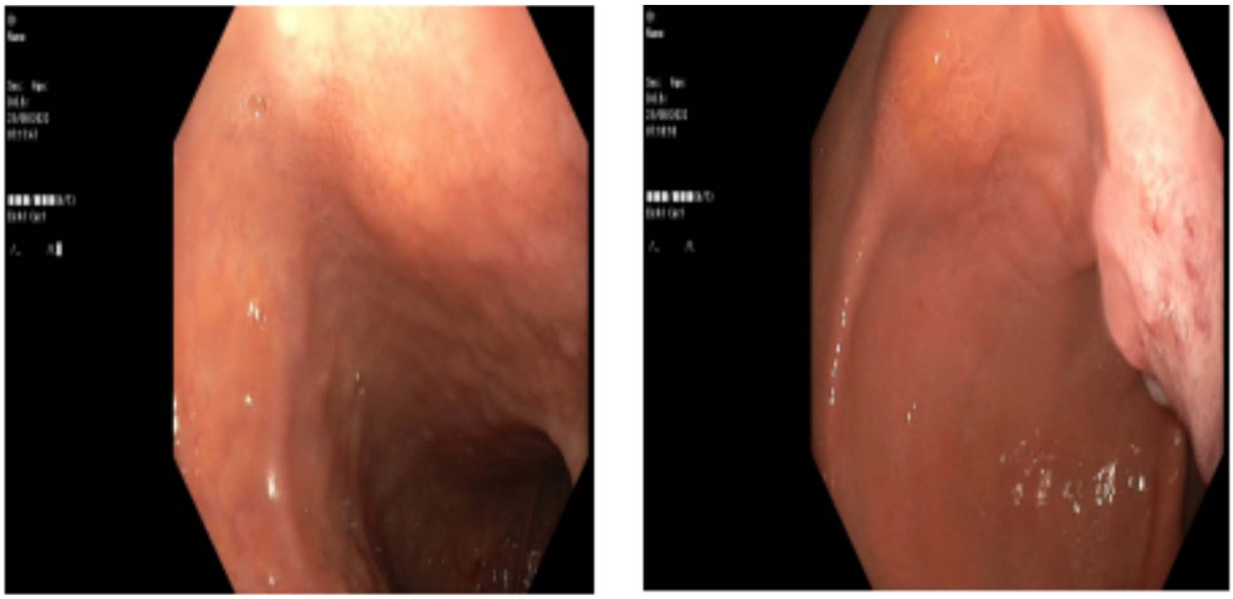

**Figure 5.** Endoscopic Image at diagnosis

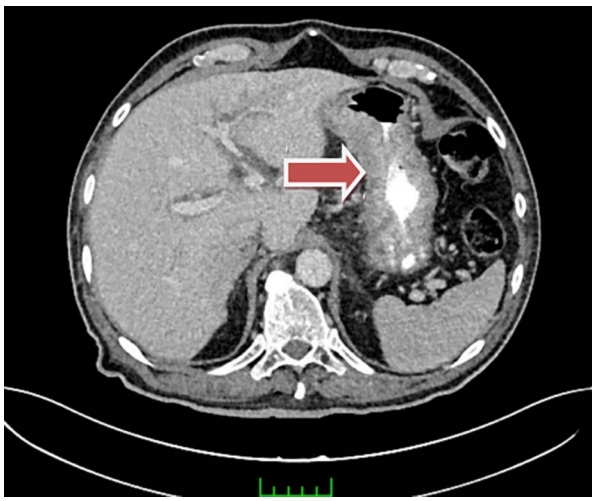

**Figure 6.** Thickness of the gastric wall

The clinical and radiological diagnosis was metastatic occult GC, and the patient was treated with a modified FOLFOX-6 chemotherapy protocol [oxaliplatin 85 mg/m$^2$, folic acid 400 mg/m$^2$, 5-fluorouracil 400 mg/m$^2$ intravenous (IV) injection and 2400 mg/m$^2$ 46-hour infusion]. The protocol was planned every 14 days. After 6 cycles of chemotherapy, a clinically significant benefit was observed in the control examination. Extensive skin lesions almost completely resolved after chemotherapy. Erythroderma and pruritus completely regressed (Fig. 8). A CT scan of the thorax and abdomen, which was performed to evaluate the response to treatment, showed that the size and number of hepatic lesions and paraaortic and mesenteric root lymphadenopathies decreased, which we considered a partial response to treatment. The patient continues this treatment.

## Discussion

Erythrodermic psoriasis is a relatively rare form of psoriasis but represents a fairly common etiology for erythrodermic phenotypes. Erythroderma is a diffuse erythema involving more than 90% of the body surface and may be exfoliative and exudative and involve hair and nail changes. It has many etiologies including infection, inflammatory skin diseases, malignancy, and systemic drug reactions [3]. However, the relationship between malignancy and psoriatic disease has not been clearly established. Studies in patients with psoriasis have documented increased rates of lymphoma and non-melanoma skin cancer, but results for other solid malignancies have not been significant [4]. Less commonly, acute myeloid leukemia and solid tumors (e.g., lung, prostate, thyroid, liver, ovaries, rectum, or skin) are associated with paraneoplastic erythroderma [5] A review of the literature identified two cases associated with EP. Both were hematological malignancies. Thus, the case of EP published by Chen et al. in 2017 [6] was accompanied by monoclonal B-cell lymphocytosis. In another study published in 2021, Li et al. [7] mentioned that B-cell chronic lymphocytic leukemia precipitated EP.

While rates of GC have been falling, over 100 000 new cases occur in Europe each year [8]. It remains one of the leading causes of cancer-related death and therefore a major health problem [9]. Patients are usually diagnosed at an advanced stage, which explains

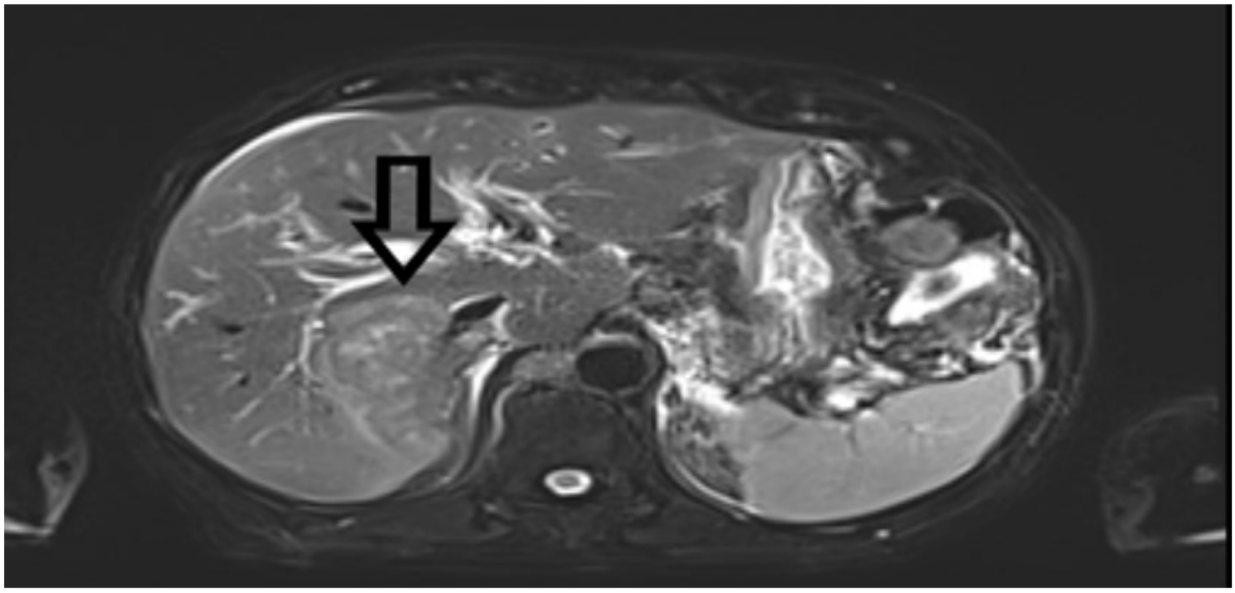

**Figure 7.** Magnetic resonance imaging of a metastatic lesion in the liver

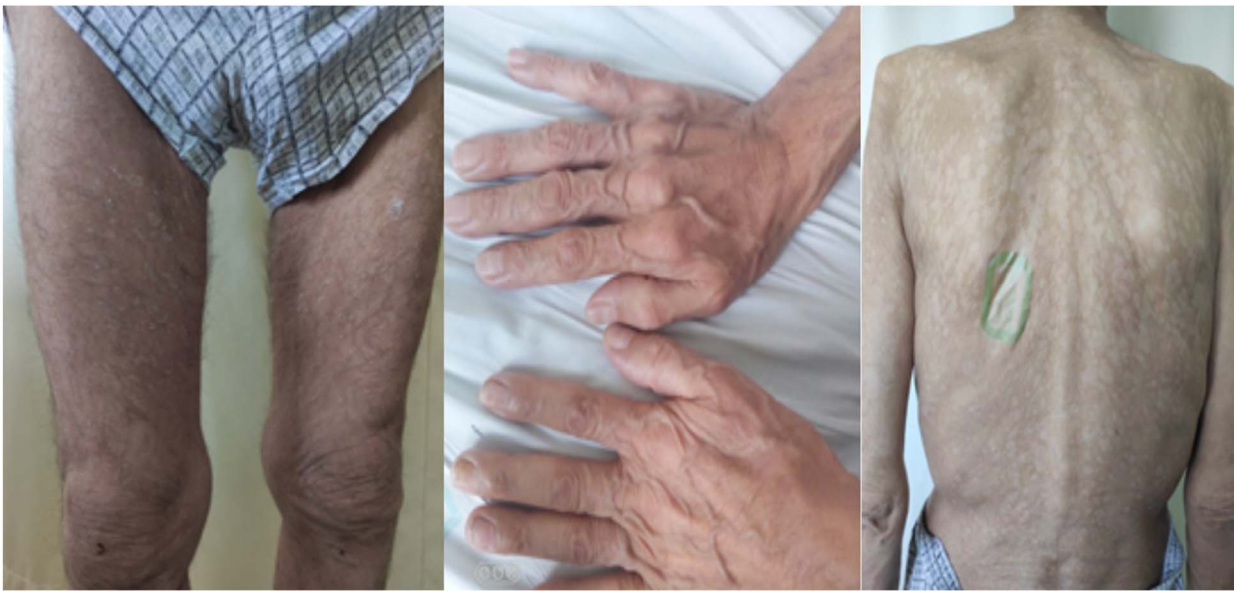

**Figure 8.** Post-chemotherapy dermatological lesions

the poor survival rate. Several dermatological paraneoplastic syndromes precede the diagnosis of GC and may therefore aid the clinician in the early detection of malignancy. In a prospective study by Tatsuat et al. [10], the frequency of false negative gastric wall biopsies in advanced gastric tumors was found to be 5.7%. The obtained results were negative because this type of tumor tissue is typically covered with gastric mucosa, and there is no apparent ulcer tissue. As a result, the biopsy is very small and superficial. Similarly, the two gastric wall biopsies performed in our case were not diagnosed as malignant as there was no obvious ulcer tissue [10].

Secukinumab is a humanized anti-IL-17A monoclonal antibody indicated for psoriasis treatment. It is indicated in moderate-to-severe psoriasis cases, psoriatic arthritis, and axial spondyloarthritis. It shows rapid responses and a safe profile in all psoriatic manifestations [11]. Although a recent case-control study in psoriasis suggested a possible increased risk of malignancy in patients using anti-TNF-alfa blockers for more than 12 months [12], studies with secukinumab failed to show an increased risk of malignancy [13, 14]. In a multicenter study of secukinumab using real-life data, 42 patients with psoriasis and a history of malignant diagnosis did not develop recurrence

or progression during a mean 56-week secukinumab treatment period [15]. In our case, we did not consider the malignancy risk due to secukinumab use because the patient had taken secukinumab for only five weeks and the treatment had been completed very recently.

The patient reported that he had experienced skin eruptions similar to psoriasis approximately 10 months before the diagnosis of GC. In fact, many dermatological paraneoplastic syndromes tend to occur as a prodrome of the underlying malignancy [16]. The severity of psoriasis in our patient was graded as a severe disease (PASI score 15) according to the clinical picture. There was no significant change in skin appearance after using topical glucocorticoids and acitretin, which is the standard treatment of psoriasis according to current guidelines in German-speaking countries [17]. Adalimumab, an anti-TNF agent, was used only for a short time. As a consequence of that ineffective treatment, our patient discontinued the therapy. After receiving 5 doses of secukinumab when the disease started to flare up again during treatment he was diagnosed with metastatic occult GC. Interestingly, within 3 months of starting chemotherapy, the lesions disappeared without any specific treatment after induced remission of gastric cancer under cytotoxic therapy. Although not confirmed, the close association between the development of lesions and cancer tumor burden is highly suggestive of paraneoplastic EP in this case. It is expected that any form of psoriasis, whether paraneoplastic or not, will improve with cytotoxic chemotherapy.

In our case, improvement of the disease was observed neither after glucocorticoid or after acitretin treatment, nor after anti-tnf and biological agents. Moreover, different temporal aspects of the disease support the hypothesis of paraneoplastic genesis. The first manifestations of EP were closely temporally related to the first diagnosis of GC. Moreover, during the first GC remission, EP also remained in remission without the need for any specific treatment.

## Conclusions

Our patient's diagnosis of metastatic occult GC occurred concurrently with a severe, new, and atypical development of EP. Whether the two conditions occurred independently as coincidental events or as a paraneoplastic syndrome with related pathogenesis remains to be established, and additional reports may be helpful to elucidate if there is a connection between these conditions. We believe that EP may be a paraneoplastic syndrome associated with malignant disorders and therefore such a possibility should be considered in the treatment of these patients.

## Article Information and Declarations

### Ethics statement

Written informed consents were obtained from patient.

### Author contributions

A.F.G.: conception, data collection, writing, editing and approval of the final draft; M.Araz: conception, data collection, editing and approval of the final draft; Fatih Kılıç: study design, writing, editing and approval of the final draft; O.Y.: study design, editing and approval of the final draft; M.U.: writing, editing; M.K.E.: editing and approval of the final draft; Fahriye Kılınç: data collection; M.Artaç: editing and approval of the final draft.

### Funding

This research did not receive any specific grant from funding agencies in the public, commercial, or not-for-profit sectors.

### Acknowledgements

None.

### Conflict of interest

The authors declare no conflict of interest.

### Supplementary material

None.

## References

1. Tomasini C, Aloi F, Solaroli C, et al. Psoriatic erythroderma: a histopathologic study of forty-five patients. Dermatology. 1997; 194(2): 102–106, doi: 10.1159/000246075, indexed in Pubmed: 9094455.
2. Gethi.org. Madrid: Grupo Español Tumores Huérfanos e Infrecuentes (GETHI). http://www.gethi.org/Portals/0/libro_digital_oncologia-V2.pd.
3. Mistry N, Gupta A, Alavi A, et al. A Review of the Diagnosis and Management of Erythroderma (Generalized Red Skin). Adv Skin Wound Care. 2015; 28(5): 228–236, doi: 10.1097/01.asw.0000463573.40637.73, indexed in Pubmed: 25882661.
4. Prizment AE, Alonso A, Folsom AR, et al. Association between psoriasis and incident cancer: the Iowa's Women's Health Study. Cancer Causes Control. 2011; 22(7): 1003–1010, doi: 10.1007/s10552-011-9773-0, indexed in Pubmed: 21553077.
5. King LE, Dufresne RG, Lovett GL, et al. Erythroderma: review of 82 cases. South Med J. 1986; 79(10): 1210–1215, doi: 10.1097/00007611-198610000-00005, indexed in Pubmed: 2945258.
6. Chen SX, Hinds BR, Goodman AM, et al. Erythrodermic Psoriasis in a Man with Monoclonal B-cell Lymphocytosis. Cureus. 2017; 9(12): e1936, doi: 10.7759/cureus.1936, indexed in Pubmed: 29464143.
7. Li Y, Wen Y, You R, et al. Erythrodermic psoriasis precipitated by B-cell chronic lymphocytic leukemia. Dermatol Ther. 2021; 34(3): e14904, doi: 10.1111/dth.14904, indexed in Pubmed: 33611837.
8. Keighley MRB. Gastrointestinal cancers in Europe. Aliment Pharmacol Ther. 2003; 18 Suppl 3: 7–30, doi: 10.1046/j.0953-0673.2003.01722.x, indexed in Pubmed: 14531737.
9. Comella P, Franco L, Casaretti R, et al. Emerging role of capecitabine in gastric cancer. Pharmacotherapy. 2009; 29(3): 318–330, doi: 10.1592/phco.29.3.318, indexed in Pubmed: 19249950.
10. Tatsuta M, Iishi H, Okuda S, et al. Prospective evaluation of diagnostic accuracy of gastrofiberscopic biopsy in diagnosis of gastric cancer. Cancer. 1989; 63(7): 1415–1420, doi: 10.1002/1097-0142(19890401)63:7<1415::aid-cncr2820630731>3.0.co;2-9.
11. Gottlieb AB, Deodhar A, Mcinnes IB, et al. Long-term safety of secukinumab in patients with moderate-to-severe plaque psoriasis, psoriatic arthritis, and ankylosing spondylitis: integrated pooled

clinical trial and post-marketing surveillance data. Arthritis Res Ther. 2019; 21(1): 111, doi: 10.1186/s13075-019-1882-2, indexed in Pubmed: 31046809.
12. Lee JW, Jung KJ, Kim TG, et al. Risk of malignancy in patients with psoriasis: a 15-year nationwide population-based prospective cohort study in Korea. J Eur Acad Dermatol Venereol. 2019; 33(12): 2296–2304, doi: 10.1111/jdv.15783, indexed in Pubmed: 31287593.
13. Valenti M, Pavia G, Gargiulo L, et al. Biologic therapies for plaque type psoriasis in patients with previous malignant cancer: long--term safety in a single- center real-life population. J Dermatolog Treat. 2022; 33(3): 1638–1642, doi: 10.1080/09546634.2021.1886231, indexed in Pubmed: 33555951.
14. Bellinato F, Gisondi P, Maurelli M, et al. IL-17A inhibitors in patients with chronic plaque psoriasis and history of malignancy: A case series with systematic literature review. Dermatol Ther. 2021; 34(2): e14889, doi: 10.1111/dth.14889, indexed in Pubmed: 33595861.
15. Pellegrini C, Esposito M, Rossi E, et al. Secukinumab in Patients with Psoriasis and a Personal History of Malignancy: A Multicenter Real-Life Observational Study. Dermatol Ther (Heidelb). 2022; 12(11): 2613–2626, doi: 10.1007/s13555-022-00797-9, indexed in Pubmed: 36169883.
16. Pelosof LC, Gerber DE. Paraneoplastic syndromes: an approach to diagnosis and treatment. Mayo Clin Proc. 2010; 85(9): 838–854, doi: 10.4065/mcp.2010.0099, indexed in Pubmed: 20810794.
17. Nast A, Altenburg A, Augustin M, et al. Deutsche S3-Leitlinie zur Therapie der Psoriasis vulgaris, adaptiert von EuroGuiDerm - Teil 2: Therapiemonitoring, besondere klinische Situationen und Komorbidität. J Dtsch Dermatol Ges. 2021; 19(7): 1092–1117, doi: 10.1111/ddg.14507_g, indexed in Pubmed: 34288473.

VIA MEDICA

CASE REPORT

Oncology in Clinical Practice
2025, Vol. 21, No. 1, 86–89
DOI: 10.5603/ocp.99588

ISSN 2450-1654
eISSN 2450-6478

# Preservation of vision through an interdisciplinary approach: a case report of intraorbital malignant solitary fibrous tumor

Andrzej Jarząbski[1,2], Tomasz Łysoń[3], Dorota Kiprian[1,2], Joanna Turkiewicz[4], Daria Kamińska[1,2], Andrzej Kawecki[4]

[1]Department of Oncology and Radiotherapy, The Maria Sklodowska-Curie National Research Institute of Oncology, Warsaw, Poland
[2]Department of Head and Neck Cancer, The Maria Sklodowska-Curie National Research Institute of Oncology, Warsaw, Poland
[3]Department of Neurosurgery, Medical University of Bialystok, Department of Interventional Neurology at the Medical University of Bialystok, Poland
[4]Department of Head and Neck Cancer, The Maria Sklodowska-Curie National Research Institute of Oncology, Warsaw, Poland

**Abstract**

A 70-year-old female with a history of subtotal surgical resection of malignant solitary fibrous tumor (SFT) located in the lateral intraconal compartment of the right orbit was referred to the Oncology Team. The patient underwent surgical treatment with adjuvant radiotherapy of the right orbit. No major complications and no new neurological deficits related to radiotherapy were observed during the 4.5 years of follow-up. The discussed case is an essential source of knowledge for the medical community, demonstrating successful interdisciplinary collaboration involving surgery and high-dose radiotherapy of intraorbital malignant solitary fibrous tumors, particularly for optic nerve protection.

**Keywords:** solitary fibrous tumour, interdisciplinary approach, case report

## Case report

The aim of our report is to present the results of a multidisciplinary approach in the treatment of intraorbital solitary fibrous tumor (SFT) after non-radical resection.

A 70-year-old female underwent surgery due to an intraorbital, intraconal tumor of the right orbit. During the first surgical treatment in 1996, the tumor was diagnosed as neurofibroma. In 2018, the patient appeared with a large tumor (37 × 21 × 25 mm) within the lateral intraconal compartment of the right orbit (Fig. 1). Right-sided exophthalmos and visual field deficits were detected before the second surgery. Using minimally invasive lateral orbitotomy, the tumor was subtotally resected. Only a small capsule fragment attached to the optic nerve was left. Immediately after surgery, no new visual deficit was observed. Histopathological examination did not confirm the initial diagnosis of neurofibroma, and a malignant solitary fibrous tumor was diagnosed [CD34(+), STAT6(+), CD(–), ERG(–)]. A few months later, a significant vision improvement was observed with normalization of the visual field.

Based on the result of histopathological examination, the patient was referred to the Oncology Team and qualified for adjuvant radiotherapy (after surgery). The plan of the treatment was based on preoperative magnetic resonance imagining (MRI) (Fig. 1) and postoperative computed tomography (CT) scan.

*Correspondence: Dorota Kiprian, MD PhD, Department of Oncology and Radiotherapy, The Maria Sklodowska-Curie National Research Institute of Oncology, ul. W. K. Roentgena 5, 02–781, Warsaw, Poland (dorotakiprian1@gmail.com)
Received: 6 March 2024; Accepted: 9 April 2024; Early publication: 30 April 2024

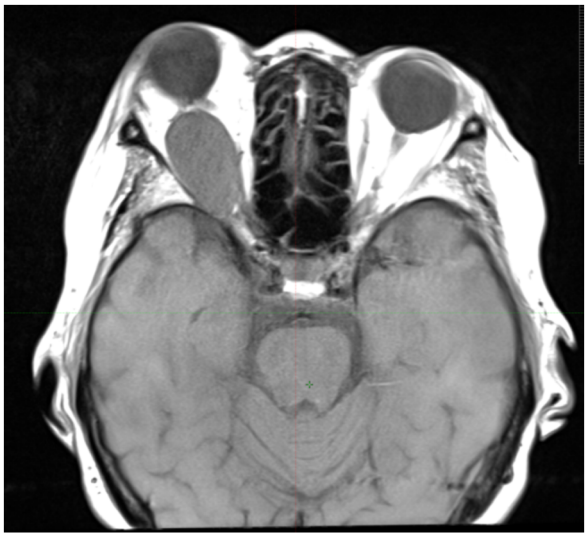

**Figure 1.** Magnetic resonance imaging before surgery

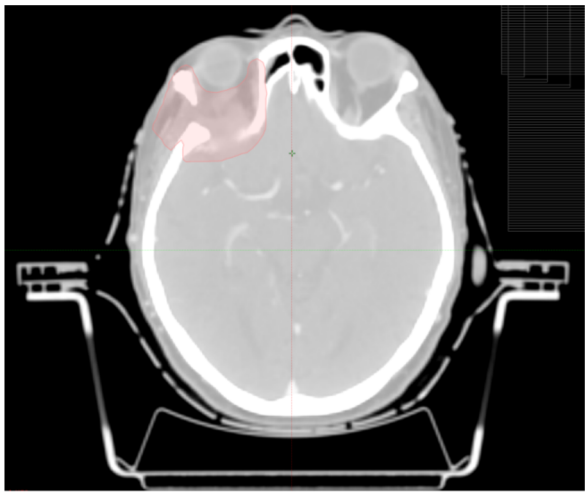

**Figure 2.** Contouring of clinical target volume (CTV) 60 Gy

Information that it was possible that a small remnant of the tumor was left attached to the optic nerve sheath and contrast enhancement within the orbital cone on postoperative MR resulted in qualifying the patient for adjuvant high-dose radiation therapy. Intensity modulated radiation therapy (IMRT) (Varian Medical Systems) was applied onto the tumor bed (space after the surgical intervention), with the treatment energy of 6 MeV photons. A total dose of 60 Gy was delivered with 30 fractions within 6 weeks. The contoured area of the tumor bed, our clinical target volume (CTV) for a 60 Gy dose, is shown in Figure 2. The distribution of treatment plan dose of 57 Gy (95% total dose) is shown in Figure 3. The maximum dose on the optic nerve was 59.4 Gy, and the mean dose was 56.99 Gy. The maximum dose on the right eye was 59.37 Gy; the mean was 38.28 Gy. The maximum dose on the right lens was 17.9 Gy; the mean dose was 14.05 Gy. The maximum dose on the left lens was 2.28 Gy; the mean dose was 1.75 Gy. The patient accepted the risk of vision deterioration after the high dose of irradiation. Ophthalmological follow-up examination revealed worse visual acuity due to a growing cataract, but there was no regrowth of the tumor within the orbit.

## Discussion

Solitary fibrous tumors are rare spindle-cell neoplasms initially documented in pleural locations by Klemperer and Rabin [1]. Westra et al. [2] were the first ones to describe STF in the orbit. The most common symptoms related to SFT are arthralgia, hypoglycemia, effusion, and exophthalmos [3].

Contribution of radiotherapy within a multidisciplinary treatment context has not been directly investigated in the literature [4–9]. In a study conducted by Krengli et al. [10], comparable overall survival (OS) rates between patients who had undergone surgery (Sx) alone and those who had received both surgery and radiotherapy (RT) were observed. The actual 5-year local control (LC) rates were 50.4% after Sx and 91.6% after Sx plus RT ($p < 0.0001$) for LC, and 50.4% after Sx and 83.1% after Sx plus RT ($p < 0.008$) for disease-free survival (DFS). However, radiotherapy demonstrated enhancements in both LC and DFS [10]. Importantly, late local recurrences were identified, even beyond ten years [7].

Complete excision of the tumor remains the preferred treatment for SFT. In our case, it was not possible without damaging the optic nerve and impacting on vision. Radical surgery may be a major prognostic factor for LC and DFS [11, 12]. With R0 and R1 resections, the status of the margin does not affect the result, but in research conducted by Krengi et al. [10], R2 operations without adjuvant treatment resulted in very high baseline local recurrences reaching up to 75%. The role of radiotherapy in SFT treatment is still disputable. According to Salas et al. [7], adjuvant radiotherapy improves LC without affecting OS. Nevertheless, factors such as tumor location, size, adhesion, potential for bleeding, and postoperative complications might occasionally preclude this approach or can be indicators for adjuvant radiotherapy [10, 13].

Different doses of adjuvant radiotherapy ranging from 45 to 68.4 Gy (mean 60 Gy) using different radiotherapy techniques are encountered in the literature [10]. The radiotherapy dose level can be conditioned by the tumor location and the margin status of the postoperative histopathological examination. Based on our review of the literature, we decided to apply the mean irradiation dose. In our case, it was difficult to assess the margin status. Information gathered

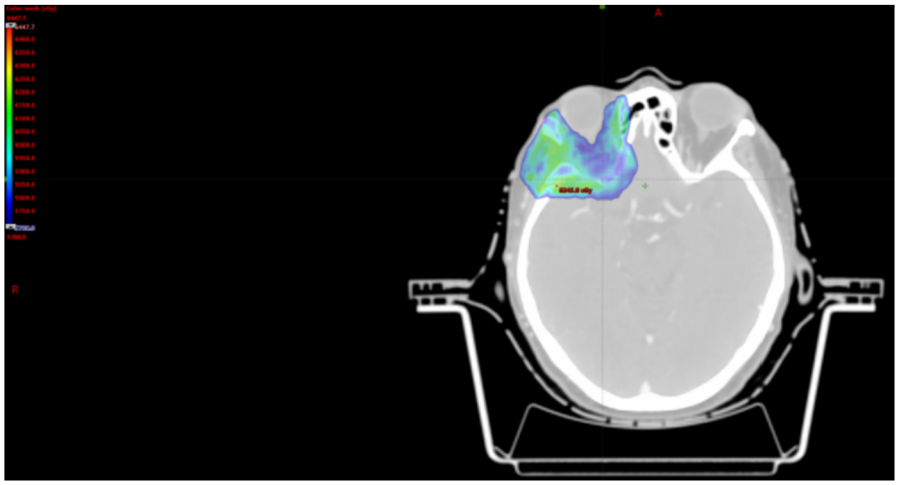

**Figure 3.** Distribution of a dose of 57 Gy

from the operative theatre and the postoperative MRI findings may have suggested residual remnants of the tumor. Therefore, the patient was qualified for adjuvant high-dose radiotherapy. This appeared to be successful and for 4.5 years of follow-up, no recurrence was diagnosed. Certainly, one can expect late radiation side effects with the risk, according to the literature, at a level above grade 2.

## Conclusions

An interdisciplinary approach with minimally invasive surgery of intraorbital malignant SFT preserving eye function combined with high-dose radiotherapy could be effective and safe for patients with nonradical surgical treatment.

## Article Information and Declarations

### Ethics statement

The patient consented to being part of this study.

### Author contributions

All authors made substantial contributions to the study design and data analysis and interpretation. All authors drafted the manuscript, revised it critically for important intellectual content, and read and approved the final version of the manuscript to be published.

### Funding

No conflict of interest or financial support to disclose.

### Acknowledgements

None.

### Conflict of interest

No conflict of interest or financial support to disclose.

### Supplementary material

None.

## References

1. Klemperer P, Rabin CB. Primary neoplasm of the pleura: a report of five cases. Arch Pathol. 1931; 11: 385–412.
2. Westra WH, Gerald WL, Rosai J. Solitary fibrous tumor. Consistent CD34 immunoreactivity and occurrence in the orbit. Am J Surg Pathol. 1994; 18(10): 992–998, doi: 10.1097/00000478-199410000-00003, indexed in Pubmed: 7522416.
3. Cereno R, Cañal J, Ranche F. Possible role of radiotherapy in the management of orbital solitary fibrous tumors. Precision Radiation Oncology. 2020; 4(4): 120–124, doi: 10.1002/pro6.1103.
4. Cardillo G, Carbone L, Carleo F, et al. Solitary fibrous tumors of the pleura: an analysis of 110 patients treated in a single institution. Ann Thorac Surg. 2009; 88(5): 1632–1637, doi: 10.1016/j.athoracsur.2009.07.026, indexed in Pubmed: 19853123.
5. Jha N, McNeese M, Barkley HT, et al. Does radiotherapy have a role in hemangiopericytoma management? Report of 14 new cases and a review of the literature. Int J Radiat Oncol Biol Phys. 1987; 13(9): 1399–1402, doi: 10.1016/0360-3016(87)90236-7, indexed in Pubmed: 3305450.
6. Mira J, Chu F, Fortner J. The role of radiotherapy in the management of malignant hemangiopericytoma.Report of eleven new cases and review of the literature. Cancer. 1977; 39(3): 1254–1259, doi: 10.1002/1097-0142(197703)39:3<1254::aid-cncr2820390335>3.0.co;2-j.
7. Salas S, Resseguier N, Blay JY, et al. Prediction of local and metastatic recurrence in solitary fibrous tumor: construction of a risk calculator in a multicenter cohort from the French Sarcoma Group (FSG) database. Ann Oncol. 2017; 28(8): 1979–1987, doi: 10.1093/annonc/mdx250, indexed in Pubmed: 28838212.
8. Wushou A, Jiang YZ, Liu YR, et al. The demographic features, clinicopathologic characteristics, treatment outcome and disease--specific prognostic factors of solitary fibrous tumor: a population--based analysis. Oncotarget. 2015; 6(39): 41875–41883, doi: 10.18632/oncotarget.6174, indexed in Pubmed: 26496033.
9. Wushou A, Miao XC, Shao ZM. Treatment outcome and prognostic factors of head and neck hemangiopericytoma: meta-analysis. Head Neck. 2015; 37(11): 1685–1690, doi: 10.1002/hed.23812, indexed in Pubmed: 24954602.
10. Krengli M, Cena T, Zilli T, et al. Radiotherapy in the treatment of extracranial hemangiopericytoma/solitary fibrous tumor: Study from the Rare Cancer Network. Radiother Oncol. 2020; 144: 114–120, doi: 10.1016/j.radonc.2019.11.011, indexed in Pubmed: 31805515.
11. Espat NJ, Lewis JJ, Leung D, et al. Conventional hemangiopericytoma: modern analysis of outcome. Cancer. 2002; 95(8): 1746–1751, doi: 10.1002/cncr.10867, indexed in Pubmed: 12365023.

12. Duval M, Hwang E, Kilty SJ. Systematic review of treatment and prognosis of sinonasal hemangiopericytoma. Head Neck. 2013; 35(8): 1205–1210, doi: 10.1002/hed.23074, indexed in Pubmed: 22733718.

13. Galiè M, Tieghi R, Cavazzini L, et al. Solitary fibrous tumor of the orbit: a case report. Int J Oral Maxillofac Surg. 2005; 34(3): 331–333, doi: 10.1016/j.ijom.2004.05.011, indexed in Pubmed: 15741045.